Molekulare Charakterisierung der cytoplasmatischen Phytochrom Funktion in *Physcomitrella patens*

Inaugural Dissertation

Zur Erlangung des akademischen Grades eines

Doktor der Naturwissenschaft (Dr. rer. nat.)

eingereicht von

Dipl. Biol. Janina Katharina Jaedicke

aus Dinslaken

Am Fachbereich Chemie und Biologie der

Justus Liebig Universität Gießen

Gießen, im Februar 2012

Erstgutachter	Prof. PhD Jon Hughes (Universität Gießen)
Zweitgutachter	PD Dr. Mathias Zeidler (Universität Gießen)

Molecular characterisation of cytoplasmic phytochrome function in *Physcomitrella patens*

Inaugural dissertation

submitted to the faculty of chemistry and biology at
Justus Liebig University Giessen
in partial fulfilment of the requirements for the degree of a
Doctor of Science (Dr. rer. nat.)

by

Dipl. Biol. Janina Katharina Jaedicke

Giessen, February 2012

First things first, but not necessarily in that order.

Doctor Who

Parts of this work were published in

Jutta Rösler, Katharina Jaedicke and Mathias Zeidler
Cytoplasmic phyotchrome action
Plant Cell Physiol. 2010 Aug;51(8):1248-54

Katharina Jaedicke, Jutta Rösler, Tanja Gans and Jon Hughes
***Bellis perennis* - a useful tool for protein localisation studies**
Planta. 2011 Oct;243(4):759-68

Katharina Jaedicke, Anna Lichtenthäler, Rabea Krikor, Mathias Zeidler and Jon Hughes
A phytochrome-phototropin light signalling complex at the plasma membrane
PNAS. (*revision submitted)*

1. Introduction

1.1. Light perception by plants

Light is the most important abiotic factor for plants as it not only serves as the primary energy source but also initiates and triggers major developmental processes. Hence plants have evolved different photoreceptors connected to specific signaling pathways for light detection, so that they are not only able to distinguish different light qualities but also light quantity, periodicity, direction and polarisation (1). The most important photoreceptors in plant development belong to the group of red and blue light (R and B, respectively) receptors. The group of R photoreceptors comprises the family of phytochromes (2) whereas several classes of photoreceptors detect B. Short wavelengths in the UV-B region are perceived by UVR8 (3), whereas longer B wavelength can be detected by phototropins (4), cryptochromes (5) and ZTL/FKF/LKP2 family members (6). Members of all photoreceptor families, except for *Zeitlupe*, are conserved in both higher and lower plants (7-10). Phytochromes and phototropins are particularly well investigated and it is known that they serve fundamental processes during plant development. The functions they serve, however, may be different from one another in either higher or lower plants (11). Zygomatic algae and certain ferns possess an additional type of photoreceptor: neochromes are chimeras of an N-terminal phytochrome photosensory module (see 1.3.4.) genetically fused to a full-length phototropin moiety (12, 13). Interestingly this special photoreceptor appears to have arisen twice during evolution. However, based on genome sequences, neochromes seem to be restricted to certain algae and ferns, as there is no evidence for the existence of these photoreceptor chimeras in either higher plants like *Arabidopsis* or other lower plants like mosses.

1.2. Higher plant phytochromes

This ancient and widespread family of R and FR sensing photoreceptors have originally been identified in plants, but to date homologs are also known in bacteria, cyanobacteria, algae, ferns, mosses and fungi (14). Phytochromes are soluble bili-proteins of a molecular mass of 124 kDa (15), physiologically acting as functional dimers (16). To sense light, plant phytochromes require PΦB as their bilin chromophore (17, 18). PΦB is derived from heme and linearised into an open tetrapyrrole through oxidation by HY1 followed by a subsequent isomerisation reaction mediated by PΦB-synthase within the chloroplast (19). The chromophore autocatalytically assembles with the apoprotein post-translationally and attaches to a conserved cystein residue (20, 21). Thereupon holophytochromes are photoconvertible and exist in two stable forms, Pr and Pfr (22). Pr preferentially absorbs R (λ_{max} ~ 660 nm) and thereon the attached chromophore undergoes a cis/trans-isomerisation at its D-rings C15-C16 bond (23, 24). Via several short-lived intermediates (25) Pfr (λ_{max} ~ 730 nm) is formed, which is considered the physiologically active form inducing responses. Pfr is converted back to Pr by either absorption of FR or by a thermal process called dark reversion (26). Although the absorption range of Pr is restricted to wavelengths around 660 nm, the absorption spectrum of Pfr overlaps in its whole range with the Pr spectrum (27). Thus Pfr predominantly absorbs wavelengths above 700 nm, but it also sufficiently absorbs R and thereupon reconverts into Pr. Therefore, even under continuous R conditions, a photoequilibrium between Pr and Pfr is established, which directly reflects the light

conditions of the environment, but can never exceed 97% Pfr.
Phytochromes initiate and regulate numerous responses in early plant development. Initially identified as the photoreceptor regulating seed germination and photomorphogenesis (22, 28, 29), phytochromes also regulate light responses of mature plants, such as circadian clock entrainment (30, 31) or flower induction (32). The detection of the light environment also influences growth adaptation of plants: in order to escape shading canopies, reflected by a low Pr:Pfr ratio, plants invest in elongation growth; a response known as shade avoidance (33, 34).
Arabidopsis thaliana possesses 5 phytochromes, PHYA to PHYE (35), which are divided into type I and type II phytochromes (36). Type I phytochromes are classified as light labile and are rapidly degraded upon light absorption. phyA is the only type I phytochrome known. Following Pfr formation, nuclear transport is initiated and shortly thereafter phyA is poly-ubiquitinated by the E3-ligase COP1, thereupon targeted for degradation by the 26S proteasome (37-39). Consequently phyA is mostly abundant in dark adapted tissues, which also matches its predominant function in early seedling development (40). In contrast, phyB and all other phytochromes of *Arabidopsis* belong to the class of light stable phytochromes (type II), which are the dominant phytochromes in green plant tissues and mature plants (36).

1.2.1. Structure and Function

Phytochromes can generally be divided into two modules: a photosensory module comprising approximately the N-terminal half and a C-terminal transmitter module. The photosensory module can be subdivided into three domains, the PAS, GAF and PHY domain (41-43). The chromophore is attached to a conserved cystein residue within the GAF-domain. Whereas both PAS and GAF domains have been identified unequivocally from their primary sequence data the structural nature of the PHY-domain remained elusive for a long time, reflected in its name: “phytochrome specific domain”. X-ray analysis of the crystallised photosensory module of a cyanobacterial phytochrome from *Synechocystis*, Cph1, recently classified the PHY domain as being a GAF-domain (44). Thus phytochromes belong to the group of tandem-GAF proteins, which also comprise phosphodiesterases and adenylate cyclases, known to be essential signal transduction components in animals and working via cyclic mononucleotide signaling (45). It was shown that the PHY domain features a tongue-like protrusion, which, together with the α-helical N-terminal extension, is necessary for sealing the tripartite chromophore pocket. The structural integrity of the photosensory module with a sealed chromophore cavity appears to be essential for proper Pfr formation as it was proposed that shielding the chromophore of the surrounding solvent is necessary for de- and re-protonation reactions involved in the cis/trans-isomerisation implied in Pfr formation (23). Furthermore it was shown that the PAS-GAF bidomain forms a figure-of-eight knot that appears to keep the PAS and GAF domains in spatial proximity and thus might help stabilising the chromophore in the pocket (44, 46, 47). Although differences exist between cyanobacterial and plant phytochromes, the structural features of the photosensory module including the tandem-GAF domain and the light-sensing knot are generally assumed for higher plants too and appear to serve signaling function. Mutations within the knot region of phyB exhibited either reduced photosensing ability or abrogation of signal transduction by inhibiting interaction with the bHLH

transcription factor PIF3 (48, 49). Homologous residues within the putative light sensing knot in phyA appear to be required for binding of PIF1 and FHY1 suggesting a role in phyA downstream signaling and nuclear transport (50).
The C-terminal transmitter module of plant phytochromes comprises two functional domains. The PAS-repeat is situated between the so-called hinge region at the end of the photosensory module and the histidine kinase related domain (HKRD) at the very C-terminus (51, 52). PAS domains are structurally conserved (53) and can function as dimerisation motifs or interaction platforms (54). Whereas bacterial phytochromes work as true histidine kinases in a two component system involving histidine auto-phosphorylation and subsequent phosphotransfer to a response regulator (55), plant phytochromes have lost the conserved histidine residue and rather function as serine/threonine kinases, also mediating autophosphorylation of phytochrome (56). Several phytochrome interacting proteins have been identified to serve as kinase substrates (57): PKS1 (58), PIF3 (59), CRY1/CRY2 (60) and members of the Aux/IAA family (61). However, despite the possibility of phytochrome acting as a kinase, phytochrome's C-terminus appears to be dispensable for downstream signaling. It rather appears to function in dimerisation and localisation, as phyB's photosensory module fused to a dimerisation motif not only enters the nucleus but is also sufficient for complementing the *phyB* phenotype (62).

1.2.2. Localisation

Phytochromes are soluble proteins and localisation studies on higher plant phytochromes phyA and phyB proved cytoplasmic localisation of Pr-phytochrome (63, 64). Interestingly, phytochromes change their localisation upon light detection, as Pfr-phytochromes are transported into the nucleus (65-68). The light quality inducing nuclear translocation is specific to the phytochrome being transported. phyA nuclear transport is most efficiently induced by FR and less efficiently by R, whereas phyB translocates into the nucleus after R perception. Both phyA and phyB differ in terms of their nuclear transport behaviour, kinetics and the associated transport mechanism. phyA accumulates in the nucleus within a few minutes (66) and it was shown that phyA nuclear transport requires the assistance of two adaptor molecules, FHY1 and FHL (69-71).
The kinetics of phyB are much slower compared to phyA and it may take up to two to four hours for phyB nuclear accumulation in continuous R (66, 72). The stringency of phyB:GFP nucleocytoplasmic partitioning differs from phyA nuclear import: although the majority of cells show cytoplasmic phyB in the dark (D), 10 % show nuclear localisation even in D conditions (73). The exact nuclear transport mechanism of phyB remains elusive, although several studies implied a role for the phyB C-terminus in nuclear transport (62, 74). The C-terminal PAS-repeat is thought to harbour a cryptic NLS, which is required for phyB nuclear translocation. In the Pr state the NLS is masked by physical interaction of the GAF-PHY domains with the PAS-repeat. Structural changes resulting from Pfr formation are thought to loosen this interaction and thereby unmask the NLS, hence inducing nuclear translocation of phyB (74). This idea is based on the findings that the C-terminal PAS-repeat is sufficient for nuclear accumulation, whereas the N-terminal photosensory module of phyB alone is unable to enter the nucleus.

1.2.3. Signaling

Consistent with the notion of nuclear localised phytochromes their primary function has been widely accepted as being regulators of gene expression (75). Numerous early target genes of both phyA and phyB have been identified by microarray analysis, the majority being connected to transcription factors: bHLH-family members (PIFs), zinc finger (COL1/2) and bZIP factors (HY5), myb-related transcription factors (CCA1) or pseudo response regulators (APRR3/5/9) (76-78). Both phyA and phyB appear to dominate induction of gene expression under continuous R conditions, whereas FR dependent gene regulation is mediated solely by phyA (77, 79). Only the minority of target genes are repressed by either phyA or phyB. Instead, phyC-E appear to substantially contribute to transcriptional repression (78).
Although phytochrome nuclear accumulation is tightly regulated and appears to play a central role in initial phytochrome signal transduction, a considerable amount of the phyA and phyB phytochrome pool always remains within the cytoplasm. As shown by abrogation of phyA nuclear transport in the *fhl/fhy1*-mutant background several phyA-specific responses were retained (abrogation of gravitropism in B, inhibition of hypocotyl elongation in B and R, enhancement of B induced phototropism) clearly pointing towards a cytoplasmic function of phyA (71, 80). Recently it was shown that phyB (and presumably phyA) control translation of PORA mRNA in the cytoplasm. The cytosolic protein PENTA1 (PNT1) interacts with and recruits phyB (phyA) to the 5' UTR, thereby inhibiting PORA mRNA translation (81). The underlying mechanism however remains elusive; translation inhibition either by steric hindrance or by phytochrome mediated phosphorylation of eukaryotic translation initiation factors are discussed as possible modes of function. As PORA expression is also transcriptionally regulated by phytochrome (82) this additionally points to a dual function of phytochromes; one in the nucleus and another within the cytoplasm.
Despite the identification of numerous nuclear interacting factors of phyA and phyB, nothing is known about possible members of a putative cytoplasmic phytochrome signaling cascade. Although there have been hints on the involvement of Ca^{2+}/calmodulin (83-87) and cGMP based signaling (88), strong evidence for such a signaling mechanism came from microinjection experiments in tomato hypocotyl cells of the phytochrome chromophore mutant *aurea* (89, 90): Expression of *CAB:GUS* and *CHS:GUS* fusion constructs were initiated by injection of either oat phyA, GTPγS, Ca^{2+} or activated calmodulin and were found to induce both anthocyanin synthesis and chloroplast development (91, 92). Additional evidence for the involvement of heterotrimeric G-proteins in phyA signaling emerged from induction of *CHS:GUS* by direct application of cGMP (91). Noteworthy, cAMP did not have positive effects within the same experimental system (91), excluding an adenylate cyclase activity of plant phytochromes. Further evidence on the involvement of G-protein signaling in phytochrome responses were gained by physiological analysis of G-protein subunit deletion mutants: R and FR hypersensitivity of GPA1-overexpressors (93), enhanced FR induced killing in *agb1* (94) and reduced germination rates of *gpa1, agb1* and *gpa1agb1* under both continuous and pulsed R (95). Although a direct involvement of heterotrimeric G-proteins in *Arabidopsis* was questioned due to the absence of a clear hypocotyl inhibition phenotype comparable to that of *phyA* or *phyB* mutants (96), G-protein

function in rapid downstream signaling still appears to be a tempting assumption to explain cytoplasmic phytochrome responses.

Noteworthy, the physiology of phyA responses within the *fhl/fhy1*-mutant are all connected to B sensing, involving participation of either cryptochromes or phototropins. Cryptochromes are nuclear localised (97, 98) and CRY1 is B dependently excluded from the nucleus (99), thus sharing compartmentalisation as a signal transduction step with phytochromes. In contrast, phototropins are plasma membrane associated (100, 101). Generally, directional responses in higher plants are B induced and connected with phototropin signaling. At the same time they are modulated by R. Although B perception induces an internalisation reaction for both phot1 and phot2 resulting in cytoplasmic accumulation (100-102). phot1 membrane association can be retained and prolonged by an R treatment prior to B detection, a phyA-mediated response (103). The phototropism of hypocotyls is fluence-rate dependently controlled by phot1 in low fluence rates and by both phot1 and phot2 in high fluence rates (104-106). In harmony with the involvement of phyA in plasma membrane retention of phot1 is the finding of R enhancement of B phototropism, likewise mediated by phyA and phot1 (107). Moreover, *Arabidopsis* roots show positive phototropic bending under R without simultaneous B application; a response mediated by both phyA and phyB (108, 109). PKS1, a target for phytochrome's kinase activity, is not only a central player in B mediated phototropism in hypocotyl cells but is also essential for R root phototropism (110). Chloroplast photorelocation are orchestrated by phot1 and phot2 with a modulating role of phyB in the inhibition of the high-light avoidance response (111, 112). Thus directional responses in higher plants, although mainly induced by phototropins, appear to require cytoplasmic phytochrome action for modulation of the response.

1.3. Mosses as model systems

Mosses were used as model systems for plant developmental studies over decades. Although mosses are separated from higher plants by approx. 400 millions years of evolution, it is their sole evolutionary position as being the first plants to conquer land which makes them an valuable system to study plant development (113). Their morphological simplicity make mosses ideal objects for any experimental approach on cellular levels but the greatest advantage over current higher plant model organisms result from their accessibility for reverse genetics (114-116). The moss *Physcomitrella* turned out to be efficiently accessible to molecular genetics in terms of gene targeting by homologous recombination (117, 118), allowing for either gene disruption (knockout) or gene introduction (knockin), a feature unique amongst plants. Due to haploidy of the dominant gametophytic phase any genetic change introduced will reveal a resulting phenotype immediately in the next generation of regenerated cells. Crossing of mosses is therefore not necessary to gain homozygous mutant lines, but is still possible by protoplast fusion (119). Two particular mosses have gained specific attention as lower plant model systems, *Physcomitrella patens* and *Ceratodon purpureus*. Both mosses were used for developmental, photobiological and cell-polarity studies during the past 40 years (120-124), as mosses are especially accessible for investigation of directional responses induced by either B or R. However, in the recent past it was *Physcomitrella* which got widely accepted as dominant model system and by the end of 2006 *Physcomitrella's* complete genome was sequenced and available to public by 2007 (125).

1.3.1. Moss phytochromes

Physcomitrella comprises four described phytochrome genes, *PHY1-PHY4* (9). Following release of the genome sequence, *in silico* analysis revealed the existence of three more putative phytochrome sequences, *PHY5a-c*, plus one additional phytochrome-like sequence; all of which have unknown expression profiles and functions. Thus eight putative phytochromes have to be assumed in *Physcomitrella,* twice the number of initially characterised sequences, likely explained by a paleo-ploidisation event millions of years ago (126). Clearly, lower plant phytochromes are evolutionary separated from their higher plant counterparts and group in a different clade from *Arabidopsis* phytochromes, sharing more phylogenetic similarities to liverworts, lycophytes and ferns (9). Despite their evolutionary differences, phytochromes of higher and lower plants are of identical domain organisation and show only minor differences on protein level. Concerning differences at the N-termini of phyA and phyB, with phyB baring a considerably longer N-terminal extension of about 35 amino acids, *Physcomitrella* phytochromes do not possess such an N-terminal extension. Nevertheless, they are functionally more similar to phyB than to phyA: Northern blot analysis indicated a light-dependent expression profile for all of the *Physcomitrella* phytochromes, with *PHY2* and *PHY4* showing light induced expression (9). Western Blot analysis showed that all of the four described phytochromes are light-stable (9), typical for type II phytochromes.

1.3.2. Moss phytochrome physiology

Contrasting the situation in higher plants in which phytochromes are responsible for transcriptional control and phototropins function in directional light sensing, mosses are able to elicit directional light responses through phytochromes. Moreover, the vast majority of described phytochrome mediated responses in mosses not only display light dependency in terms of their initiation but also inherit vectorial character. Both spore germination and protoplast regeneration show directionality with primary chloronemata outgrowth occurring in the direction of light or perpendicular to the electrical vector (E-vector) of polarised red light (R_{pol}) (120, 127). Similarly, protonemal tip cells grow photo- and polarotropically according to either unilateral or polarised R (123, 124, 128). All of the described responses also share strong fluence rate dependency. This is manifested quantitatively in the case of spore germination and protoplast regeneration (120, 129-132), but can also be seen in protonematal tip cell bending in a qualitative manner. Low fluence rates (< 0.5 µmol · m^{-2} · s^{-1}) as well as fluence rates higher than 5 µmol · m^{-2} · s^{-1} lead to negative phototropism, whereas medium fluence rates (1.0 - 2.5 µmol · m^{-2} · s^{-1}) induce positive phototropism (9). Exposure to R_{pol} induces perpendicular growth to the orientation of the E-vector (9, 133, 134). Physiological analyses of *Physcomitrella* phytochrome knockout lines have identified phy4 as the phytochrome to predominantly mediate directional light sensing in *Physcomitrella,* as dark adapted *phy4*$^{-}$ protonemata tip cells retained negative phototropic responses while losing polarotropic and positive phototropic responses.
Directional responses of lower plants can also be induced by B. Inhibition of gravitropism in *Ceratodon* filaments is inhibited by R, but inverted by B, as shown by class 2 mutant lines, which are specifically defective in phototropic responses (135,

136). Chloroplast avoidance and accumulation responses in *Physcomitrella* are inducible by both high and low fluence rates of B and were shown to be processed by phototropins, as is the case in *Arabidopsis* (8, 104, 137). At the same time these responses can be induced by R in a phytochrome dependent manner (8, 138). Positioning of side branch formation is induced and enhanced by both B and R (139, 140) and cryptochromes and phototropins are involved in B induced side branch positioning (141-143). Phytochromes were implied in processing the R enhancement of B responses (142). Although it remains unclear how exactly phytochrome integrates into these B responses, both phototropins and phytochromes were proposed to mediate side branch positioning as cytoplasmically localised photoreceptors via action dichroism (142) (see 1.3.4).

1.3.3. The paradox of phytochrome directional light sensing

Although unquestionable in its existence, phytochrome mediated regulation of directional and vectorial responses, as evident in *Physcomitrella*, are in strong disagreement with the observed functional and molecular characteristics of higher plant phytochromes. As is described in detail in *Arabidopsis*, phytochromes are soluble proteins which translocate light dependently into the nucleus. There they interact mostly with transcription factors, regulating expression of downstream target genes involved in complex responses such as photomorphogenesis. This notion of phytochrome function is in its exclusivity simply incompatible with the transduction of directional and / or vectorial cues, as this information necessarily gets lost at every of the subsequent steps underlying transcriptional regulation: nuclear translocation of the photoreceptor, interaction with downstream signaling components, initiation or repression of transcription, cytoplasmic translocation of the resulting mRNA and finally ribosomal translation of the gene product. However, nuclear localisation of *Physcomitrella* remains unclear at this point and an interaction with described transcription factors as found in *Arabidopsis* has not been established. In higher plants, numerous phytochrome-mediated responses are known, which occur too quickly to be explained by transcriptional regulation. Changes of ion fluxes within the pulvini of *Salmanea* leafs are detectable within 2 min (144), alterations of the surface potential of *Hordeum* coleoptiles occur within 30 sec following an R pulse (145). The fastest phytochrome response reported is the local stimulation of cytoplasmic streaming in the water plant *Vallisneria* measurable with 2.5 sec (146). Meanwhile, nuclear translocation of both phyA and phyB requires essentially more time (66, 68) and is not detectable earlier than 20 min after light treatment even in the case of phyA. Therefore, also in higher plants a cytoplasmic signaling route might exist, which is much more prominent in *Physcomitrella*, but both might share a common mechanism.

1.3.4. Directional light sensing and the Jaffe/Etzold/Haupt hypothesis

Phytochrome directional responses are explainable by formation of a Pfr gradient reflecting the light gradient established within the cell (147). Irradiation of the cell under continuous light will rapidly lead to a homogenous illumination of the whole cell, thus no light gradient will be formed. But given the free movement of both Pfr and Pr molecules, a cytoplasmic Pfr gradient could be principally maintained even

under continuous illumination, due to constant movement of the photoreceptor molecules and photocycling between Pr and Pfr under continuous R. However, many of the R induced directional responses described are inducible by light pulses rather than continuous illumination. Under pulsed light conditions, however, a cytoplasmic gradient is less likely formed among soluble molecules, as R absorption quickly forms Pfr, but the R induced Pfr conversion into Pr is not as efficient. Consequently, Pfr molecules formed upon a light pulse will eventually diffuse throughout the cell and may not be reconverted by a subsequent light pulse. In the mean time, Pfr molecules may undergo dark conversion, additionally contributing to the loss of a local Pfr-Pr gradient. Consequently, a Pfr gradient cannot be formed by a soluble, freely floating phytochrome molecule pool under pulsed light conditions, thereby neglecting the possibility of directional responses under pulsed light conditions.

Adding to the problem of local Pfr gradient formation, polarotropic responses require anisotropic photoreceptors for detection of the vibrational plane of the E-vector (147). Light absorption by dichroic photoreceptors occurs under preferred E-vector orientation in dependence of the dipole moment of the chromophore: Parallel orientation of the E-vector to the transition dipole moment of the chromophore results in a high probability of light absorption, the opposite effect is the case for perpendicular orientation. To account for these spectral prerequisites, the Jaffe/Etzold/Haupt model postulates a plasma membrane attachment for phytochromes. The transition dipole moments of Pr molecules are thought to be oriented parallel to the cell surface while those of Pfr molecules are oriented perpendicularly, due to 90° rotation upon isomerisation (128, 148-150). Hence, the cis/trans-isomerisation of the chromophore following light absorption (flip-flop-dichroism (151-153)) allows for the establishment of a tetrapolar gradient of activated photoreceptors within a cylindrical protonemata cell. Plasma membrane association of phytochrome as proposed could also enable formation and maintenance of a Pfr-Pr gradient under both continuous and pulsed light conditions.

Intriguingly, the specifications of chloroplast movement responses in both B and R in *Physcomitrella* are comparable to the responses observed in *Mougeotia scalaris* (149), *Mesotaenium caldariorum* (154) and *Adiantum capillus-veneris* (150). However, they are fundamentally different on a molecular level. In both the green algae *Mougeotia* and the fern *Adiantum* a novel type of convergently evolved photoreceptor could be identified, which appears to be responsible for the characteristic directional responses in R and B (12). Neochromes are made up of a phytochrome photosensory module fused to a full-length phototropin module. As phototropins are indeed localised to the plasma membrane through a yet unidentified mechanism, such an arrangement would simultaneously explain the required action dichroism as well as R and B responsiveness. Although experimental attempts were undertaken to prove plasma membrane attachment (155, 156), phytochrome membrane association was never unequivocally shown. Furthermore, phytochromes do not show inherent characteristics of hydrophobic attachments or transmembrane domains (157, 158). However, such a direct or indirect interaction between phototropins and phytochromes, which could principally explain the observed dichroism in mosses, has never been shown, neither in higher nor in lower plants.

Anisotropic phytochrome arrangement could principally also be achieved by

association with other cellular structures. Studies with cytoskeleton inhibitors revealed phototropic bending of *Ceratodon* tip cells to be dependent on re-orientation of actin filaments (159, 160). Additional evidence on cytoskeletal involvement came from physiological analysis of *Physcomitrella* knockout lines lacking subunits of the ARP2/3-complex. Those cells are disrupted in polymerisation of actin filaments and not only show severe defects in protoplast regeneration and polar tip growth but are also compromised in their response towards polarised light (161). Chloroplast photomovements in *Physcomitrella* were recently shown to involve formation of specific thin and short actin filaments between the chloroplasts and the plasma membrane (162). Chloroplast positioning in *Arabidopsis* is likewise connected to the cytoskeleton, as chloroplasts movements are mediated along actin filaments by interaction with CHUP1 (163, 164) and also involve formation of chloroplast-specific actin filaments (cp-actin) for chloroplast positioning (165). Interestingly, even the formation of cp-actin filaments appears to be light-dependent, with an involvement of phototropins, and is independently regulated from the actual chloroplast movement (166). Although a direct association of phytochrome to actin filaments could not be drawn from these observations, a close connection between directional light sensing of phytochromes and the mediation of directional responses by cytoskeletal filaments in both higher and lower plants is likely.

1.3.5. Physiology & Signaling

As in seed plants, light affects moss development throughout its whole life cycle (131). Spore germination in *Physcomitrella* is induced by either B or R, the effect being reversed by subsequent FR, thus classifying R induced spore germination as a phytochrome response (130, 131). Likewise, regeneration of protoplasts was shown to be light-dependent on R or B, with B being more efficient than R (122). Side branch formation is also induced and enhanced by both B and R respectively, with an involvement of both cryptochrome and phytochrome, at least partially requiring both photoreceptors to be nuclear localised (142, 143). Likewise, the transition of a side-branch initial cell into a bud-precursor cell is cryptochrome inhibited in B and phytochrome induced in R (141). Light and hormone signals are also tightly connected in photomorphogenic processes of higher plants (167). Hormone levels are integrated by light either via the phytochrome or the cryptochrome pathway, both culminating in the regulation of HY5, a central integrator of auxin, GA and ABA signaling, by the COP1 (+SPA1) degradation pathway (168-171).

Although an involvement of phytochrome in the developmental processes described above is apparent, almost nothing is known about phytochrome nuclear function in lower plants. Although nuclear localisation of *Physcomitrella* phytochrome appears to be required for side branch formation (142), it has not been reported so far. Instead, *Physcomitrella* phytochromes were repeatedly reported to be cytoplasmically localised, matching a role in directional light sensing (9, 172).

Recently, nuclear phytochrome functions and localisations in lower plants became of interest. Nuclear translocation of *Adiantum* phytochrome 2 was observed after partial spore-irradiation with R, inducing germination of imbibed *Adiantum* spores (173). Homologs of the bZIP transcription factor HY5 were identified in *Physcomitrella*, *Pp.HY5a* and *Pp.HY5b*. However, as double knockouts of *hy5ahy5b*

displayed disturbed protrusion of caulonema cells in both light and dark conditions (174), it remains unclear how Pp.HY5 is integrated into a light signaling pathway in *Physcomitrella.*

1.4. Aims

Although phytochromes are accepted to primarily function by regulation of gene expression within the nucleus, cytoplasmic functions of phytochromes in both higher and lower plants have been described (71, 80, 81). Such cytoplasmic phytochrome responses appear to be often, but not exclusively connected with directional light sensing. In higher plants this might happen through sensitizing B responsiveness of phototropins, but in lower plants it appears to be even tighter and more directly linked, manifesting phototropism and polarotropism in R.
This work aims at the elucidation of cytoplasmic phytochrome function, especially in regard to R mediated directional light sensing. The role of *Physcomitrella* phy4 and its signaling mechanism in these responses is of particular interest.

(i) phy4 was shown to be the predominant phytochrome in *Physcomitrella* responsible for directional R sensing (9). To consolidate this role of phy4, a transient phenotypic rescue by overexpression of PHY4:YFP in the *phy4*$^{-}$ knockout background was addressed, additionally confirming phy4:YFP as a functional photoreceptor to be used in further localisation studies.

(ii) Although higher plants light-dependent phytochrome localisation has been studied extensively, nothing is known about lower plants photoreceptor localisation. As earlier studies implied that the configuration of fluorescent fusions to phytochrome is crucial for its function, both N- and C-terminal fusions where employed for localisation studies of phy4. Being of outstanding interest, localisation studies on *Physcomitrella* phototropins photA1-photB2 was approached similarly.

(iii) Directional light sensing of lower plants appears to necessitate a fast acting, cytoplasmic signaling system, possibly connected to a fixed or plasma membrane associated phytochrome pool. To identify components of this yet unknown signaling cascade, a *Physcomitrella* cDNA library was screened for interacting proteins of phy4. Also, a second Y2H system should be established, which enables holo-phy4 assembly and therefore characterisation of putative light-dependent interactions revealed by Y2H screening.

(iv) *In vivo* interaction of eventually identified phy4 interacting proteins should be confirmed with a bimolecular fluorescence complementation (BiFC) assay using sYFP-methods.

(v) B signaling is implied to play a fundamental role in higher plant directional light perception and to be tightly connected to R directional responses in lower plants (8, 175). In order to elucidate this R / B connection in perception and signaling a direct interaction between phytochrome and phototropin photoreceptors in both higher and lower plants was investigated.

2. Material

2.1. Organisms

2.1.1. *Escherichia coli*

DB3.1
TOP10
TOP10F'
XL1Blue

2.1.2. *Saccharomyces cerevisae*

AH109
Y187

2.1.3. *Physcomitrella patens*

WT Gransden 2004	
phy4	(9)
photA2/photB1	(8)
photB1/photB2	(8)
photA2/photB1/photB2	(8)

2.1.4. Other plants

Allium cepa

2.2. Buffer and solutions

If not stated otherwise, purified water of millipore-grade was used for all experiments.

2.2.1. For RNA methods

<u>10 x MOPS buffer</u>
200 mM MOPS (pH 7.0)
50 mM Sodium acetate
5 mM EDTA (pH 8.0)
filled up with DEPC-H_2O

<u>RNA agarose gels</u>
1.2 % (w/v) Agarose
1 x MOPS buffer
filled up with H_2O
boiled up
plus 5% Formaldehyde

<u>3 x RNA loading dye</u>
1.5 ml Formaldehyde
5 ml Formamide
1 ml MOPS buffer [10 x]
10 µl EtBr stock solution
ad 10 ml with H_2O

<u>EtBr stock solution</u>
20 mg/ml Ethidium bromide
dissolved in H_2O

2.2.2. For DNA methods

Agarose gel electrophoresis

5 x TBE buffer
500 mM Tris
425 mM Boric acid
50 mM EDTA (pH 8.0)

Agarose gel
0.8 – 1.2 % (w/v) Agarose
in 0.5 % TBE buffer
boiled up

EtBr staining solution
1 : 20,000 EtBr
in 0.5 % TBE buffer

6 x loading dye
0.03 % (w/v) Bromophenol blue
0.03 % (w/v) Xylene blue
60 % (v/v) Glycerol
60 mM EDTA
10 mM Tris

DNA ladder
100 bp / 1 kb marker from NEB
diluted in 6 x loading dye (1 : 4)

Plasmid DNA Maxi preparation

STE
0.1 M NaCl
10 mM Tris/HCl (pH 8.0)
1 mM EDTA (pH 8.0)
5 % (v/v) Triton X100
stored at 4 °C

Solution I
50 mM Glucose monohydrate
25 mM Tris/HCl (pH 8.0)
10 mM EDTA (pH 8.0)
stored at 4 °C

Solution II
200 mM NaOH
1% SDS (v/v) (from 10 % stock)
prepared fresh on the day of use

Solution III
3 M Potassium acetate
11.5 % (v/v) Acetic acid
stored at 4 °C

Lysozyme solution
1 mg/ml Lysozyme
10 mM Tris/HCl (pH 8.0)
prepared fresh on the day of use

TE buffer
20 mM Tris/HCl (pH 8.0)
1 mM EDTA (pH 8.0)

RNAse solution
2 µg/ml RNAaseA
in 20 mM TE-buffer

Proteinase K solution
20 mg/ml Proteinase K
in 20 mM TE-buffer

PEG/NaCL
13 % PEG 8000
1.6 M NaCl
dissolved in H_2O

Sodium acetate
3 M Sodium acetate
pH 5.2 – 5.8 (with acetic acid)

Ethanol
pure, stored at 4 °C or -20 °C

Isopropyl alcohol
pure, stored at -20 °C

2.2.3. For protein methods

SDS-PAGE

2 x Lämmli-buffer
4 ml SDS-solution [10 %]
2 ml Glycerol
2.5 ml DTT [1 M]
1.2 ml Tris/HCl [1 M] (pH 6.8)
0.09 % (w/v) Bromophenol blue
ad 10 ml with H_2O
500 µl β-mercaptoethanol

SDS-PAGE running buffer
25 mM Tris
192 mM Glycine
0.1 % (w/v) SDS

10 % APS
10 % (w/v) Ammonium persulphate
dissolved in H_2O

Acrylamide solution
30 % Acrylamide 4 K solution
(37,5:1 Acrylamide:Bis-Arylamide)

Buffer of the separating gel (4x)
1.5 M Tris/HCl (pH 8.8)
0.6 % (w/v) SDS

Buffer of the stacking gel (4x)
0.5 M Tris/HCl (pH 6.8)
0.6 % (w/v) SDS

Separating gel (10 %)
5 ml Acrylamide solution
3.75 ml Buffer (separating gel)
6.25 ml H_2O
90 µl APS [10 %]
15 µl TEMED

Stacking gel (4 %)
650 µl Acrylamide solution
1.25 ml Buffer (stacking gel)
3.1 ml H_2O
25 µl APS [10 %]
5 µl TEMED

Coomassie Stain

Hot Coomassie solution
0.5 % (w/v) Coomassie brilliant blue R250
25 % (v/v) Isopropoanol
10 % (v/v) Acetic acid

Destain solution
10 % Acetic acid

Western Blots

Washing buffer
10 mM Tris/HCl (pH 7.4)
0.05 % (v/v) Tween 20
0.9 % (w/v) NaCl

Blocking buffer
5 % (w/v) Skimmed milk powder dissolved in washing buffer

Blotting buffer
2.5 mM Tris
150 mM Glycin
pH 8.3
20 % (v/v) Methanol

Detection buffer
100 mM Tris/HCl (pH 9.5)
150 mM NaCl

NBT stock solution
50 mg/ml NBT
dissolved in dimethylformamide (DMF)

BCIP stock solution
50 mg/ml BCIP
dissolve in H_2O

NBT/BCIP solution
17.5 µl BCIP stock solution
34 µl NBT stock solution
ad 5 ml with detection buffer

2.2.4. For bacterial methods

Cultivation of bacteria

Liquid LB medium
1 % (w/v)Tryptone
0.5 % (w/v) Yeast extract
10 mM NaCl
pH 7.5

TB buffer
12.54 g (0.72 M) K_2HPO_4
2.31 g (0.17 M) KH_2PO_4
ad 100 ml with H_2O
pH 7.4
sterilised by autoclaving

Liquid TB medium
12 g Tryptone
24 g Yeast extract
4 g Glycerol
ad 900 ml with H_2O
sterilised by autoclaving
plus 100 ml TB buffer immediately before use

Preparation of electro-competent cells

H_2O
sterilised by autoclaving
cold (on ice)

DMSO
7 % (v/v) Dimethyl sulfoxide (DMSO) in H_2O

Transformation of bacteria

LB + $MgSO_4$
1 % (w/v) Tryptone
0.5 % (w/v) Yeast extract
10 mM NaCl
1 mM $MgSO_4$
pH 7.5

Selection media for *E. coli*
Liquid LB medium
1.5 % (w/v) Agar
Antibiotics and/or IPTG/X-Gal as indicated

IPTG stock solution
100 mM IPTG
sterilised by filtration
diluted 1:500

SOC medium
2 % (w/v) Tryptone
0.5 % (w/v) Yeast extract
10 mM NaCl
2.5 mM KCl
10 mM $MgCl_2$
20 mM $MgSO_4$
20 mM Glucose
sterilised by filtration

X-Gal stock solution
20 mg/ml X-β-Gal
sterilised by filtration
diluted 1:1000

2.2.5. For yeast methods

Cultivation of yeast

Liquid YPDA medium
10 g Yeast extract
20 g Tryptone
ad 885 ml with H_2O
sterilised by autoclaving
100 ml Glucose stock solution
(2 % final conc.)
15 ml Adenine stock solution
(0.003 % final conc.)

Glucose stock solution
20 % (w/v) glucose monohydrate
dissolved in H_2O
sterilised by filtration
stored at 4 °C

Adenine stock solution
0.2 % (w/v) Adenosine hemisulfate
dissolved in H_2O
sterilised by filtration
stored at 4 °C

Solid YPDA medium
Liquid YPDA medium
1.5 % (w/v) Agar
sterilised by autoclaving
100 ml Glucose [20 %]
15 ml Adenine stock

Transformation of yeast

1 M LiAc
1 M Lithium acetate
pH 8.4 – 8.9
sterilised by filtration

100 mM LiAc
100 mM Lithium acetate
pH 8.4 – 8.9
sterilised by filtration

Salmon sperm DNA
2 mg/ml sonicated salmon sperm DNA
denatured 5 min at 100 °C
stored at -20 °C

PEG solution
50 g PEG 3550
dissolved in H_2O
ad 100 ml with H_2O
sterilised by autoclaving

H_2O
Autoclaved H_2O
cold

Transformation mix
240 µl PEG solution
50 µl single-stranded
salmon sperm DNA
36 µl 1 M LiAc
x µl plasmid DNA
34 µl H_2O – x µl plasmid DNA

Selection media

Dropout supplements (Clontech)
SDO : 0.74 g/l -Trp
SDO : 0.69 g/l -Leu
DDO: 0.64 g /l -Trp/-Leu
TDO : 0.62 g/l -Trp/-Leu/-His
QDO : 0.60 g/l -Trp/-Leu/-His/-Ade

3-AT stock solution
1 M 3-Amino-1,2,4-triazole
sterilised by filtration
stored at -20 °C

Liquid dropout medium
6.7 g Yeast nitrogen base (DIFCO)
Dropout supplement (Clontech)
dissolved in H_2O
pH 5.8 (NaOH)
ad 900 ml H_2O
sterilised by autoclaving
100 ml Glucose stock solution
if indicated, supplemented with
0.5 mM – 2.5 mM 3-AT
30 µM PCB

Solid dropout medium
Liquid dropout medium
1.5 % (w/v) Agar
sterilised by autoclaving
100 ml Glucose stock solution
if indicated supplemented with
0.5 mM – 2.5 mM 3-AT
20 mg Xα-Gal
30 µM PCB

10 x Leucine
1000 mg L-Leucine
dissolved in H_2O
sterilised by filtration
stored at 4 °C

10 x Tryptophan
200 mg L-Tryptophan
dissolved in H_2O
sterilised by filtration
stored at 4 °C

-Trp/-His dropout medium
6.7 g Yeast nitrogen base (DIFCO)
0.62 g -Trp/-Leu/-His DO supplement
dissolved in H_2O
pH 5.8 (NaOH)
ad 800 ml H_2O
sterilised by autoclaving
100 ml Glucose stock solution
100 ml Leucine stock solution
if indicated, supplemented with
0.5 mM – 2.5 mM 3-AT

X-α-Gal stock solution
10 mg/ml 5-Bromo-4-chloro-3-indoxyl-α-D-galactopyranosid
dissolved in DMF
sterilised by filtration
stored lightproof at -20 °C

-Leu/-His dropout medium
6.7 g Yeast nitrogen base (DIFCO)
0.62 g -Trp/-Leu/-His DO supplement
dissolved in H_2O
pH 5.8 (NaOH)
ad 800 ml H_2O
sterilised by autoclaving
100 ml Glucose stock solution
100 ml Tryptophan stock solution [10 x]
if indicated, supplemented with
0.5 mM – 2.5 mM 3-AT

PCB preparation from *Spirulina*

Cyanobacteria buffer
100 mM KPO_4 buffer
5 mM EDTA
pH 7.0

Spirulina
Tamil Nadu, article no. 1240
Green Valley, N*aturprodukte* GmbH, Berlin, Germany

ONPG assay

Liquid DDO medium
6.7 g Yeast nitrogen base (DIFCO)
0.64 g -Trp/-Leu DO supplement
dissolved in H_2O
pH 5.8 (NaOH)
ad 900 ml H_2O
sterilised by autoclaving
100 ml glucose stock solution
30 µM PCB

Z-buffer
16.1 g Na_2HPO_4
5.50 g NaH_2PO_4
0.75 g KCl
0.25 g $MgSO_4$
dissolved in H_2O
pH 7.0
sterilised by autoclaving

Z buffer + β-mercaptoethanol
100 ml Z- buffer
0.27 ml β-mercaptoethanol
prepared freshly

o-nitrophenyl-β-D-galactopyranoside
4 mg/ml ONPG (Sigma)
dissolved in Z buffer (1-2 h, vortex)
pH 7.0
prepared freshly

1M Na_2CO_3
1M Na_2CO_3
dissolved in H_2O

DNA extraction from yeast

Zymolase stock solution (60 U/ml)
10 mg/ml Zymolase from *Arthrobacter* (Sigma)
dissolved in H_2O
stored at -20 °C

Zymolase solution
100 µl zymolase stock solution
ad 1 ml with H_2O
prepared freshly

Protein extraction from yeast

NaOH solution
200 mM NaOH
dissolved in H_2O
stored on ice
prepared freshly

2.2.6. For plant methods

Moss cultivation

Media for moss cultivation were optimised by Hughes and Cove and are based recipes from (119, 176).

Solution B (100 x)
100 mM $MgSO_4$
dissolve in H_2O
stored at 4 °C

Solution C (100 x)
180 mM KH_2PO_4
dissolved in H_2O
stored at 4 °C
pH 6.5

Solution D (100x)
1 M KNO_3
45 mM $FeSO_4 \cdot 7\ H_2O$
dissolved in H_2O
stored at 4 °C

Solution E (100 x)
1 M KNO_3
1.4 mM $Fe(III)C_6H_5O_7$
dissolved in H_2O
stored at 4 °C

Solution Ca (100 x)
200 mM $CaCl_2 \cdot 2\ H_2O$
dissolved in H_2O
stored at 4 °C

Solution N (100 x)
500 mM Di-ammonium tartrate ($C_4H_{12}N_2O_6$)
dissolved in H_2O
stored at 4 °C

Solid BCE225 medium
liquid BCE225 medium
0.8 % (w/v) agar
if indicated:
supplemented with antibiotics
overlaid with cellophane foil

3er medium
1 mM KNO_3
0.1 mM $CaCl_2$
1 mM KH_2HPO_4
40 µM $MgSO_4$
10 µm $Fe(III)C_6H_5O_7$
1 x Hoagland's trace elements
27 mM glucose
0.3 % (w/v) Yeast extract
1.2 % Agar
sterilised by autoclaving

Hoagland's trace elemens (1000 x)
9.93 mM H_3BO_3
0.23 mM $AlK(SO_4)_2 \cdot 12\ H_2O$
0.22 mM $CuSO_4 \cdot 5\ H_2O$
0.24 mM KBr
0.66 mM LiCl
0.10 mM $Na_2MoO_4 \cdot 2\ H_2O$
1.97 mM $MnCl_2 \cdot 4\ H_2O$
0.23 mM $CoCl_2 \cdot 6\ H_2O$
0.19 mM $ZnSO_4 \cdot 7\ H_2O$
0.17 mM KI
0.12 mM $SnCl_2 \cdot 2\ H_2O$
0.25 mM $NiCl_2 \cdot 6\ H_2O$
dissolved in H_2O
stored at 4 °C

Liquid BCE225 medium (800 ml)
8 ml solution B
8 ml solution C
8 ml solution E
800 µl Hoagland's trace elements
0.2 % (w/v) $C_6H_{12}O_6$
dissolved in H_2O
ad 784 ml with H_2O
sterilised by autoclaving
added through sterile filter:
8 ml solution Ca (100 x)
8 ml solution N (100 x)

Protoplast isolation & transformation

Mannitol solution
8 % (w/v) D-mannitol
dissolved in H_2O
sterilised by autoclaving
stored at 4 °C

Driselase stock solution
2 % (w/v) Driselase from *Basidiomycota* (Sigma)
dissolved in mannitol solution
sterilised by filtration
stored at -20 °C

Driselase solution
0.5 % Driselase (from stock solution)
diluted with mannitol solution
prepared freshly, kept on ice

$Ca(NO_3)_2$ stock solution (10 x)
1 M $Ca(NO_3)_2$
dissolved in H_2O
sterilised by filtration
stored at 4 °C

Tris buffer (10 x)
100 mM Tris (pH 8.0)
dissolved in H_2O
sterilised by filtration

3 M solution
5.05 mM D-mannitol
15.15 mM $MgCl_2$
0.1 % (v/v) MES solution (pH 5.6)
sterilised by filtration

PEGT solution
2 g PEG 6000
melt in waterbath
1 ml mannitol solution
10 µl $Ca(NO_3)_2$ stock solution
10 µl Tris buffer (pH 8.0)
mixed by vigorous vortexing
prepared fresh
(2 h prior transformation)

Protoplast regeneration

Overnight regeneration medium
1x solution B
1x solution C
1x solution D
10 mM $CaCl_2$
0.2 % (w/v) Glucose
sterilised by autoclaving
5 mM Di-ammonium tartrate
8 % (w/v) D-mannitol

Top layer
1x solution B
1x solution C
1x solution D
8 % (w/v) D-mannitol
0.2 % (w/v) Glucose
0.4 % (w/v) Agar
sterilised by autoclaving
10 mM $CaCl_2$
5 mM Di-ammonium tartrate

Bottom layer
1x solution B
1x solution C
1x solution D
8 % (w/v) D-mannitol
1 x Hoagland's trace elements
0.2 % (w/v) Glucose
0.8 % (w/v) Agar
sterilised by autoclaving
10 mM $CaCl_2$
5 mM Di-ammonium tartrate
overlaid with cellophane foil

Transient transformation by particle inflow gun

Solid BCE225 + Mannitol
BCE225 medium
0.2 M D-mannitol
0.8 % (w/v) agar
dissolved in H_2O
sterilised by autoclaving

50 % glycerol
50 % (v/v) glycerol
in H_2O
sterilised by autoclaving

$CaCl_2$
2.5 M $CaCl_2$
dissolved in H_2O
sterilised by filtration
stored at 4 °C

Spermidine stock solution (10 x)
1 M spermidine (Sigma)
dissolved in H_2O
sterilised by filtration
stored at -20 °C

Ethanol
pure, store at RT

Spermidine solution
100 mM spermidine
diluted from stock solution with sterile H_2O

Particle suspension
Spherical gold particles, 1.6 µm (InBio Gold, Eltham, Australia) or
Tungsten beads M17, 1.1 µm (BioRad)
washed with ethanol
stored in ethanol suspension at 4 °C

2.3. Oligonucleotides and vectors

2.3.1. Oligonucleotides

Table 1: Oligonucleotides used for cloning purposes

Name	Sequence	Description
KJ 16	GGGCTCGGCCTGACCGGCCTTTTTTTTTTTTTTTTT	r/v oligodT for cDNA synthesis of full-length Phy4 CDS
KJ 17	CATATGATGTCGACCACCAAGTTGGCA	f/w Phy4 5' full length cDNA + NdeI header
KJ 27	GCATGCAAAGAGGGGGTTTG	r/v Sequencing SphI site of Phy4
KJ 28	CAAGCTCCTCAGGAAGTCCC	r/v Phy4 sequencing -300 from M13
KJ 29	TCGGCAACACATAAGTTGCATTC	r/v Phy4 sequencing
KJ 30	TCCAGTTGGAGAAGCCATGG	f/w Phy4 sequencing
KJ 31	CCCATGTATTGCGCATGGCA	r/v Phy4 sequencing
KJ 39	ATGAAGCTACTGTCTTCTATCG	f/w GAL4 BD 5' end
KJ 41	GCATACAATCAACTCCAAGC	f/w sequencing of pGADT7 fusions, end of ADH1 promoter
KJ 43	CCACTATCCTTCGCAAGACC	f/w 35S promoter sequencing
KJ 44	CCCGGGCTATCTCACACTGCCTGCATC	r/v 3´Phy4 terminal partial + SmaI header
KJ 50	ATTGTTCTCGTTCCCTTTC	f/w GAL4 BD sequencing
KJ 59	GAGTCCAAGCTCAGCTAA	r/v sequencing primer starting in ADH1 terminator
KJ 60	CTATTCGATGATGAAGATACCCCACCAAACC	f/w 5' AD Y2H-Insert Screening Oligo
KJ 61	GTGAACTTGCGGGGTTTTTCAGTATCTACGATT	r/v 3' AD Y2H-Insert Screening Oligo
KJ 62	CTATTCGATGATGAAGATACCCCAC	f/w like KJ 60, lower Tan
KJ 63	GTGAACTTGCGGGGTTTTTCAGTAT	r/v like KJ 60, lower Tan
KJ 65	CATATGTCGACCACCAAGTTGGC	f/w Phy4 FL 5' 1/2 of NdeI site, pBRIDGE_C
KJ 67	GAGCTCATGTCGACCACCAAGTTGGCAT	f/w Phy4_FL 5' + SacI header. Cloning in pBRIDGE_C
KJ 68	TTAATTAATCTCACACTGCCTGCATCATCT	r/v Phy4_FL 3' + PacI header. Cloning in pBRIDGE_C
KJ 69	TTAATTAAGCCCTGGAGCTTTAAGTCGTT	r/v Phy4_N 3' + PacI header. Cloning in pBRIDGE_C
KJ 70	GAGCTCATGGGCATGGATGAACTCAGTAC	f/w Phy4_C 5' + SacI header. Cloning in pBRIDGE_C
KJ 76	TAATACGACTCACTATAGGG	f/w Y2H Sequencing primer T7 promoter
KJ 77	AGATGGTGCACGATGCACAG	r/v Y2H Sequencing primer
KJ 78	CTGCACAATATTTCAAGCTATACCAAGC	f/w ADH 1 promoter
KJ 79	CTTGTTCGATAGAAGACAGTAGCTTCAT	r/v Gal4 BD
KJ 80	AATGCTTTTATATCCTGTAAAG	r/v GAL4 BD sequencing primer
KJ 81	GAATTCATGTCGTTTGATTCCACGTTTGGA	f/w PHOTA1 + EcoRI header, in pGADT7
KJ 82	ATCGATTAAAAAGTGTCACCGAAATTCGAG	r/v PHOTA1 + ClaI header, in pGADT7
KJ 84	ATCGATCAAAAAGTATCATTGAACGTTGAGTC	r/v PHOTA2 + ClaI header, in pGADT7
KJ 86	GGATCCTAGAAAACATCGGACGTAAATGTG	r/v PHOTB2 + BamHI header, pGADT7
KJ 88	GAGCTCCAGAATTCCTGAAATGTGGAAATAG	r/v PHOTB1 +SacI header, in pGADT7
KJ 90	GAGCTCCACTTCTTCTTCGCAGCGG	r/v EF1alpha + SacI header, in pGADT7
KJ 92	GAGCTCCACGGGTATCCGTCATCCTG	r/v ZFprotein + SacI header, in pGADT7
KJ 93	GAATTCATGGGTAGCGTTCCCGCTG	f/w Pirin + EcoRI header, in pGADT7
KJ 94	ATCGATTATGGTGTGGACTGGGCCTTG	r/v Pirin + ClaI header, in pGADT7
KJ 95	ATCGATATGCCGGCCTCGGGGGGA	f/w PRL + ClaI header, in pGADT7
KJ 96	GAGCTCTAGAACCGGCGCATGTCCTTCG	r/v PRL + SacI header, in pGADT7
KJ 100	GTAGGCAGCGTCATCGACAC	r/v PHOTB1 5' end sequencing

KJ 101	CACAGGTACCTCCTCTGAC	r/v PHOTA2 5' end sequencing
KJ 102	CATTGTGAAGAATCCCGCACTC	r/v PHOTA1 5' sequencing
KJ 105	ATCTACCAGGAGTGGCA	f/w sequencing PHOTB2
KJ 106	TCTATCGACGTTCCAACAG	f/w sequencing PHOTB2
KJ 107	ACTATGAGGAACGGCC	f/w sequencing PHOTB2
KJ 108	GAGTGCGGGATTCTTCA	f/w sequencing PHOTA1
KJ 109	ATTCTGCAAGGTTCTACG	f/w sequencing PHOTA1
KJ 110	TGACGAGTTCTTGGAATTG	f/w sequencing PHOTA2
KJ 111	TTCGTCGACCTCTCGATCATG	r/v EF1alpha 5' end sequencing
KJ 112	GACCTGTTTGTCATCACCAGCT	r/v PRL1 5' end sequencing
KJ 113	ATCGATTAATGGGTAAGGAGAAGGTGCAC	f/w EF1alpha + ClaI header, in pGADT7
KJ 114	ATCGATTAATGGTGGAAAAGAATGCATCTAGG	f/w ZFprotein + ClaI header, in pGADT7
KJ 116	ATCGATTAATGGACGAATTTGGGAGAGTG	f/w PHOTA2 + ClaI header, in pGADT7
KJ 117	ATCGATTAATGGAGGAGCAGGATCCCG	f/w PHOTB1 + ClaI header, in pGADT7
KJ 118	GGATCCTAATGGAGGGTCTGAATCCTATTTCC	f/w PHOTB2 + BamHI header, in pGADT7
KJ 119	ATCGATGTATGCCGGCCTCGGGGG	f/w PRL1 + ClaI header, in pGADT7
KJ 127	ATGTCGACCACCAAGTTGGCA	f/w Phy4 FL cloning in pCR8/GW/TOPO
KJ 128	CTATCTCACACTGCCTGCATC	r/v Phy4 FL w/ Stopp in pCR8/GW/TOPO
KJ 129	TCTCACACTGCCTGCATCATC	r/v Phy4 FL w/o stopp in pCR8/GW/TOPO
KJ 130	CTACTGGAGCTTTAAGTCGTTGAG	r/v Phy4 N w/ Stopp in pCR8/GW/TOPO
KJ 131	CTGGAGCTTTAAGTCGTTGAGTCG	r/v Phy4 N w/o Stopp in pCR8/GW/TOPO
KJ 132	ATGTCGTTTGATTCCACGTTTGGA	f/w PhotA1 in pCR8/GW/TOPO
KJ 133	CTAAAAAGTGTCACCGAAATTCGAG	r/v PhotA1 w/ Stopp in pCR8/GW/TOPO
KJ 134	AAAAGTGTCACCGAAATTCGAGGC	r/v PhotA1 w/o in pCR8/GW/TOPO
KJ 135	ATGGACGAATTTGGGAGAGTGAGT	f/w PhotA2 in pCR8/GW/TOPO
KJ 136	GCTGACTCAACGTTCAATGATACTTTT	r/v PhotA2 w/o Stopp in pCR8/GW/TOPO
KJ 137	TCAAAAAGTATCATTGAACGTTGAGTC	r/v PhotA2 w/ Stopp in pCR8/GW/TOPO
KJ 138	ATGGAGGAGCAGGATCCCG	f/w PhotB1 in pCR8/GW/TOPO
KJ 139	CTAGAATTCCTGAAATGTGGAAATAG	r/v PhotB1 w/ stopp in pCR8/GW/TOPO
KJ 140	GAATTCCTGAAATGTGGAAATAGGAG	r/v PhotB1w/o in pCR8/GW/TOPO
KJ 141	ATGGAGGGTCTGAATCCTATTTCC	f/w PhotB2 in pCR8/GW/TOPO
KJ 142	TCAGAAAACATCGGACGTAAATGTGGT	r/v PhoB2 w/ stopp in pCR8/GW/TOPO
KJ 143	GAAAACATCGGACGTAAATGTGGTT	r/v PhotB2 w/o stpp in pCR8/GW/TOPO
KJ 144	ATGGGTAAGGAGAAGGTGCAC	f/w EF1a in pCR8/GW/TOPO
KJ 145	CTACCACTTCTTCTTCGCAGC	r/v EF1a w/ Stopp in pCR8/GW/TOPO
KJ 146	CCACTTCTTCTTCGCAGCGG	r/v EF1a w/o Stopp in pCR8/GW/TOPO
KJ 147	ATGGGTAGCGTTCCCGCTGAT	f/w Pirin for cloning in pCR8/GW/TOPO
KJ 148	TTATGGTGTGGACTGGGCCTTG	r/v Pirin w/ stopp in pCR8/GW/TOPO
KJ 149	TGGTGTGGACTGGGCCTTG	r/v Pirin w/o stopp in pCR8/GW/TOPO
KJ 150	ATGCCGGCCTCGGGGGGA	f/w PRL1 for cloning in pCR8/GW/TOPO
KJ 151	CTAGAACCGGCGCATGTCCTT	r/v PRL1w/ stopp in pCR8/GW/TOPO
KJ 152	GAACCGGCGCATGTCCTTCG	r/v PRL1 w/o stopp in pCR8/GW/TOPO
KJ 153	ATGGTGGAAAAGAATGCATCTAGG	f/w ZF fw in pCR8/GW/TOPO
KJ 154	CTAGGAGCTCCACGGGTATC	r/v ZF rev w/ stopp in pCR8/GW/TOPO
KJ 155	GGAGCTCCACGGGTATCC	r/v ZF rev w/o stopp in pCR8/GW/TOPO
KJ 156	GAGCTCTAATGGGCATGGATGAACTCAGT	f/w Phy4_C + SacI header, in pBRIDGE_C
KJ 157	TCGTTTTAAAACCTAAGAGTCACT	r/v Phy4C_BAC, use with KJ41
KJ 159	ATTCATGTCATGCATCTGG	f/w seq. primer Tan 54 °C Phy4 3'end
KJ 160	ATGGATGAACTCAGTACAGTTGCT	f/w primer Phy4_C for GW Entry Tan 62°C
KJ 161	TCTCACACTGCCTGCATCATC	r/v 3' Phy4C Entry w/o Stopp Tan 62 °C
KJ 162	CTATCTCACACTGCCTGCATC	r/v 3' Phy4C w/ Stopp Entry Tan 62 °C
KJ 163	ATTATCACCCGATCGTCGAATTGT	r/v PhotB2 Tan 62 °C
KJ 170	GATGCCTCACAACTGGTTTCG	f/w Tan 61 °C PhotB2
KJ 171	GCTGCTTGAGCTTCTCAATTG	f/w Tan 60 °C PhotB1
KJ 172	ATGACAACTTCCACGCCATCT	f/w Tan 60 °C Pirin
KJ 173	AGCAGCACTATTCAGCCAATC	f/w Tan 60 °C ZF
KJ 174	ATATGAGCTCTCAACATGTGGAGCACGACAC	f/w SacI header, Tan 61 °C 2x35S

		promoter from SAT6 mCherry construct
KJ 175	ATATACTAGTTGGCTATCGTTCGTAAATGGTGA	r/v SpeI header, Tan 61 °C, 2x35S promoter from SAT6 mCherry construct
KJ 176	ATATGAGCTCCATAATAGCTGTTTGCCAACCGGT	f/w Tan 64 °C SacI header + ATAT for PCR digestion
KJ 185	CTACTTCTTGTTTGCTGCAGCGAGTTC	r/v phyA 3' w/ stopp Tan 71 °C
KJ 186	ATGTCAGGCTCTAGGCCGACTCAGTCC	f/w phyA 5' Tan 72 °C
KJ 187	ATGGTTTCCGGAGTCGGGGGTAGT	f/w phy B 5' Tan 68 °C
KJ 188	CTAATATGGCATCATCAGCATCATGTCACC	r/v phy B 3'Tan 69 °C
KJ 189	ATTGCCTTGGATTAAAACGTT	r/v phot1 sequencing primr Tan 54 °C
KJ 190	ATGCCCGCCAAAAAGATAT	f/w phot1 sequencing primer Tan 53 °C
KJ 191	TGGACGTGTTTCTACTCC	f/w phot2 sequencing primer Tan 54 °C
KJ 192	CAGTTACTTGAAACAAGTGTTT	f/w phyB sequencing primer Tan54 °C
KJ 193	CCCGGGTATGTCAGGCTCTAGGCCGAC	f/w XmaI header + T + phyA CDS Tan 62°C
KJ 194	GGATCCCTACTTGTTTGCTGCAGCGA	r/v BamHI header + phyA CDS 3´Tan 59 °C
KJ 222	CGTTGTAAAACGACGGCCAG	f/w f222fw Tm60 °C
KJ 223	TATGTTGTGTGGAATTGTGAGC	r/v f223 rev Tm 62 °C
ALL 2	CATATGGGCATGGATGAACTCAGTACA	f/w NdeI header + Phy4_C partial
EG 09	TACCTGAGCACCCAGTCC	f/w GFP
EG 10	CACGAACTCCAGCAGGACCATGTGATC	r/v GFP
EG 35	TAATACGACTCACTATAGGGC	T7 Seq forward
EG 41	TATGATTGCATTAAATAGTGCA	ALPP4 forward
J 62	GGGCTCGGCCTGACCGGCCTTTTTTTTTTTTTTTTV	lock docking oligo dT + SfiI header + 6 base clamp
MZ 104	GGGATGACGCACAATCCCACTA	35S Promoter 5'-->3'
MZ 311	GCCGGACACGCTGAACTTG	PSPYNE YN reverse@9520 in YFP-Nterm
MZ 312	GGTGTTCTGCTGGTAGTGGT	PSPYCE YC reverse@9520 in YFP-Cterm
MZ 403	CACCATGGAACCAACAGAAAAACCATC	PHOT1 5' for ENTR-D directional cloning (CACC header)
MZ 404	TCAAAAAACATTTGTTTGCAGATCTTC	PHOT1 3' for Gateway cloning with STOP
MZ 406	CACCATGGAGAGGCCAAGAGCCCCTCCATCT	PHOT2 5' for ENTR-D with CACC overhang for directional cloning
MZ 407	TTAGAAGAGGTCAATGTCCAAGTCCGTAG	PHOT2 3' for Gateway cloning with STOP
MZ 408	GAAGAGGTCAATGTCCAAGTCCGTAG	PHOT2 3' for Gateway cloning w/o STOP
MZ 409	AAAAACATTTGTTTGCAGATCTTCTAG	PHOT1 3' for Gateway cloning w/o STOP
M13FW	GTAAAACGACGGCCAG	f/w derivative of Invitrogen M13 FP
M13RV	CAGGAAACAGCTATGAC	r/v derivative of Invitrogen M13 RP

Oligonucleotides were purchased from Invitrogen.

2.3.2. Vectors and Plasmids

Table 2: Vectors for cloning purposes and plasmids used

Vector	Purpose	Reference
pCR-BluntII-TOPO	subcloning	Invitrogen
pGBKT7	Y2H bait constructs	Clontech
pGADT7	Y2H prey constructs	Clontech
p_BRIDGE_C	Y2H bait constructs, C-term. fused	Jutta Rösler (177)
pCR8/GW/TOPO	GW Entry vector for LR-recombination	Invitrogen
p2CGW7,0-CFP	GW destination vector, N-term CFP fusion	(178)
p2FGW7,0-GFP	GW destination vector, N-term GFP fusion	(178)
p2GWC7,0-CFP	GW destination vector, C-term CFP fusion	(178)
p2GWF7,0-GFP	GW destination vector, C-term GFP fusion	(178)
p2CGW7,0-CFP+2x35S	as above, + 2x35S promoter + TL enhancer	recloned
p2FGW7,0-GFP+2x35S	as above, + 2x35S promoter + TL enhancer	recloned
p2GWC7,0-CFP+2x35S	as above, + 2x35S promoter + TL enhancer	recloned
p2GWF7,0-GFP+2x35S	as above, + 2x35S promoter + TL enhancer	recloned
pSAT4(A)-DEST-n(1-174)EYFP-N1	sYFP, N-terminus of YFP, fused C-terminally	(179)
pSAT4-DEST-n(1-174)EYFP-Cl	sYFP, N-terminus of YFP, fused N-terminally	(179)
pSAT5(A)-DEST-c(175-End)EYFP-N1	sYFP, C-terminus of YFP, fused C-terminally	(179)
pSAT5-DEST-C(175-END)EYFP-C1(B)	sYFP, C-terminus of YFP, fused N-terminally	(179)
pSAT6_mCherry_VIRD2_NLS	nuclear marker ($Cherry_{NLS}$)	(179)
pM-GK	PIP2a:GFP, plasma membrane marker	(180)
pWEN18_YFP	35S::YFP	(181)
pWEN18_CFP	35S::CFP	(181)
pM304.2	35S::phyA:GFP	(68)
pPhyB_GFP	35S::phyB:GFP	Philipp Gasch (182)
pPhy4:YFP	phy4:YFP for phenotypic rescue	(9)
pBACPA	phyA_BD, control in Y2H experiments	Jutta Rösler (177)
pGADFHY1	AD:FHY1, control in Y2H experiments	(183)
pGBKT7-p53	Clontech Y2H system control	Clontech
pGBKT7-lamin C	Clontech Y2H system control	Clontech
pGADT7 Control	Clontech Y2H system control	Clontech

2.4. Enzymes and antibodies

2.4.1. Enzymes

Restriction enzymes used for cloning (NEB)

BamHI^{HF}	SacI
ClaI	ScaI
EcoRI^{HF}	SmaI
NdeI	SpeI
NotI^{HF}	SphI
PacI	XmaI

Other enzymes used

Antarctic Phosphatase	NEB
Driselase	Fluka
LR-Clonase enzyme mix	Invitrogen
Lysozyme	Applichem
Phusion Hot Start Polymerase	Finnzymes
Proteinase K	Applichem
RNAse A	Sigma
RNAse H	Invitrogen
SuperscriptII reverse transcriptase	Invitrogen
TaKaRa Ex Taq Polymerase	TAKARA BIO INC.
Taq Polymerase	home-made
T4DNA Ligase	NEB
Zymolase	Sigma

2.4.2. Antibodies

Mouse α c-myc monoclonal	1:5,000	Sigma Aldrich
Goat α mouse IgG alkaline phosphatase coupled	1:30,000	Sigma Aldrich

2.5. Growth chambers

Longday conditions, 16 h light (Osram L58 W/77, 50 µmol · m^{-2} · s^{-1}), 8 h dark, 22 °C.

2.6. Illumination devices

R LED660-66-60, 660 nm, 210 mW at 240 mA (Roithner Lasertechnik, Vienna)

R Kingbright Cluster/52mm LED-spot red (660 nm) (Conrad Elektronik SE, Hirschau, Germany); used in Y2H assays

FR LED735-66-60, 735 nm, 1000 mW at 240 mA (Roithner Lasertechnik, Vienna), with filter (*Plexiglas Formmasse* black 90053 0.2 mm (Röhm GmbH))

B H4-AR58G05B24BC-C 460 nm 1.5 W at 350 mA +/- 40°(Roithner Lasertechnik, Vienna)

2.7. Microscopy

2.7.1. Macroscope

For macroscopic observations, as used for protoplast regeneration assay and screening of transient transformed cells, a fluorescence macroscope (Leica Z16 APO zoom system) equipped with a CCD-camera (DFX 500, Leica) was used. Table 3 lists filter cubes used for fluorescence observations.

Table 3: Filter cubes used with the Leica Z16 APO zoom system

Filter cube	Excitation	Dichroic mirror	Emission
CFP	BP 436 / 20	455	BP 480 / 40
I3	BP 450-490	510	LP 515
GFP	BP 470/40	500	BP 525/50
N3	BP 546/12	565	BP 600/40

2.7.2. Epifluorescence microscope

For microscopic observations as mainly used for localisation studies employing transient expression of fluorescent reporter fusion proteins, an automated, upright epifluorescence microscope (Leica DM6000B) equipped with a CCD-camera (DFX 500, Leica) was used. The system was run by the manufacturer's software Leica Application Suite 3.7. DIC filter cube was used for interference contrast presentation. Table 4 lists filter cubes used for fluorescence observations.

Table 4: Filter cubes used with the epifluorescence microscope DM6000B

Filter cube	Excitation	Dichroic mirror	Emission
CFP	BP 436 / 20	455	BP 480 / 40
I3	BP 450-490	510	LP 515
YFP	BP 500 /20	515	BP 535 / 30
N3	BP 546/12	565	BP 600/40

2.7.3. Confocal laser scanning microscope

For advanced microscopic observations, as required for studies on plasma membrane localisation of fluorescent fusion proteins and sYFP-experiments, a confocal laser scanning unit equipped with an upright fluorescence microscope (TCS-SP2 AOBS, Leica) was used with the manufacturers software (Leica confocal software). This facility was made accessible by Prof. Adriaan Dorresteijn and Dr. Anne Holz (Institute of Zoology and Developmental Biology, JLU Giessen). For high resolution observation, a state of the art confocal laser scanning microscope (TCS-SP5 AOBS) was made accessible at Leica Microsystems (Mannheim, Germany) by Manfred Jung and Dr. Olga Levai. Table 5 gives the colour lookup table with the respective excitation and emission wavelengths used.

Table 5: Colour lookup table, excitation and detection wavelengths used with TCS-SP2 AOBS

Fluorophore	Excitation [nm]	Detection [nm]	LUT
CFP	458	468-478	Cyan
Chlorophyll	496	675-700	Red
GFP	488	500-535	Green
mCherry	543	605-675	Red
YFP	514	530-560	Yellow
Transmission	488	500-535	Grey scale
		555-620	Grey scale
		650-750	Grey scale

Single scans were carried out with 4x line average and 6x frame average. For enhancement of brightness and contrast and the generation of overlay pictures Paint Shop Pro 7 (Corel), Adobe Photoshop CS3 (Adobe) and CorelDRAW X5 (Corel) were used.

2.8. Fine chemicals

A. A. Packaging Limited, Liverpool, UK
Cellophane discs, 8.0 mm

Agilent Technologies, St. Clara, CA, USA
Plant RNA Isolation Mini Kit

Amersham Biosciences, Little Chalfont, UK
PvDF membrane

Applichem GmbH, Darmstadt, Germany
Acetic acid
Acrylamide 4K solution, 30 %
Agar Kobe
Ammonium sulfate
Ammonium acetate
Ammonium persulfate
Ampicillin
Bromophenol blue
BCIP
BSA
Calcium chloride
Calcium nitrate
Chloroform
Coomassie R250
D-Mannitol
Dipotassium hydrogen phosphate
Dithiothreitol (DTT)
Ethanol, pure
Formaldehyde
Formamide
Glucose monohydrate
Glycerine
Glycine
IPTG
Isoamyl alcohol
Isopropyl alcohol
Kanamycin sulfate
L-Leucin
L-Tryptophane
MES buffer grade
Methanol
β-mercaptoethanol
MOPS
NBT
PEG 6000
Phenol
Potassium acetate
Potassium dihydrogen phosphate
Potassium hydroxide
Rubidium chloride
Sodium chloride
Sodium hydroxide
TEMED
Tris, ultrapure
Tryptone
X-β-Gal
Yeast extract

BioRad Laboratories, Hercules, USA
SDS-PAGE gel chamber and Tank Blot apparatus
Prestained Marker Precision Plus

Biosynth AG, Staad, Switzerland
X-α-Gal

Carl Roth GmbH + Co. KG, Karlsruhe, Germany
Potassium chloride
Sodium acetate
Sodium dodecyl sulfate (SDS)
Triton X100

Fisher Scientific Chemicals, Loughborough, Leics., UK
Diammonium tartrate

Fluka Chemie, Buchs, Switzerland
PEG 8000
Driselase

Invitrogen Corporation, Carlsbad, USA
DB3.1 *E. coli* cells
Gateway ENTR-cloning kit
Gateway LR-clonase mix
Oligonucleotides (see table 1)
SuperScript II first strand synthesis kit
TOP10 *E. coli* cells
TA-cloning kit
TOPO blunt cloning kit
TOP10F' *E. coli* cells

Merck KgaA, Darmstad, Germany
Ammonium nitrate
Boric acid
DMSO
EDTA
Potassium hydroxide
Sodium chloride, concentrated

MP Biomedicals, Illkirch, France
LB medium

NEB, New England Biolabs Inc., Beverly USA
1 kb & 100 bp DNA ladder
Restriction enzymes + buffers

PEQLab, Erlangen, Germany
PEG 3550
Agarose

QIAGEN GmbH, Hilden, Germany
QIAquick Gel Extraction kit
QIAprep Spin Miniprep kit

Serva GmbH, Heidelberg, Germany
Dimethyl formamide
Tween 20

Sigma-Aldrich Chemie GmbH, Steinheim, Germany
Ethidium bromide
Spermidine
Xylene blue

Whatman Ltd., Maidstone, UK
Filterpaper

3. Methods

3.1. Cloning procedures

3.1.1. RNA extraction and gel electrophoresis

RNA from 200 mg of WT *Physcomitrella patens* filaments from fresh liquid culture was extracted using the Plant RNA Isolation Mini Kit (Agilent) according to manufacturer's instructions. Yield and quality were checked by RNA agarose gel electrophoresis. 1.2 % agarose were dissolved in 1 x MOPS buffer, boiled up, poured into a gel chamber equipped with combs as appropriate, cooled down, the gel was completely covered with 1 x MOPS buffer. RNA samples were taken up in 3 x RNA loading dye and loaded onto the gel. Gel electrophoreses was run at 120 V for 45 min, thereafter the gel was transferred into an ethidium bromide bath for 10 minutes. RNA samples were observed and documented using a UV-B transilluminator (fluorescent lamp, 312 nm, TCP20M) equipped with a CCD-camera (Nikon).

3.1.2. RT-PCR

First strand cDNA synthesis was carried out using the SuperScript II first strand synthesis kit (Invitrogen) according to manufacturer's conditions. 3.5 µg of fresh *Physcomitrella patens* WT RNA were used as template. Initial cDNA was synthesised using an oligo-dT-lock docking primer (J62). Resulting cDNA was diluted 1:10 and used as template for subsequent PCR amplification with cDNA-specific primers, as appropriate. Resulting PCR-products were further analysed by agarose gel electrophoresis.

3.1.3. Agarose gel electrophoresis and DNA staining

Dissolved agarose was poured into gel chambers equipped with combs as appropriate. After cool down, the gel was completely covered with 0.5 x TBE-buffer and combs were removed. Samples were taken up in 6 x loading dye and loaded onto the gel. Gel electrophoresis was run at 200 V for 25-35 min, thereafter the gel was transferred into an ethidium bromide bath for 10 minutes. DNA samples were observed and documented using a UV-B transilluminator (fluorescent lamp, 312 nm, TCP20M) equipped with a CCD-camera (Nikon).

3.1.4. Molecular cloning

If not stated otherwise, molecular cloning procedures were carried out according to Sambrook and Russel 2001 (184). Enzymes and related buffers were used as demanded by manufactures instructions; digested vectors were de-phosphorylated by antarctic phosphatase (NEB). Purification of fragments for insertion and vector backbones was achieved by gel-extraction using a MinElute Gel extraction kit (Qiagen). Generally 50 ng of vector backbone were ligated with 3 x amount insert. T4-DNA-Ligase mediated ligation was carried out at 14 °C (blunt) or 16 °C (sticky) for 4 to 16 h. Small-scale plasmid preparation was done using a QIAprep Spin Miniprep Kit (Qiagen).

3.1.5. TOPO blunt cloning

Cloning of cDNAs into pCR-BluntII-TOPO was carried out with the Zero Blunt TOPO PCR cloning kit (Invitrogen) according to manufacturer's instructions with halved reaction volumina. Blunt-end cDNAs were PCR-amplified using Phusion Polymerase (Finnzymes) and purified by gel-extraction with the help of a MinElute Gel extraction kit (Qiagen). Reaction time for TOPO-ligation was increased up to 15 minutes for PCR-products larger 1500 bp.

3.1.6. Gateway cloning

3.1.6.1. ENTR-Vectors

The pCR8/GW/TOPO/TA-system (Invitrogen) was used for creation of GW entry vectors for subsequent cloning of fluorescent fusion plasmids and sYFP plasmids. cDNAs of the respective genes of interest were PCR-amplified with TaKaRaEx Taq Polymerase (Takara Bio Inc.), generating A-overhangs at each 3' end of double-stranded PCR-products. TOPO-mediated TA-ligation of gel-purified PCR-products into pCR8/GW/TOPO/TA was carried out according to manufacturers' instructions using halved reaction volumina. For PCR-products larger 1500 bp reaction time was increased to 15 min. Since this entry vector does not allow for directional insertion of the fragment, orientation of the insert was checked by asymmetric restriction digest. Depending on further cloning approaches two versions of each cDNA were prepared as GW entry clones. For N-terminal fusions to fluorescent tags stop-codons were introduced at the cDNAs end. For C-terminal fusions, stop-codons were omitted.

3.1.6.2. Cloning of 2 x 35S GW destination vectors

For construction of fluorescent fusions a GW destination vector set by Karimi *et al.* 2002 (178) was used. Those vectors comprise single 35S promoters and enable both N- or C-terminal fusions of GFP or CFP to the cDNA of interest. Initial expression test involving transiently transformed onion epidermis cells and *Physcomitrella* filaments proved GFP and CFP expression only for onion cells; no GFP or CFP was observed in *Physcomitrella*. To circumvent problems arising from expression levels in *Physcomitrella* the single 35S promoter of these destination vectors was exchanged by a double 35S promoter and a TL-enhancer of the pSAT6-mCherry-VirD2-NLS construct. Promoter und enhancer were isolated from pSAT6-mCherry-VirD2-NLS by SacI & SpeI digestion and purified by gel-extraction. New promoter and enhancer were ligated into the new destination vectors by conventional cloning. Resulting new set of destination vectors is shown in Fig. 1. Functionality of the new destination vectors were checked by transient expression in both onion epidermis and *Physcomitrella*. All vectors proofed to express efficiently in both plant cell types.

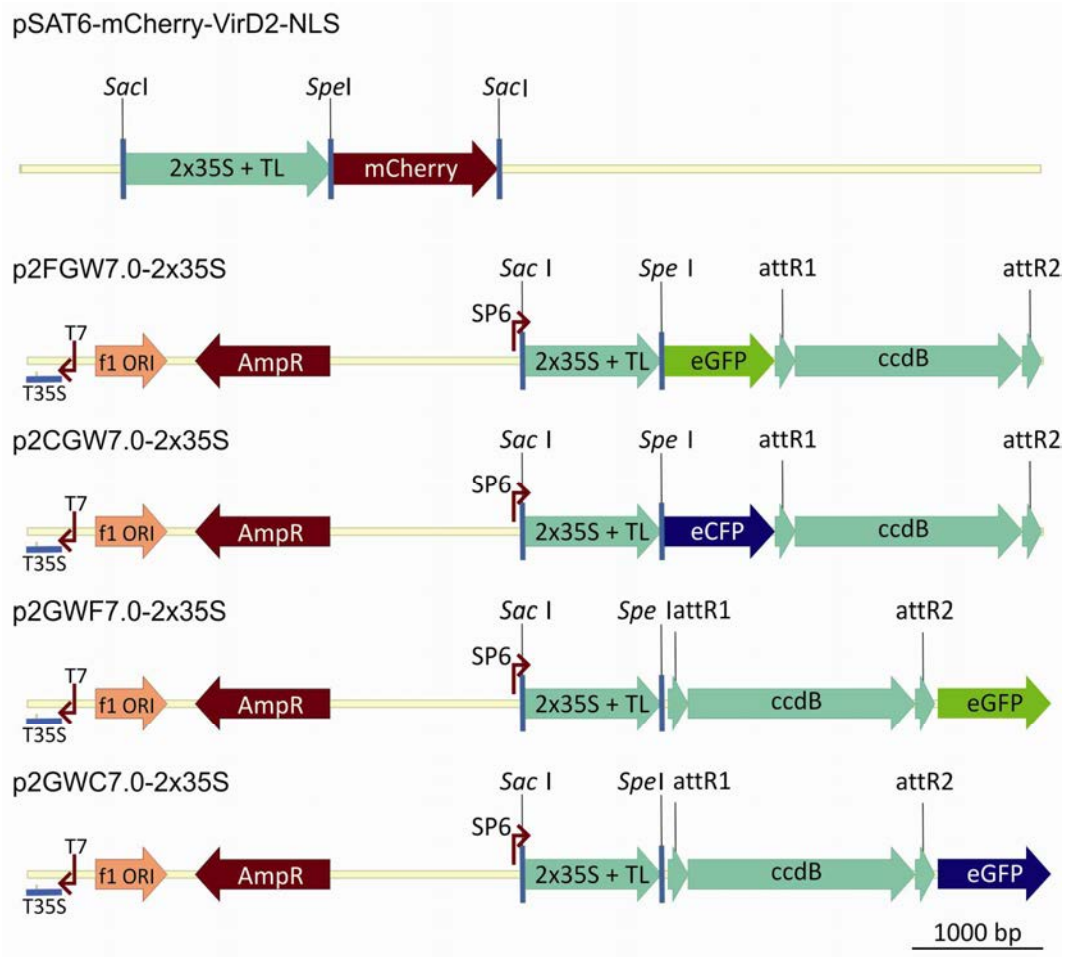

Fig. 1: Re-cloned destination vectors for over expression of N- & C-terminal fluorescent fusions.
Single 35S promoters were exchanged by SacI & SpeI based cloning. Fluorescence markers are placed either in front or after attR sites for N- or C-terminal fusions. attR1 and attR2: recognition sites for clonase mediated recombination. ccdB: lethality marker. Scale bar as indicated.

3.1.6.3. LR-reaction cloning of fluorescent fusions and sYFP-constructs

Both fluorescent fusion and sYFP constructs were prepared on the basis of the Gateway system. For fluorescent fusion constructs, above described destination vectors were used to generate either N-terminal GFP or CFP fusions or C-terminal GFP or CFP fusions. LR-mediated recombination was carried out using the LR clonase II mix (Invitrogen) according to manufacturer's conditions. 150 ng entryclone and 150 ng of the appropriate destination vector were used; otherwise reaction volumina were halved. Integrities of the resulting clones were checked by restriction digest. sYFP-constructs were generated similarly using pSAT-series destination vectors for either N- (pSAT4-Dest-N / pSAT5-Dest-C) or C-terminal fusions (pSAT4a-Dest-N / pSAT5a-Dest-C) of the YFP-moieties (179). All of the four available sYFP-vectors of the pSAT-series contained a double 35S promoter + enhancer and were used as purchased.

3.2. Protein methods

3.2.1. SDS-PAGE and protein staining

SDS-PAGE gels were prepared according to Sambrook and Russel (184) . 10 % acryl amide gels were used for detection of phytochrome fusion proteins. Protein samples were taken up in 2 x loading dye and loaded onto the gel. For Western Blot analysis, 4 x sample volume was loaded. High range marker was used for coomassie stained gels, pre-stained marker was used for western blot analysis. Gel was run at 100 V for ca. 1.5 h until the dye front completely ran off. Subsequently gels were either coomassie stained or blotted.
For staining, the gel was shortly boiled up (microwave, 600 W) in hot coomassie solution. After a short cool down, staining solution was discarded and the gel was likewise boiled up in destaining solution, thereafter incubated for 30 min while shaking. Destaining was repeated three times, until background staining was completely washed out. The gel was dried in cellophane foil for storage after documentation

3.2.2. Western Blot and immunodetection

SDS-PAGE gels were blotted onto a methanol-activated PvDF membrane. For this, two layers of tank blot buffer soaked filterpaper were placed both underneath the gel and upon the membrane. The blotting chamber (Protean Tank Blot, Biorad) was placed into the tank filled with tank blot buffer; additionally a cooling aggregate was added. Under constant stirring, tank blot was run at 100 V (20 mA) in the cold room (4 °C) for 2 h. After protein transfer was finished the membrane was blocked in blocking buffer for 1 h. Incubation with the first antibody for 1h followed. The membrane was incubated for 15 min in washing buffer (slow shaking, repeated three times) to remove excess of the first antibody and was incubated with the second antibody for one further hour. Following three washing steps as before detection of proteins was carried out by NBT/BCIP staining. NBT and BCIP were added to detection buffer; the membrane was incubated until immunostaining of protein samples was sufficient for documentation.

3.3. Bacteria

3.3.1. Preparation of electro-competent *E. coli* cells

XL1blue cells from a -80 °C glycerol stock were streaked out on fresh LB + tetracycline and incubated at 37 °C. On overnight liquid LB + tetracycline (5 mg/ml) culture was inoculated with a single colony from this culture. Incubation was carried out at 37 °C while shaking at 180 rpm. 250 ml liquid TB + tetrazycline was incubated with 500 µl of liquid overnight culture and further incubated at 18 °C while shaking at 160 rpm until OD_{600} reached 0.4 (approx. 32 h). Cells were harvested by centrifugation at 5.000 g, supernatant was discarded, washed twice in ice-cold sterile water and subsequently taken up in 800 µl sterile, ice-cold 7 % DMSO-solution. Aliquots of 100 µl were instantly frozen in liquid nitrogen and further stored at -80 °C. Competence, as determined by transformation with 1 ng pUC19, reached 1 x 10^8 - 1x 10^9 cfu per µg DNA.

3.3.2. Transformation of *E. coli* cells by electroporation

Cells were thawed on ice for approx. 30 min; simultaneously electro-cuvettes (2 mm width, Biorad or PeqLab) were pre-cooled on ice. Depending on the approach, either 100 ng plasmid DNA, a whole ligation volume or 5 -10 µl of yeast DNA extract (see 3.4.7) were added to the cells. The reaction volume was mixed while carefully transferring the cells into the cuvettes. Cells were electroporated at 1,550 V, 21 µF and 400 Ω (Wave Controller 400, Genezapper). Afterwards 500 µl hand-warm LB-Mg was added, cells were transferred into 2 ml reaction tubes and incubated at 37 °C and constant shaking at 180 rpm for 1 h. Ultimately transformed cells were streaked out on selection medium and incubated overnight at 37 °C.

3.3.3. Transformation of *E. coli* cells by heat-shock

Commercially available competent cells were used as available from purchased kits. Transformation was carried out according to Hanahan (185). Cells from -80 °C were thawed on ice for approx. 30 min and mixed with the appropriate amount of plasmid DNA or a whole ligation reaction. Following further 30 min incubation on ice, cells were first heat-shocked at 42 °C for 45 sec and then cold-shocked on ice for 2 min. 500 µl of hand-warm SOC medium was added and cells were incubated at 37 °C on a shaker (180 rpm) for 1 h before being streaked out on selection medium.

3.3.4. Small scale plasmid preparation (Mini-Prep)

3 ml liquid LB + selection marker were inoculated with a single *E. coli* colony and incubated on a shaker (180 rpm) at 37 °C overnight. Plasmid DNA was extracted with the help of a QIAprep Spin Miniprep kit (Qiagen) according to manufacturer's suggestions.

3.3.5. Large scale plasmid preparation (Maxi-Prep)

250 ml TB + selection were inoculated from a small LB + selection marker overnight culture (1:1000) and incubated on a shaker (160 rpm) at 37 °C. Large scale extraction of plasmid DNA was carried out as described in Sambrook and Russel (184). Purity and concentration were determined spectral photometrically (spectrum between 200 - 300 nm, and OD_{260} respectively). For transformation purposes DNA concentration was usually adjusted to 1 or 2 µg/µl.

3.4. Yeast

3.4.1. Growth and cultivation

Generally, all yeast cells used in the work presented here, were grown as 3 ml liquid culture in their respective full (YPDA) or selection (dropout-) medium at 30 °C shaken at 220 rpm overnight. Cells were harvested at 3,000 g (5 min) and taken up in 750 µl medium. 750 µl cell-suspension were mixed with 250 µl glycerol and instantly transferred to -80 °C for storage. Constantly used strains, such as AH109, Y187 or pre-transformed cells, were periodically streaked out on YPDA-medium or selection medium respectively and grown for 4 d at 30 °C. Such streaks were kept at 4 °C and

used for experiments for up to 6 weeks, after which new cells were grown from -80 °C stocks.

3.4.2. Cloning of Y2H bait and prey plasmids

Both bait and prey constructs for Y2H analysis were conventionally cloned using vectors provided by Clontech's Y2H matchmaker system, pBGKT7 and pGADT7. Both vectors yield fusion constructs carrying the BD and AD respectively at the N-terminus of the protein of interest. Phytochrome 4 bait and prey fusions were cloned with NdeI and SmaI. To achieve C-terminal fusions of the BD, phytochrome 4 inserts were PacI / SacI cloned into pBAC, a derivative of pBRIDGE (Y3H system, Clontech). pBAC was cloned and kindly provided by Jutta Rösler (177).

3.4.3. Yeast transformation

3.4.3.1. Transformation

25 ml YPDA-medium were inoculated with 3 to 5 colonies (AH109 and Y187) and grown at 30 °C shaking at 220 rpm overnight. Cell density was determined by counting with the help of a *Fuchs-Rosenthal*-chamber. A 50 ml pre-warmed YPDA culture was then inoculated with 2.5 x 10^8 cells, previously washed in cold water. The expansion culture was grown to a cell density of 2 x 10^7 cells/ml (OD_{600}: 0.8 - 1.0) under conditions described before (4 - 6 h). Cells were harvested at 5,000 g for 5 min, washed twice with 25 ml of ice-cold, sterile water and taken up in 1 ml sterile water. Following centrifugation as before, pelleted cells were resuspended in 1 ml sterile water and aliquots à 100 µl/transformation (i.e. 1 x 10^9 cells) were prepared. Aliquots were kept on ice. Meanwhile the transformation-mix was prepared (see 2.2.5.); 1 µg plasmid DNA was used for single transformation, two plasmids (1 µg each) were added for simultaneous double transformation. The DNA-volume added to the transformation mix remained 36 µl per transformation, regardless of the number of plasmids transformed. Cell-aliquots were spun down (13,000 g, 1 min), supernatant was discarded and cells were resuspended in 360 µl transformation mix / transformation, vigorously vortexed if necessary. Cell suspensions were heat-shocked at 42 °C for 40 min with short vortexing in 10 min intervals. Afterwards cells were spun down in a table top centrifuge as before and taken up in 500 µl of sterile water before being plated on selection medium as appropriate. Transformed cells were incubated for 4 d at 30 °C.

3.4.3.2. Sequential transformation

25 ml selection medium were inoculated with 3 to 5 colonies of pre-transformed yeast from selection medium. Culture was grown for up to 24 h at 30 °C and 220 rpm. Cell density was determined by counting with a *Fuchs-Rosenthal*-chamber. As for single transformation, 2.5 x 10^8 cells were used for inoculation of an YPDA-expansion culture as described before (see 3.4.2.1.). After cell harvest and two washing steps, the cell pellet was resuspended in 3 ml 100 mM LiAc. Cells were incubated at 30°C, 220 rpm for 15 min. After homogenisation of the cell suspension by short vortexing, 300 µl cell aliquots were prepared and kept on ice. Meanwhile the transformation mix was prepared as described (containing only

one plasmid). Cell-aliquots were spun down (13,000 g, 2 min) and vigorously mixed with 360 µl transformation mix. Cells were incubated within the transformation mix shaking at 180 rpm at 30 °C for 30 min and thereafter heat-shocked (42 °C) for 30 min, with vortexing in 5 min intervals to prevent sedimentation. The transformation mix was removed after centrifugation (13,000 g, 2 min) and cells were finally resuspended in 500 µl of sterile water and plated on double or triple-dropout medium as appropriate. Transformed cells were incubated for 4 d at 30 °C.
For large scale transformation, as needed for cDNA library screening, a 40 x scale up of this procedure was used (see 3.4.6.).

3.4.4. Protein extraction

For total protein extraction 1 -3 yeast colonies were used to inoculate an overnight culture of appropriate selection medium. Cells were harvested (5,000 g, 5 min) and resuspended in 2 ml freshly prepared cold 0.1 M NaOH then incubated on ice for 5 min. Following centrifugation at 5,000 g (5 min), pelleted cells were boiled up in 50 µl 6 x Lämmli-buffer for 5 min. Suspension was clarified at 10,000 g for 15 min. The supernatant was transferred to a new reaction tube; both the supernatant and the pellet were stored at -20 °C.

3.4.5. Adjustment to auto-activation growth with 3-AT

The Y2H principle is based on the reconstitution of a functional GAL4 transcription factor upon and it is a well known drawback of any Y2H approach based on this principle that the BD-hybrid protein might on its own be able to activate gene expression, for instance if the BD-fusion either contains itself a transcription factor or strongly interacts with transcription factors. Therefore it is essential to determine the bait proteins autoactivation capacity, as too low amounts will lead to false positive clones in the screening process, amounts too high will hamper identification of weak interactions.
In order to determine the lowest concentration needed for repression of auto activity, yeast cells expressing the respective bait constructs were quantitatively (1 x 10^6 cells) streaked out on selection medium lacking Trp and His. 3-AT was added in increasing concentrations, starting with 0.25 mM, 0.5 mM, 1 mM then increasing in 1 mM steps up to 7 mM. Cells were incubated in the respective selection media for 4 d at 30 °C. Colony growth was monitored over the whole incubation period. The suitable 3-AT concentration was determined as the point at which colony background growth was reduced to small numbers of tiny colonies, with the next highest concentration of 3-AT completely repressing colony growth after 4 d. Complete growth repression was omitted to enable low interaction strength to be monitored in Y2H assays. Concentrations determined were as follows: 2.5 mM for both full-length BD:PHY4 and BD:PHY4_C and 1 mM for BD:PHY4_N constructs.
No autoactivation was observed for AD:fusions or the cDNA library containing yeast cells when tested on -Leu/-His selection medium.

Table 6: Amounts of 3-AT added to dropout medium for suppression of *HIS3* autoactivation by BD-fusion proteins.

Bait constructs	final concentraion of 3-AT [mM]
BD:PHY4	2.5
BD:PHY4_N	0.5
BD:PHY4_C	2.5
PHY4:BD	1.0
PHY4_N:BD	1.0
PHY4_C:BD	0.5

3.4.6. Y2H cDNA library screening

For Y2H library screening a sequential double transformation was carried out at a 40 x scale up. This scale up was calculated on the basis of generally reached transformation efficiency with this transformation method, in order to be able to cover the whole library. To screen 28,000 different genes presumably contained in the library a minimum of 8.5 x 10^5 were needed.
One aliquot of AH109 cells, pre-transformed with a putative full-length cDNA library from *Physcomitrella* (kindly provided by Dr. Hans Sommer, MPI cologne) was used for inoculation of 75 ml overnight culture in liquid -Leu medium. Cells were grown at 30 °C shaking at 220 rpm. 1 x 10^9 cells were taken from this overnight culture to inoculate 200 ml of an YPDA expansion culture (6 h at 30 °C and 220 rpm) until OD_{600} reached 0.9. Cells were harvested as before (5,000 g, 4 min at 4 °C), washed with 100 ml cold, sterile water, finally resuspended in 4ml of 100 mM LiAc and incubated at 30 °C and 220 rpm for 15 min. Meanwhile the transformation mix was prepared as described before (i.e. amounts for 40 single transformations, 40 µg of sterile bait-plasmids were transformed). Cells were then taken up in the transformation mix and mixed well by vigorous vortexing. Following incubation of the cells in transformation mix suspenstion at 30 °C for further 30 min, cells were heat shocked (42 °C, 45 min) with short vortexing in 5 min intervals. Cells were collected by centrifugation (5,000 g, 5 min) and resuspended in 40 ml of sterile water.
Finally, transformed cells were streaked out on 100 large Petri dishes (ø 14.5 cm) containing Trp/-Leu/-His dropout medium + 2.5 mM 3-AT and incubated in a temperature-adjusted room at 30 °C for 21 d. To determine the transformation efficiency, 1:100 and 1:1000 dilution of the transformation suspension was plated onto -Trp/-Leu selection medium, colony growth monitored and documented, transformation efficiency was then calculated per µg DNA and number of cells initially used for transformation. A transformation efficiency of 1 x 10^4 was reached.

3.4.7. DNA extraction

For total DNA extractopm from yeast, a 3 ml 3DO overnight culture was inoculated with the respective yeast colony and incubated at 30 °C and 220 rpm until the culture reached sufficient cell density (up to 30 h). Cells were harvested (5,000 g 3 min) and washed with sterile water. The pellet was resuspended in 100 µl zymolase solution and incubated at 37 °C for 30 min. Following addition of approx. 25 µl glass beads (ø 0.45 - 0.5 mm) the samples were cracked by strong vortexing (Mixermill, full

speed, 5 min) and thereafter boiled up for 10 min and incubated for further 5 min on ice. Finally the sample was centrifuged for 1 min in a desktop centrifuge (full speed) and the supernatant transferred into a fresh reaction tube. 100 µl TE buffer were added, DNA was extracted by addition of phenol:chloroform:isopropyl alcohol (25:24:1). Following centrifugation (13,000 g, 1 min) the supernatant was transferred into a new reaction tube and DNA was precipitated by addition of 8 µl 10 M ammonium acetate and 500 µl pure ethanol and incubated for at least 1 h at -20 °C. Precipitated DNA was pelleted at 20,000 g, washed with ethanol, finally solved in 10 µl of sterile water and stored at -20 °C.

3.4.8. Analysis of positive interaction partner from Y2H screen

After 21 d of incubation on 3DO selection medium plates were stored at 4 °C. 1120 yeast colonies (approx. 10 % of all grown yeast colonies) were transferred to 2DO and 3DO (+2.5 mM 3-AT), incubated at 30 °C for 7 d and finally transferred to 4DO (with and without +2.5 mM 3-AT) and 4DO + Xα-Gal selection medium (masterplate) and incubated at 30 °C for further 7 d. 75 yeast colonies survived this second round of selection and were further evaluated in regard to their growth, colony size and colour and sorted accordingly. Colonies grown under highest stringency conditions possible (4DO + 2.5 mM 3-AT + Xα-Gal) were sorted three groups: pink colonies (mostly correlating with large colony size), white colonies (correlating with medium colony size) and blue colony (mainly correlating with only small to tiny colony size). Masterplates were stored at 4 °C, yeast colonies were streaked out on new plates for further analysis.
DNA was extracted as described (see 3.4.7.) and presence of prey constructs was checked by PCR analysis with KJ60/KJ61 and KJ62/KJ63 respectively using 1 - 2 µl of yeast DNA extract. KJ60/61 were suggested by Clontech's Y2H manual. KJ62 and KJ63 each are 7 bps shorter than KJ60/61, which results in a considerably lower annealing temperature (64 °C *vers*. 71 °C). The possibility to work with lower annealing temperatures increased chances of obtaining PCR products from suboptimal DNA extracts from yeast cells. Both primer pairs were used for all colonies tested; the majority gave different results in terms of either product sizes or the general capability to generate PCR products at all.

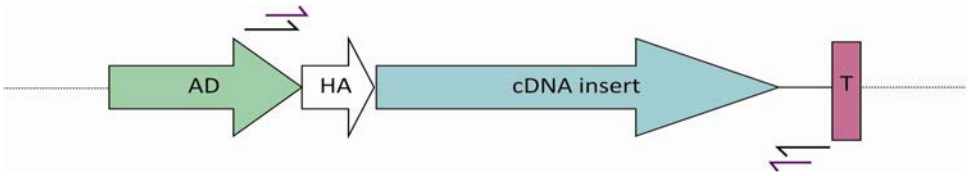

Fig. 2: Simplified scheme of prey constructs with positioning of primers used for sorting and sequencing of cDNA inserts.
cDNA inserts of putative positive clones isolated from Y2H screen were sorted according to PCR products sizes resulting from amplification with primers KJ60 & KJ61 (black arrows). Clones comprising different cDNA insert sizes were subsequently sequenced using primers KJ76 / KJ77 (purple arrows). Not to scale.

Finally, 69 colonies produced positive results in PCR analysis; however, a majority of those produced more than one PCR-product, putatively correlating with the existence of more than one prey-plasmid; positive clones were categorised according

to PCR-fragment sizes. The selected yeast plasmids were shuttled into *E. coli* by electroporation using 2 - 5 µl of the yeast DNA extract (selection on LB + Amp for pGADT7). Following numerous attempts, 33 of 75 yeast colonies were successfully shuttled into *E. coli*, plasmid DNA was extracted as described (see 3.3.4.). From each category of fragment size, 1 to 4 putative positive colonies were sequenced (GATC, Constance). The obtained sequences for selected colonies were further analysed in depth by BLAST against the *Physcomitrella* genome database. Identified cDNA sequences were *in silico* translated into protein sequences, which were used for protein BLAST against and both the *Physcomitrella* and *Arabidopsis* non-redundant protein databases. Further *in silico* analysis comprised reciprocal BLAST on protein level, protein domain and motif analysis (CDD and SMART), subcellular localisation predication (Wolf P-SORT) and phylogenetic analysis (see 3.7.5.).

3.4.9. Preparation of PCB

100 g *Spirulina* pellets were ground to fine powder which was then taken up in 1 l of Cyanobuffer under constant stirring in a light-proof Erlenmeyer flask for at least 5 h. Subsequently the *Spirulina*-mash was clarified by centrifugation (5,000 g, 15 min). The volume of the soluble fraction was determined and kept light-proof, the pellet was discarded. Ammonium sulfate of appropriate amounts (0.37 g / 1 ml *Spirulina*-solution) was ground and added to the solution. Following complete dilution of the ammonium powder, the solution was kept light-proof for 16 h at 4 °C. Thereafter, the light-blue *Spirulina*-solution was centrifuged (6,000 g, 4 °C, 30 min). In dim green-light conditions (540 nm) the supernatant was discarded, the pellets were resuspended in ice-cold methanol with a homogeniser (ART *Labortechnik*). This was repeated until the supernatant was of clear light-blue colour. Pellets were then methanolysed in 400 ml methanol and slowly stirred for 16 h at 54 °C under light-proof conditions. Methanolysed PCB was separated from other proteins by centrifugation (5,000 g, 4 °C, and 15 min). Resulting pellets were again methanolysed as described above, meanwhile the clear dark blue supernatant was stored at -80 °C. Supernatants of both menthanolysis steps were united and volume was reduced to approx 30 ml by vacuum evaporation. PCB purity and concentration was determined spectral photometrically in methanol solution. To determine PCB concentration an absorption coefficient of 37.9 $mM^{-1} \cdot cm^{-1}$ at 690 nm was used. Further purification, if needed, was achieved by reverse phase chromatography.
Yeast media for light-dependent interaction assays usually contained 30 µM for solid media and 20 µM for liquid media. Before adding PCB to the medium, PCB solution was sonicated for 1 min and added to hand-warm medium after autoclaving.

3.4.10. Light dependent Y2H interaction assay on PCB-selection medium

In a first attempt, interaction in yeast was confirmed by independent cloning the cDNAs of putative interacting proteins from *Physcomitrella* mRNA into Y2H prey vectors; table 6 gives an overview.

Table 7: Cloning of prey constructs for interaction validation in yeast.

Gene	Vector	Restriction enzyme
Pp.PHOTA1	pGADT7	EcoRI & ClaI
Pp.PHOTA2	pGADT7	ClaI
Pp.PHOTB1	pGADT7	ClaI & SacI
Pp.PHOTB2	pGADT7	BamHI
Pp.EF1α	pGADT7	ClaI & SacI
Pp.PLP	pGADT7	ClaI & SacI
Pp.PRL1	pGADT7	ClaI & SacI
Pp.Pirin	pGADT7	EcoRI & ClaI

To test for light dependent interaction with phy4 yeast colonies also containing the putative interacting partners were pre-selected on 3DO selection medium. One colony of interest was used for inoculation of a liquid overnight culture in 3DO medium. Cell density was determined by counting with the help of a *Fuchs-Rosenthal*-chamber. In a quantitative approach 2.5 x 10^5 cells were spotted on different selection media: 2DO to test for growth conditions, 3DO and 4DO, either with or without 30 µM PCB (all of which containing an appropriate amount of 3-AT). Thereafter cells were incubated for 4 d at 30 °C under light conditions as appropriate (R 0.7 µmol · m^{-2} · s^{-1}, FR 3.0 µmol · m^{-2} · s^{-1} or B 0.7 µmol · m^{-2} · s^{-1}). Colony growth was documented by photography after 4 d.

3.5. Moss

3.5.1. Moss cultivation

Axenic *Physcomitrella* cultures were grown on cellophane-overlaid BCE225 medium under long day conditions. Mutant lines were kept on BCE225 additionally containing the respective antibiotic to maintain selection pressure. Long-term cultures were transferred to fresh BCE225 medium every 6-8 weeks.
A small liquid BCE225 culture (approx. 25 ml) was inoculated with filament cells from solid BCE225 medium to grow larger amounts of fresh *Physcomitrella* filaments, as needed for transformation purposes or physiological analysis, a small liquid BCE225 culture (approx. 25 ml) was inoculated with filament cells from solid BCE225 medium. To reduce formation of gametophores liquid cultures were shortly homogenised with the help of an Ultra-Turrax (T18 basic Ultra-Turrax, IKA, Staufen, Germany) twice a week. After having reached sufficient cell density (after 10 - 14 d) filaments were transferred into 200 ml liquid BCE225 for further growth. Such cultures were used up to 4 weeks. In this case BCE225 medium was renewed every 10 - 12 d.

3.5.2. Protoplast isolation and transformation

Protoplasts were isolated from fresh *Physcomitrella* filament culture by driselase digestion under sterile conditions. 2 x 500 mg of cells were harvested and shortly dried from residual medium, thereafter transferred into 2 petri dishes and incubated in 0.5 % freshly prepared Driselase solution for up to 1 h. Isolated protoplasts were separated from undigested tissue by two filtration steps. A 100 x 100 µm nylon mesh was used for initial filtration. Protoplasts were simultaneously washed with 5 ml of 8 % mannitol solution and afterwards harvested by mild centrifugation (200g, 5 min).

Pelleted protoplasts were subsequently further filtrated through a 50 x 50 µm nylon mesh and washed as before. Living protoplasts were quantified by counting using a *Fuchs-Rosenthal*-chamber.
For transformation protoplasts were carefully resuspended in an appropriate amount of MMM-solution to give $1.6 \cdot 10^6$ protoplasts / ml (min. 300 µl) and aliquoted for transformation. 30 µg of sterile plasmid DNA were placed in 15 ml incubation tubes (round bottomed), 300 µl protoplasts suspension was carefully added and finally supplemented with 300 µl PEGT. Protoplasts were heat shocked for 5 min (45 °C) in a thermo block and cooled down in a water bath (RT) for 5 min. Five times 300 µl of 8 % mannitol solution were stepwise added in 5 min intervals; then five times 1 ml of 8 % mannitol solution were stepwise added in 3 min intervals. Protoplasts were spun down (200 g, 5 min), supernatant was removed and finally protoplasts were taken up in 3 - 5 ml PRML and incubated 24 h in darkness. Afterwards the supernatant was removed and protoplasts were resuspended in 2.5 ml hand-warm PRMT and dispensed on cellophane-overlaid PRMB (1 ml protoplast suspension / plate). Transformed protoplasts were regenerated in continuous white light conditions in a longday chamber until further treatments.

3.5.3. Filament transformation

The procedure of biolistic transfection is described in detail in Jaedicke *et al.* (186). In brief, after homogenisation *Physcomitrella* protonemata were transferred from liquid culture to cellophane-overlaid BCE225 solid medium and incubated for 5 d in standard cultivation conditions. Cells were incubated on BCE225 + Mannitol to reduce cells turgor pressure 5 h prior to transformation. Meanwhile micro particles were prepared. 0.5 mg gold particles (1.6 µm, Inbio Gold) were used per transformation. Particles were spun down at 9,000 *g* for 2 minutes and resuspended in 16.5 µl 50 % glycerol. 2 µg of plasmid DNA, then 10 µl of 2.5 M CaCl2 and 4 µl of 0.1 M spermidine were sequentially added with vigorous vortexing after every step. Particles were spun at 5,000 *g* for 10 s, the DNA-coated gold particles washed in 100 µl ethanol and finally taken up in 15 µl pure ethanol. Biolistic transfection was achieved using a home-made particle inflow gun (187). 15 µl particle suspension were loaded per shot into the centre of the teflon screen. The chamber was evacuated rapidly to 200 millibar (20 kPa), biolistic transfection was carried out via a single shot of helium at 9 bar (0.9 MPa). The vacuum was released immediately thereafter. Following transfection, filaments were transferred back to BCE225 medium for further incubation until observation.
Onion epidermis cells were transformed likewise, without pre-incubation on mannitol medium. Whole onion scale leaves were used for transfection, the epidermis was removed from the leaves immediately before observation.

3.5.4. Photobiological experiments

3.5.4.1. Protoplast regeneration

Following protoplast isolation and overnight recovery (see 3.5.2.), protoplasts were taken up in top layer and transferred to cellophane-overlaid PRMB medium. For regeneration of protoplasts under directional light conditions Petri dishes

were covered with glass lids overlaid with a polarising filter (commercial-quality film polarisers, grey, 25 % transmission, Edmund Optics GmbH, Karlsruhe, Germany) and placed in red light. Fluence rate (with polarising filter) was adjusted to 0.8 µmol · m^{-2} · s^{-1} using the PAR meter (see 3.6.1.). Protoplasts were regenerated under these conditions for 7-8 d. Thereafter plates were observed with the Fluo Makro and regeneration of protoplasts was documented by photography. Directionality of outgrowth was evaluated from pictures taken by using Image Tool 3.0 (UTHSCA, San Antonio, TX). Statistic analysis was done by Excel (Microsoft, Redmond, WA); to simplify presentation of directionality values measured were clustered into one class of 90° (as directionality to the E-vector was concerned only normal or parallel orientation was possibly observed). Results were presented as circular histograms using Origin 7.5 (OriginLab, Northampton, MA).

3.5.4.2. Phototropism of filaments

Thin lines (1-2 mm) of *Physcomitrella* filaments were prepared on BCE225 medium in squared Petri dishes (12 cm). 4 filament lines were placed on each half of the Petri dish with every line being inclined by approx 30° to prevent shading in directional light conditions. Prepared filaments were incubated standing upright in dark boxes for 10 d. For phototropism, filaments were placed in directional red or blue light (1.0 µmol m^{-2} · s^{-1} each) for 24 h. Bending of filament tip cells was observed with the Fluo Marko and documented by photography. Similar to protoplast regeneration experiments (see. 3.5.4.1.) evaluation of bending was done using Image tool, Excel and Origin.

3.5.4.3. Polarotropism of filaments

Filaments were prepared in thin lines as described in 3.5.4.2. Petri dishes were covered with thin glass plates overlaid with polarising filters. Filaments were immediately placed in red light (0.03 µmol m^{-2} · s^{-1}) from above and grown for 7 d. Subsequently the plane of the polarising filter was turned by 45° and filaments were incubated in red light for further 24 h. Polarotropic bending of filament tip cells was evaluated as described for phototropism experiments (see 3.5.4.2.).

3.6. Light measurements

3.6.1. PAR meter

R and B were measured with a PAR-meter (Skype Quantum Sensor) connected to a voltmeter (Voltcraft M-4660A). First the dark current was determined by completely light proof shielding of the light sensor, then the sensor head was put into the light and voltage was measured. From the voltage measured dark current was subtracted and residual voltage in mV was multiplied with a factor of 3 (according to the calibration of the sensor head) to get the actual fluence rate in µmol · m^{-2} · s^{-1}. For accurate light measurement, the distance of the sensor head to the experimental base was determined and experimental conditions were height-adjusted accordingly.

3.6.2. Spectral radiometer

To measure either very low fluence rates or light beyond PAR (i.e. FR) a spectral radiometer (Ocean optics SD2000) was used with the manufacturer's software. Following calibration with a special light source, absolute intensity of the incident light was measured with the spectral radiometers sensor head (8.9×10^{-4} m^2). Output was given as number of photons per m^2 and sec; the actual fluence rate in $\mu mol \cdot m^{-2} \cdot s^{-1}$ was calculated from this as: (photons $cm^{-2} \cdot s^{-1}$) $\cdot$ ($6.022 \cdot 10^{13}$).

3.7. *In silico* analysis

3.7.1. BLAST

For identification of cDNA sequences obtained from Y2H screening, nucleotide and subsequently also protein BLAST services from NCBI (http://blast.ncbi.nlm.nih.gov/) and cosmoss (https://www.cosmoss.org/) databases were used.

3.7.2. Protein domain and motif analysis

Identified protein sequences from BLAST search were further analysed regarding conserved functional domains or motifs using CDD-database search from NCBI (http://www.ncbi.nlm.nih.gov/Structure/cdd/cdd.shtml) and SMART (http://smart.embl-heidelberg.de/) were used.

3.7.3. Subcellular localisation prediction

Prediction of protein localisation was carried out with WoLF PSORT (http://wolfpsort.org/).

3.7.4. Alignments

Alignments were done using ClustalW2 from EMBL-EBI (http://www.ebi.ac.uk/Tools/msa/clustalw2/).

3.7.5. Phylogenetic trees

As it was aimed at a comparison of the conservation of the identified proteins amongst several plant species, sequences of currently available plant model systems were aligned and one of the closest homologs of each of the model systems listed was used in phylogenetic analysis.
Phylogenetic trees were generated using Geneious Pro 4.8.5 software (www.geneious.com; (188). Trees are bootstrapped and in un-rooted presentation; distances and groupings were determined by Jukes-Cantor and Neighbour-Joining method and correspond to 500 replications. Protein distances are calculated as substitutions per site.

4. Results

4.1. Phytochrome 4 sequence analysis

Full-length phytochrome 4 cDNA was first cloned by Mittmann *et al.* in 2004, three years before the draft genome sequence of *Physcomitrella* was published (125). This *PHY4* cDNA sequence was deposited at GenBank (accession number AY123145.1), the resulting protein sequence was stored with the accession number AAM94952.1. These sequences will be subsequently referred to in the text as *PHY4*^{2004}. After having completed genome sequencing of *Physcomitrella* by the end of 2007 the full-length sequence of *PHY4* was available on the Joint Genome Institute (JGI) server (sequence version 1). Shortly thereafter a new, moss-specific database server was set up and is curated by the University of Freiburg (www.cosmoss.de), currently providing the best cultivated *Physcomitrella* sequence database (accession number of the current gene model version 6 is Pp1s164_65V6.1, with the accession numbers for both cDNA and protein sequences being identical). *PHY4* and PHY4 sequences are also found on NCBI, annotated as XM_001773498 and XP_001773550.1.

Detailed *in silico* analysis of the initially cloned *PHY4*^{2004} and the later cloned *PHY4* cDNA sequences revealed 6 single nucleotide exchanges within the original *PHY4*^{2004} sequence, all of them located within the GAF, PHY and the HKRD domain. Alignment of both *PHY4* protein sequences revealed that 4 of 6 point mutations indeed cause amino acids changes within PHY4 protein sequence, whereas 2 resemble silent mutations. Subsequent alignments with both PHYA and PHYB (see suppl. fig. 1) revealed three of these four mutations (Q388L, L471F and L579S) affect conserved residues in both phyA and phyB. The fourth detected point mutation, R1021K, concerns an arginine residue which is conserved in phyB, whereas phyA carries an asparagine at this position.

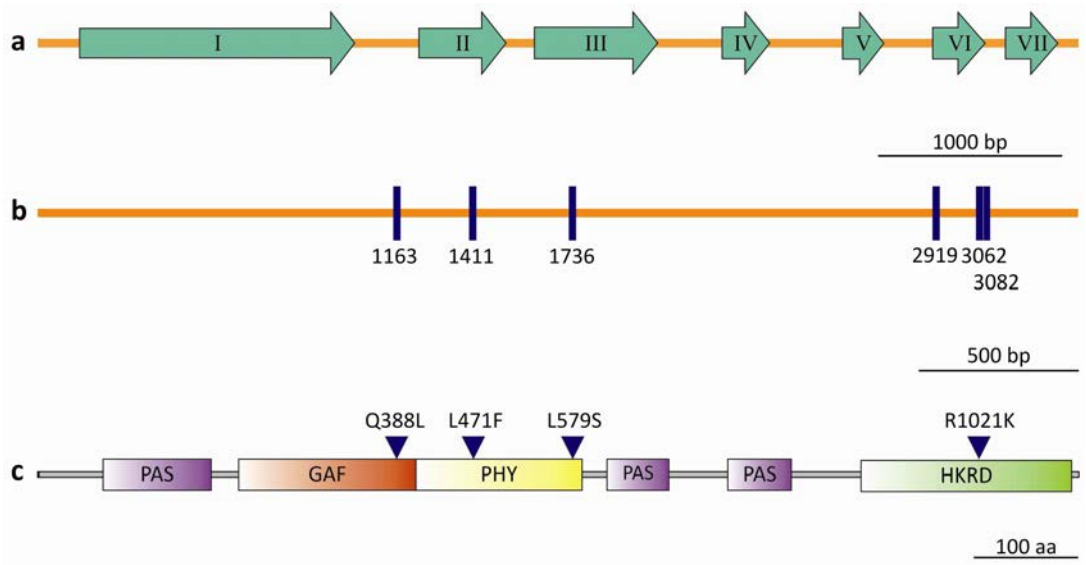

Fig. 3: Schematic representation of genomic DNA (a), coding DNA (b) and the protein sequence (c) of *Physcomitrella* phytochrome 4.

Green arrows designate 7 exons of *PHY4* gDNA (**a**). The initially cloned coding sequence of *PHY4*^{2004} contained 6 point mutations (in purple), which were identified after alignment with the genome sequence published in 2007 (**b**). Those point mutations result in four amino acid changes located at the designated positions (purple arrow heads) within the GAF, PHY and HKRD domains (**c**). Scale bars as indicated.

To verify the actual *PHY4* sequence and to exclude sequencing artefacts, a full-length *PHY4* cDNA sequence was cloned from fresh *Physcomitrella* WT mRNA. Sequencing of the resulting PCR product confirmed the *PHY4* cDNA sequence from the draft genome sequence as correct.
To investigate possible functional differences resulting from the point mutations identified in *PHY4*^{2004}, further analyses regarding light-dependent localisation of phytochrome 4 were carried out using two constructs carrying both versions, *PHY4*^{2004} and *PHY4* cDNA (see section 4.3.1).

4.2. Establishment of a transient phenotype rescue assay for *phy4*$^{-}$

4.2.1. Polarotropic outgrowth during protoplast regeneration

phy4^{-} knockout lines have been extensively investigated regarding directional R- light responses by Mittmann *et al.* To affirm the loss-of-function phenotype in directional R sensing in *phy4*$^{-}$ cells, a transient phenotype rescue assay for regenerating protoplasts was established. Regeneration of WT, *phy4*$^{-}$ and transformed *phy4*$^{-}$+ phy4^{2004}:YFP protoplasts was assayed in low (0.8 µmol·m^{-2}·sec^{-1}) and high (10 µmol·m^{-2}·sec^{-1}) fluence rates of R_{pol} and analysed in respect to (i) the directionality of the response and (ii) its dependence on the fluence rates applied.

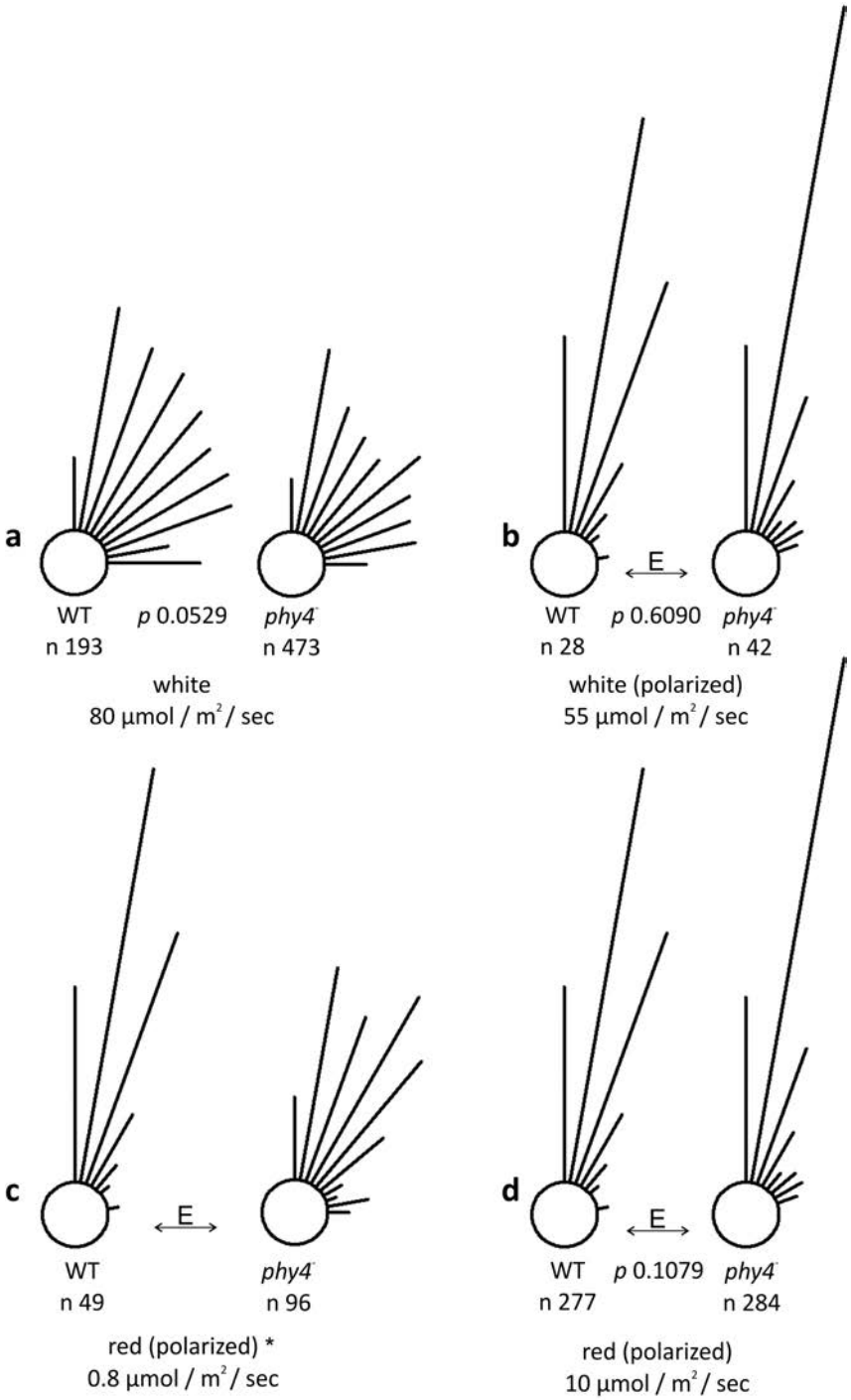

Fig. 4: R_{pol}-phenotypes of regenerating WT and *phy4*⁻ protoplasts in low and high fluence rates. In unpolarised white light, both WT and *phy4*⁻ protoplasts regenerate new filaments cells in random orientation (**a**). Under polarised light conditions direction of outgrowth was perpendicular to the orientation of the E-vector (**b**, **c**, **d**). In *phy4*⁻ protoplasts under low fluence rates (0.8 µmol·m^{-2}·sec^{-1}) this orientation is lost and regeneration occurs randomly (**c**), whereas perpendicular orientation was maintained in fluence rate conditions under 10 µmol·m^{-2}·sec^{-1} (**d**). *p*-values of student's t-tests are given, statistical significance ($p < 0.05$) is indicated by an asterisk (**c**). Orientation of the E-vector as indicated.

In unpolarised light conditions, filament outgrowth resulted in random orientation of both WT and *phy4*⁻ protoplasts. Under all polarised light conditions tested, WT protoplasts directed filament outgrowth in perpendicular orientation to the E-vector.

phy4^{-} shows a similar polarotropic behaviour as WT in high fluence rate conditions and student's t-test proved datasets of WT and *phy4*$^{-}$ being statistically not different under such light conditions.
However, the polarotropic phenotype of *phy4*$^{-}$ is absent in low fluence rates of R_{pol} fluence rates (0.8 µmol·m^{-2}·sec^{-1}). Instead, filament outgrowth under those conditions occurs randomly. As the loss of polarotropism occurred only under low fluence rates, this phenotype resembles the phenotype observed for polarotropic responses of *phy4*$^{-}$ tip cells (9). Thus the protoplast regeneration assay confirmed the loss-of-function phenotype of *phy4*$^{-}$ regarding polarotropism and can be used for transient complementation assays of phy4.

4.2.2. Phenotypic rescue of *phy4*$^{-}$ by transient overexpression of *PHY4*^{2004}*:YFP*

An assay based on protoplast regeneration additionally opened the possibility to access a transient phenotypic rescue of the investigated R_{pol} phenotype. *phy4*$^{-}$ and WT protoplasts were transformed with *PHY4*^{2004}*:YFP* constructs and transformation was confirmed via microscopic observation of YFP fluorescence. Outgrowth of transformed protoplasts was subsequently measured and compared with untransformed control protoplasts. Indeed, expression of *PHY4*^{2004}*: YFP* in *phy4*$^{-}$ leads to enhanced polarotropic filament outgrowth in low fluence rate conditions, similar to WT. Under the same conditions, polarotropic regeneration was strongly reduced in *phy4*$^{-}$ (see fig. 4). This further supports the role of phy4 in responses to R_{pol} and confirms the functionality of phy4^{2004}:YFP as a functional photoreceptor-fusion.

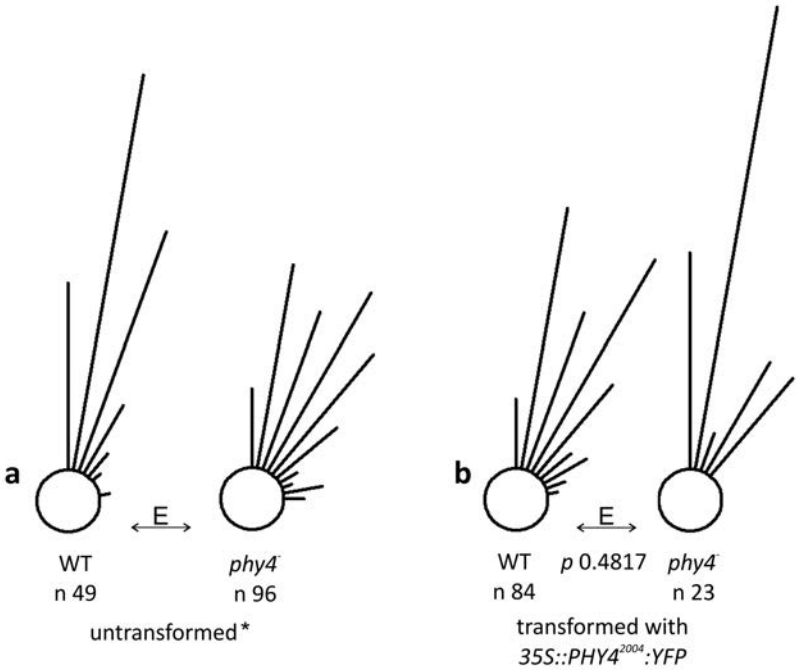

Fig. 5: Transient phenotypic rescue of *phy4*$^{-}$ protoplasts under low fluence rates (0.8 µmol · m^{-2} · sec^{-1}) of polarised red light.
The inability of *phy4*$^{-}$ protoplasts to direct outgrowth of regenerated filament cells towards the E-vector (**a**) can be abolished by overexpression of PHY4:YFP (**b**). *p*-values of student's t-tests are given, statistical significance ($p < 0.05$) is indicated by an asterisk (**a**). Orientation of the E-vector as indicated.

4.3. Localisation studies of fluorescently tagged phytochrome 4 fusion proteins

Higher plant phytochromes have been extensively studied regarding their light dependent localisation (65, 66, 68). Both phyA and phyB were shown to translocate to the nucleus in an R dependent manner, which led to the model of phytochrome functioning primarily through transcriptional regulation within the nucleus (75). Since moss phytochromes regulate physiological responses which are clearly connected to a cytoplasmic and putatively membrane bound localisation, a detailed analysis of phy4's *in vivo* localisation is of great interest. Fluorescent tags were fused either N- terminally or C-terminally to full length *PHY4* cDNAs. Both cDNAs (*PHY4*^{2004}and *PHY4*) were investigated regarding the localisation of the resulting fluorescent fusion proteins.

4.3.1. Light dependent localisation of C-terminally tagged phy4 fluorescent fusions

Previous work on phyA and phyB localisation was done exclusively using C-terminally tagged fusions, probably due to the fact that phyA was shown to contain functionally relevant parts within its N-terminal domain (189, 190). From the first phytochrome crystal structures it is now known that the structural integrity of both the extreme N-terminus and the photosensory module is fundamental to the photoconversion mechanism of phytochrome (44, 191). Moreover it has been shown that phytochromes comprise a figure-of-eight knot within their N-terminal modules (44, 46, 47). Although it is unknown how this complicated structure is achieved exactly, it can be assumed that further extension of the N-terminus may complicate knot-formation. Thus, it is assumed that C-terminal fusions have a lesser potential to harm phytochrome function. To identify transformed cells and to unequivocally locate the nucleus, a red fluorescent marker protein was used, which was co-transformed with all *PHY4:YFP* constructs into filament cells. Cherry$_{NLS}$, driven by a double 35S promoter, comprises a nuclear localisation sequence (NLS) of the VirD2 protein from *Agrobacterium tumefaciens* (192), resulting in constitutive nuclear localisation of the expressed reporter (179).

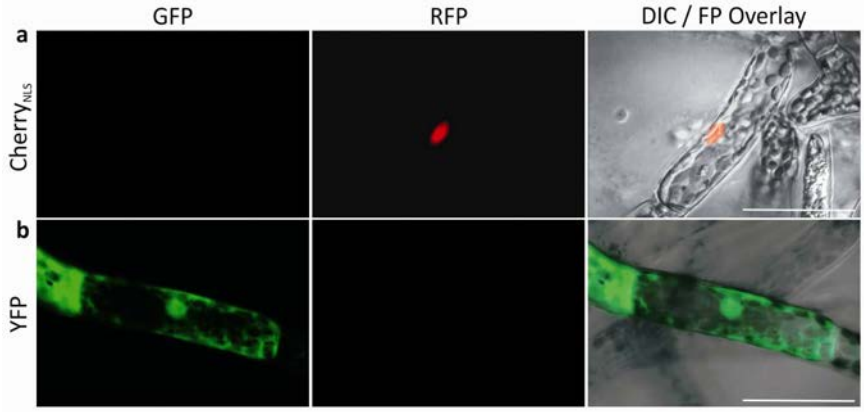

Fig. 6: Localisation of YFP and Cherry$_{NLS}$ controls.
Expression of Cherry$_{NLS}$ (**a**) results in a fluorescence signal exclusively within the nucleus. YFP fluorescence (**b**) is visible in both the cytoplasm and the nucleus. No chloroplast auto-fluorescence or other bleed through could be detected with the chosen filter cubes, even for strong fluorescence signals. Scale bars 50 µm.

Expression of both *Cherry$_{NLS}$* and *YFP* in moss filament cells shows a similar distribution as previously observed (179, 193). Cherry$_{NLS}$ was exclusively localised to the nucleus, whereas YFP was localised to both compartments, the cytoplasm and the nucleus. Although both proteins were overexpressed no bleed through-effect was observed for the filters used. Thus false positive signals are minimal and co-transformation with phytochrome fusion constructs is suitable.

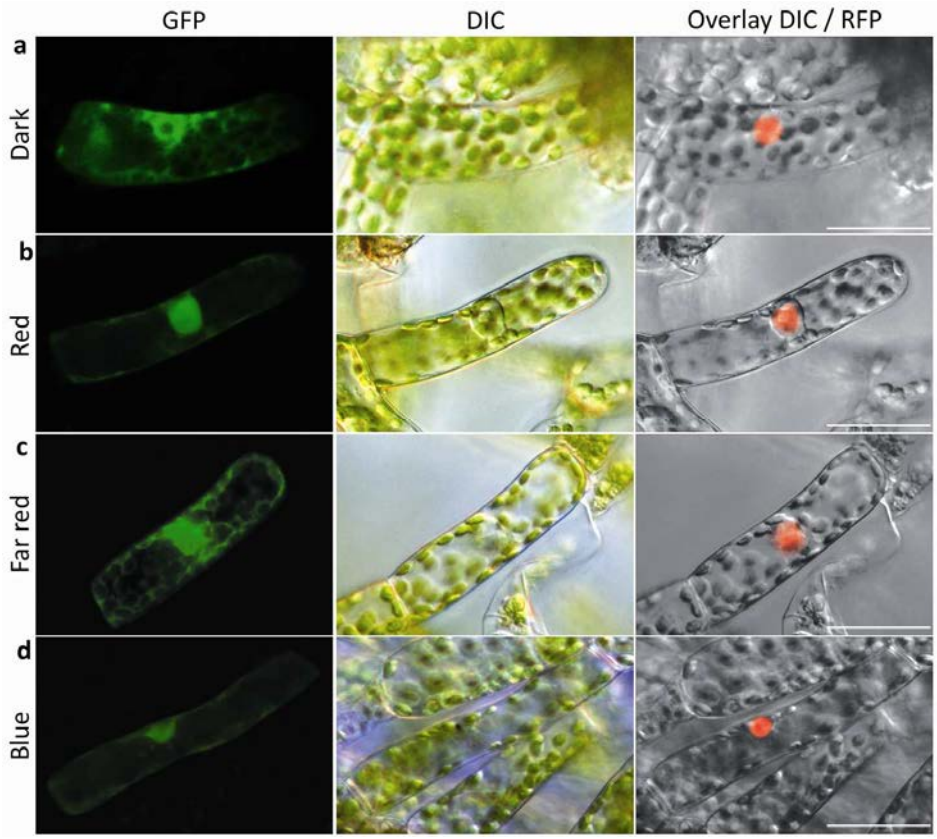

Fig. 7: Light dependent localisation of phy4^{2004}:YFP in *Physcomitrella* protonemata cells.
phy4 appeared to be localised mostly to the cytoplasm localised but showed nuclear accumulation in R and partially in FR and B. Scale bars 50 µm.

Expression of *PHY4^{2004}:YFP* in dark incubated protonemata cells lead to a strong fluorescence signal located to the cytoplasm. A possible nuclear accumulation in dark conditions was not unequivocally detectable from this data, but cannot be generally excluded. Likewise, expression of *PHY4:CFP* resulted in localisation of the fusion protein to both the cytoplasm and the nucleus in all light conditions tested (Fig. 7).

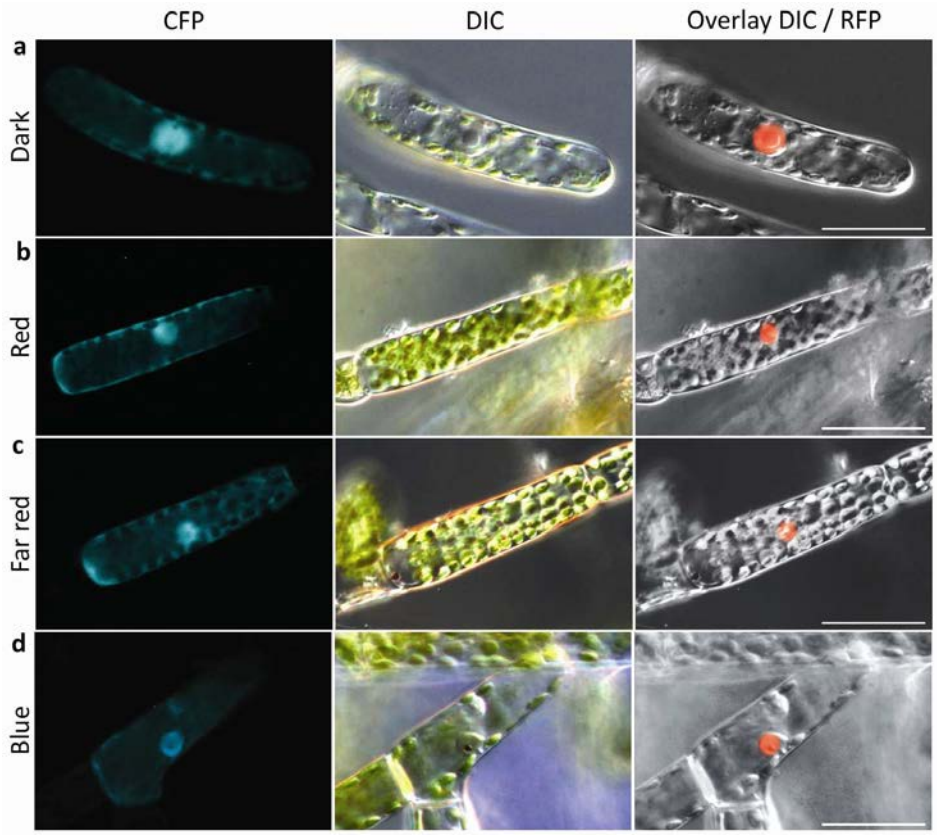

Fig. 8: Light dependent localisation of phy4:CFP in *Physcomitrella* protonemata cells.
phy4 appeared predominantly localised to the cytoplasm and showed partial nuclear accumulation under all light conditions. Scale bars 50 µm.

Both phy4 species are mainly localised to the cytoplasm and show weak nuclear accumulation independent of light. This is in contrast with Arabidopsis phyA and phyB, which migrate light dependently into the nucleus (65), Figure 10). A potential enhancement of nuclear accumulation in R and FR light, as seen for phy4^{2004} is not as pronounced in case of phy4:CFP.

4.3.2. Light dependent localisation of N-terminally tagged phy4 fluorescent fusions

Since phy4^{2004} and phy4 did not show significant differences concerning their light dependent localisation pattern when C-terminally fused to a FP-tag, N-terminal fusions of *PHY4* cDNA only were constructed and tested for their subcellular localisation.

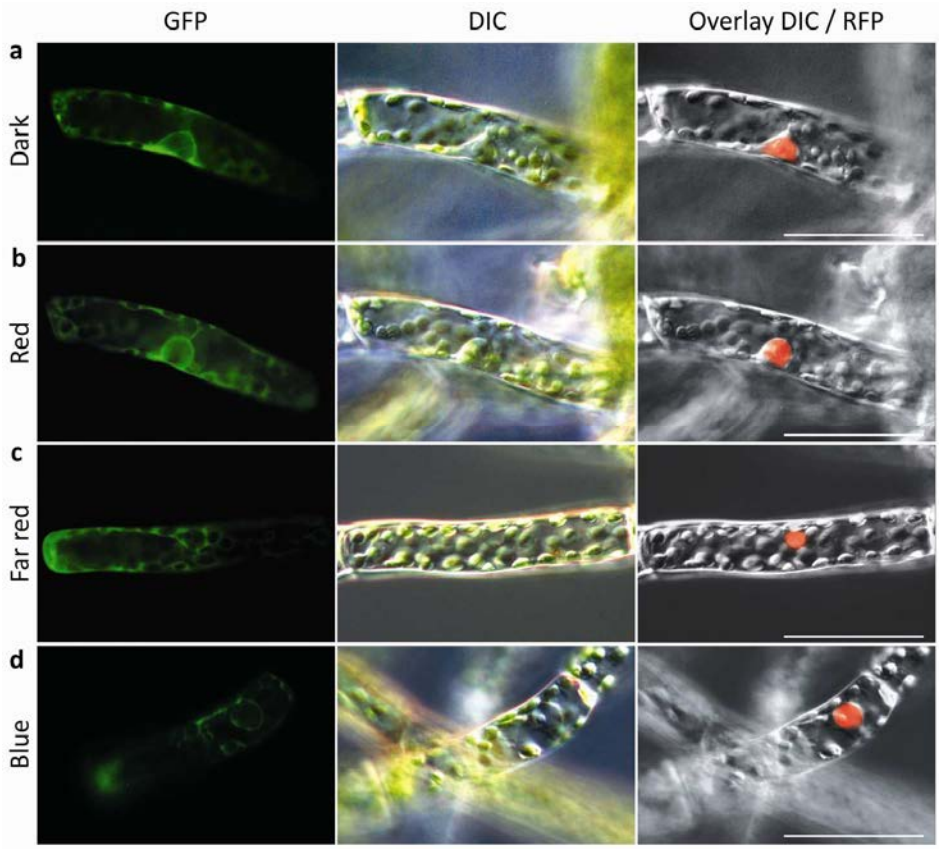

Fig. 9: Light dependent localisation of GFP:phy4 in *Physcomitrella* protonemata cells.
N-terminally tagged phy4 is strictly localised to the cytoplasm, no nuclear accumulation is apparent under all light conditions tested. Scale bars 50 µm.

Intriguingly, GFP:phy4 localised strictly to the cytoplasm under all light conditions tested. No nuclear accumulation of the fusion proteins was observed; instead the nuclei were surrounded by a strong cytoplasmic fluorescence signal, similar to a corona. This localisation pattern is obviously different from C-terminally tagged phy4 and different to any described localisation pattern of C-terminally tagged higher plant phyA or phyB. Adding a reporter protein to the phy4 N-terminus blocks nuclear import phy4. As these fusion constructs have not been tested in a transient complementation assay, the functionality and integrity of the photoreceptor is unknown and might also be compromised.

4.3.3. Localisation of phy4 fluorescent fusion proteins within higher plant cells

Having observed partial nuclear accumulation of phy4 fluorescent fusion proteins in *Physcomitrella* cells, nuclear translocation of phy4 was investigated in higher plant cells. To gain insight into a possible nuclear import mechanism, phyA and phyB localisation were accordingly observed for their light dependent translocation behaviour in *Physcomitrella* cells (see figs. 14 and 15).

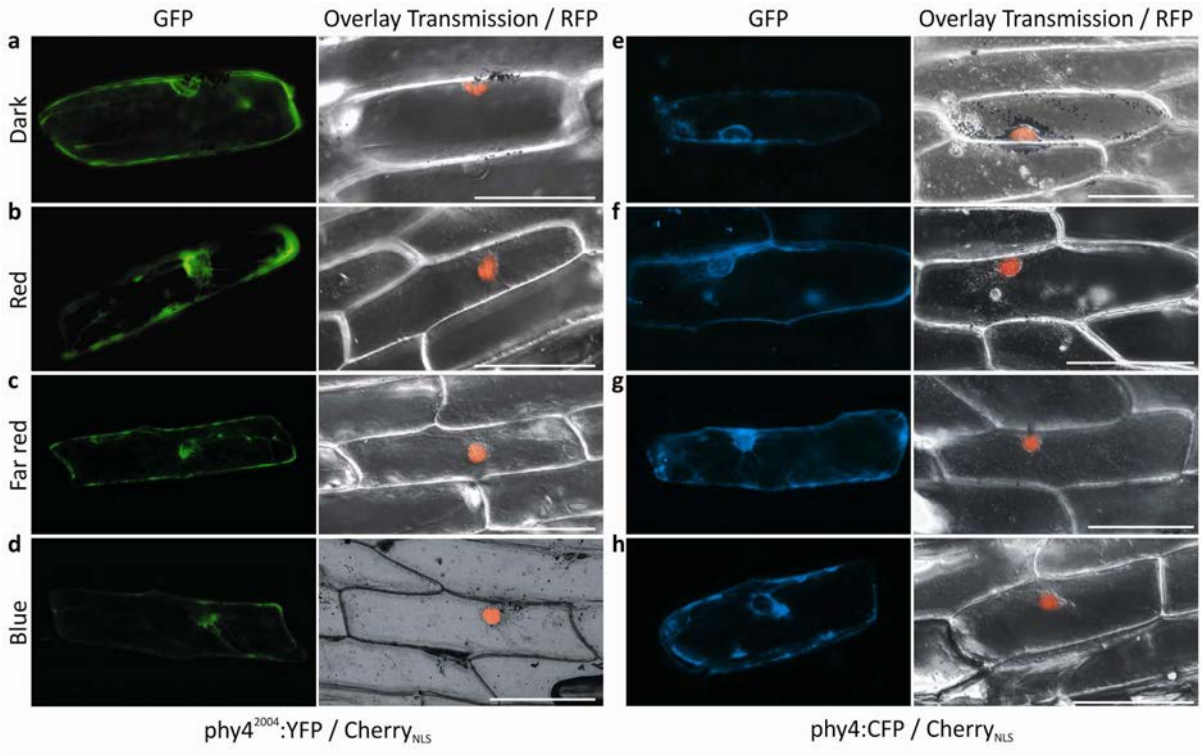

Fig. 10: Light dependent localisation of phy4^{2004}:YFP and phy4:CFP in onion epidermis cells.
Both C-terminally fused phy4 species were localised exclusively to the cytoplasm under all light conditions tested. Scale bars 100 µm.

Both phy4^{2004}:YFP and phy4:CFP localised exclusively to the cytoplasm in onion epidermis cells under all light conditions tested. Cytoplasmic strands were well depicted in the cell periphery and appeared densely around the nucleus. Thus, phy4 localisation in higher plant cells is different from the localisation pattern observed in *Physcomitrella*, where partial nuclear translocation of the same fusion constructs was observed (see Figs. 7 and 8).

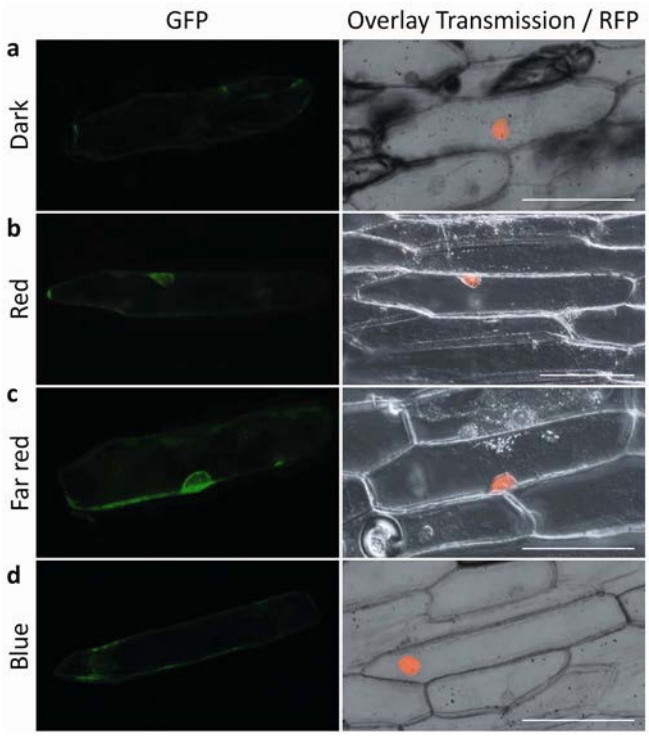

Fig. 11: Light dependent localisation of GFP:phy4 in onion epidermis cells.
N-terminal fusions of phy4 to GFP resulted in strict cytoplasmic localisation in all light conditions tested. Scale bars 100 µm.

The N-terminal fusion GFP:phy4 is also localised exclusively to the cytoplasm, as previously observed in *Physcomitrella* protonemata cells. Therefore, phy4 can generally be considered not to be translocated to the nucleus in higher plant cells, regardless of the position of the fusion tag. Since the ability of the fusion proteins to enter the nucleus was demonstrated in *Physcomitrella* cells, either a specialised phy4 import mechanism is present in moss cells, which is significantly different from higher plant phytochrome import mechanisms, or higher plant nuclei have fundamentally different properties from lower plant nuclei, e.g. such as exclusion limits. The possibility exists that phy4 is actively exported from the nucleus of higher plants but not from those of lower plants, although we consider this unlikely.

4.3.4. Light dependent localisation of N-terminally tagged phyA and phyB fluorescent fusions

Since N-terminally tagged phy4 fusions showed a complete abrogation of nuclear translocation, the ability of nuclear translocation of other N-terminally tagged phytochromes was investigated. Onion (*Allium cepa*) epidermal cells were transiently transformed with *GFP:PHYA* or *GFP:PHYB*. To control the ability of light dependent nuclear accumulation, C-terminally fused *PHYA:GFP* and *PHYB:GFP* constructs were also transformed into onion epidermis cells.

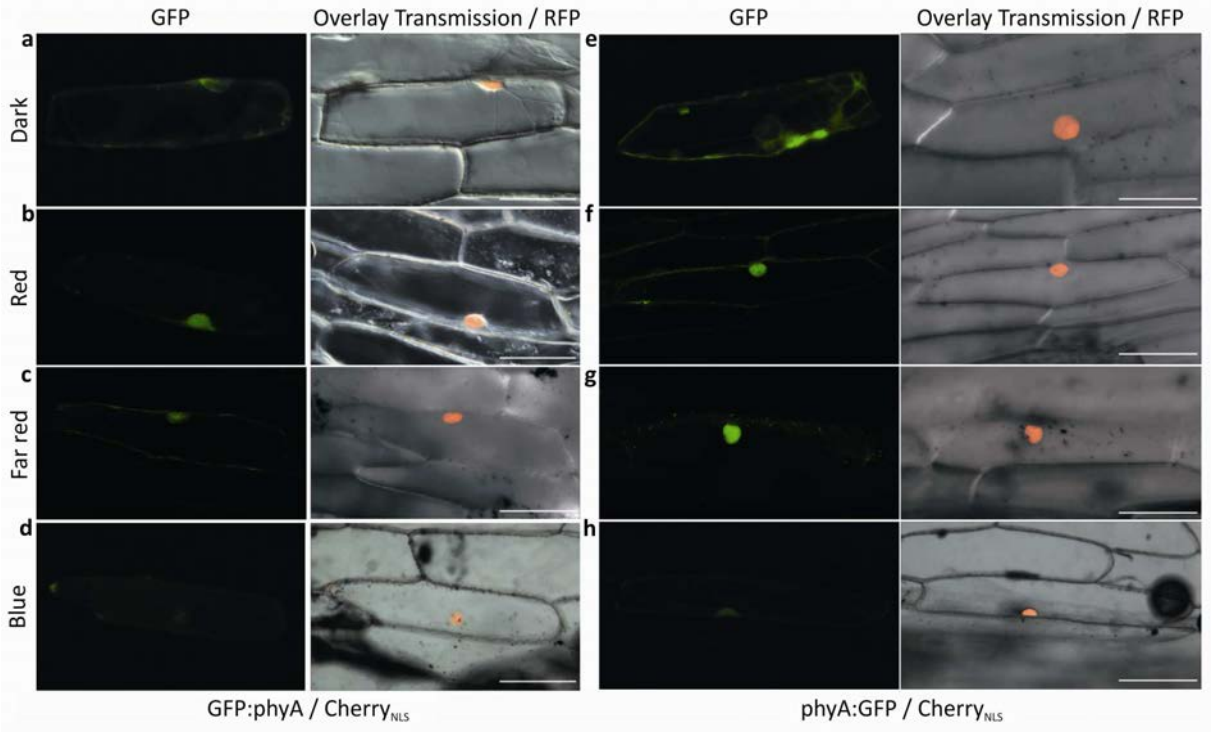

Fig. 12: Light dependent localisation of N- and C-terminally tagged phyA.
Both N and C-terminal fusions of GFP to phyA result in light dependent nuclear accumulation of the photoreceptor under red and far red light. Scale bar 100 µm.

Expression of *PHYA:GFP* (right panel) showed R and FR dependent localisation to the nucleus. No nuclear but exclusively cytoplasmic localisation was seen in darkness, and only a weak fluorescence signal in the nucleus could be observed after B irradiation. Remarkably, the position of the GFP-tag did not affect phyA's ability for light dependent transport into the nucleus: both GFP:phyA and phyA:GFP show R and FR induced translocation to the nucleus. These results contrast *Physcomitrella* phy4, for which localisation is sensitive to the positioning of the tag in the fusion protein (Figs. 6 and 7).

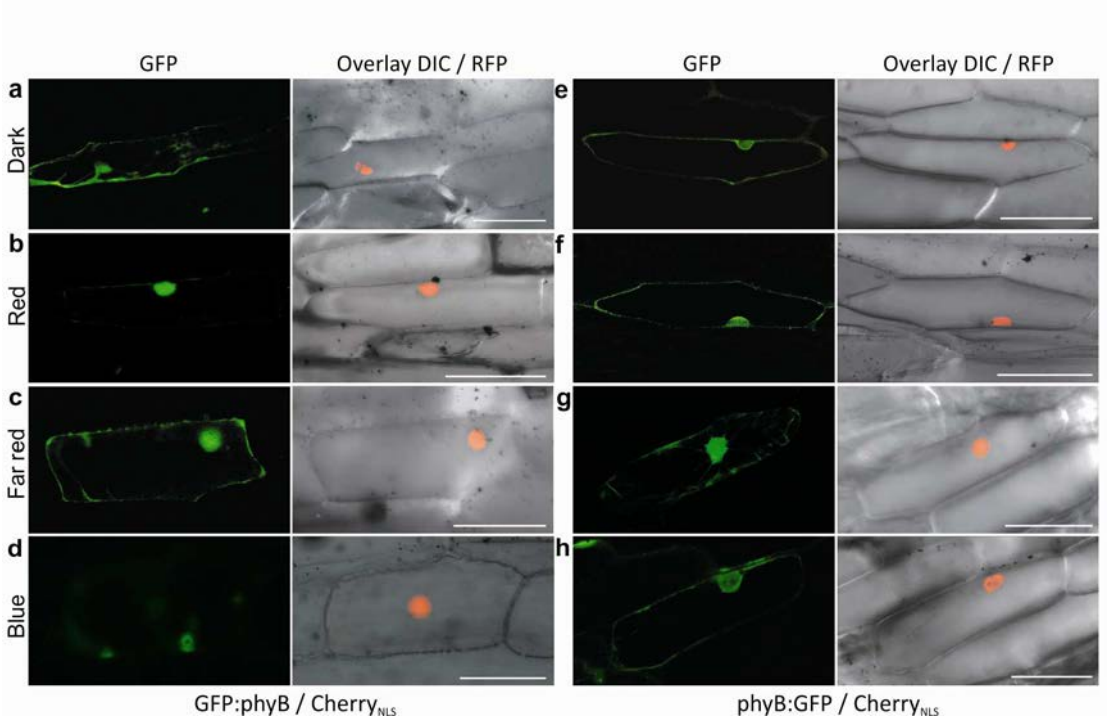

Fig. 13 Light dependent localisation of N- and C-terminally tagged phyB.
Both N- and C-terminal fusions of GFP to phyB result in light dependent accumulation of the photoreceptor in the nucleus under R and FR. Scale bars 100 µm.

Similar to phyA, phyB:GFP fusion proteins were also subjected to localisation studies in onion cells. phyB:GFP was almost exclusively localised to the cytoplasm in both D and B conditions, whereas strong accumulation of the fluorescence signal was seen after R illumination. Even in continuous FR conditions a fluorescence signal within the nucleus could be observed after 1 hour time, although a considerable cytoplasmic signal remained. As for phyA, the positioning of the GFP-tag did not affect light dependent nuclear translocation of phyB in onion cells. The localisation of GFP:phyB was equivalent to phyB:GFP.
Taken the results together, the N-terminal positioning of the GFP-tag only affected localisation of phy4 in *Physcomitrella*. All three phytochromes investigated, phyA, phyB and phy4 showed nuclear translocation when C-terminally fused to a fluorescence tag and expressed in their respective native cells types. Generally no nuclear translocation of phy4 was seen in higher plant cells.

4.3.5. Light dependent localisation of phyA in *Physcomitrella* protonemata cells

Since in higher plants cells the localisation pattern of phy4 was considerably different from the localisation pattern of the same constructs within *Physcomitrella* cells, comparable localisation of higher plant phytochromes was investigated in lower plant cells. To address this question, fluorescently tagged phyA and phyB were transformed transiently into *Physcomitrella* cells. This experiment was part of a bachelor thesis project under my supervision; data shown for R and FR conditions were obtained by Milva Mateblowski.

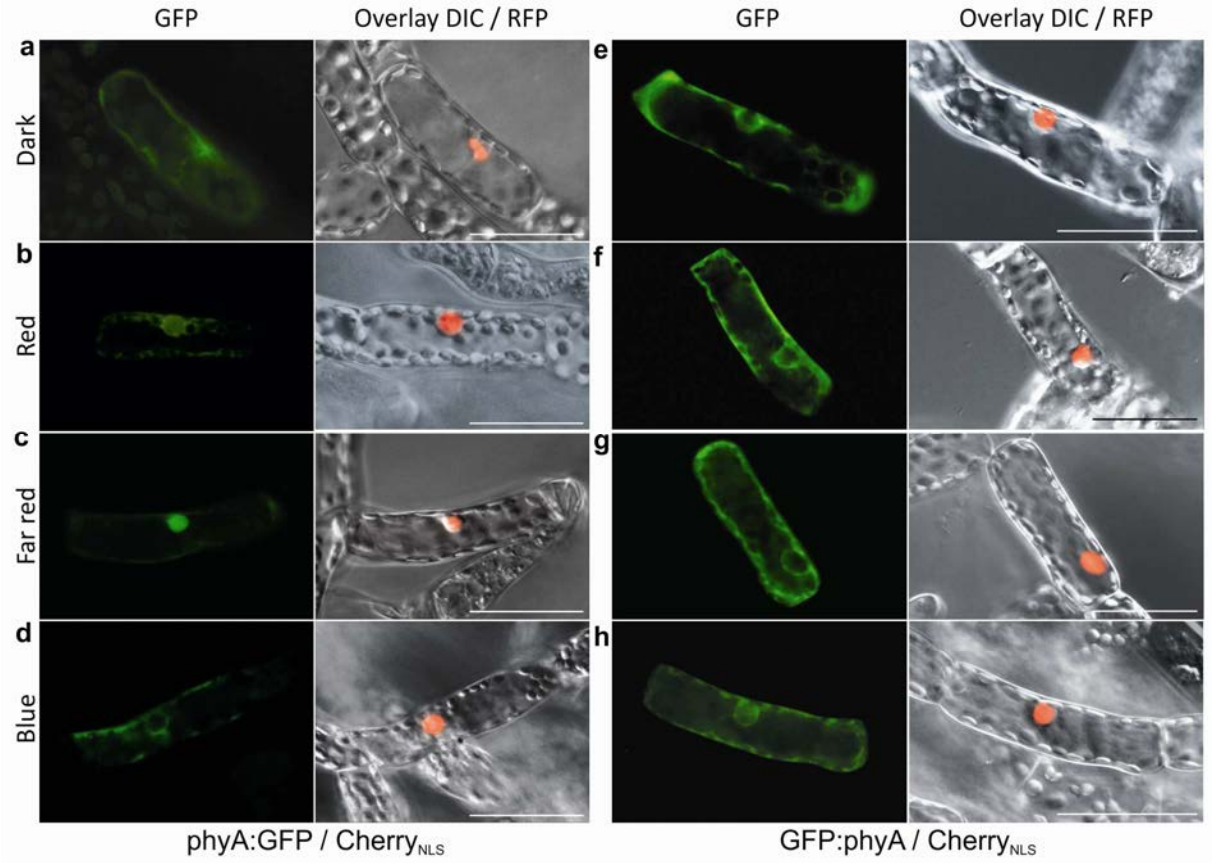

Fig. 14: Light dependent localisation of N- and C-terminally tagged phyA in *Physcomitrella* filament cells.
phyA:GFP shows light dependent accumulation within the nucleus in R- and more pronounced in FR-light, whereas GFP:phyA fusions loose their ability to enter the nucleus under any light condition. Scale bars 50 µm.

Surprisingly, phyA:GFP showed light dependent nuclear localisation in *Physcomitrella* filaments, as previously observed in onion cells. In darkness and under B conditions, phyA:GFP remained exclusively within the cytoplasm, whereas after R illumination a weak fluorescence signal within the nucleus arose, which became more pronounced after FR absorption. These results resemble previous findings for phyA:GFP localisation when transiently expressed in onion epidermal cells (see Fig. 12). However, GFP:phyA was exclusively localised to the cytoplasm and nuclear accumulation could not be induced by any light stimulus given. This localisation is clearly different from GFP:phyA observed in onion cells. The N-terminal fusion of PHYA abolishes the nuclear accumulation phenotype in *Physcomitrella*, similarly to the N-terminal fusion of phy4. It thus seems that nuclear translocation in *Physcomitrella* is possible for higher plant phyA and lower plant phy4 only when the N-terminus is accessible and not hindered by a GFP-tag. The import mechanism of PHY4 appears to be different from FHY1/FHL, since this transport route is principally accessible higher plants phytochromes but did not lead to nuclear accumulation of phy4 in onion cells.

4.3.6. Light dependent localisation of phyB in *Physcomitrella* protonemata cells

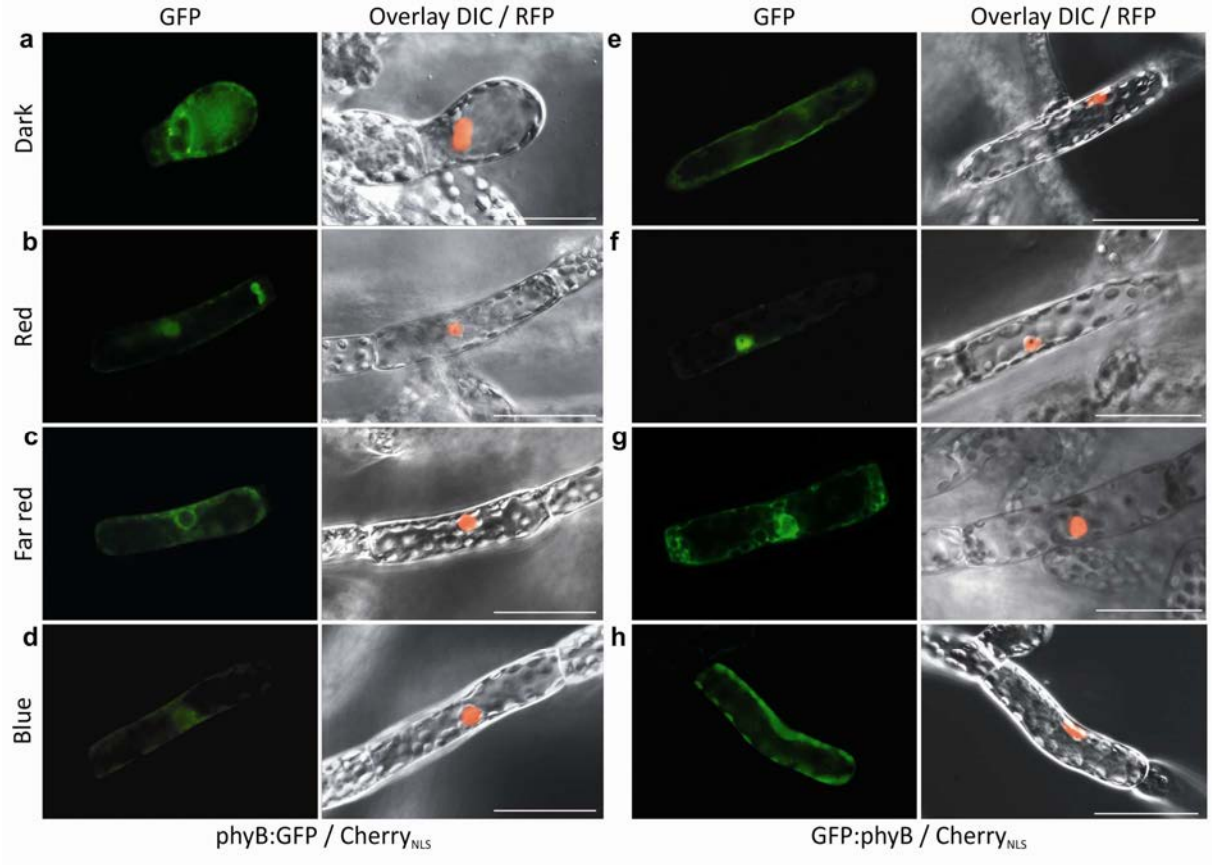

Fig. 15: Light dependent localisation of phyB:GFP in *Physcomitrella* protonemata cells.
Both N- and C-terminally tagged phyB show R-dependent nuclear translocation in *Physcomitrella*, whereas all other light conditions result in strict cytoplasmic localisation. Scale bars 50 µm.

Localisation of both phyB:GFP and GFP:phyB in *Physcomitrella* resembled the localisation pattern of phyB observed in onion cells. Both fusion constructs, phyB:GFP and GFP:phyB showed nuclear accumulation after R treatment. phyB nuclear transport was accomplished in both model systems, which is accordance with the notion that moss phytochromes are functionally more related to the light stabile type-II class phytochromes to which phyB belongs. However, phy4 was under no conditions able to enter the nucleus in higher plant cells. Thus it has to be assumed that phy4 nuclear transport is also different from the transport mechanism of phyB, which is thought to be brought about by unmasking of a cryptic NLS (74).

Comparison of the localisation data resulting from the expression of either phyA or phyB in *Physcomitrella* showed that phyA nuclear transport worked in *Physcomitrella* as reliable as it did in onion epidermal cells (Fig. 10). PHYA:GFP exhibited the well established R/FR- dependency of nuclear translocation in both model systems. Thus, a functionally conserved nuclear transport mechanism has to be available in *Physcomitrella*. Nuclear transport in *Physcomitrella* seems to be dependent on a freely accessibly N-terminus of phyA and phy4 but not phyB. However, the actual FHY1-based nuclear transport of phyA in higher plant cells appears to be different from the *Physcomitrella* system, as phy4 was not nuclear translocated in higher plant cells.

4.4. Identification of putative phy4 interacting partners by Y2H library screening

The work presented aimed to identify phy4 interacting partners, particularly such proteins involved in either (i) the probable cytoplasmic signaling pathway of phy4 and / or (ii) the hypothesised fixation of phy4 at cellular structures enabling phytochrome anisotropy as required for the directional light sensing competence of phy4. To identify qualifying interacting proteins, Y2H approaches were employed.
As expression of any full-length phytochrome generally proved difficult in the past, two further phy4 partial constructs, comprising either the full N-terminal photosensory module or the complete C-terminal transmitter module, were constructed additional to the full-length protein for expression in yeast cells.

4.4.1. Construction and expression of PHY4 bait constructs in yeast

For determination of sites suitable for construction of phy4 partial constructs sequences of all known *Physcomitrella* phytochromes were aligned and conserved residues of both phyA and phyB were identified. Specific residues within the hinge region have previously been used for successful expression of phyA or phyB partials in plants and yeast (**a)** (194), **b)** (65), **c)** (195)). Based on comparison with phyB partial constructs used in Y2H screens (195) the equivalent site was chosen for construction of phy4 N- and C-terminal partial constructs for use in the current Y2H experiments.

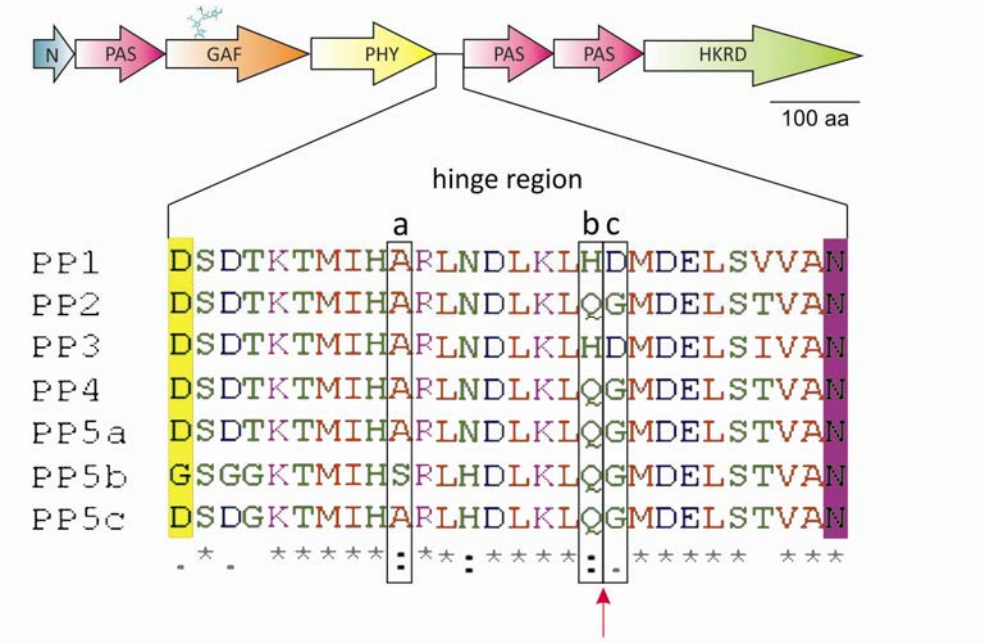

Fig. 16: Determination of suitable sites for creation of phytochrome 4 partial constructs.
ClustalW2 alignments of all *bona fide Physcomitrella* phytochrome sequences reveal a high degree of sequence conservation within the hinge region. Arrow indicates site used for creation of phy4 N- and C-terminal partial constructs. Scale bar as indicated.

The respective phy4 cDNA sequences were N-terminally fused with the GAL4-BD according to conventional Y2H approaches as proposed by Clontech's matchmaker system. The phy4_N terminal construct was cloned by Anna Lena Lichtenthäler as part of a *Diplomarbeits* project under my supervision.

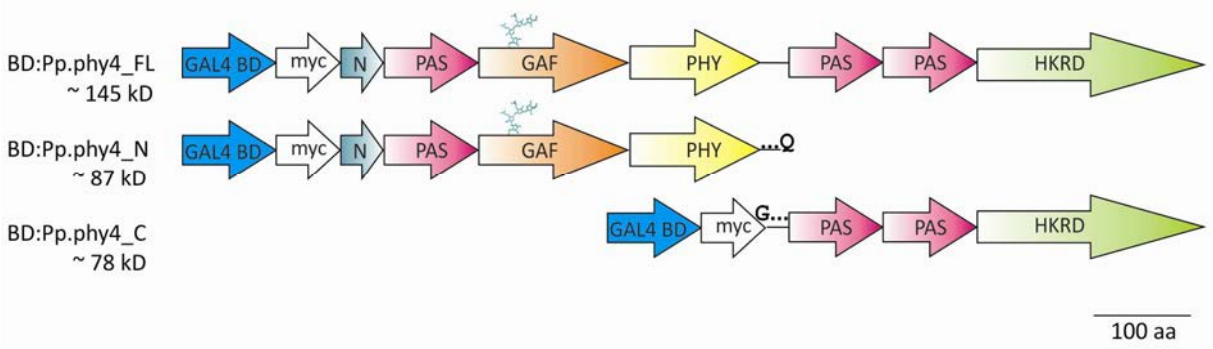

Fig. 17: Schematic of phy4 fusion proteins used as baits in Y2H experiments.
N-terminal fusions of the GAL4-BD and a myc-tag to either full-length phy4 or the N-terminal and C-terminal phy4 partial constructs are shown. No chromophor will be attached to the fusion protein comprising only the phy4 C-terminal module. Scale bar as indicated.

The bait constructs described above were transformed into yeast and following nutritional selection the expression of bait proteins was assayed by SDS-PAGE and immunodetection on western blot using anti-myc antibodies (6xmyc:At.FHY1 kindly provided by Ilse Klein was used as positive control).

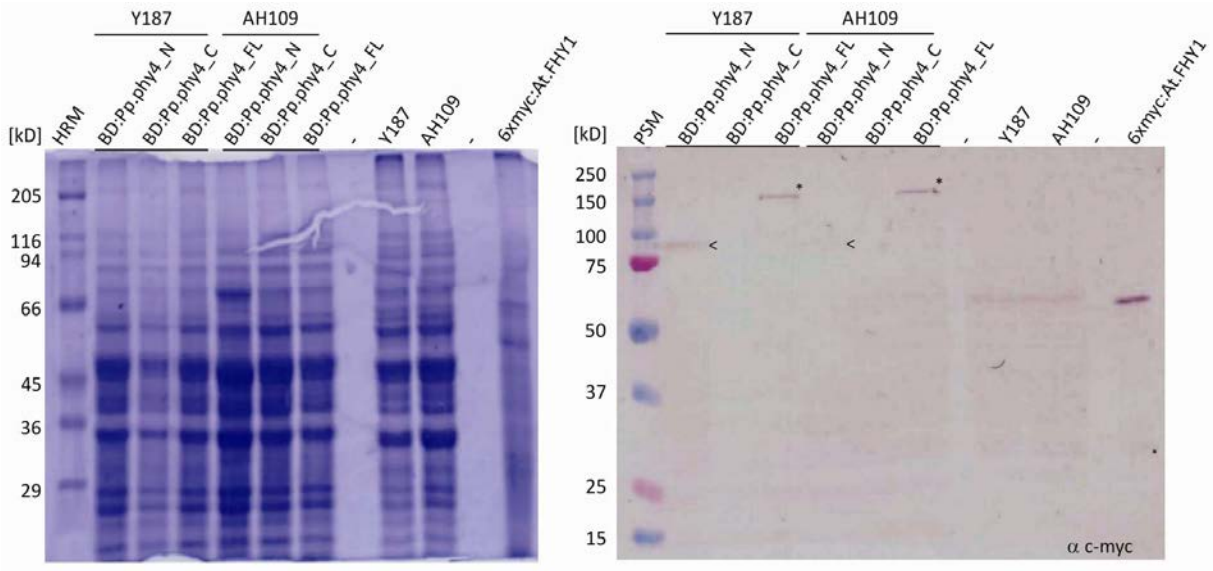

Fig. 18: Analysis of phy4 bait protein expression in two yeast strains by immunoblotting.
Signals corresponding to either BD:phy4_N or BD:phy4_FL are marked (< and *, respectively). Protein amount SDS-PAGE:WB =1:4.

Immunodetection of myc-tagged phy4 bait proteins verified expression of both the phy4 N-terminal partial and full-length phy4 in the yeast strains tested. Expression of phy4 C-terminal partial bait proteins could not be confirmed through western blot analysis. Since the expression level of full-length phy4 appeared to be unexpectedly high, the full-length phy4 construct was used for further Y2H experiments and the cDNA library screening (see 4.4.3).

4.4.2. Establishment of external and internal Y2H system controls

Although Clontech's matchmaker Y2H system comes with internal controls for specific protein-protein-interaction, those controls are only suitable as systematic controls. Therefore, advantage was taken of the light independent dimerisation of phytochromes. Phytochromes function as stable dimmers (16) and the C-terminal transmitter module was described as comprising the responsible dimerisation motifs (62). Consequently, both the full-length protein and the C-terminal partial construct should exhibit constitutive, light-independent dimerisation. To establish phytochrome dimerisation as an internal positive control, the above described phy4 constructs were cloned into the prey-vector, containing the GAL4-activation domain (AD). Upon co-expression of both phytochrome constructs, phy4 dimerisation could be established as a light independent control.

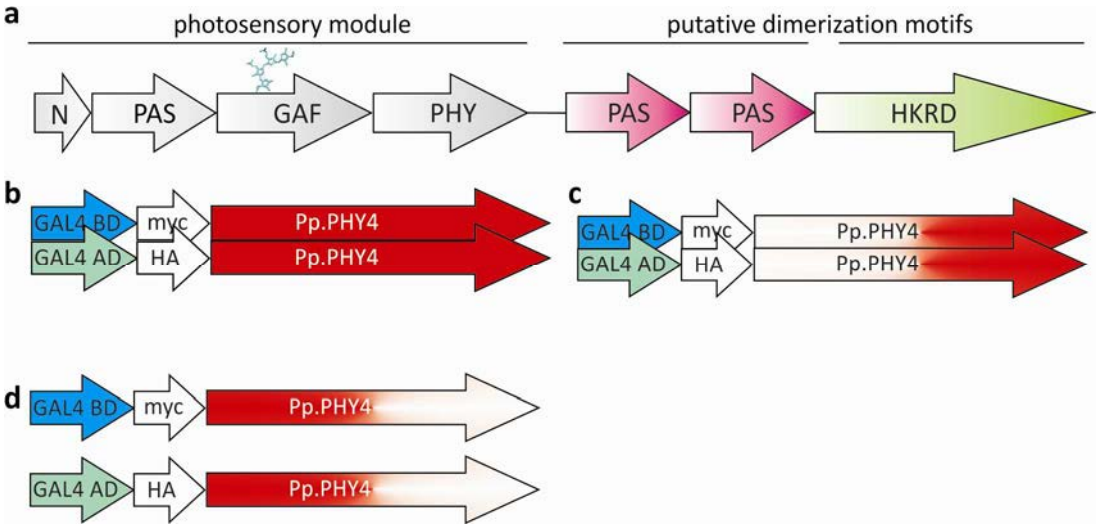

Fig. 19: Schematic of internal positive controls based on phy4 dimerisation.
Both full-length (**b**) and the C-terminal partial constructs (**c**) can serve as positive controls. N-terminal constructs lack the motif necessary for phytochrome dimerisation (**a**) and consequently will not form phy4-dimers (**d**).

Functionality of the described internal positive control was confirmed following yeast nutritional selection under both medium (TDO) and high (QDO) stringency conditions. Combinations of phy4_FL/phy4_FL and phy4_FL/phy4_C proved suitable by positive selection (see suppl. fig. 3), whereas a combination of phy4_N/phy4_N did not lead to a positive growth of colonies, as expected.

4.4.3. Isolation and identification of putative PHY4 interactors

A pretransformed cDNA library from light grown *Physcomitrella* was obtained from the MPI Cologne. To be able to cover the complete cDNA library, putatively containing the whole *Physcomitrella* transcriptome with roughly 28,000 expressed genes in all three reading frames, a minimum requirement of *ca.* 8.5 x 10^5 clones/transformation were calculated. During screening a transformation efficiency of 1 x 10^4 clones was achieved, correlating to approx. 23,500 out of 28,000 transcripts. In a 10 % approach, 1,120 colonies were transferred from medium

stringency (TDO + 2.5mM 3-AT) to high stringency selection (QDO + 2.5mM 3-AT). Of these 1,120 transferred clones, 75 putative positive clones survived the 2nd round of selection. Those yeast colonies were further kept under high stringency conditions and sorted by PCR according to the different cDNA inserts contained within the prey-plasmids. In total, it was possible to amplify PCR products from 69 out of 75 yeast colonies. PCR products were sorted according to their sizes and their abundance with which they were generated from different yeast clones. Table 8 summarises the results from PCR analysis.

Table 8: Sorting of yeast colonies isolated from Y2H screen according to the sizes of amplified PCR products from inherited prey plasmids.

PCR product approx. size [kb]	Qunatity of products with identical sizes	unique [# colony]	<3 [# colony]	>4 [# colony]
0.5	1	42		
0.75	3		7, 47, 68	
0.8	1	45		
0.9	5			2, 5, 10, 46, 52
1.0	4			37, 59, 60, 64
1.1	5			4, 24, 38, 44, 66
1.2	4			16, 31, 53, 62
1.3	1	12		
1.4	4			1, 20, 32, 48, 63
1.5	2		29, 39	
1.55	5			8, 13, 21, 40, 65
1.6	1	50		
1.7	5			3, 17, 19, 34, 67
1.8	6			9, 22, 30, 41, 43, 54
1.9	3		6, 11, 56	
2.0	5			26, 28, 36, 58, 69
2.1	5			25, 33, 49, 51, 61
2.2	2		55, 57	
2.7	1	50		
3.1	1	15		
3.2	1	18		

PCR-sorting identified 17 colonies yielding either unique (7 colonies) or a small number of different PCR products (10 colonies). In a further approach prey-plasmids of all initially sorted prey-containing colonies were shuttled into *E. coli* for further analysis. 33 of 75 plasmids were successfully isolated from yeast and shuttled into TOP10 or XL1Blue *E. coli* cells.

Table 9: Prey plasmids of yeast colonies listed were successfully shuttled into *E. coli* cells.
Selected prey plasmids were finally sequenced for cDNA insert identification (bold red).

E. coli unique [# colony]	*E. coli* <3 [# colony]	*E. coli* >4 [# colony]
	47, 68	
		2, 10, **46**
		59, 60
		44, 66
		16, 31, 53, 62
12		
		1, 20, **32**
	39	
		8, 21
		3, 17, 19, **34, 67**
		9, 30, 54
	11	
		26
		25, 33, 61

Restriction digest of isolated plasmids showed some of the transformed *E. coli* cells to contain more than one different prey-plasmid. Those were subsequently labelled regarding to their initial colony number (e.g. #1) followed by ascending numeration (e.g. #1.1, #1.2 etc.). In those cases two different populations of prey plasmids were finally sequenced.

4.4.4. *In silico* analysis of putative PHY4 interactors

Sequence data was further analysed by BLAST searches against the current version of the *Physcomitrella* nucleotide database on both the cosmoss and the NCBI database server. Alignments of the sequencing data with the CDS identified from BLAST searches revealed that 62 % of the analysed sequences were indeed represented as full-length sequences within the cDNA library, whereas the majority of the remaining 38 % missed parts of the 5 ´end.
cDNA hits were then translated into protein sequences and verified by protein BLAST against the non-redundant protein database of *Physcomitrella*. To identify *bona fide* phytochrome interacting/signaling partners it was one criterion whether or not isolated proteins share homologs in *Arabidopsis* thaliana and/or other plants. Isolated proteins were further analysed by BLAST searches of the non redundant *Arabidopsis* protein database. Identified protein sequences were further analysed regarding conserved protein domains or motifs and their predicted functions using SMART (http://smart.embl-heidelberg.de) and NCBI CDD (conserved domains database) search. The cDNA hits as well as the identified conserved domains and their related/predicted function are listed in table 10.

Table 10: *In silico* analysis of sequences isolated from Y2H screen.
Hits of outstanding interest and chosen for further analysis are marked in orange, hits of minor interest are marked in yellow. TM: transmembrane domain.

Clone	*Physcomitrella* hit	Conserved domains or motifs	Function
#1.7	predicted protein	no hits	no hits
#2.3	predicted protein	DUF151 & EpcC superfamily	heterochromatin formation
#8.5	predicted protein	GIY_YIG superfamily	class I homing endonuclease
#9.2	lipoxygenase Lox8b	PLAT, lipoxygenase	fatty acid oxidation
#10.3	40s ribosomal protein s15	ribosomal S19 superfamily	ribosome assembly
#10.7	40s ribosomal protein s16	ribosomal S19 superfamily	ribosome assembly
#11.5	60s ribosomal protein	ribosomal S19 superfamily	ribosome assembly
#12.5	proteophosphoglycan ppg1	no hits	secreted proteins of Leishmania
#16.1	predicted protein	TM & sulfotransferase domain, p-loop	phosphate binding, binding of ATP/GTP
#21.3	porphobilinogen deaminase	HMBS superfamily	porphyrin biosynthesis
#21.4	porphobilinogen deaminase	HMBS superfamily	porphyrin biosynthesis
#25.3	pore protein of 24 kd	no hits	no hits
#25.4	pore protein of 24 kd	no hits	no hits
#25.7	pore protein of 24 kd	no hits	no hits
#26.7	porphobilinogen deaminase	HMBS superfamily	porphyrin biosynthesis
#31.4	predicted protein	ACE1-Sec16 like	mediation of vesicle transport
#32.2	predicted protein	dehydrin domain	temperature, drought and salt stress
#33.7	pleiotropic regulator 1	WD40 domain repeats (7x)	adaptor/regulator in signal transduction
#34.1	cysteine proteinase inhibitor	cystatin like domain	cysteine protease inhibitor (PRL1 interactor?)
#39.3	small RuBisCO subunit	small RuBisCO multimerization interface	RuBisCO assembly
#44.4	small RuBisCO subunit	small RuBisCO multimerization interface	RuBisCO assembly
#46.3	dna gyrase subunit b	HATPase-c, TOPOII-trans-DNA-gyrase	Histidine kinase like ATPase, DNA toposiomerase
#53.2	PSAD-1	PSAD superfamily	Photosystem protein D1
#53.45	PSAD-1	PSAD superfamily	Photosystem protein D1
#54.1	elongation factor 1 alpha	Ras-like GTPase, GTP binding site, EF1a II & III	G box protein, cytosceleton binding
#59.5	small RuBisCO subunit	small RuBisCO multimerization interface	RuBisCO assembly
#61.4	pirin-like protein	Cupin2, Pirin_C	interaction with GPA1
#62.3	PSI reaction center subunit II	PSAD superfamily	Photosystem protein D1
#66.5	predicted protein	OTU superfamily	Cysteine protease
#68.6	predicted protein	no hits	no hits

As expected, a considerable number of identified sequences were related to plant housekeeping genes like 40 and 60 S ribosomal proteins, proteins related to chlorophyll synthesis or photosynthesis or membrane pores and are likely false positives. Since annotation of the *Physcomitrella* genome is still an ongoing process, a large amount of genes have not been annotated yet. If possible, such sequences were further classified according to conserved domain or motifs contained in their sequence. Following cDNA and protein identification and *in silico* analysis, protein sequences were analysed regarding their predicted subcellular localisation. Putative interacting partners may be excluded from further analysis due to localisation into compartments phytochromes do not access. Literature provides examples for predicted phytochrome interacting partners of such controversial nature (186, 196, 197). Prediction of subcellular localisation was carried out using WoLF PSORT (http://wolfpsort.org). Results are presented in table 11.

Table 11: Prediction of subcellular protein localisation of putative PHY4 interactors.
Cp: chloroplasts, Cyto: cytoplasm, Cytosk: cytoskeleton, ER: endoplasmatic reticulum, Mito: mitochondrion, Nuc: nucleus, PM: plasma membrane, Vac: vacuole. Colour code as in table 4.

Clone	*Physcomitrella* hit	Predicted Localization
#1.7	predicted protein	Mito, Nuc
#2.3	predicted protein	Nuc, Cyto, Cytosk
#8.5	predicted protein	Cp
#9.2	lipoxygenase Lox8b	Cp, Mito
#10.3	40s ribosomal protein s15	Cyto
#10.7	40s ribosomal protein s16	Cyto
#11.5	60s ribosomal protein	Cyto
#12.5	proteophosphoglycan ppg1	Nuc, Cp
#16.1	predicted protein (F10M10.190)	Cyto
#21.3	porphobilinogen deaminase	Cp
#21.4	porphobilinogen deaminase	Cp
#25.3	pore protein of 24 kd	Cp, PM
#25.4	pore protein of 24 kd	Cp, PM
#25.7	pore protein of 24 kd	Cp, PM
#26.7	porphobilinogen deaminase	Cp
#31.4	predicted protein	ER, Cp, Vac, Cytosc, Nuc
#32.2	predicted protein	Mito
#33.7	pleiotropic regulator 1	Cyto, Nuc
#34.1	cysteine proteinase inhibitor	Cyto
#39.3	small RuBisCO subunit	Cp
#44.4	small RuBisCO subunit	Cp
#46.3	dna gyrase subunit b	Cyto
#53.2	PSAD-1 (photosystem I subunit D-1)	Cp
#53.45	PSAD-1 (photosystem I subunit D-1)	Cp
#54.1	elongation factor 1 alpha	Cyto
#59.5	small RuBisCO subunit	Cp
#61.4	pirin-like protein	Cyto, Nuc
#62.3	photosystem I reaction center subunit II	Cp
#66.5	predicted protein	Cp, Nuc, Cyto
#68.6	predicted protein	Cp, Mito, ER, Nuc

Although exact prediction of subcellular protein localisation is difficult, especially for organellar targeted proteins, proteins predicted to localise in other compartments as either the cytoplasm or the nucleus were formally excluded from further analysis. The following sections present putative candidates chosen from analysed Y2H screening data.

4.4.4.1. #16.1 - predicted protein containing a p-loop motif (PLP)

The sequence obtained from yeast colony #16 contained cDNA of a yet unknown "predicted" protein and was the only sequence chosen for further analysis, which could not be unequivocally identified by *in silico* analysis. The reason for it being of interest as a probable phy4 interacting partner is based on its conserved functional domain. When initially analysed in 2009, CDD search identified a C3HC4 RING zinc finger motif. Since phytochrome interacting partners containing RING type zinc fingers have been described in *Arabidopsis*, this protein appeared to make a good candidate for further analysis. As was realised, prediction algorithms changed by the beginning of 2011 (198). Using current algorithms of

CDD search and SMART-prediction both searches are to date unable to identify a RING-type zinc finger motif. Instead, a transmembrane domain located at the N-terminus and a sulfotransferase domain containing a phosphate binding loop, a so-called Walker-motif (or p-loop motif) were predicted. p-loops are made up by a sequence of GXXXXGK(T/S) resulting in a structure containing a β-sheet followed by a glycine rich loop and a α-helix (199). This motif is capable of binding ATP, or less common, also GTP at the β-γ-phosphate moiety (200) and is commonly found in nucleotide binding proteins, but also in ATP-synthases, helicases or kinases (201). Thus, the "predicted protein" identified from Y2H apparently is grouped into the superfamily of p-loop containing nucleoside triphophate hydrolyses. Plant sulfotransferases are either soluble or transmembrane proteins and transfer a sulfate group to proteins or glycosaminoglycans (202).

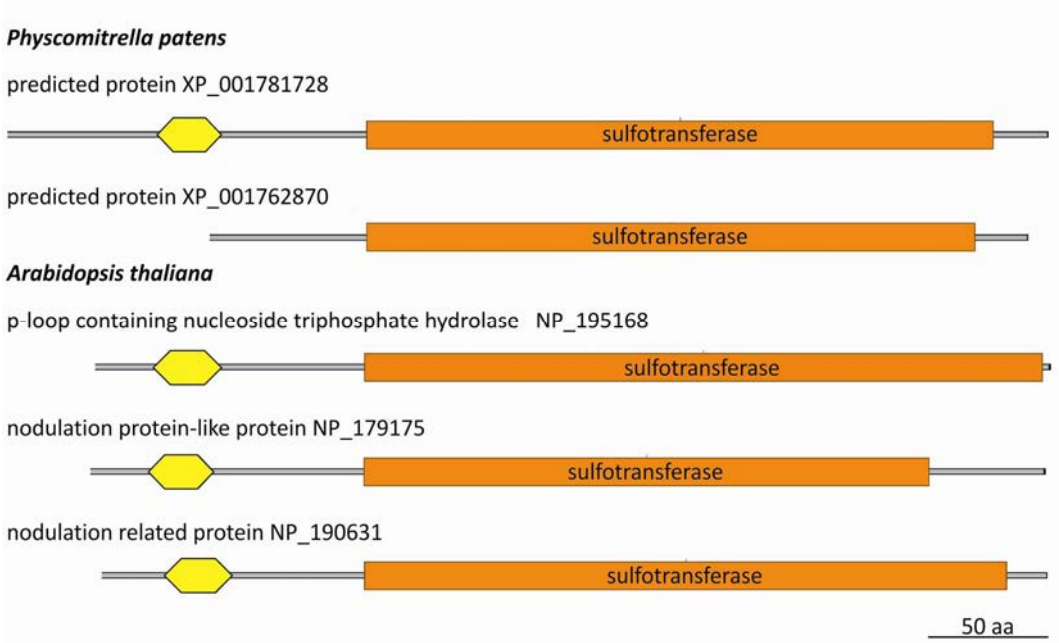

Fig. 20: Alignment of *Physcomitrella* PLP and its putative *Physcomitrella* and *Arabidopsis* homologs.
Transmembrane domains in yellow, sulfotransferase domains in orange. Scale bar as indicated.

Protein BLAST identified one close homolog in *Physcomitrella*. This protein lacks the transmembrane domain and was presumably listed due to its high degree of similarity originating from the sulfotransferase domain.
PLP contains three homologs in *Arabidopsis* with the closest homolog being designated as a p-loop containing nucleoside triphosphate hydrolyse family protein – like protein, the two remaining homologs are annotated as nodulation proteins. ClustalW2-alignment of both the *Physcomitrella* and *Arabidopsis* proteins yielded 58.5 % consensus with 42.9 % sequence identity. Additional homologs are found in several other species from lower to higher plants and theirs phylogenetic relation are depicted in suppl. figure 21.

Fig. 21: Alignment (ClustalW2) of PLP isolated from a *Physcomitrella* cNDA library and its *Physcomitrella* and *Arabidopsis* homologs.
Predicted transmembrane domains (yellow) and p-loop containing sulfotransferase domains (red) are highlighted.

4.4.4.2. #33.7 - pleiotropic regulator locus (PRL)

Although no annotation for the *Physcomitrella* protein was available at the time of BLAST searches this sequence could be assigned to the pleiotropic regulator locus 1 (PRL1) on the basis of its high homology to the respective *Arabidopsis* protein. PRL1 appears to be a single copy gene in *Physcomitrella* whereas *Arabidopsis* carries two PRL homologs, PRL1 and PRL2. CLUSTALW2 alignment of Pp.PRL with At.PRL1 and At.PRL2 yielded 64.8 % consensus with 27.3 % sequence identity.

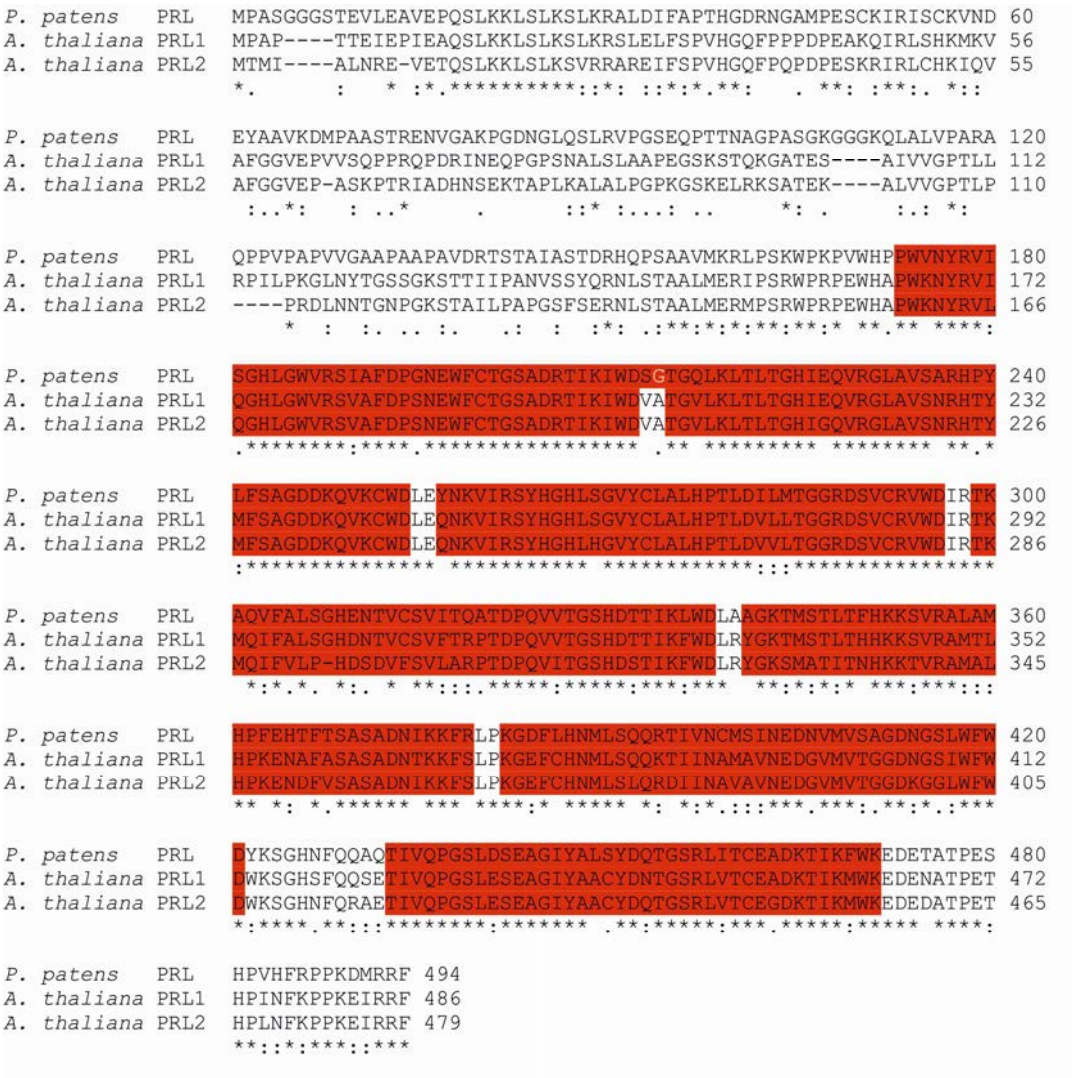

Fig. 22 Alignment (ClustalW2) of PRL isolated from a *Physcomitrella* cNDA library and its *Arabidopsis* homologs PRL1 and PRL2.
WD40 repeats are highlighted in red.

SMART analysis of both the *Physcomitrella* and the *Arabidopsis* protein sequence revealed a 7 x repeat of a WD40 motif, structurally forming a circular 7 sheeted beta-propeller (203). Commonly WD40-domain proteins function as platforms in multi-protein-complex assembly, with the propeller serving as a rigid scaffold for protein-protein-interactions, as in the case of the β-subunit of heterotrimeric G-proteins or E3-ubiqitin ligases. As such, WD40-domain proteins mostly serve in signal transduction or transcriptional regulation (204, 205). Other than the WD40-motifs, no particular domains or motifs were identified.
Protein BLAST identified PRL-homologs in many different plant species (see suppl. fig. 5); all of which were single copy genes with the exception of *Arabidopsis thaliana*, which bears two copies.

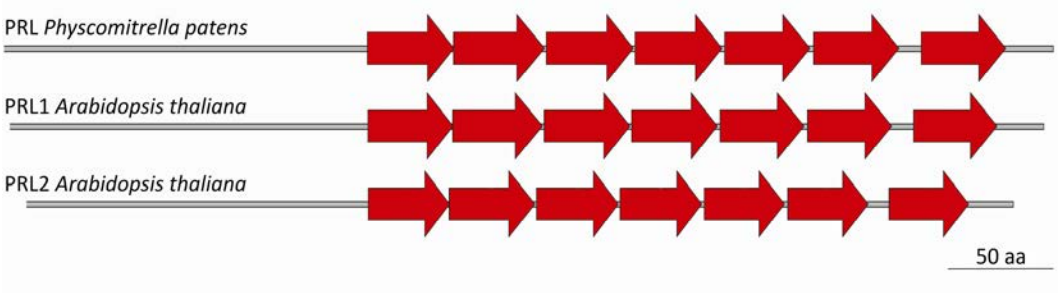

Fig. 23: Schematic of *Physcomitrella* PRL with its *Arabidopsis* homologs PRL1 and PRL2.
WD40 motifs in red. Scale bar as indicted.

4.4.4.3. #54.1 - elongation factor 1 α (EF1α)

This clone was assigned to the elongation factor 1 α (EF1α). EF1α is a ubiquitous protein from bacteria to the animal kingdom and exhibits a high degree of conservation even on protein level throughout all species.

```
P. patens   EF1α   MGKEKVHINIVVIGHVDSGKSTTTGHLIYKLGGIDKRVIERFEKEAAEMNKRSFKYAWVL 60
A. thaliana EF1α   MGKEKFHINIVVIGHVDSGKSTTTGHLIYKLGGIDKRVIERFEKEAAEMNKRSFKYAWVL 60
                   *****.************************************************

P. patens   EF1α   DKLKAERERGITIDIALWKFETMKYYCTVIDAPGHRDFIKNMITGTSQADCAVLIIDSTT 120
A. thaliana EF1α   DKLKAERERGITIDIALWKFETTKYYCTVIDAPGHRDFIKNMITGTSQADCAVLIIDSTT 120
                   ********************* ************************************

P. patens   EF1α   GGFEAGISKDGQTREHALLAFTLGVKQMICCCNKMDATTPKYSKARYEEIVKEVSAYLKK 180
A. thaliana EF1α   GGFEAGISKDGQTREHALLAFTLGVKQMICCCNKMDATTPKYSKARYDEIIKEVSSYLKK 180
                   ********************************************:**:****:****

P. patens   EF1α   VGYNPEKVPFVPISGFEGDNMIERSTNLDWYKGPTLLEALDNVSEPKRPSDKPLRLPLQD 240
A. thaliana EF1α   VGYNPDKIPFVPISGFEGDNMIERSTNLDWYKGPTLLEALDQINEPKRPSDKPLRLPLQD 240
                   *****:*:***********************************::.***************

P. patens   EF1α   VYKIGGIGTVPVGRVETGIIRPGMLVCFAPTGLTTEVKSVEMHHESMPEAHPGDNVGFNV 300
A. thaliana EF1α   VYKIGGIGTVPVGRVETGMIKPGMVVTFAPTGLTTEVKSVEMHHESLLEALPGDNVGFNV 300
                   *****************:*:***:* ******************: ** *********

P. patens   EF1α   KNVAVKDLKRGYVASDSKNDPAKEAANFTAQVIIMNHPGQIGNGYAPVLDCHTSHIAVKF 360
A. thaliana EF1α   KNVAVKDLKRGYVASNSKDDPAKGAANFTSQVIIMNHPGQIGNGYAPVLDCHTSHIAVKF 360
                   ***************:**:**** *****:******************************

P. patens   EF1α   AEILTKVDRRSGKELEKEPKFLKNGDAGFVKMIPTKPMTVETFAEYPPLGRFAVRDMRQT 420
A. thaliana EF1α   SEILTKIDRRSGKEIEKEPKFLKNGDAGMVKMTPTKPMVVETFSEYPPLGRFAVRDMRQT 420
                   :*****:*******:*************:*** *****.****:*****************

P. patens   EF1α   VAVGVIKAVEKKEPTGAKVTKAAAKKK-- 447
A. thaliana EF1α   VAVGVIKSVDKKDPTGAKVTKAAVKKGAK 449
                   *******:*:**:**********.**
```

Fig. 24 Alignment (ClustalW2) of EF1α isolated from a *Physcomitrella* cNDA library and its closest *Arabidopsis* homolog.
EFTU domains (EF-TU1, EF-TU_D2 and EF-TU_D3) are highlighted in purple.

EF1α proteins belong to the family of Ras-like GTPases and thus comprise of several GTP binding sites, as well as binding sites for other interacting proteins of the EF-family like EF-Tu proteins. The binding motif of the β-γ-phosphate moiety of an ATP or GTP is comprised within the first domain of EF1α. GTP_EFTU_D2 structurally forms a β-barrel and is responsible for binding of charged tRNAs and probably also for cytoskeletal association of the protein. GTP_EFTU_D3 domain generally exhibits GTP hydrolysis capacity.

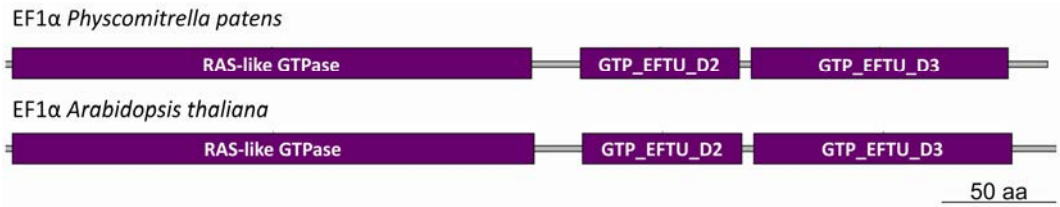

Fig. 25: Schematic of EF1α protein's domain organisation in *Physcomitrella* and *Arabidopsis.*
Conserved domains in purple. Scale bar as indicated.

In *Physcomitrella* 6 copies of EF1α proteins were detected by BLAST search; *Arabidopsis* posses 4 homologous proteins of EF1α, EF1A1-EF1A4 (206). As such, EF1α has to be considered a ubiquitous protein although the number of protein homologs in other plant species may vary in a great range (e.g. more than 10 homologs in *Zea mays*) (207).

4.4.4.4. # 61.4 - pirin-like protein (Pirin)

This sequence was assigned to a pirin-like protein in *Physcomitrella* by its high degree of homology to the *Arabidopsis* pirin-like protein. *Arabidopsis* carries 3 homologous proteins of the Pirin-family: Pirin, a putative Pirin lacking approx 30 amino acids of the N-terminus and a Pirin-like protein that carries an N-terminal extension of about 20 amino acids. The protein identified in *Physcomitrella* exhibits highest homology to the pirin-like protein of *Arabidopsis* with 63 % consensus positions and 54 % sequence identity.

```
P. patens    PRN        -------------------------MGSVPADFSKPRKVVKKVLSQAQPEGDGATVRRSI 35
A. thaliana  PRN-like   MRAAINRANSLGGLFSFRFIRNIKSMSSSTSQDFVSRPVIKKVFAKLQKEGDGAVVRRGI 60
A. thaliana  PRN        -------------------------MTYENNSVPRIVIKKVLAKLEKEGEGAVVRNGI 33
A. thaliana  PRN-put.   ----------------------------------------MKVMVLSLGKASP-------- 13
                                                               :* :. .    .

P. patens    PRN        GRPELKQLDPFLLLDYFEASGPAGFPDHPHRGFETVTYMLQGSFTHEDFAGHKGILEAGD 95
A. thaliana  PRN-like   SRSEQKLLDPFLMLDEFSVSPPAGFPDHPHRGFETVTYVLEGGITHQDFKGHKGTIYAGD 120
A. thaliana  PRN        TKIDQKLLDPFVLLVEFSFSLSAGFPDHPHRGFESVTYMLQGGIIHKDPKGHKGTIQAGD 93
A. thaliana  PRN-put.   SKSDHELLDPFVSLVEFSVSPPGGFKDHPHRGFESVTYMFQGGIIHQDCNGNKGTIHEGD 73
                          : : : ****: *  *. * ..** ********:***:::*.: *:*  *:** :  **

P. patens    PRN        VQWMTAGRGIVHSEMPSPVGVQRGLQLWVNLAGKDKMIEPNYQELKAKDIPRIEKDGVEV 155
A. thaliana  PRN-like   VQWMTAGRGIIHSEMPEEE-VNKGLQLWINLSSNEKMIEPNYQELSHSDIPKAEQNGVEV 179
A. thaliana  PRN        VQWMTAGRGIIHSEFPEEE-VNNGLQLWINLPSTEKMTEPKYKELSSLDIPRAEENGVEV 152
A. thaliana  PRN-put.   VQWMTAGRGIIHSEMPEEQ-VNKGLQLWINLPSSAKMIEPKNIEISSSEIPSADDYGVEV 132
                         **********:***:*.   *:.*****:**... ** **:  *:.  :**  :. ****

P. patens    PRN        VIIAGESFGVKSPVYTRTPTMYLDFYLQPGASLHQAIPEGWNAFTFVL---KGSMVFGKE 212
A. thaliana  PRN-like   KVIAGESMGIQSPVYTRTPTMFLDFTLQPGAQIHQNVPESWNAFAYILESGEGGGVFSSS 239
A. thaliana  PRN        KVIAGDSMGIKSPVYTRTPTMFLDFTLKPGSQTHQTVPESWTAFAYIIEGDEG--VFGSL 210
A. thaliana  PRN-put.   KVIAGESMGVKSPFYTKTPIMFLDFTLDPKAQTHQAVPESWTAFAYIVEGDEG--VFSSS 190
                         :***:*:*::**.**:** *:*** *.* :. ** :**.*.**:::::   :*  **..

P. patens    PRN        DAPPIGPSHTVVLSDG-DGLSAWNKG-TEPAQFVLVGGKPLNEPVAQYGPFVMNTQAQLM 270
A. thaliana  PRN-like   NSSPIPAHSVVVFGPGNDGVSVWNKSSSKQLRFVLIAGEPIGEPVVQYGPFVMNTQAEID 299
A. thaliana  PRN        NSSAISAHHVVVFGPG-DLVSVWNKSTSRSLRFLLIAGEPIGEPVVQCGPFVMNSQAEID 269
A. thaliana  PRN-put.   DSSTVQAHNVVVFGTG-DEVSVWNTSNSRPLRFLLIAGEPIGEPVVQHGPFVMNSQDEIE 249
                         ::..: .  .**:. * * :*.**.. :.  :*:*:.*:*:.***.* ******:* ::

P. patens    PRN        EAVRDYQYGKNGFERAHSWRSEAKAQSTP 299
A. thaliana  PRN-like   MTIEDYHYGKNGFEMAKYWRSQ------- 321
A. thaliana  PRN        MAFDDYQNAKNGFEMAKC---------- 287
A. thaliana  PRN-put.   MTIGDYRNGMNGFEMAKHWRSE------- 271
                         :. **: . **** *:
```

Fig. 26 Alignment (ClustalW2) of Pirin isolated from a *Physcomitrella* cNDA library and its putative *Arabidopsis* homologs.
The cupin domain (light blue) and the C-terminal domain of pirin-proteins (dark blue) are highlighted.

SMART identified a conserved Cupin-domain in all of the proteins. Cupin domains were named after their conserved structure, forming a barrel out of 6 β-strands. The C-terminus is a conserved part of all pirin-proteins.

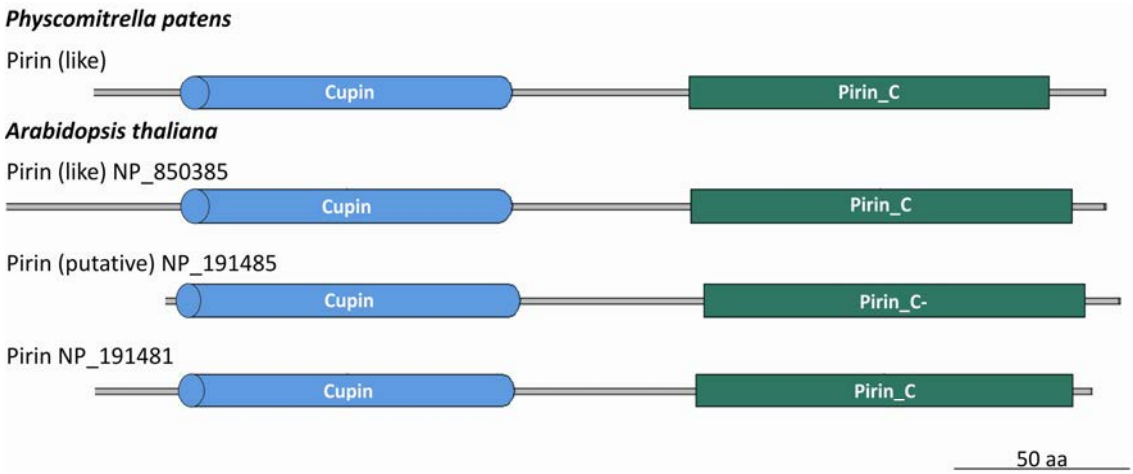

Fig. 27: Schematic of pirin proteins domain organisation in *Physcomitrella* and *Arabidopsis*.
Cupin domains in light blue, conserved C-terminal domains in green. Scale bar as indicated.

Pirin is a single copy gene in *Physcomitrella*, whereas *Arabidopsis*posses3 related sequences. Pirin proteins were identified in many other plant species, but not within tobacco or colza.

4.5. Light dependent interaction of phy4 with its putative interactors in yeast

4.5.1. Quantitative growth assay on PCB-complemented medium

After having identified putative phy4-interacting proteins by Y2H cDNA library screening, protein-protein interaction had to be further confirmed. All of the considered cDNAs were cloned as full length products from light grown *Physcomitrella* tissue. A first step aimed at the reproduction of the protein-protein-interaction and a possible state (i.e. Pfr)-dependency of the interaction. For this, the described cDNAs were cloned into the Y2H prey-vector pGADT7. Yeast cells containing BD:PHY4-baits were co-transformed with the respective prey-plasmids. Subsequently, equal amounts of yeast cells were spotted on PCB complemented dropout medium under high stringency conditions and incubated in D, R and FR conditions for 3 to 5 d.

A constitutive homodimerisation of apo-PHY4 was seen under all selection conditions, indicating that chromophor incorporation does not generally abolish interaction. Negative controls lacking either only the prey-, or both the bait and the prey-hybrids did not show colony growth under selective conditions. This emphasizes the stringency of the selection pressure and reduces chances for false positives.

Apo-PHY4 interacted constitutively with all of its putative interactors under medium stringency conditions. Interaction with EF1α and PRL1 was detected even under high stringency conditions. This resembles conditions used in the Y2H-screen and thus reproduces the previous findings. Interaction strength is additionally underlined by the strong blue colouring of the colonies resulting from

breakdown of Xα-Gal contained in the 4DO medium into blue 5-bromo-4-chloro-3-hydroxyindole. This is due to activation of the *MEL1* promoter by GAL4, leading to secretion of a α-galactosidase into the medium.

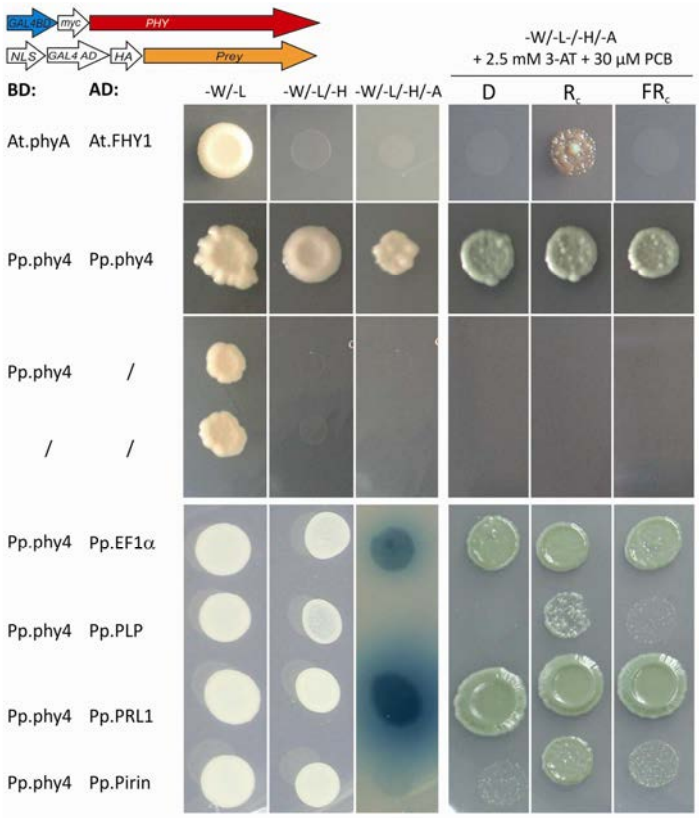

Fig. 28 Analysis of light dependent BD:phy4 interaction with putative interacting proteins.
Scheme in the upper left corner indicates bait and prey molecules used. Left panel: yeast cells were spotted on DDO, TDO and QDO (+Xα-Gal); TDO and QDO containing 2.5 mM 3-AT. Right panel: yeast cells on PCB-complemented QDO were incubated in different light conditions. Continuous red light induced interaction of BD:phy4 with both AD:PLP and AD:Pirin.

In order to further elucidate interaction with functional holo-phy4, interaction studies were continued on PCB-complemented medium. Assembly of functional holo-phytochrome with PCB was shown for moss phytochromes using recombinant phytochrome 2 from *Ceratodon purpureus* (208), likewise formation of functional *Arabidopsis* phyA from PCB-complemented yeast medium was demonstrated (70). A Pfr specific interaction was seen for phyA:BD with AD:FHY1, which occurred only in PCB-fed yeast under continuous R; no interaction was seen for apo-PHYA:BD/AD:FHY1. Thus fusion of the BD to the N-terminus of phyA did neither inhibit chromophor attachment nor Pfr-formation and photosensing. Interestingly, holo-phy4, as indicated by the apparent green colouring of the growing yeast colonies, showed state-dependent binding of PLP and Pirin in continuous R. This not only verifies previous interaction but also further indicates phy4-Pfr-specificity for binding PLP and Pirin. However, a state-independent interaction is observed in the cases of EF1α and PRL1. This is in harmony with the strong interaction of apo-PHY4 even under highest selection pressure applied. Remarkably, no interaction was observed for C-terminal fusions of the BD to phy4 (phy4:BD; see suppl. fig. 8). Whether this is due to inhibition of Pfr-formation or

the effect of any other structural impairment of PHY4 cannot be determined as this point. As PHYA:BD hybrids showed no influence on Pfr-formation and proper binding of FHY1 in R, impairment of Pfr formation in case of PHY4:BD seems rather unlikely. Thus, phytochromes were established as functional, i.e. photoconvertible photoreceptors within living yeast cells.

4.5.2. Photoreversibility of state-dependent interactions by β-galactosidase assay

PLP and Pirin exhibited interaction with BD:PHY4 only in its Pfr-form, a fact that raised the question of photoreversibility of this interaction. Quantitative growth assays, as described in the previous section, were carried out under continuous light conditions; photoreversibility cannot be accessed under such conditions. Growth assays would theoretically be feasible also in pulsed-light conditions, but unclear parameters concerning the growth behaviour of yeast cells make it difficult to determine a lag-phase and/or escape time of the activation of the GAL4 promoter. Therefore, a liquid β-galactosidase assay was performed to investigate photoreversibility of the state-dependent phy4-interaction with PLP and Pirin. Using yeast strain Y187 it was possible to monitor phy4-interaction strength quantitatively by activation of the *lacZ* gene expression under the control of the GAL1 promoter. In this assay, ONPG is used as substrate which is enzymatically broken down by β-galactosidase resulting in the accumulation of yellow o-nitrophenol, the amount of which can be measured photometrically. This experiment was performed by Rabea Krikor as part of her master thesis project under my supervision.

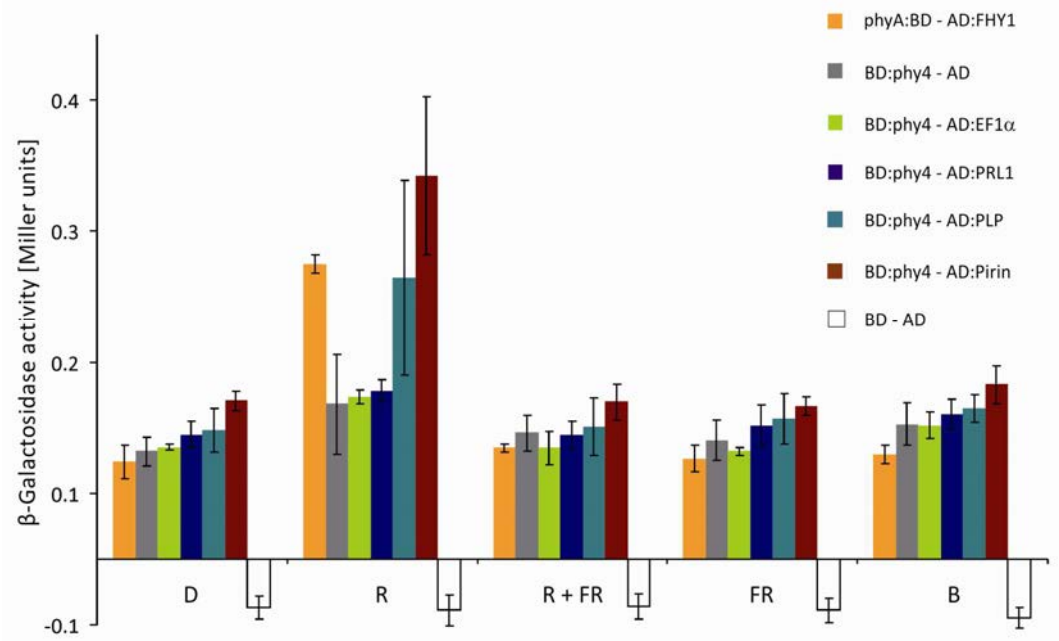

Fig. 29: Light dependent β-galactosidase assay analysing FR-reversibility of R-induced interaction of phy4 with putative interactors.

R-strengthened interaction of both PLP and Pirin with holo-phy4 was FR-reversible. Background activity of β-galactosidase is displayed as negative activity (white bars) and was subtracted from every measured value. Standard errors are given.

As expected from the results of the quantitative growth assays, only PLP and Pirin, along with the positive control phyA/FHY1, exhibited an increase in interaction strength of about 3 to 3.5-fold after retrieving an R-pulse. Remarkably, this reaction is reversed by a subsequent FR-pulse given immediately afterwards, mainly reducing the interaction strength to dark-levels. No such change in interaction strength was observed for phy4 interaction with either EF1α or PRL1 in any light condition, as expected from results of the growth assays. Apparently FR or B-pulses alone did not have an effect on phy4 interaction with any of the proteins investigated.

4.5.3. Quantitative growth assay of phy4 partials with putative interactors

In order to access whether a particular part of phy4 is necessary and sufficient for binding its putative interactor, the afore mentioned phy4 partial baits were employed in another Y2H growth assay for interaction with the previously identified interacting proteins (see 4.4.).

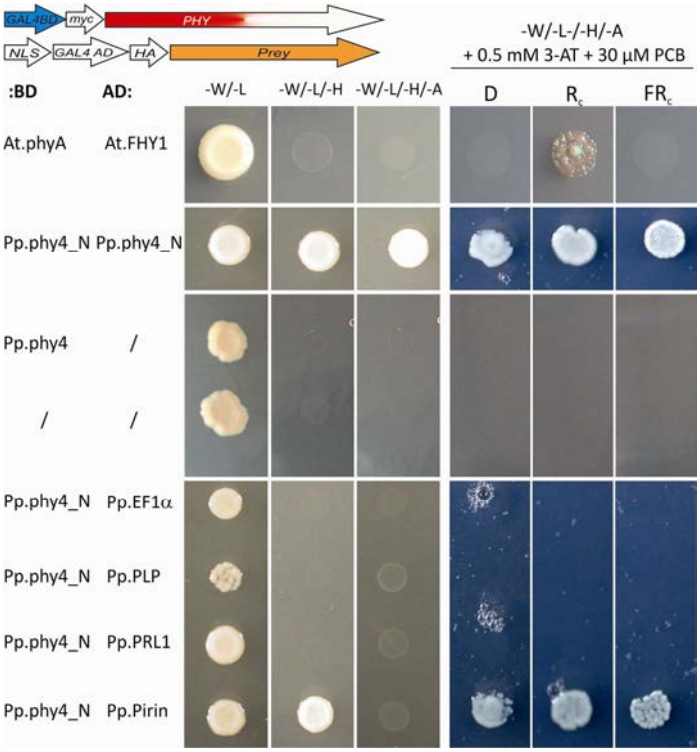

Fig. 30: Analysis of light dependent interaction of BD:phy4_N with putative interactors.
Scheme in the upper left corner indicates bait and prey molecules used. Left: Yeast cells were spotted on DDO, TDO and QDO; TDO and QDO contained 0.5 mM 3-AT. Right: yeast cells on PCB-complemented QDO were incubated in different light conditions.

Surprisingly, constitutive dimerisation of the two N-terminal parts lacking the putative dimerisation module located at the phy4 C-terminus was observed. This behaviour contrasts previous observations where PHY4_N bait and prey molecules showed no dimerisation (see suppl. fig. 3). The dimerisation of PHY4_N partials might be due to high protein concentrations within yeast cells, as observed for the Cph1 photosensory module (209). Homodimerisation of full-length holo-phy4 and apo-PHY4 were state-independent, as observed before.

In contrast to phy4_N homodimerisation, BD:phy4_N interaction with Pirin is at least partially dependent on the holo-protein, since no interaction of (apo-) PHY4_N with Pirin is observed under high selection pressure containing no PCB. Although it seems that phy4_N interaction with Pirin is dependent on holo-phytochrome assembly, no light dependency of the interaction is observed. Thus holo-phy4 appears to be structurally different from apo-PHY4 in providing an interaction surface for pirin. All other proteins investigated did not show interaction with phy4_N. No interaction is seen for C-terminal fusions to PHY4_N (Pp.phy4_N:BD, see suppl. fig. 9).

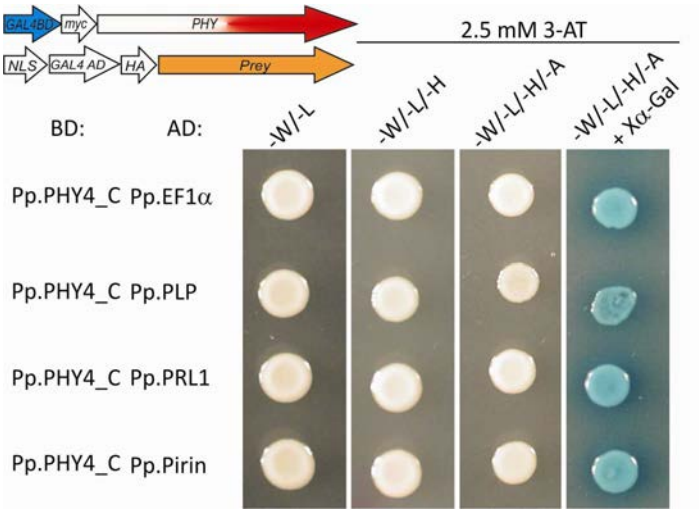

Fig. 31: Analysis of light dependent interaction of Pp.PHY4_C with putative interactors.
Scheme in the upper left corner indicates bait and prey molecules used. Apo-PHY4_C interacts strongly with all prey-proteins even under most stringent selection conditions (4DO + Xα-Gal).

Plant phytochromes bind the chromophor at a conserved cystein residue of the GAF-domain located within the N-terminal photosensory module. Constructs bearing only the C-terminal half of the apoprotein are thus unable to assemble the chromophor. Hence, no light-dependent interaction can be possibly observed using the C-terminal half of phy4. Consequently growth assays with Pp.PHY4_C baits were carried out only on media without PCB.

All proteins previously shown to bind full-length phy4 interacted constitutively with PHY4_C under all selection conditions tested. Both EF1α and PRL1 interacted strongly but state-independently with full-length apo-PHY4 and holo-phy4; however no interaction was observed for PHY4_N and phy4_N (see fig. 30). From these observations EF1α and PRL1 are concluded to interact with full-length phy4 within its C-terminus. Binding of EF1α and PRL1 with PHY4_C:BD, however, was only very weak even under medium stringent selection conditions (suppl. fig. 10). This might hint on a necessity for a freely accessible C-terminus for the binding of phy4.

Interaction of both PLP and Pirin with full length BD:phy4 was state-dependent and constitutive for the C-terminal phy4 partial (BD:PHY4_C). Interestingly, PLP exhibited no interaction with (holo-)BD:phy4_N. Binding of PLP to phy4 thus seems to be mediated rather by the C-terminal transmitter module of phytochrome, with the N-terminus mediating exclusively state-dependency of the interaction. Contrary to PLP, Pirin interacted constitutively with BD:PHY4_C and state-independently with holoBD:phy4_N. Therefore, binding of pirin to phy4 appears to be accomplished within the photosensory module.

4.6. sYFP-based i*n vivo* interaction studies of phy4 with putative interactors

Following verification of phy4-interaction in yeast, *in vivo* interaction was investigated using a bimolecular fluorescence complementation assay. YFP-moieties (YFP_N and YFP_C) were fused to either full-length *PHY4* or the putative interactor respectively, yielding a functional YFP-barrel upon protein-protein-interaction.
Once the fluorescence reporter is successfully reconstituted, it remains locked in this conformation and thereby also locks the interacting fusion partners (210). This allows detection of temporal interactions and their localisation simultaneously, but has the disadvantage to render R/FR reversibility impossible to detect with this method.

4.6.1. Homodimerisation of phy4

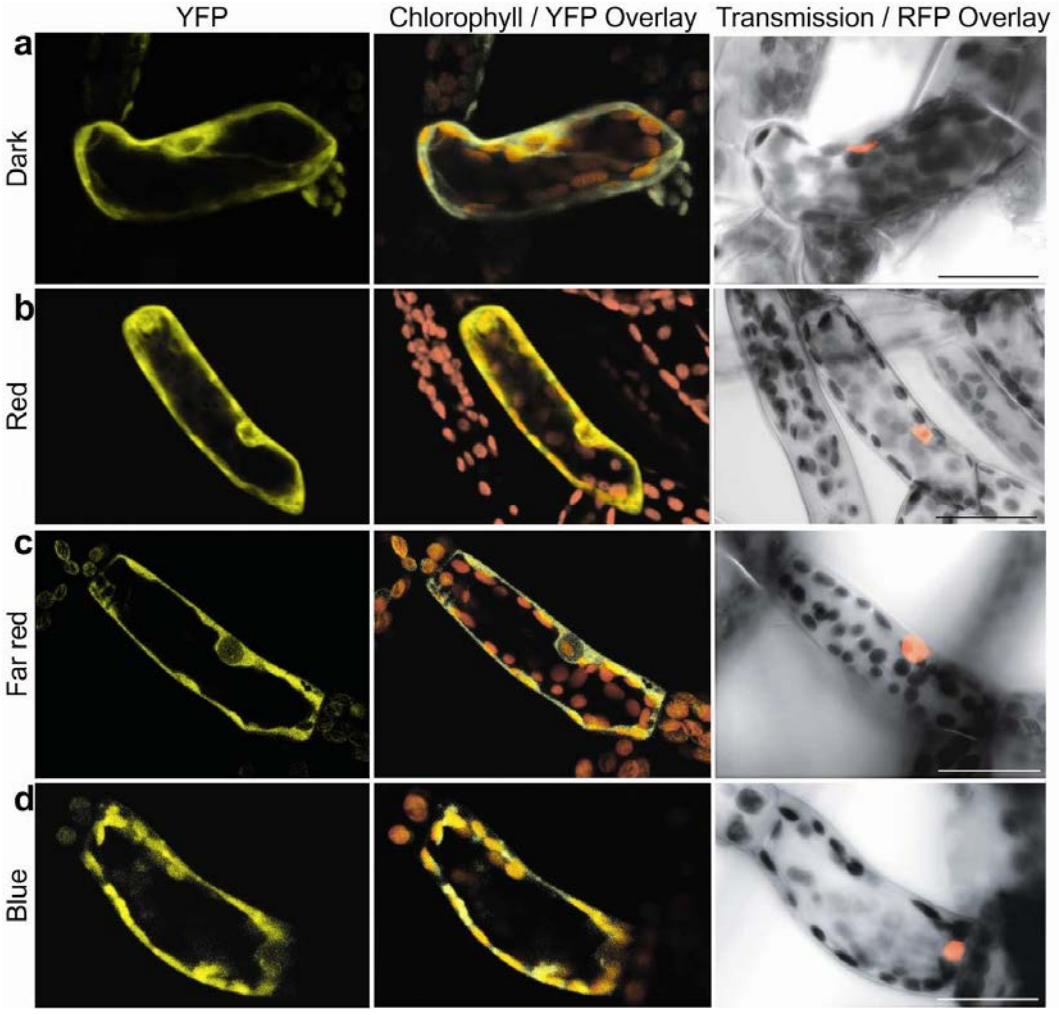

Fig. 32: Light dependent localisation of phy4-homodimers in *Physcomitrella* protonemata.
N-terminal phy4 fusions to either of the two YFP moieties (YFP_N:Pp.phy4 – YFP_C:Pp.phy4) form homodimers. Under all light conditions tested, phy4 homodimers remain localised to the cytoplasm. Expression of $Cherry_{NLS}$ marks positioning of the nucleus. Scale bars 50 µm.

Similar to Y2H experiments, homodimerisation of phy4 was exploited as a system positive control. Indeed fluorescence derived from phy4-homodimers could be detected and it remained localised to the cytoplasm under all light conditions tested, resembling the localisation pattern of N-terminal phy4 fluorescence fusions observed before (see fig. 9).

In order to exclude false positive signals resulting from self-assembly of the two YFP-halves, YFP-moieties without protein fusions were expressed in both *Physcomitrella* and onion cells as a negative control. No fluorescence signal was observed even when cells were overexposed to excitation light (see suppl. fig. 11).

4.6.2. phy4-EF1α and phy4-PRL1 interaction

Since EF1α and PRL1 did not show phy4-Pfr-dependent interaction in previous studies, interaction of phy4 was investigated without any light pre-treatments.

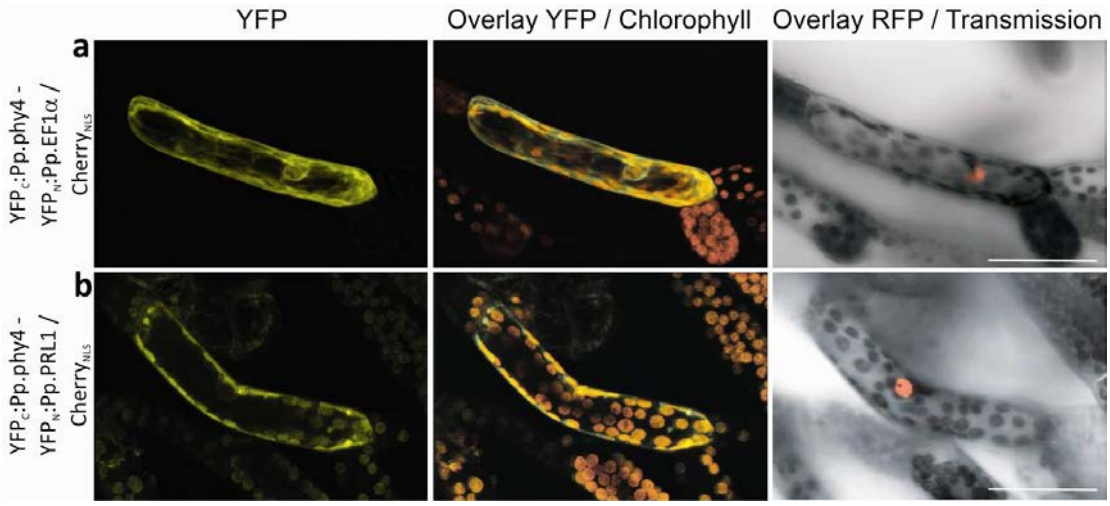

Fig. 33: *In vivo* interaction of phy4 with EF1α and PRL1 in *Physcomitrella* protonemata.
Scale bars 50 µm.

Both EF1α and PRL1 interacted *in vivo* with full-length phy4 in *Physcomitrella* as shown by emission of YFP signals. The localisation of the EF1α-signal was restrained to numerous distinct and fine branches throughout the whole cell, explicitly excluding the nucleus and also the chloroplasts, which appeared to be embedded in a dense network of those filamentous structures. Comparison with localisation data derived from expression of conventional N-terminal FP-fusions (see suppl. fig. 12) also showed clear restriction of the signal to the cytoplasm. A restraint to particular structures within the cytoplasm, as observed for the sYFP-signal, however could not be observed. A comparably weak sYFP-signal for phy4-PRL1-interaction was localised to the cytoplasm as well, exhibiting a more homogenous distribution compared to EF1α. In contrast to observations made with CFP:PRL1-fusions (see suppl. fig. 12), no sYFP-signal was detected within the nucleus.

4.6.3. Interaction of phy4 with PLP and Pirin

Previous Y2H-studies have shown both PLP- and Pirin-binding to phy4 to be dependent upon formation of Pfr. Therefore, sYFP studies involving those two proteins were carried out either in darkness (i.e. without light treatment prior to observation) or with 1 h pre-incubation in R. FR-treatments for reversibility tests were omitted, for the reasons described in 4.6.

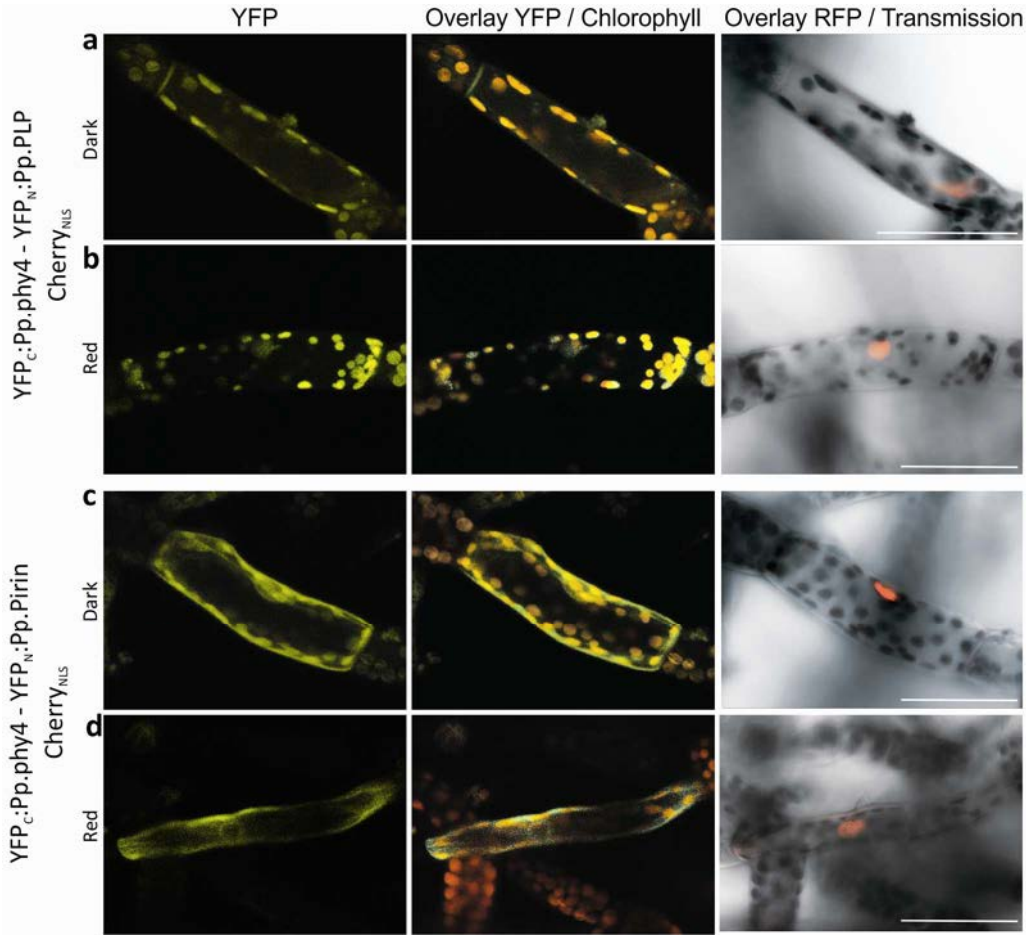

Fig. 34: *In vivo* interaction of phy4 with PLP and Pirin in *Physcomitrella* protonemata.
Scale bars 50 µm.

phy4-PLP interaction lead to the emission of only very weak sYFP-signals, which were localised to the cytoplasm in darkness and appeared to be localised to the nucleus upon R pre-treatment. This contrasts the localisation pattern of CFP:PLP observed in either D or R where CFP:PLP emitted a homogenous cytoplasmic signal (see suppl. fig. 13). No difference in the localisation of the fluorescence signal was seen between D and R samples of CFP:PLP.

Pirin generally yielded stronger sYFP-signals, with the signals being localised to the cytoplasm in both D and after R-treatment. Other than CFP:Pirin, which showed clear nuclear accumulation of the fluorescence signal in both D and R (see suppl. fig. 13), sYFP-signals of phy4/pirin remained cytoplasmic in both conditions tested.

Taken the results of the sYFP-experiments together, interaction of full-length phy4 with all of the four isolated proteins could be verified *in vivo*.

4.7. Studies on *Physcomitrella* phytochrome 4-phototropin interaction

Different physiological studies in both higher and lower plants indicated a close interplay between R and B signaling. Although phytochromes are generally capable of absorbing B, to date no phytochrome specific blue light responses are known. Thus the idea emerged that phytochromes might share a signaling cascade with another photoreceptor group specific for B. In higher plants, phototropins are responsible for direction responses, such as phototropic bending of the hypocotyls or coleoptiles and chloroplast movement

responses (104-106, 137, 211, 212). Phototropins are also conserved in mosses; *Physcomitrella* contains at least 4 phototropins, with additional putative phototropin sequences identified by BLAST search of the genome sequence. In *Physcomitrella* phototropins are only responsible for B induced chloroplast movements, whereas other directional responses are phytochrome mediated. Moreover, chloroplast movements are also inducible by R with an involvement of phy2 and phy4 (172). As the functions of both photoreceptors seem to be tightly cross-linked with each other, a direct interaction of phy4 and all four described phototropins was hypothesised. This question was addressed by both Y2H- and sYFP-methods.

4.7.1. Quantitative growth assay on PCB-complemented medium

To elucidate interaction of full-length phy4 with Pp.phot, all four phototropin cDNAs (*Pp.PHOTA1-Pp.PHOTB2*) were cloned into pGADT7 to yield AD:fusions for Y2H interaction assays. To account for state-dependent interaction of both phytochrome and phototropin, growth assays were carried out under continuous R, FR and B conditions.

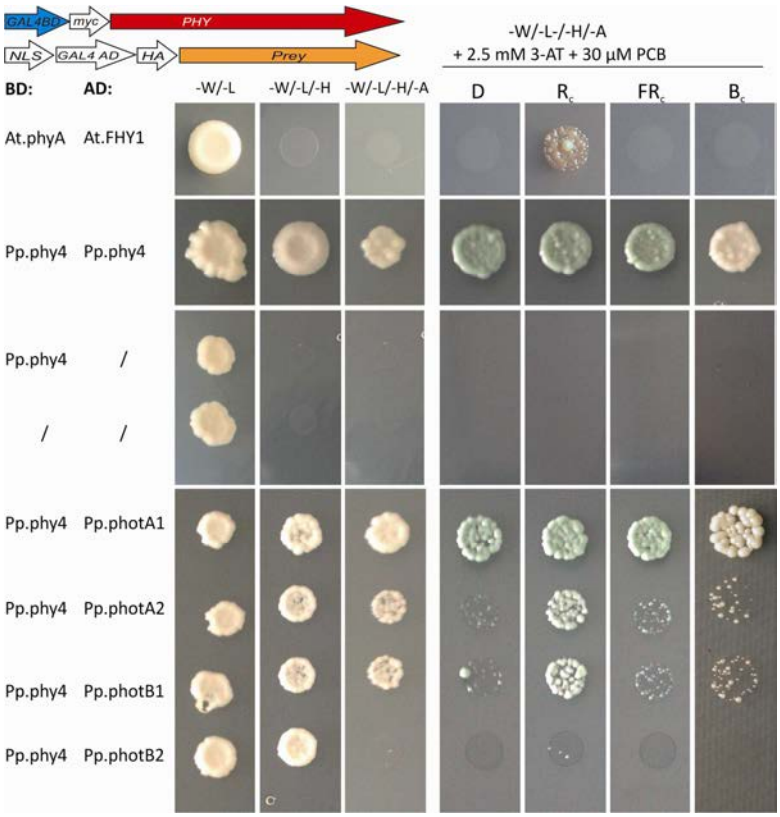

Fig. 35: Analysis of light dependent interaction of BD:phy4 with any of the four phototropins by Y2H.

Scheme in the upper left corner indicates bait and prey molecules used. Left panel: yeast cells were spotted on DDO, TDO and 4QDO containing 2.5 mM 3-AT. Right panel: yeast cells incubated on PCB-complemented 4DO medium were placed in different light conditions.

Remarkably, full-length BD:phy4 bound phototropins A2, B1 and B2 red light dependently. Binding to Pp.photA1 initially appeared to be constitutive under all light conditions tested, but a Pfr-dependency was shown by ONPG-assays (compare 4.7.2.). Binding of Pp.photB2, however, was very weak even in

continuous R. No phy4/phototropin interaction was observed in D, FR or B.
In contrast to phy4 Pfr-specific interactions observed previously for PLP and Pirin, Pp.photA1, A2 and B1 showed interaction under high stringency selection even with apo-PHY4. Interestingly, this binding is lost for the holo-phytochrome, which exhibited no binding to phototropins in D, FR or B but only under R conditions. No interaction was observed for the equivalent phy4 C-terminal fusions (phy4:BD, suppl. fig. 14)

4.7.2. Photoreversibility of state-dependent interactions by β-galactosidase assay

After observation of phy4-Pfr-dependent interaction with photA2, photB1 and photB2, FR-reversibility of these interactions was approached by liquid β-galactosidase assay. The specific interaction of phyA/FHY1 was employed as a state-dependent positive control, as described before. The data shown here was obtained by Anna Lena Lichtenthäler, under my supervision.

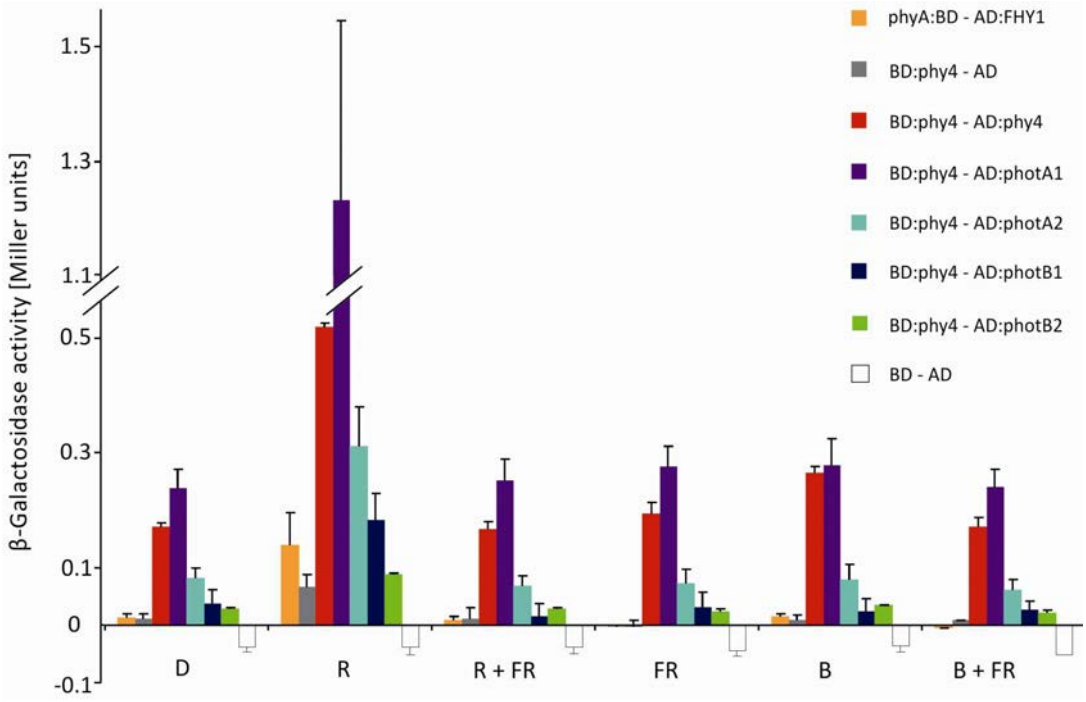

Fig. 36: Light dependent β-galactosidase assay analysing R/FR-reversibility of phy4-phototropin interaction.
Interaction strength of BD:phy4 with any of the phototropins investigated increased after red light treatment. This reaction was photoreversible by a subsequent far red pulse. Background β-galactosidase activity is displayed as negative activity and was subtracted from every value. Standard errors are given.

phy4-homodimerisation, initially set up as a state-independent control, exhibited comparably strong interaction under all light conditions but moreover showed a approx. 2-fold increase in interaction strength following R-pulses. This increase was reverted by a subsequent FR-pulse. This enhanced phy4/phy4 binding might be due to a greater stability of the dimer in Pfr-formation.
phyA/FHY1 interacted only under R conditions, with a subsequent FR-pulse

completely reverting interaction. Almost no binding of phyA to FHY1 was detected in D, FR or B conditions.
Interestingly, all of the four phototropins exhibited an approx. 3-fold increase in interaction strength after an R-pulse. All of these reactions were reverted to dark-levels by a subsequent FR-pulse. No such reaction was observed in FR or B. Thus interaction of phy4 with phototropin appears to be phytochrome dependent and Pfr-specific.

4.7.3. Quantitative growth analysis of phytochrome partials

To possibly identify the phytochrome-module responsible for phototropin binding, quantitative growth assays using the N- or C-terminal partials of phy4 as bait were used in light-dependent Y2H assays with phototropins.

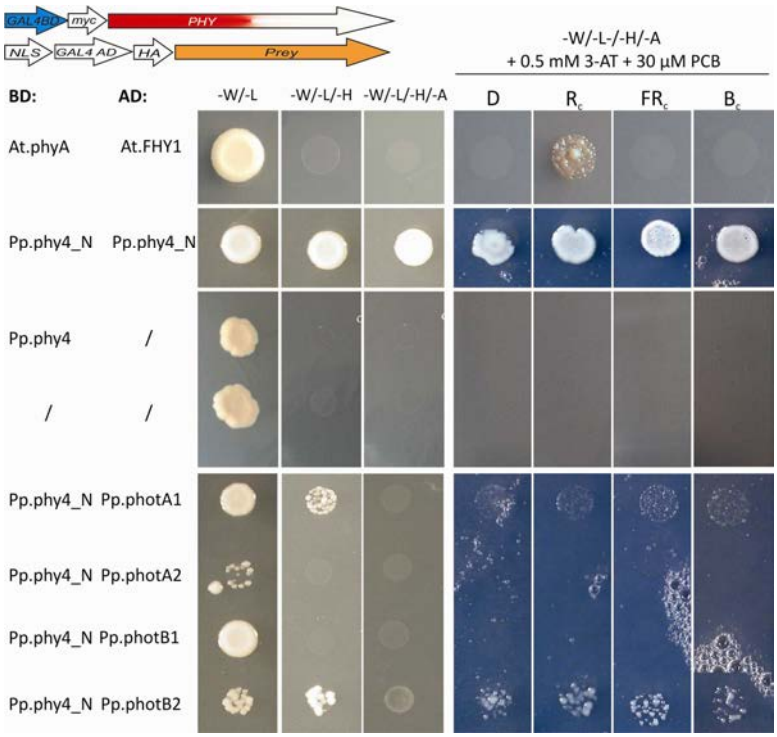

Fig. 37: Analysis of light dependent interaction of BD:phy4_N with *Physcomitrella* phototropins.
Scheme in the upper left corner indicates bait and prey molecules used. Left panel: yeast cells were spotted on DDO, TDO and QDO containing 0.5 mM 3-AT. Right panel: yeast cells on PCB-complemented 4DO were incubated in different light conditions.

Although Pfr-specific binding of full-length phy4 to each of the phototropins was seen before, no interaction of phototropins with BD:phy4_N was observed under any light condition tested. Despite positive selection for both BD:PHY4 and AD:PHOT on DDO medium, no quantitative interaction was seen for apo-PHY4 on medium or high stringency selection conditions. No interaction was seen for C-terminally fused bait constructs (phy4_N:BD) either (suppl. fig. 15).

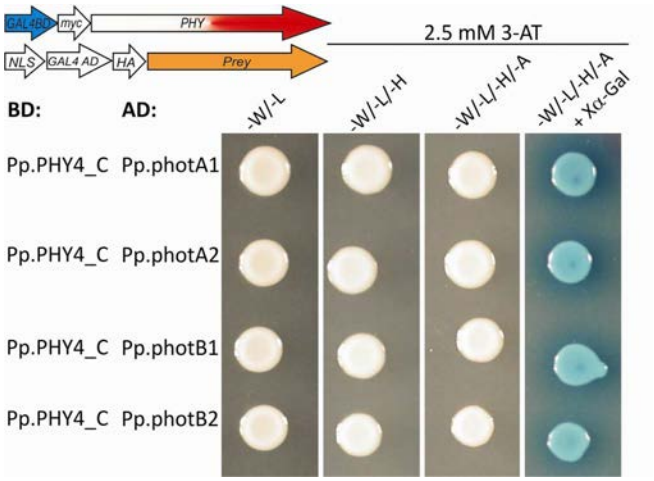

Fig. 38: Analysis of light dependent interaction of BD:PHY4_C with *Physcomitrella* phototropins.
Scheme in the upper left corner indicates bait and prey molecules used. Apo-PHY4_C interacted strongly with all phototropins (4DO + Xα-Gal).

As observed previously for the putative phy4 interacting proteins, BD:PHY4_C partials bound all of the four phototropins constitutively under all selection conditions. A lower but still clearly detectable interaction with PHY4_C:BD was observed only for photA1 (suppl. fig. 16).

4.7.4. Localisation studies of *Physcomitrella* phototropins

In order to visualise cell structures and compartments, fluorescent dyes and marker fusion proteins were established. These markers were subsequently used to determine the localisation of phototropin fluorescent fusion proteins.

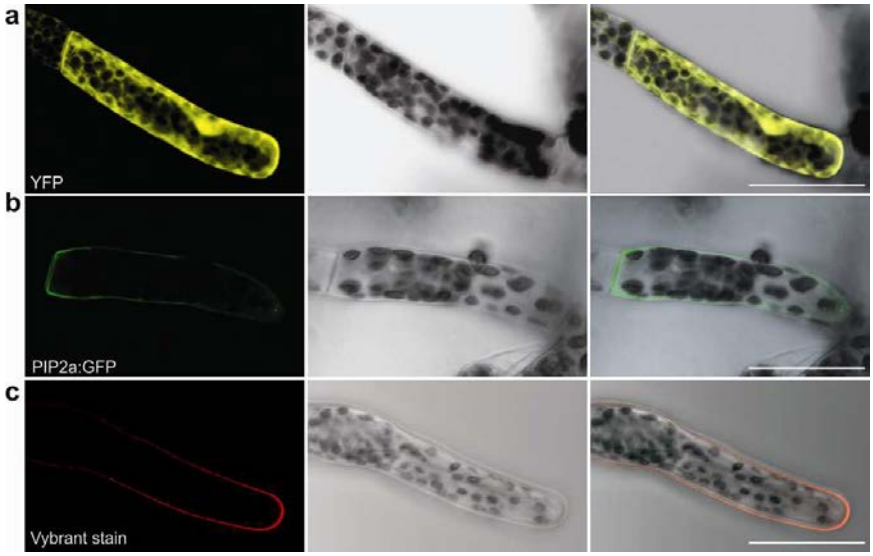

Fig. 39: Expression and localisation of cytosolic, nuclear and plasma membrane localised markers in *Physcomitrella* protonemata.
YFP (**a**) localised to both the cytoplasm and the nucleus, whereas PIP2a:GFP (**b**) exhibited strict plasma membrane localisation. A Vybrant (Molecular Probes) fluorescence signal (**c**) is emitted only when incorporated into membranous environment. Scale bars 50 µm.

Extensive studies on *Arabidopsis* phototropins showed that both phot1 and phot2 are localised to the plasma membrane and that this localisation is influenced by light. The mechanism by which phot1 and phot2 are bound to the plasma membrane however remains unknown. Since it is apparent from sequence analysis that phototropins themselves do not posses properties to integrate in or associate with the plasma membrane directly, it has been hypothesised that a hitherto unknown phototropin-interacting membrane protein mediates plasma membrane localisation. Although *Physcomitrella* phototropins have been physiologically characterised (8) to date nothing is known about their localisation either. To answer this question, N-terminally CFP-tagged fusion proteins were transformed into *Physcomitrella* and co-expressed with YFP as a cytoplasmic marker.

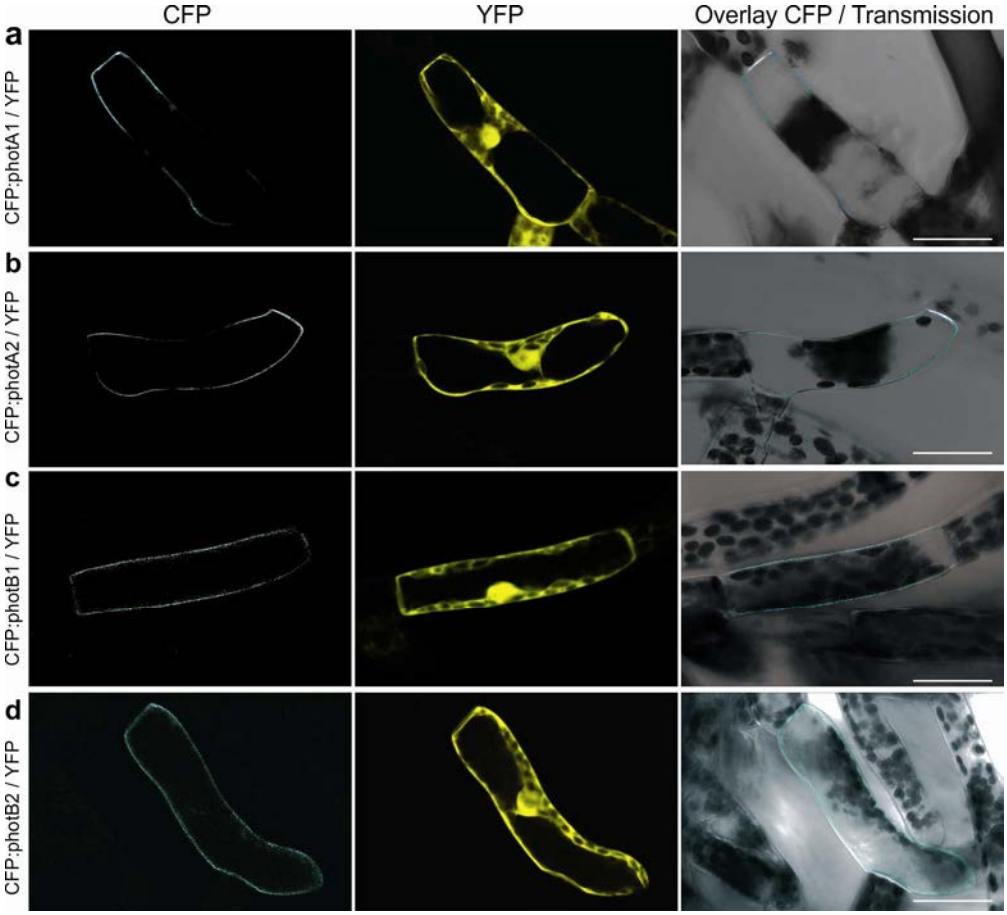

Fig. 40: *Physcomitrella* phototropins are plasma membrane localised.
Fluorescence of *Physcomitrella* CFP:phototropin is detected in the cells outer periphery. YFP is localised to the cytoplasm and to the nucleus. Scale bars 50 µm.

CFP:Pp.phot-fusions were localised to the outer periphery of the cell. Co-expression of YFP results in a strong nuclear signal and homogenous fluorescence within the cytoplasm, defining the thin border between the plasma membrane and locally restricted cytoplasm. Both fluorescence signals, either emerging from phototropin-fusions or from YFP, can be clearly differentiated. Comparison with the plasma membrane protein PIP2a:GFP and a membrane specific dye (see Fig. 38) strongly suggest plasma membrane association of *Physcomitrella* phototropins.

4.7.5. Homodimerisation of *Physcomitrella* phototropins

Arabidopsis phototropins have been described as functional dimers (213). In order to elucidate whether *Physcomitrella* phototropins dimerise as well, sYFP-fusions of all four phototropins were transformed into *Physcomitrella* cells and investigated homodimerisation.

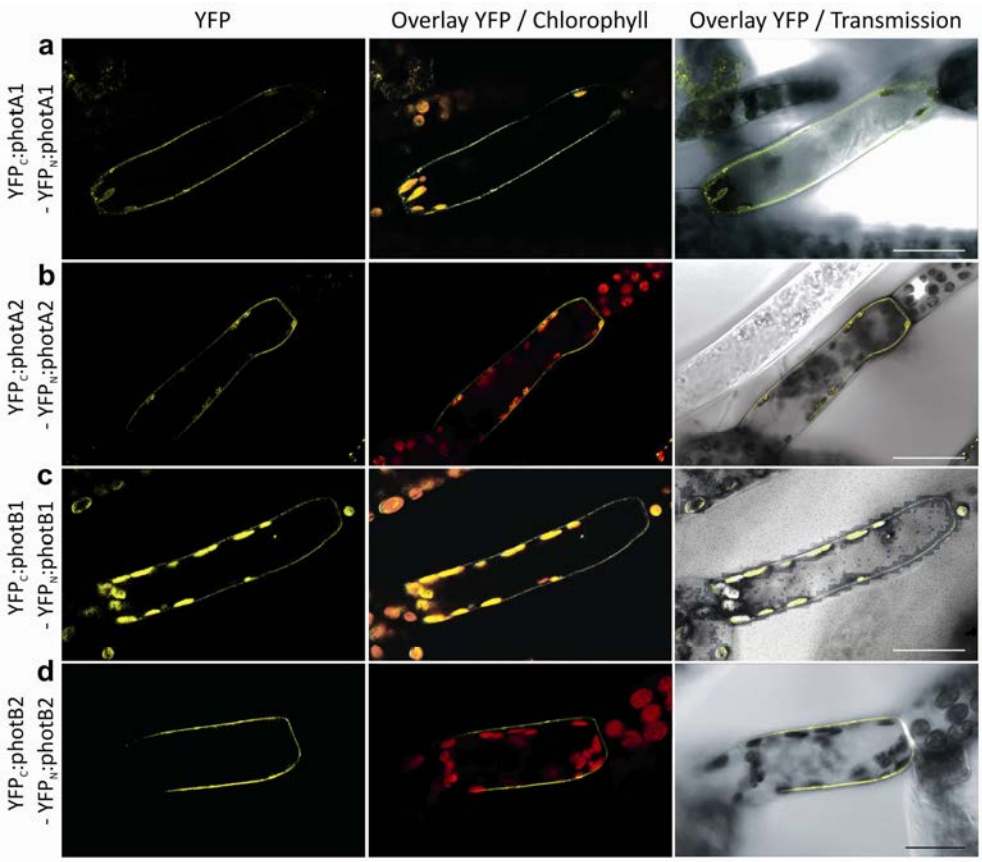

Fig. 41: *Physcomitrella* phototropins form homodimers *in vivo*.
N-terminal sYFP-fusions of all four phototropins yield fluorescence signals located to the outer cell periphery. Scale bars 50 µm.

YFP-fluorescence was reconstituted by the interaction of two phototropin-molecules each fused to one YFP-moiety. Reconstitution of YFP fluorescence demonstrates that *Physcomitrella* phototropins homodimerise *in vivo* as described for *Arabidopsis* phototropins. As previously observed for conventional FP-fusions to the N-termini of *Physcomitrella* phototropins (see fig. 40), fluorescence signals of sYFP-fusions resemble the phototropin localisation pattern at the plasma membrane. Additionally, plasma membrane localisation appeared to be independent of light treatments. No B induced internalisation of *Physcomitrella* phototropins was observed when expressed in onion epidermal cells (experiments carried out by Rabea Krikor). Consequently no possible R-enhanced plasma membrane attachment was observed either. Light-dependent analysis of homodimer formation exhibited no evidence for R or B influence on dimerisation of the photoreceptors or their localisation (suppl. figs. 17, 18).

4.7.6. sYFP-based *in vivo* studies on phy4-phot interaction in *Physcomitrella*

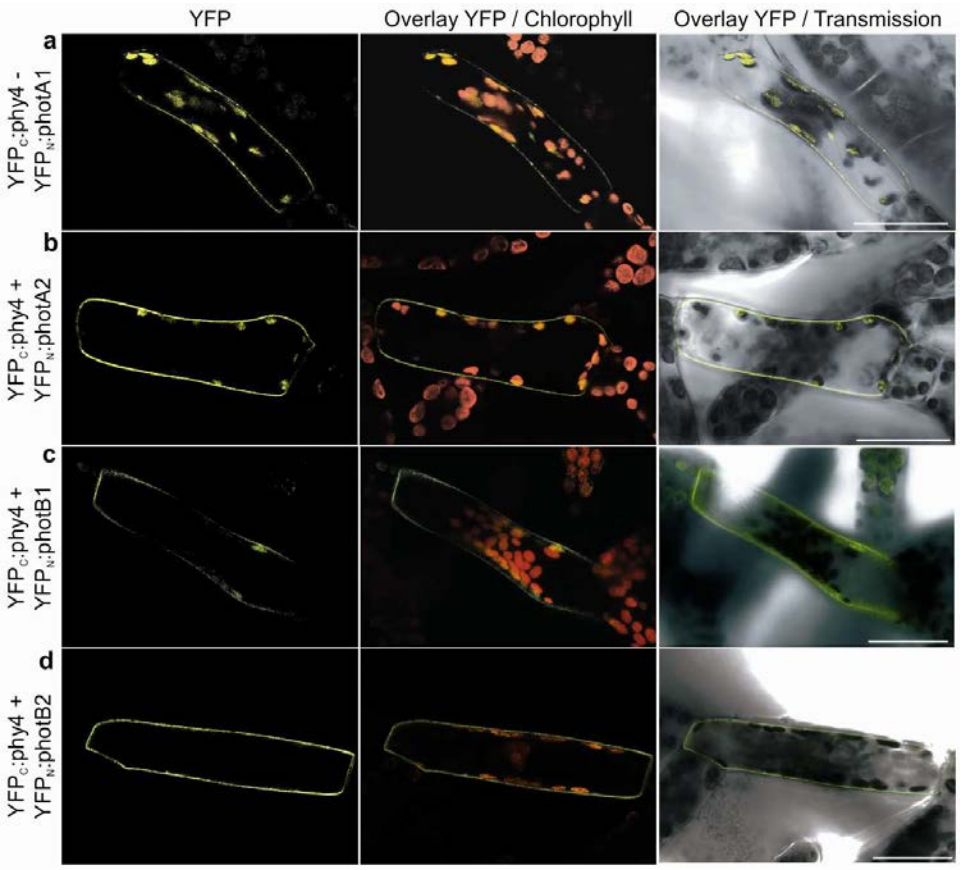

Fig. 42: phy4 interacts with *Physcomitrella* phototropins at the plasma membrane.
N-terminal fusions to phy4 and any of the four phototropins yield sYFP-signals at the plasma membrane after R-illumination. Scale bars 50 µm.

The phytochrome-phototropin interaction observed in both Y2H growth and ONPG-assays was confirmed *in vivo* using the sYFP-complementation assay.
Consistent with the observed localisation pattern of CFP:phot fusions and the sYFP-phototropin homodimers, interaction of phy4 with every of the four phototropins investigated takes place at the plasma membrane. Thus it seems that a proportion of the phytochrome pool binds to phototropin molecules at the plasma membrane. Since no localisation experiments before pointed on a comparable plasma membrane signal for FP-phy4 fusions (see fig. 9), it has to be assumed that only a small proportion of the cell's phy4-pool binds to phototropin at any one time.

4.7.7. *In vivo* interaction studies of phy4-phot in higher plant cells

As moss phototropins interact with phytochrome *in vivo* and *in vitro*, the interaction capability of higher plant phytochromes and phototropins was investigated.
In both *Arabidopsis* and *Physcomitrella* the mechanism by which phototropin is bound to the plasma membrane is as yet unknown; previously reported *Arabidopsis* candidates seem to be only partially conserved in *Physcomitrella*. NPH3 and EHB1-homologs can be identified within the genome sequence, whereas PKS-family homologs appear to be absent in *Physcomitrella* and other lower plants, like *Selaginella* (214). Nevertheless, none of these candidates were confirmed to function

in plasma membrane attachment of phototropins.

To find out if the membrane attachment mechanism is conserved between higher and lower plants, *Physcomitrella* phototropin B1 and B2 association to the plasma membrane and phy4-phot interaction were investigated in higher plant cells. Therefore onion epidermis cells were transiently transformed with *CFP:PHOT* and *YFP_N:PHOT / YFP_C:PHOT*sYFP-fusion constructs, as described in 4.7.4 and 4.7.5. Microscopic observations were carried out in cooperation with Dr. Olga Levai using the TCS-SP5 AOBS facility at Leica Microsystems in Mannheim.

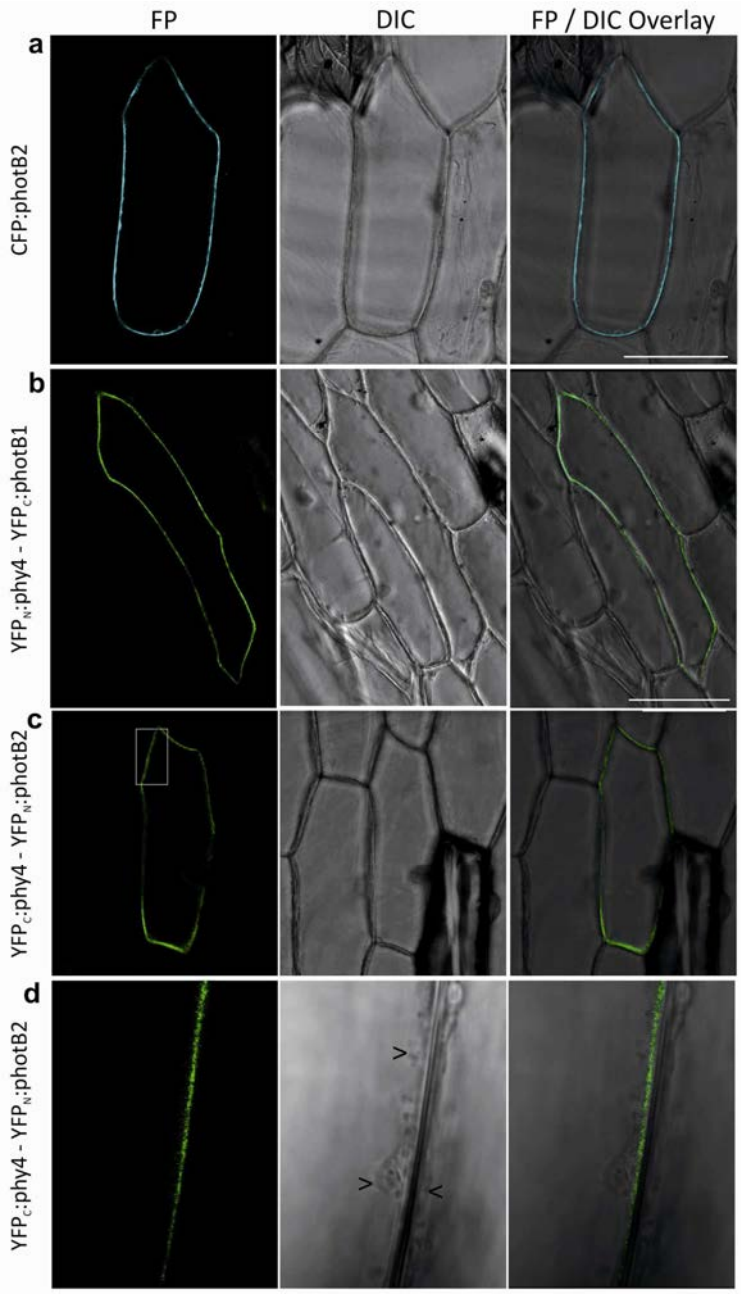

Fig. 43: Localisation of CFP:photB2 and sYFP-interaction of phy4 with photB1 and photB2 in onion epidermis cells.

CFP:photB2 was expressed as a localisation control; notably both phototropin and the phy4 - phototropin interaction are plasma membrane localised in onion cells. Arrow heads indicate positioning of cytoplasmic accumulation at the cell border. Scale bars 100 µm.

Both the localisation of conventional CFP:photB1 fusion and the phy4-photB1 and phy4/photB2-interaction at the plasma membrane could be detected in onion epidermis cells. A close-up view on a region at a cell-cell-conjunction explicitly demonstrated phy4-phot interaction occurring at the plasma membrane, since the cytoplasm (restricted to the cell periphery by vacuole-mediated spatial constriction) was completely free from any fluorescence signal (Fig. 44, **d**).

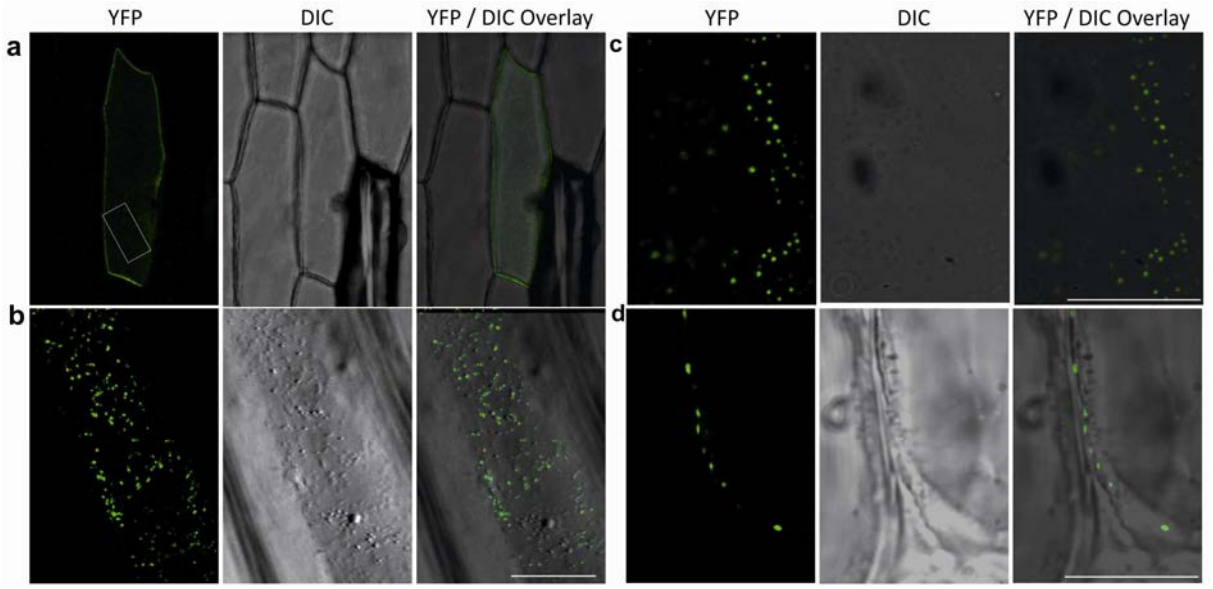

Fig. 44: Structurally distinct fluorescent signals resulting from sYFP-based YFP_C:phy4 + YFP_N:photB2 interaction.
Those signals were observed at the cell surface and the cells outer periphery, possibly related to membrane vesicles or lipid rafts. Scale bars 25 µm.

Microscopic observation at higher resolution allowed identification of locally restricted fluorescence signals. Those signals appeared as spot-like structures distributed all over the cell surface (Fig. 45, **b**) but were also apparent within the signals at the cell periphery (Fig. 45, **d**). It is in the realms of possibility that these local signals refer to membranous structures such as vesicles or lipid rafts; not unlikely, since first steps of some directional responses, like phototropic bending of tip cells rely on membranous rearrangements.
Since those structures were only apparent in a few samples and only visible at highest resolution, it is thus not clear whether they display spatially restricted foci of distinct function, or if they result from overexpression of the sYFP-constructs and are therefore artefacts.

4.8. Analysis of vectorial responses in *Physcomitrella* phototropin mutants

Directional responses in *Physcomitrella* are mainly perceived and further processed by phy4, the predominant receptor for those responses. With the discovery of a plasma membrane localised phy4-phototropin complex, a possible mechanism to detect and induce directional responses such as phototropism and polarotropism is offered. Thus loss of phototropin might result in a phenotype similar to *phy4*$^-$. To verify this hypothesis, phototropin double and triple mutants, kindly provided by Masahiro Kasahara were analyzed regarding their polarotropism and phototropism in R.

4.8.1. Red light phototropism

Loss of phy4 was shown to have a severe impact on phototropism in a fluence rate dependent manner; positive phototropic curvature of tip cells was most affected in medium fluence rates between 1.0 – 2.5 µmol · m^{-2} · sec^{-1} (9). The phototropic bending of filament tip cells in stable knockout lines for *phy4*, *photA2/B1, photB1/B2 and photA2/B1/B2* were analysed according to Mittmann *et al.* Dark-adapted filaments were grown negatively gravitropically before being exposed to unidirectional R of 1.0 µmol · m^{-2} · sec^{-1}.

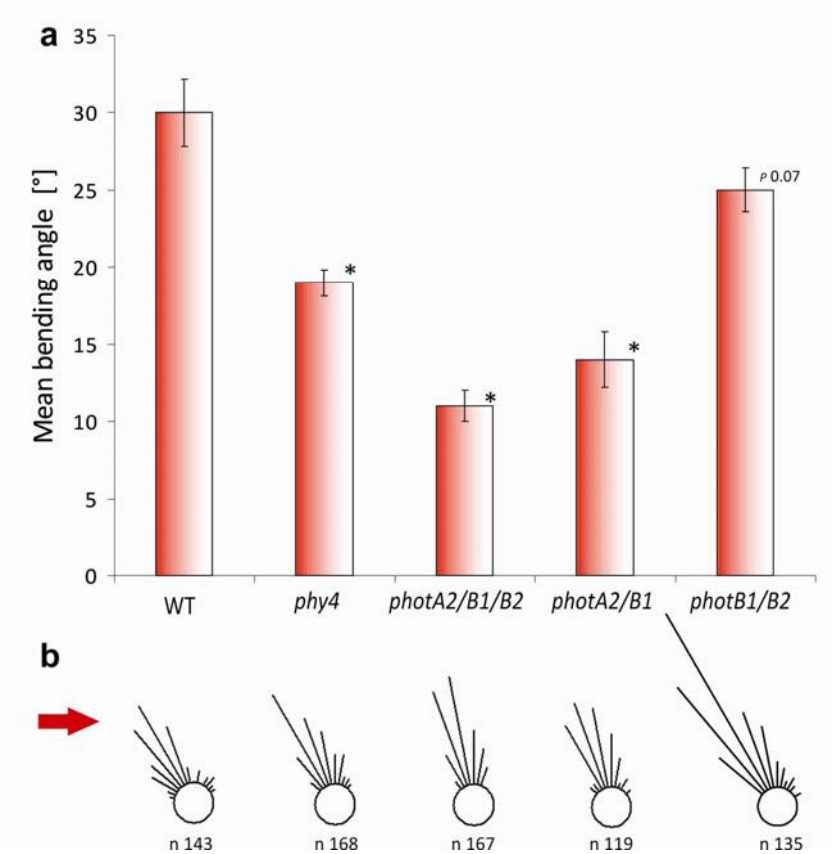

Fig. 45: Red light phototropism is affected in phototropin double and triple knockout mutants.
Red light phototropism is strongly reduced in *phy4* cells and almost abolished in the triple (*photA2photB1photB2*) and one of the double (*photA2photB1*) phototropin knockout lines, as represented by the mean bending angle (**a**) and bending direction as plotted in circular histograms (**b**). Asterisks mark values with statistically significant difference compared to WT (student's t-test, *p 0.01*). Standard errors are given.

Physiological analysis revealed both phototropin double and the triple knockout line to be indeed severely affected in their positive R phototropism; the triple knockout line showed the strongest phenotype amongst all lines investigated, with a further 2 fold reduction in positive curvature compared to *phy4* tip cells and a 3 fold reduction compared to WT. The phototropin double knockout lines differed from each other in their extent of the response. Loss of both photA2 and photB1 had a stronger effect on phototropic bending than loss of photB1 and photB2. These observations reflect the interaction strength of phy4 with those three phototropins; binding of phy4 was strongest to photA1, photA2 and photB1, whereas binding to photB2 was comparably weak (see figs. 34 and 35).

4.8.2. Red light polarotropism

Lower plants are capable of adjusting their growth orientation towards the polarisation plane of incident light, another directional response to R mediated by phy4 (9). The role of phy4-phot interaction for polarotropic responses was thus tested similarly to phototropic experiments described in 4.8.1. Hence, negative gravitropically grown filaments were exposed to 30 nmol·m^{-2}·sec^{-1} of R_{pol}.

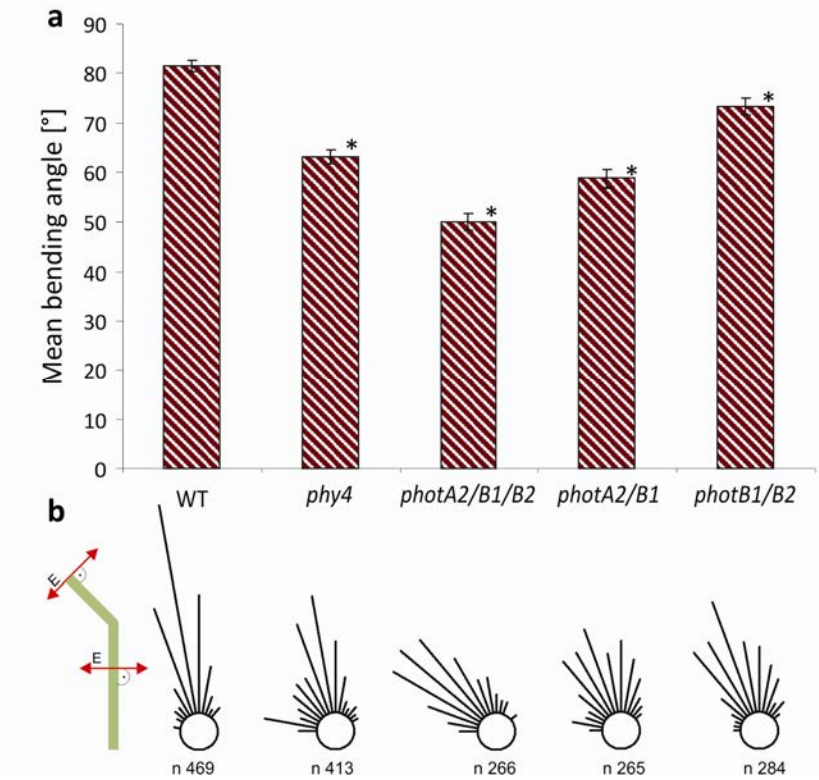

Fig. 46: R polarotropic responses are abolished in phototropin triple mutants.
The angle of the growing tip cells onto the E-vector was measured after rotation of the E-vector by 45°. Consequently, positive responses to R_{pol} are measured as a maximum angle of 90°, no responses are measured as angles of 45°. *phy4*$^{-}$ and phototropin double mutants show reduced polarotropism, whereas polarotropism of phototropin triple mutants was almost abolished, as represented by mean bending angles (**a**) and growth orientation (**b**). Asterisks mark values with significant statistical difference compared to WT (student's t-test, *p 0.01*). Standard errors are given.

Polarotropic responses of the different knockout lines mainly resemble the phenotypes observed for phototropism in unilateral R (see fig. 45).
WT tip cells bent normal to the E-vector of incident R, whereas this response was considerably reduced in *phy4*$^{-}$ and the *photB1/photB2* double knockout. Curvature was further reduced in the *photA2/photB1* double mutant and almost completely lost in the *photA2/photB1/photB2* triple knockout.

4.8.3. Blue light phototropism

Phototropins mediate B induced chloroplast movement responses in lower plants (8), but to date no B induced phototropism or polarotropism was reported for *Physcomitrella.* A possible B induced phototropism was therefore investigated using the before mentioned phytochrome and phototropin knockout lines.

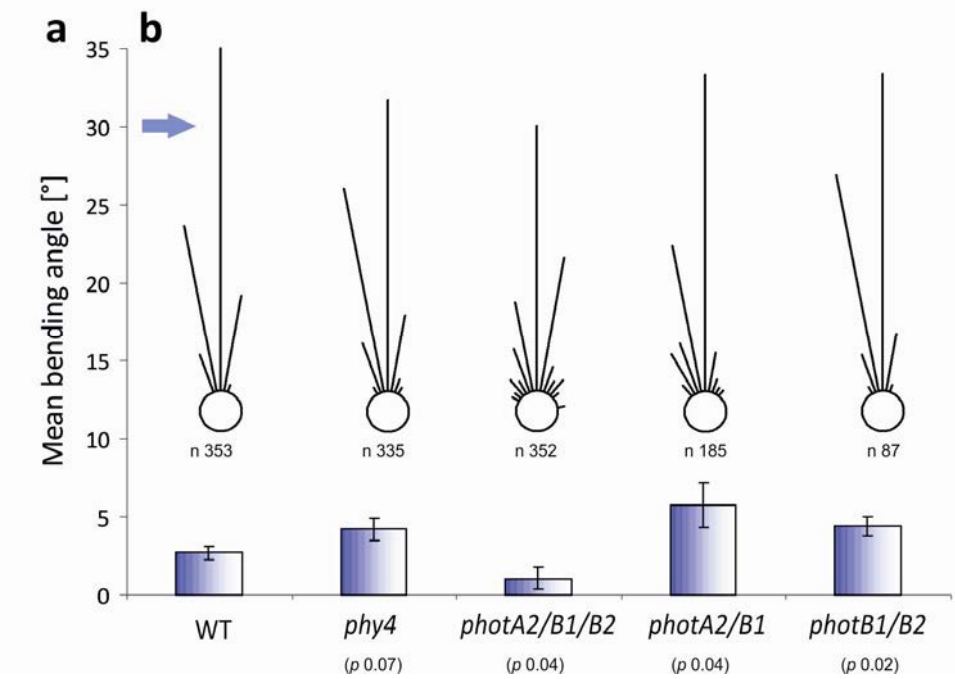

Fig. 47: *Physcomitrella* tip cells do not respond to medium fluence rates of unilateral blue light. None of the moss lines investigated respond to unilateral blue light under medium fluence rates of blue light (1.0 µmol·m^{-2}·sec^{-1}), as represented by the mean bending angle (**a**) and growth orientation displayed in circular histograms (**b**). None of the values measured is statistically different from WT. Standard errors and student's t-test *p*-values are given.

To clarify the role of phototropins in B phototropic responses, unidirectional B at 1.0 µmol·m^{-2}·sec^{-1} was applied to dark-adapted negatively gravitropically grown filament cells of the knockout lines indicated above. This fluence rate was chosen as it is within the range of fluence rates having the highest impact on positive phototropism in R (9). Nevertheless, no effect of unilateral B was detected for WT or any of the knockout lines investigated. Statistical analysis verified first observations of curvatures between 3° and 7°; none of the datasets is significantly different from WT. Thus, no B dependent phototropism exists in *Physcomitrella*. Moreover it can be assumed that (i) the role of phototropins in R phototropism is restricted to phy4's anisotropic binding at the plasma membrane and (ii) chloroplast movement responses in B (8) are differently regulated than R induced directional responses, which rely on phototropin interaction.

4.9. Studies on *Arabidopsis* phyA interaction with phot1

Physiological evidence point to a tight connection between R and B signaling in higher plants too, like R-enhanced B phototropism of hypocotyl cells (107, 215) or root phototropism (108, 109, 216) in *Arabidopsis*. Thus, a similar interaction of higher plant phyA and phot1, the two major players in these responses, was hypothesised. To test for *in vivo* interaction of phyA with phot1, sYFP-assays employing N-terminal fusions were performed.

4.9.1. *In vivo h*omodimerisation of phyA

To ensure functionality of N-terminal sYFP-fusions, YFP_N/YFP_C:phyA were tested for their ability to form homodimers with proper light-dependent localisation, as previously observed for simple FP:fusions (see fig. 12). Onion epidermis cells were transiently co-transfected with the above mentioned constructs and the nuclear marker $Cherry_{NLS}$.

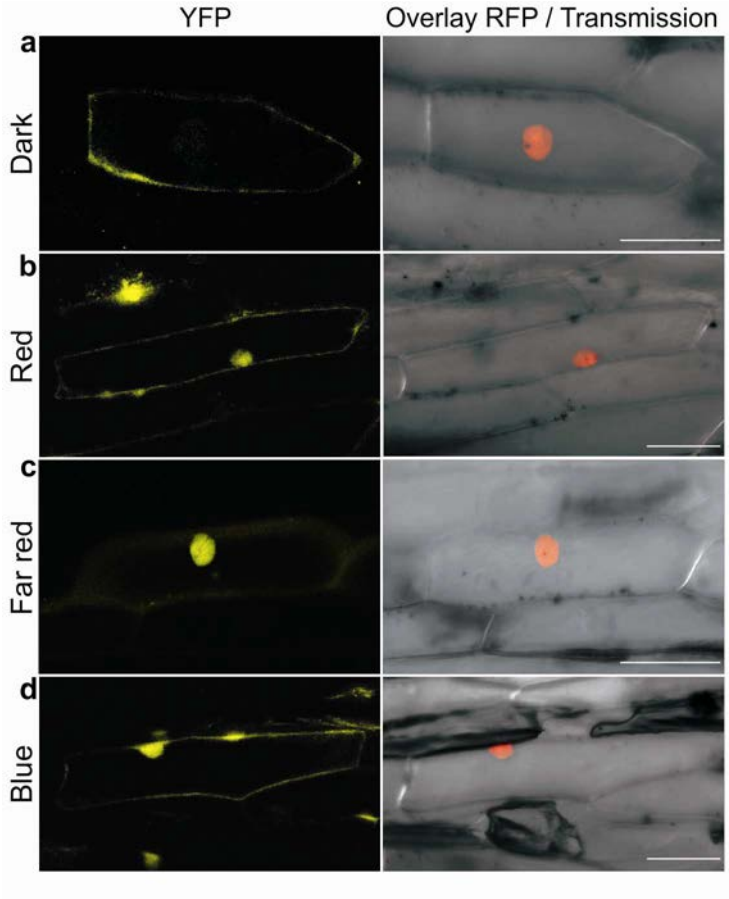

Fig. 48: Light dependent localisation of phyA homodimers in onion epidermis cells.
N-terminal phyA fusions to either of the two YFP moieties form homodimers as revealed by sYFP. Expression of $Cherry_{NLS}$ marks positioning of the nucleus. Scale bars 100 µm.

As shown before for phy4 sYFP-fusions, N-terminal sYFP-fusions to phyA formed homodimers in onion epidermis cells. The localisation of the YFP-signal under the given light conditions resembles the state-dependent localisation pattern of simple phyA fluorescence fusions (see fig. 12). Thus YFP_N/$_C$:phyA-fusions constitute functional photoreceptors.

4.9.2. *In vivo h*omodimerisation of phot1

To visualise and identify cell structures and compartments, marker proteins were expressed in onion epidermal cells.

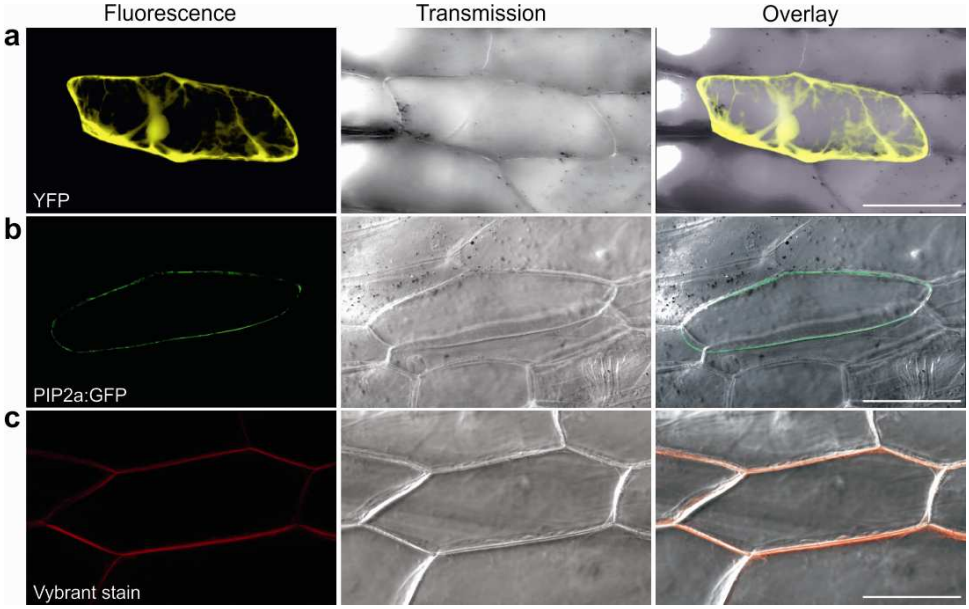

Fig. 49: Expression and localisation of cytosolic, nuclear and plasma membrane localised markers in onion epidermis cells.
YFP (**a**) is localised to both the cytoplasm and the nucleus, whereas PIP2a:GFP (**b**) shows strict plasma membrane localisation. Vybrant (Molecular Probes) fluorescence signals (**c**) are emitted only when incorporated into membranous environment. Scale bars 100 µm.

Expression of marker proteins and visualisation with a membrane specific dye in onion cells yielded the same fluorescence signals as previously observed in *Physcomitrella* filament cells (see fig. 39).
After having established functional sYFP-phyA fusions in onion epidermis cells, plasma membrane localisation of N-terminal sYFP-fusions of phot1 was analyzed in the same model system. Therefore $YFP_N/_C$:phot1 fusions were transfected into onion epidermis cells and tested for homodimerisation. The localisation pattern was compared to previously reported light-dependent localisation of phot1 in *Arabidopsis* (100, 217).

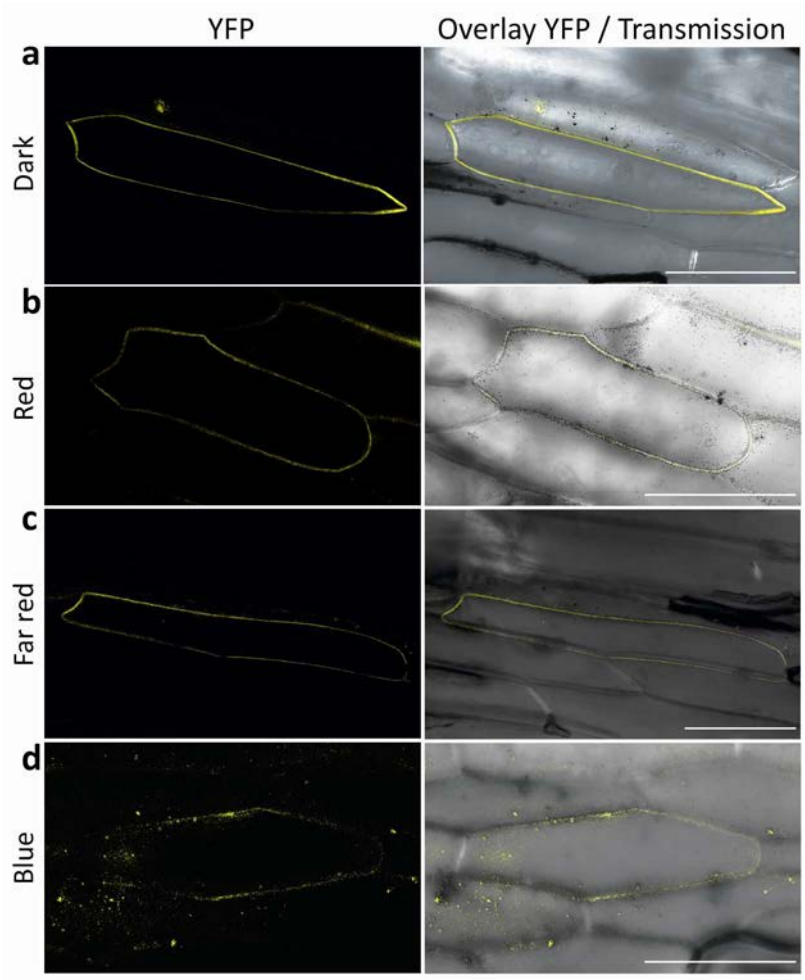

Fig. 50: Light dependent localisation of phot1 homodimers in onion epidermis cells.
N-terminal phot1 fusions to either of the two YFP moieties form homodimers as revealed by sYFP. Scale bars 100 µm.

Expression of N-terminal sYFP-fusion of phot1 yielded reconstitution of the YFP signal. From comparison with plasma membrane markers, the YFP signal is localised to the plasma membrane (see figure 49). phot1 homodimerises under all light conditions tested. Notably, the before observed distinct plasma membrane localisation of phot1 appeared to diffuse after blue light incubation, presumably resembling B induced internalisation as described in Sakamoto & Briggs (2002). Thus, N-terminal phot1-fusion proteins constitute functional phototropins.

4.9.3. *In vivo* interaction of phyA and phot1 in onion epidermis cells

After having established both photoreceptors as functional N-terminal fusions in the sYFP-system, *in vivo* interaction of phyA and phot1 was investigated in onion epidermis cells.
Interaction of *Physcomitrella* phy4 with phototropins was observed even without previous light-treatments in Y2H assays; however, it was shown that R seems to promote plasma membrane localisation of phot1 in hypocotyls cells of *Arabidopsis* (103). Despite the experimental limitations of the sYFP-system explained earlier (see 4.6), phyA-phot1 interaction was assayed both without light pre-treatment and after 1 h of R incubation.

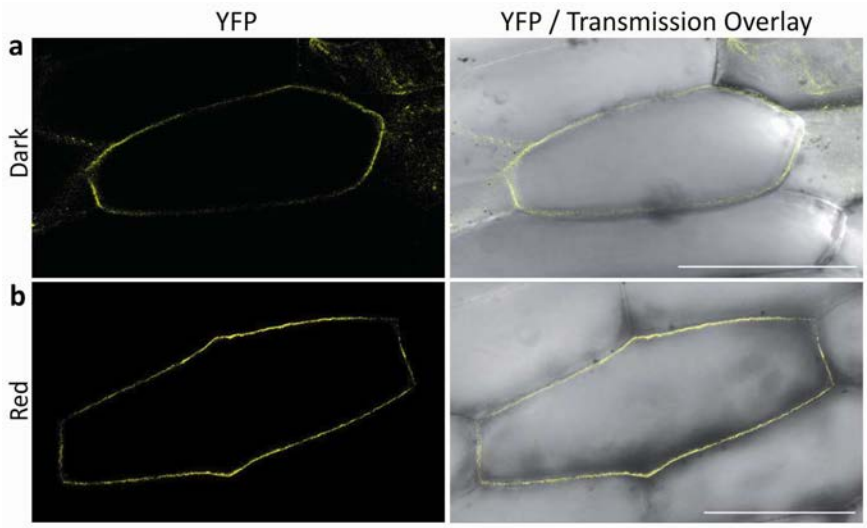

Fig. 51: *In vivo* interaction of phyA with phot1 in onion epidermal cells as revealed by sYFP.
YFP_C:phyA-YFP_N:phot1 emit a strong sYFP-signal after 1 h of R incubation. Scale bars 100 µm.

Astonishingly, phyA and phot1 interacted *in vivo* at the plasma membrane when N-terminally fused to either of the two YFP moieties. The signal strength was comparably low in darkness (i.e. without light-treatment prior to observation) and seemed to increase after R incubation to a strong distinct signal, resembling the localisation of phot1-homodimers previously observed (see Fig. 50). phyA and phot1 interaction at the plasma membrane thus seems to exist not only in lower plants but also in higher plants.

The finding of phytochrome-phototropin interaction might be the basis for understanding phytochrome involvement in directional responses in general and its modulating role in directional B responses. Plasma membrane association of phytochrome mediated by interaction with phototropins has a dramatic impact in directional R sensing in mosses, while it has a more subtle implication in the R modulation of B induced directional responses in higher plants. Furthermore, this finding supports the idea of a cytoplasmic phytochrome function and presumably connected signaling route and questions gene expression as the exclusive mode of action of phytochrome. Moreover it appears that phytochromes act through two equally important functional *modi*: by both regulation of gene expression within the nucleus to regulate complex developmental programs such as photomorphogenesis and by perception and mediation of directional / vectorial cues, which are partially integrated into the B signaling route of phototropins by (in)direct interaction within the cytoplasm.

5. Discussion

5.1. Directional phenotype of regeneration protoplasts in R_{pol} and transient phenotype rescue

Phytochrome-mediated directional responses in *Ceratodon* and *Physcomitrella* were assayed by moss protoplast regeneration. While phytochrome specificity was shown by R/FR-reversibility *Ceratodon* protoplast regeneration (120), directional *Physcomitrella* in protoplast regeneration were assessed in polarised white light, leaving the possibility of both B and R photoreceptor participation undetermined (161, 218). Polarisation of germinating spores was shown to be phytochrome-mediated (123, 124) and physiological analyses of single phytochrome knockout lines indicated phy4 to be responsible for directional responses in protonemata (9). In accordance with those previously reported observations, a protoplast regeneration phenotype of *phy4*$^-$ could indeed be established in the studies presented here. Regeneration of both WT and *phy4*$^-$ protoplasts revealed a strong fluence rate dependency regarding both the efficiency of regeneration and the occurrence of directional outgrowth. In accordance with previous reports (122, 131) the efficiency of protoplast regeneration increased with the fluence rates of R (10 µmol · m^{-2} · s^{-1}). However, regenerating protoplasts of the *phy4*$^-$ line did not develop a directional phenotype under such fluence rates of R_{pol} (see fig. 4). With decreasing fluence rates (0.8 µmol · m^{-2} · s^{-1}) regeneration efficiency dropped but at the same time phenotypic differences between WT and *phy4*$^-$ protoplasts became apparent: while WT protoplasts regenerated primary cells in normal orientation to the applied E-vector, this response was abrogated in *phy4*$^-$ protoplasts (see fig. 4). This observation further confirmed phy4 as the phytochrome responsible for directional light sensing in *Physcomitrella.*

Both protoplast regeneration and the directionality of primary cell outgrowth are light-dependently regulated by phytochrome, with a special involvement of phy4. While directional responses such as polarotropic primary cell growth are presumably explained by a hitherto unknown signaling cascade of cytoplasmic phytochrome, regeneration of daughter cells from isolated protoplasts might be additionally dependent on transcriptionally regulated processes. Such regulation might be brought in line with fluence rate dependency as nuclear signaling - if not nuclear transport of phy4 itself (see 5.2.1.) - might be more efficiently triggered under higher fluence rates of R. However, responses in different directions are much more difficult to connect with varying fluence rates. Phototropic responses are either in positive (low to medium fluence rates) or negative (very low and high fluence rates) direction of unilateral R (9). Assuming the establishment of a Pfr gradient and the prerequisite of anisotropic phytochrome (see 5.5.2. and 5.5.3.), kinetics of either Pfr formation at the flank of illumination or photocycling between Pr and Pfr could account for the formation of a Pfr gradient either at the illuminated or the opposite flank of the cell. Under medium fluence rates, a Pfr gradient might be formed at the side of illumination, as R on the opposing flank is not sufficient for Pfr formation. Thus, bending will occur towards the side of illumination, i.e. bending in positive direction. Under high fluence rates, the cell might be more homogenously illuminated within a short time and even though a Pfr gradient will be formed at the illuminated side first, enough R will be available for Pfr formation on the opposite flank. Within a short time frame, the initially formed Pfr gradient at the

illuminated cell flank might be disintegrated by photocylcing and reconversion of Pfr to Pr. Thus a Pfr gradient on the opposite side might be more easily maintained leading to negative phototropic bending. Polarotropic responses, on the other hand, only exist under very low fluence rates and are not observable under any other light condition. While phototropic responses are triggered by the directionality of the incident light stimulus (i.e. directionality in a strict sense), polarotropic responses are induced by the orientation of the E-vector. As this information should not differ depending on the fluence rates applied, other information of the incident light stimulus have to affect polarotropic responses. Maybe cellular rearrangements induced by the information given by the E-vector are overdriven by simulatenously induced responses resulting from other information of the incidient light stimulus; thus polarotropism would not be possible to be observed under higher fluence rates.

Loss of phy4 affected both positive phototropic and polarotropic responses in medium (1 µmol · m^{-2} · s^{-1}) and low fluence rates (30 nmol · m^{-2} · s^{-1}) (9). Likewise, polarotropic outgrowth and phenotypic rescue of regenerating *phy4*$^{-}$ protoplasts were affected under the same light conditions in this study. As protoplast regeneration is the earliest step following standard protoplast transformation procedures, this phenotype was used for transient complementation assays. Transient overexpression of *PHY4:YFP* was judged by observation of YFP fluorescence 48 h post transfection. Further investigation on protoplast regeneration in R_{pol} showed no influence of phy4:YFP regarding WT protoplast regeneration, neither affecting regeneration itself nor directionality of filament outgrowth (see fig. 5). However, *phy4*$^{-}$ protoplasts recovered their ability for directional sensing by expression of *PHY4:YFP* and showed phenotypic rescue under very low fluence rates of R_{pol}. The fusion of a fluorescent tag to PHY4 therefore does not interfere with physiological responses but constitutes a functional photoreceptor compensating the loss of phy4 (see fig. 5).

Investigation of protoplast regeneration offers the possibility to observe early events of polarity determination, connecting fluence rate dependence of the initiation of regeneration with the directional character of the resulting response. As soon as a phenotype of *phy4*$^{-}$ protoplasts in R_{pol} is established, phenotypic rescue could be assessed under the same experimental conditions by transient overexpression of *PHY4:YFP*. A transient assay holds the advantage of circumventing problems possibly associated with the stable, ectopic integration of a *PHY4:YFP* construct in the background of the *phy4*$^{-}$ knockout line. Moss mutant lines derived from homologous recombination events mostly contain concatemeric copies of the knockout constructs integrated either at the genomic locus and / or additionally at ectopic sites (219). As long as the genomic locus is targeted, this will result in gene knockout but may generate a mutant line additionally affected by the integration of large amounts of DNA made up by DNA concatemers. The additional integration of a construct containing the cDNA of the initially targeted locus may thus further cause peculiarities in growth and development. To circumvent possible problems associated with conventionally targeted mutant lines, a new generation of knockout constructs generated by the CRE/lox system offers the possibility to excise the targeted genomic locus together with the inserted marker. The excision of the whole targeted genomic locus opens the possibility for a clean deletion mutant. The use of this technique could thus improve gene targeting by circumventing problems arising from concatemeric integration and offers the possibility for consecutive insertion of multiple knockouts without the need for several different marker genes.

5.2. Phytochrome localisation studies

5.2.1. Intracellular localisation of phy4

The phenotypic rescue of *phy4*$^-$ by transient overexpression of *PHY4:YFP* confirmed C-terminal phytochrome fluorescent fusions as functional photoreceptors (see 4.4.2). To be able to connect phy4 directional light sensing with phy4 localisation, two different phy4-fluorescent fusion proteins were analysed regarding their light-dependent localisation. Comparison of the *PHY4* cDNA sequences cloned by Mittmann *et al.* and the sequence obtained after genome sequencing revealed 6 single nucleotide exchanges. Those mutations lead to four changes within the protein sequence, three of which are located within the photosensory module and one within the HKRD. Although only one mutation within the photosensory module was located in the GAF-domain, probably involved in the formation of a light sensing knot in phy4 (see fig. 3), both *PHY4* cDNAs were used for the generation of fluorescent fusions to exclude effects deriving from the mutations identified. C-terminal fluorescent fusions from both *PHY4* constructs predominantly localised to the cytoplasm in *Physcomitrella* cells with only weak nuclear accumulation (see fig. 7 and 8).

So far, nuclear localisation has not been shown for moss phytochromes. Instead, an exclusively cytoplasmic localisation has been reported for all 4 characterised phytochromes in dark-adapted *Physcomitrella* protoplasts (172). This localisation also matches their function in R induced chloroplast avoidance responses, as irradiation with high fluences of R (2.5 h of 25 µmol · m^{-2} · s^{-1}) did not lead to nuclear accumulation of either phy1:YFP or phy2:YFP (172). In accordance with these observations, NLS-fusions to PHY1 and PHY2 resulted in abrogation of the chloroplast avoidance response under the same R conditions, clearly pointing to a cytoplasmic function of phy1 and phy2. *phy4*$^-$ protonemata were not affected in regard to chloroplast photorelocation under R_{pol} conditions but were impaired in directional responses of the protonematal tip cells (9), also pointing to cytoplasmic phytochrome function. As both *PHY2* and *PHY4* group within the same phylogenetic clade (9), it seems that they both serve detection of directionality but that they mediate different responses.

Nuclear translocation of both phyA and phyB has been analysed in great detail for C-terminal fusion proteins and is, in contrast to moss phytochromes, strongly light dependent. phyA nuclear-cytoplasmic partitioning occurs rapidly and to a great extent in FR conditions (66, 68) while nuclear translocation of phyB is not only considerably slower but even detectable in D (73). Likewise, phy4:CFP is predominantly cytoplasmic, but also shows a weak nuclear accumulation in dark conditions. This reflects the situation observed for phyB nuclear cytoplasmic partitioning and once more points to a functionally conserved similarity between both phy4 and phyB. On the other hand, nuclear localisation of phy4:CFP appears to not change upon further illumination neither in R nor in FR. Thus, a light-dependent nuclear transport is questionable and certainly reflects higher plant phytochromes nuclear localisation only to a minor extent.

Nuclear translocation of phyA and phyB is a prerequisite for their function in regulating gene transcription (75, 220, 221). While nuclear interacting proteins have been described for both phyA and phyB (PIFs, HY5, COP1, CCA1 and others) and were

connected to phytochrome's gene regulatory function, nuclear functions of moss phytochromes are not as evident. Nevertheless, moss phytochromes may also have nuclear functions, which require partial nuclear localisation. They may function within the nucleus in cooperation with cryptochromes in regulating the change of generation phases as in the hormonal controlled transition from chloronemata to caulonemata, induction of bud-initials and gametophore formation (141, 142). *Arabidopsis* phytochromes and cryptochromes also work together in higher plants in integrating light signals into the circadian clock by interaction with clock components like CCA1 and LHY. The interaction of phytochrome and/or cryptochrome with clock components either happens directly by protein-protein interaction or indirectly by transcriptional control, which is regulated by phytochrome in concert with ELF3 and SPA1 (repression) or TIC, ZTL and GI (induction) (77, 222, 223).
Many features of the circadian clock are also conserved in *Physcomitrella* and photoperiodic regulation of the day-length sensitive transition from the gametophore into the sporophyte generation (224). Specific clock components homologous to the respective *Arabidopsis* proteins have been characterised (PpCOL, PpCCA1a, PpCCA1b, PpPRR2) and showed functional redundancy (224-229) and *Physcomitrella c*ryptochromes have been shown to be at least in parts responsible for B entrainment of the clock (228). Very recently *Adiantum* phy2 was indeed reported to be R dependently translocated into the nucleus thereby mediating spore germination (173). Possible nuclear responses in *Physcomitrella* may also include induction of spore germination and protoplast regeneration (130, 131), which could be regulated independently of directional responses related with either germination or regeneration. Homologs of certain *Arabidopsis* interacting partners involved in nuclear regulation of photomorphogenic responses were identified in *Physcomitrella* too, like PIF1 (50) or HY5 (174). Their role in integrating light stimuli in the developmental program of *Physcomitrella* as yet remains elusive, as mosses do not exhibit photomorphogenesis in a strict sense and therefore might exhibit different responses than those observed in *Arabidopsis*.

5.2.2. Intracellular localisation of N-terminal tagged phytochromes

Functional integrity was assumed to be retained by C- rather than N-terminal phytochrome fusions, as transgenic plants overexpressing phyA implied a critical role for the N-terminal extension (189, 190). Ever since, this assumption was confirmed by positive outcomes of light-dependent nuclear translocation studies with C-terminally positioned tags (65, 66). Nowadays structural information on the photosensory module is available, additionally pointing to a crucial role for the N-terminal module in formation of functional phytochromes (44). Although to date no related information on plant phytochromes exists, the structural features of cyanobacterial and bacterial phytochromes suggest an important function of the N-terminal module. It has thus to be assumed that N-terminal positioning of a tag might influence formation of functional phytochrome in terms of either its photoconvertibility into stable Pfr or other structure-related signaling or translocation events.
In order to investigate the significance of tag-positioning regarding phytochrome's light-dependent nuclear translocation, fluorescent fusions to the N-termini of *PHY4* and both *PHYA* and *PHYB* were also transiently expressed in *Physcomitrella* and onion

epidermis cells. As partially expected from structural consideration, GFP:phy4 indeed exhibited exclusive cytoplasmic localisation in *Physcomitrella* protonemata cells. Any nuclear accumulation, as partially observed for C-terminal fusion proteins (see fig. 7 and 8), was abrogated when using *GFP:PHY4* (see fig. 9). Thus subcellular localisation of phy4 is predominantly cytoplasmic but also sensitive to tag-positioning, as N-terminally fused fusion proteins do not show nuclear fluorescence signals.
Controls using conventional C-terminal fluorescent fusions (*PHYA:GFP* and *PHYB:GFP*) showed light-dependent nuclear translocation of both phyA and phyB as described before. phyA:GFP was exclusively localised to the cytoplasm in darkness and showed strong nuclear accumulation after FR and R irradiation (see fig. 12). Likewise phyB:GFP exhibited nuclear accumulation after R and weakly upon FR irradiation. Only very weak nuclear signals were observed for phyB:GFP in dark conditions (see fig. 13). Interestingly, neither phyA:GFP nor phyB:GFP showed nuclear translocation after B irradiation. Although phytochromes are able of absorbing in the B range, this apparently does not lead to photoreceptor nuclear accumulation. In contrast to the observations made for GFP:phy4 in *Physcomitrella* (see fig. 9), N-terminal fusions to both phyA and phyB resulted in a light-dependent intracellular localisation pattern similar to C-terminal fusions in onion epidermal cells (see figs. 12 and 13). Nuclear import of phyA and phyB was not affected by positioning of the fluorescence tag at the N-terminus. As the light dependency still persists and a specificity towards spectral quality can be observed, these fusions likely maintain their spectral integrity and therefore proper folding of the molecule.

5.2.3. Differences and similarities of phy4 and phyA/phyB nuclear transport mechanisms

The localisation pattern observed for C-terminal fluorescent fusions of PHY4 showed weak nuclear accumulation, which was not enhanced through light as observed for phyA or phyB. However, the cytoplasmic localisation of phy4 became more pronounced when expressed in a higher plant background, as both C-terminal and N-terminal fluorescent fusions were exclusively localised to the cytoplasm (see fig. 11). phyA:GFP surprisingly exhibited light-dependent nuclear translocation in *Physcomitrella* (see fig. 14) as observed in higher plant cells (see fig. 12). Nuclear accumulation under FR conditions was most effective, less nuclear accumulation was observed after R treatments. Strict cytoplasmic localisation was observed for both D and after B treatment. Expression of the reciprocal fusion in *Physcomitrella*, GFP:phyA resulted in strict cytoplasmic localisation under all light conditions tested (see fig. 14). This observation is especially interesting as GFP-tag positioning to phyA did not affect light-dependent localisation of phyA in onion epidermis cells (see fig.12).
Nuclear transport of phyA in *Arabidopsis* is facilitated by adaptor molecules FHY1 and FHL (69, 70) and loss of both results in strict cytoplasmic localisation of phyA (71). Consequently, this might hint towards a conserved nuclear transport mechanism for phytochromes between higher and lower plants. Although BLAST searches involving the full length sequence of FHY1 did not yield an obvious homolog, more detailed *in silico* search with the C-terminus of FHY1 revealed a potential candidate from the *Physcomitrella* genome (XP_001772262.1). FHY1's C-terminus also comprises the

conserved phyA binding motif (69). As far as light-dependent nuclear import of phyA:GFP in *Physcomitrella* is concerned, this *Physcomitrella* protein is able to facilitate proper nuclear translocation of phyA. Interestingly, phyA's nuclear transport is impaired in *Physcomitrella* in dependence of GFP-tag positioning, as is phy4. This hints towards a functional conservation of the nuclear transport machinery including the putative FHY1 homolog of *Physcomitrella*. Very recently, the group of Andreas Hiltbrunner presented data on light-dependent nuclear translocation of *Physcomitrella* phytochromes, reporting nuclear accumulation of moss phytochromes being brought about by a *Physcomitrella* homolog of FHY1 (230); at least to some extent supporting the findings of the work presented here.

However, the differences regarding light-dependency of phyA and phy4 nuclear transport point towards differently regulated nuclear transport processes. Assuming phy4 nuclear transport in *Physcomitrella* being generally facilitated by the *Physcomitrella* FHY1 homolog, it is questionable why phy4 is not light-dependently transported in *Physcomitrella* and why phy4 is not nuclear translocated in higher plant cells. FHY1 was shown to bind phyA within its N-terminal photosensory module (70) and this binding is a prerequisite for nuclear transport. Recently, single residues within the N-terminal extension of phyA were identified as being necessary for FHY1 binding and phyA nuclear transport (231). Although phyA appears to require a freely accessible photosensory module, addition of a 25 kDa protein tag at the N-terminus does not impair interaction with the FHY1/FHL-transport machinery as this construct is still capable of entering the nucleus in a light dependent manner (see fig 12). Seemingly, moss phytochromes are not recognised by either FHY1 or FHL in higher plants, questioning the structural determinations of the FHY1 binding site. It was shown that FHY1 preferentially binds phyA in its Pfr form (232) and although no specific residues have yet been identified, it was reported that FHY1 binds to phyA within the region of the N-terminal residues 100-406 (70). Alignment of the first 500 amino acids of phyA and phy4 exhibited considerable differences within the first ~ 75 amino acids comprising the N-terminal extension domain (NTE). The NTE of phyA was very recently shown to add to the binding efficiency of FHY1 to phyA (231) and the differences within the NTEs of both phyA and phy4 might lead to a considerable structural difference, possibly explaining why phy4 is not recognised by FHY1 in higher plant cells. Seemingly the functional homologous protein in *Physcomitrella* is sensitive to other features of the N-terminus of phytochrome, as it recognises the apparently different NTEs of both phyA and phy4. At the same time this protein appears to be extremely sensitive to changes within the photosensory module as both GFP:phyA and GFP:phy4 show complete abrogation of nuclear import in *Physcomitrella*. However, FHY1 appears to not be as sensitive to changes within the N-terminus of phyA, as both phyA:GFP and GFP:phyA are light-dependently nuclear translocated. It can only be speculated that the *Physcomitrella* FHY1 recognises other features of the N-terminal module, or is more restricted to the very N-terminal part of phytochrome, whereas *Arabidopsis* FHY1 recognises different and/or additional sites of the (complete) photosensory module. Consequently GFP tagging of phyA's NTE does not influence FHY1 binding as much since other remaining binding sites within phyA are sufficient for nuclear transport. Due to further differences within the protein sequences, phy4 may not exhibit such additional binding sites and is therefore not transported by FHY1 at all. However, such gradual differences in

GFP:phyA transport were not in the range of observation possibilities using transiently overexpressing plant cells. It is possible that further downstream signaling is at least partially impaired through the N-terminal tagging of phytochromes. Subsequent signaling events, such as PIF binding happens at the photosensory module and it is therefore likely that phytochrome is sensitive to N-terminal tagging. However, this would require detailed complementation assays of the mutants.
In contrast, localisation of phyB in *Physcomitrella* was comparable to the pattern observed in onion cells (see figs. 13 and 15). As in the case of higher plant cells, considerable amounts of phyB remained cytoplasmically localised, even when nuclear accumulation in R occurred. As observed before, tag-positioning left nuclearcytoplasmic partitioning of phyB unaffected. The import mechanism of phyB is unknown so far, but it was suggested that phyB itself contains a cryptic NLS in between the PAS repeat and the HKRD, which is masked and unmasked through photoconversion (74). N-terminal fusions of phyB would not impair this mechanism and nuclear accumulation could be maintained, as seen in onion cells (see fig. 13). As phyB nuclear transport in *Physcomitrella* showed no sensitivity towards N-terminal tagging, unlike phyA and phy4, the nuclear transport machinery of phyB and phy4 appears to be different from each other. Unmasking of a cryptic NLS within the phyB sequence as proposed could facilitate nuclear transport in *Physcomitrella* too, as no specific adaptor proteins are needed as in the case of phyA. This again underlines the fundamentally different transport mechanisms of phyA and phyB. Whether or not phy4 is nuclear translocated in a specifically regulated manner and if so by which transport mechanism this translocation is mediated cannot be unequivocally determined at this point. Also a possible nuclear function of phy4 remains elusive. As supported by the localisation studies shown (see figs. 7-9 and (172)), moss phytochromes are majorily localised to the cytoplasm with only a partial nuclear localisation. Thus further experiments were focussed on the cytoplasmic moss phytochrome function and the elucidation of the underlying cytoplasmic signaling route.

5.3. Identification of putative phy4 interacting proteins and verification of phytochrome-specific interaction

In order to identify components of the putative cytoplasmic signaling route of phy4, an Y2H screen of a *Physcomitrella* cDNA library against a full-length phy4 sequence was performed. Following cDNA library screening and sequencing of the isolated clones, numerous interacting proteins were identified from which four clones were chosen for further analysis based on their predicted function and subcellular localisation. Those proteins were named: Pirin, PLP, PLR, EF1α in accordance with their annotation or predominant domains or motifs. Those putative interacting partners are discussed in the following sections.

5.3.1. PLP, a p-loop containing protein

PLP is annotated as an unknown protein in the *Physcomitrella* database. Comparison of protein sequence similarity revealed a C3HC4 RING zinc finger motif, which classified this protein as an interesting candidate for a phytochrome signaling pathway. Several zinc finger proteins have been identified as members of higher

plant phytochromes signaling pathways. Due to their DNA binding capacity, zinc finger motifs are classified as transcription factors and have been shown to control several light-regulated developmental processes. CONSTANS, a CHC3H2 zinc finger protein, promotes flowering in *Arabidopsis* (233). SOMNUS, a CCCH-type zinc finger protein, negatively regulates light-dependent seed germination downstream of PIL5 and becomes itself transcriptionally repressed by both phyB and phyA (234, 235). HRB1 (HYPERSENSITIVE TO RED AND BLUE-1), a ZZ-type zinc finger, regulates expression of PIF4 in both R and B dependent manner mediated by phyB and CRY1 (236, 237). RFI2 (RED AND FAR-RED INSENSITIVE 2) and COP1 contain the specific C3HC4 type RING zinc finger motif which is also present in PLP. RFI2 acts as a positive regulator of both phyA and phyB mediated de-etiolation of young *Arabidopsis* seedlings (238). Furthermore, RFI2 negatively regulates CONSTANS expression and thereby represses photoperiodic flowering (238). COP1 is a central player of early *Arabidopsis* development and regulates photomorphogenesis in different light qualities (239). Additionally to the C3HC4 zinc finger, COP1 contains several WD40 repeats (240). However, the similarity of the RING motif is higher between PLP and RFI2 than COP1. The mutant *cop1* displays the strongest phenotype of any signaling intermediate identified so far: constitutive photomorphogenesis in D. In darkness, COP1 acts as a E3 ubiquitin ligase of HY5, a positive regulator of photomorphogenesis and strikingly, the amount of HY5 can be directly correlated to hypocotyl elongation in *Arabidopsis* (170, 241, 242). Additionally, COP1 acts as an E3-ubiquitin ligase on both phyA and phyB within the nucleus (38, 243). Upon light detection, active exclusion of COP1 from the nucleus is mediated by phyA, phyB and CRY1 (244). However, COP1 cytoplasmic function still remains elusive.

Since the algorithm of CDD searches having been changed in 2011 (198), the initially identified C3HC4 RING zinc finger motif unfortunately could not be reproduced in Pp.PLP. Instead, a transmembrane domain, a p-loop motif and a sulfotransferase domain were annotated for PLP, overall classifying it into the group of p-loop nucleoside triphosphatases (NTPases).

In *Arabidopsis*, 18 sulfotransferase (SOTs) are encoded within one gene family. SOTs transfer a sulfate group form 3'-phosphoadenosine 5'-phosphosulfate (PAPS) to a hydroxyl group of one of their various substrates. Thereby SOTs control the function of a wide variety of biological compounds by posttranslational addition of sulfate. The expression of SOTs appears to be tightly controlled in an organ and tissue-specific manner and as well in regard to the developmental stage. One specific SOT, AtSOT17, exhibited expression in a circadian rhythm with the highest mRNA content at the end of the light phase (245). SOTs appear to be functional in diverse processes such as the regulation of hormone synthesis or activity, mostly concerning BR or JA (246-248). Tyrosylprotein sulfotransferases apparently function in the maintenance of root stem cells by modification of peptide hormones (249-251). Still, plant SOT function and the specific compounds modified by the respective SOTs are poorly characterised yet (202).

Homologs of Pp.PLP identified from the protein database of *Arabidopsis* were annotated as nodulation proteins. Formation of root nodules is initiated by symbiotic interaction with rhizobia under nitrogen-limiting conditions. Nodulation mainly occurs on the roots of *Fabaceae* family members, but are also found in other species within the rosid clade (252). Nodulation is light dependent and seems to be

photomorphogenically controlled. It was recently reported that the R/FR ratio sensed by phyB and further processed by JA-signaling significantly influences nodulation in *Lotus* (253). JA is reported to promote root nodule formation in *Lotus* and the expression of JA-activating genes (MYC2, JAR1 previously known as FIN219, a cytoplasmic phyA signaling component) is negatively regulated by phyB (254, 255). Addition of sulfate inactivates JA and might therefore give a hint on an interplay between phytochrome light signaling and JA-action on photomorphogenically mediated nodulation events. Despite this connection, *Arabidopsis* as a non-nodule plant triggers a system resistance response upon root colonisation by *Pseudomonas* (256) and obviously, no nodulation occurs on *Physcomitrella.* Therefore, an implication of Pp.PLP in phytochrome controlled nodulation events is inexplicable.

Since sulfotransferases are poorly characterised in *Arabidopsis* and roles for sulfonation in regulation of development and plant defence reactions are only just emerging, it is not surprising that there is almost no information about sulfotransferase action in *Physcomitrella*. Also, JA, in a strict sense, is not amongst the conserved hormones regulating development in *Physcomitrella*; only cyclopentenones, precursors of JA-synthesis, are present and analyses of knockout mutants have revealed a possible role connected with sexual reproduction (257). For these reasons, a conclusion on a putative role of Pp.PLP on phytochrome signaling might only be drawn from BR-based mechanisms. However, as the BR-synthesis and signaling routes in *Physcomitrella* and their impact on moss development are only just emerging (258), it is hard to conclude a connection between light induced responses and downstream responses mediated by BR in *Physcomitrella.*

Pp.PLP was one of two candidate proteins identified from cDNA library screening to interact with phy4-Pfr, the interaction being reversible by subsequent FR irradiation (see figs. 28 and 29). Light-dependent interaction with phy4 was only detected for the full-length protein (see fig. 28), whereas constitutive interaction was detected with apo-PHY4_C (see fig. 31). No binding was observed for the photosensory module (see fig. 30) suggesting the binding site of Pp.PLP being located within the phy4 C-terminal module, but with a structural influence on conformation dependency from the N-terminus. In both the Y2H-spot assay and the *in vivo* sYFP-complementation assay, interaction between Pp.PLP and phy4 appeared to be comparatively weak. Interestingly, the localisation of the Pp.PLP-phy4 interaction complex changed from cytoplasmic in darkness to nuclear upon R irradiation (see fig. 34). This observation contrasts localisation studies with CFP:PLP alone, as CFP:Pp.PLP was strictly localised to the cytoplasm under both D and R conditions (see suppl. fig. 13). This points towards a phytochrome-induced nuclear translocation of the interaction complex and supports a light-dependent nuclear import of phy4, which has not been obvious from localisation studies either. Localisation of fluorescent fusion proteins is also inconsistent with the prediction of a transmembrane domain by SMART analysis; but membrane integration of the fusion protein could likely be prohibited by the N-terminally placed CFP-tag. Localisation of a C-terminal fluorescent fusion and its consequences for phytochrome interaction remain to be investigated.

5.3.2. PRL1, pleiotropic regulator locus

Mutations in the *PRL1* locus of *Arabidopsis* result in a great variety of different phenotypes as the name "pleiotropic regulator" implies (259). Initially reported to play a role in cell polarity determination by acting on the assembly of the actin cytoskeleton within the heterologous system of fission yeast (260), PRL1 was later suggested to play a central role in integrating light signals with both the BR-synthesis and signaling and sugar response pathways (261)). *prl1's* COP-phenotype of the inhibition of hypocotyl elongation in darkness has been in parts correlated with a repressing action of PRL1 on *CPD* transcription in light-grown plants (261). As this phenotype occurred only in dark conditions while under R, FR and B *prl1* seedlings were comparable to WT, it was not possible to connect PRL1 action on *CPD* gene expression to a specific photoreceptor (261). Further protein analysis described PRL1 as a basically charged protein with both localisation to the cytoplasm and association with microsomal membranes. It was also shown that a proportion of PRL1 is nuclear localised in *Arabidopsis* (261). PRL1 binds specifically to importin-α (ATHKAP2) and carries an NLS variant, which is not constitutively recognised. Therefore, it was hypothesized that PRL1 might be a target for protein kinases. Phosphorylation could be involved in nuclear import by targeting either the NLS sequence or importin-α itself. Later it was shown that PRL1 acts on BR biosynthesis not only by influencing *CPD* transcription but also by regulating the *Arabidopsis* SNF1 kinase homologs Akin10 and Akin11, which (as members of the SnRK family) have been implicated in sugar signaling and nowadays also ABA perception (262-265). Thereby PRL1 could have a function in integrating light signals antagonistically with a glucose signaling pathway: PRL1 might negatively regulate SNF1 kinases in light-grown plants whereas glucose increases SNF1 activity under the same light conditions. Dark grown plants consequently exhibit the reciprocal effects of PRL1 and glucose on SNF1 kinase activity.

In *Physcomitrella*, the transition between caulonemata and chloronemata growth and developmental processes are also regulated by light, sugar and phytohormones, especially cytokinins and auxins (266-269). Analyses of knockout lines of *Physcomitrella HXK1* (*Pp.HXK1*), a homolog of At.HXK1 acting as both a glycolytic enzyme and a sugar response regulator, revealed deficiency in glucose responses and formation of caulonemata (270, 271). This response was later also connected to hypersensitivity to both cytokinin and abscisic acid, but not to auxin (266). *Pp.hxk1* showed reduced caulonema formation, which could be stimulated by addition of glucose, high light conditions or auxin; conditions under which chloronemal branching was severely inhibited (270). This synergistic effect on controlling developmental processes in dependence of external energy sources resembles the situation described for *Arabidopsis* SNF1-kinase activity under light or dark conditions. SNF1-homologs are also conserved in *Physcomitrella* (266, 272) and are possible candidates for sensing the energy level crucial for developmental transition between caulonemata and chloronemata. The possibility of integrating light signals with phytohormone signaling was provided in *Physcomitrella* by analysis of the cryptochrome mutants. The cryptochrome mediated inhibition of auxin effects on branching and side branch position was downregulated in B conditions (141). Although a tight interconnection between light, sugar and phytohormone signaling is apparent from the observations made, no photoreceptor could be assigned to either

glucose or phytohormone signaling in *Physcomitrella* (266).
Pp.PRL interacted constitutively with phy4 as no light-dependency was observed for full-length holo-phy4 (see fig. 28). Analysis of Pp.PRL interaction with phy4 partials showed no binding to holo-phy4_N but constitutive binding to PHY4_C in Y2H (see figs. 30 and 31). Consistent with colony growth assays on PCB-complemented medium, liquid ONPG-assays did also not support R interaction enhancement of Pp.PRL and phy4 (see fig. 29). *In vivo* interaction in *Physcomitrella* occurred within the cytoplasm and was clearly excluded from the nucleus, although intracellular localisation revealed light-independent nuclear accumulation of CFP:Pp.PRL1 (see figs. 33 and suppl. fig. 13). As sYFP experiments were carried out without previous light treatments, it can only be stated that phy4-PRL1 interaction initially occurs within the cytoplasm. Whether or not Pp.PRL1 is retained within the cytoplasm by phy4 after R irradiation has not been investigated so far.
The identification of Pp.PRL1 from the cDNA library as a putative interacting partner of phy4 could possibly provide a link between light signaling by phytochrome and integration into either sugar and/or phytohormone signaling in *Physcomitrella*. From observations made in *Arabidopsis*, PRL1 is a repressor of photomorphogenesis, as it apparently negatively regulates early de-etiolation responses. Mosses do not undergo photomorphogenesis and although COP1 and HY5 homologs have been recently identified from the genome sequence, their role in light-dependent development in *Physcomitrella* is not yet clear (174). The transition between caulonemata and chloronemata may probably qualify as a related developmental process to photomorphogenesis. The transition between both cell forms is dependent on both high light conditions and auxin, both of which promote the formation of caulonemata from chloronemata, whereas cytokinin induces bud formation (267). A possible role for Pp.PRL1 could thus derive from its impact on auxin homeostasis. PRL1 negatively regulates the activity of SNF1 kinases in light, whereas in darkness, due to competition of the binding site within the C-terminus of SNF1 (273), SCF^{TIR1} is bound to SNF1, which as an active kinase could subsequently phosphorylate SCF^{TIR1} and affect its function in auxin signaling. The competitive binding of PRL1 or SCF^{TIR1} to SNF1 kinases appears to be regulated by light and might be regulated by phytochrome. As PRL1 is proposed to require phosphorylation of its NLS for nuclear transport and as the interaction with either SNF1 or SCF^{TIR1} presumably occurs within the nucleus, phytochrome could mediate phosphorylation of PRL1 either directly or indirectly by activation of other kinases, e.g. CDPKs (see section 5.4.4.).
Interestingly, a putative PRL1 interacting protein was isolated by cDNA library screening (see table 10). This protein was annotated as a cystein proteinase inhibitor, perhaps pointing towards the role of degradation in the responses described above. Interaction of phy4 with both PRL1 and the putative PRL1-interacting protein could provide a mechanism of PRL1 stability in terms of degradation prevention. This could provide another regulatory level in the competition of PRL1 and SCF^{TIR1} with SNF1.

5.3.3. EF1α, elongation factor 1 alpha

EF1α is a multifunctional protein, which, apart from its role in translation (274), also reversibly binds and bundles actin (275, 276), binds and severs microtubules in a Ca^{2+} and calmodulin dependent manner (277) and interacts with the 26S-proteasome in protein degradation of N^{α}-acetylated proteins, like actin or α-crystallin (278). Additionally, EF1α also plays a role in signaling events as it activates PIP kinase 4 (279) and serves as a substrate for Rho-associated and Ca^{2+}-dependent protein kinases (280, 281).

Actin binding by EF1α is dependent on both EF1α's binding to GTP and its phosphorylation status. EF1α_GTP shows low affinity for monomeric G-actin, whereas binding to F-actin is unaffected (276) but decreases upon phosphorylation of EF1α (280). This state-dependent binding capacity of EF1α to the cytoskeleton appears to culminate in the Ca^{2+} mediated regulation of tip growth in both *Arabidopsis* and *Physcomitrella.* Higher plants show polarised growth especially during pollen tube and root hair development, while *Physcomitrella* generally propagates by tip growth (282). Interestingly, Rho-GTPases are involved in the control of polarised growth by mediation of F-actin dynamics in both cases (283-285). Root development in *Arabidopsis* is stimulated by light; especially root hair formation is light sensitive and phytochromes are the photoreceptors involved (286). Recently regulation was shown to be mediated by cytoplasmic phytochrome together with a Rho-GTPase exchange factor, PIRF 1 (287). As the actin binding of EF1α is also regulated by its GTP-binding status, small G-protein factors might influence actin dynamics by regulation of EF1α binding to G-actin. RAC/ROP-GTPases and their connected signaling partners are also conserved in *Physcomitrella* and may very likely play a homologous role in tip growth mediation as they do in *Arabidopsis* (283).

Tip growth also underlies a tight regulation by actin polymerisation and depolymerisation factors which mediate actin turnover in relation to Ca^{2+}-gradients. The dynamics of actin reorganisation during tip growth have been especially well characterised in *Physcomitrella* protonemata cells. ArpC1, ArpC4 and BRICK, all of which are components of the Arp2/3- and the WACE/SCAR-complex respectively, were shown to be essential for cell morphogenesis and polarised cell growth in *Physcomitrella* protonemata (161, 218, 288, 289)). Interestingly, *Arabidopsis* T-DNA insertion lines of the respective genes (289-291) did not result in a loss of function in tip growth (292, 293), pointing to different mechanisms regulating tip growth in higher and lower plants. ACTIN DEPOLYMERISATION FACTOR (ADF) is a central regulator of actin turnover in *Physcomitrella* and loss of ADF results in the loss of tip growth and cortical F-actin dynamics (294, 295). ADF-function is regulated by phosphorylation of a conserved serin (Ser-6) within the N-terminus, similarly to the binding capacity of EF1α to F-actin. Although CDPKs are discussed as possible phosphor donors, the kinase specific for ADF1 phosphorylation has not yet been identified (294). ADFs are also associated with F-actin organisation in *Arabidopsis*, but their involvement in regulation of tip growth processes is not well understood (296).

F-actin organisation and actin-mediated vesicular trafficking is also the basis for light-induced directional responses in mosses. Tip cells of moss protonemata possess a cortical network of actin bundles which are directed towards the apex (159). Their alignment is connected with a tip-to-base Ca^{2+}-gradient and is also coupled with Ca^{2+} influx (160, 297). In unilateral R, a Pfr gradient is formed and a Ca^{2+} gradient is

established towards the side of illumination. Consequently the actin-network rearranges towards the light-perceiving flank mediated by a local synthesis of new actin filaments. As a result, a directionally-translocated actin cap forms which builds the new centre of polarised outgrowth. Finally, outgrowth is accomplished by polarised vesicle transport alongside the rearranged actin bundles (160, 298, 299) or, less efficiently, the microtubules (300).

Profilin 2 has been recently shown to be involved in actin turnover and in actin-cytoskeleton mediated vesicular trafficking together with EF1α in *Arabidopsis* root cells (301) and profilin was also reported to be essential for tip growth in *Physcomitrella* (302). Additionally, profilin is a central player in chloroplast movement responses in *Arabidopsis*, another directional response accomplished by the actin cytoskeleton (303) and possibly EF1α. Chloroplasts in *Physcomitrella* are either transported along microtubules or microfilaments, depending on the inducing light conditions. While both phytochromes and phototropins induce microtubule mediated movements, microfilaments are involved only upon B irradiation (304). In contrast, chloroplast photorelocation in *Arabidopsis* is exclusively initiated by B via phototropins (106) and transport is solely mediated by microfilaments (305). The connection between chloroplast relocation and actin filament association was made by the discovery of a protein located on the outer chloroplast envelope. CHUP1 (CHLOROPLAST UNUSUAL POSITIONING 1) was shown to interact with both actin and profilin (303) and to be indispensable for chloroplast photomovements (163, 164). Additionally to the F-actin network, chloroplast positioning is based on short actin filaments formed on the surface of the chloroplasts, the so called cp-actin. Accumulation of cp-actin filaments and the association of chloroplasts to the F, G, and cp-actin filaments are all mediated by CHUP1 (162, 165, 306, 307). Although chloroplast movements are induced by B, a modulating role of R, especially within the avoidance response under high light conditions, is apparent from enhanced chloroplast movements under high B in phytochrome mutants (111). Recently it was shown that phyB together with JAC1 is involved in this reaction (112) and that R induces disappearance of cp-actin, thereby delaying chloroplast movements upon recurring B treatments (165). The existence of an organised cp-actin network and of CHUP1 homologs (CHUP1a and CHUP1b) in *Physcomitrella* suggests the existence of a similar chloroplast movement machinery connecting profilin, EF1α and the actin-filament network.

Due to its promiscuous role in multiple cellular functions, EF1α's association with the cytoskeleton and its role in Ca^{2+}-dependent signaling events make it a good candidate to serve as a cytoplasmic phytochrome interactor in directional light signaling. Holo-phy4 showed constitutive interaction with EF1α under all light conditions tested in the Y2H spot assay (see fig. 28). Only very weak enhancement of interaction was induced by R pulses within the Y2H ONPG-assay, still this enhancement was FR reversible (see fig. 29). *In vivo* interaction, as shown by sYFP-complementation in *Physcomitrella* cells, revealed a local association between phy4 and EF1α at distinct structures throughout the whole cell (see fig. 33). Comparison with marked actin-filaments in *Physcomitrella* cells suggests a cytoskeleton association for the phy4-EF1α complex (308). By direct interaction with phy4, EF1α could mediate F-actin filament association with phy4 and its putative cytoplasmic signaling pathway. Additionally, EF1α itself could be part of this signaling route. It has long been

assumed that phytochromes are able to light-dependently change Ca^{2+} fluxes over plasma membranes (87) and changes in Ca^{2+} concentrations are also connected to directional responses like phototropism (160) (see 5.4.3.). Phytochrome-dependent increase in Ca^{2+} could activate CDPKs which subsequently phosphorylate EF1α and thereby induce loosening of EF1α association of the F-actin cytoskeleton. A disconnection of EF1α from the cytoskeleton could possibly lead to changes in actin turnover and synthesis of new F-actin filaments with the additional involvement of ADFs, which are phosphor-regulated themselves, by either the same CDPKs or different kinases. As phytochrome would consequently be disconnected from the remnant F-actin network together with EF1α, this could imply a possible feedback regulation. As phytochromes exhibit kinase activity themselves (56) EF1α could also be phosphorylated directly by phytochrome upon Pfr formation without the involvement of CDPKs. Additionally, Rho-GTPases, which are involved in polarised growth by mediation of F-actin dynamics in both *Physcomitrella* and *Arabidopsis*, could Ca^{2+}-dependently regulate the activity of EF1α via its GTP-binding status.

5.3.4. PRN, Pirin

As a further Pfr-specific interaction candidate, Pirin was discovered by Y2H. Alignment with the putative *Arabidopsis* homologs revealed overall high homology (see fig. 26), even with the pirin-like protein that carries an exceptional N-terminal extension. Pirin was the first interacting protein of the α-subunit (GPA1) of the *Arabidopsis* heterotrimeric G-protein.

In *Arabidopsis* only one G-protein coupled receptor and one heterotrimeric G-protein are known. GPA1 was identified as the single α-subunit for a heterotrimeric G-protein (309). *gpa1* mutant analyses allowed pinpointing first roles in plant development: positive regulation of cell division (310) and seed germination in response to gibberellic acid (GA), abscisic acid (ABA) and brassinosteroids (BR) (311). Meanwhile, GCR1 was identified as the only putative G-protein coupled receptor (312), bearing sequence similarities with 7TM domains (313), localisation to the plasma membrane (314) and interaction with GPA1 (314, 315). Although GCR1 was reported to act independently of heterotrimeric G-proteins in responses to BR and GA in seed germination (316), a direct interaction with GPA1 was shown for several other responses mostly involving ABA-signaling, seed germination and early seedling development (314, 315, 317). Overexpression of GPA1 resulted in R and FR hypersensitivity (93), whereas disruption of GPA1 enhanced FR-induced killing (94) and in addition negatively affected seed germination rates together with loss of AGB1 (95). Detailed analysis of double mutants of G-protein subunits and phyA and phyB respectively gave further insight in the connection of photoreceptor signaling with G-protein action and proposed GPA1 as a positive regulator of phyA and phyB downstream signaling (95).

PRN1 was shown to specifically interact with GPA1 in both Y2H and *in vitro*, the cupin domain located at the N-terminus of PRN1 was dispensable for interaction, hinting on a binding site located within the well conserved C-terminal domain (318). PRN1 expression is upregulated by both ABA and a single pulse of low fluence R (318). Although analysis of the genomic locus identified a *cis*-element (ACGT) potentially related to B sensitivity of transcriptional activation, low fluences of B did not enhance PRN1 transcription levels. *prn1* mutants showed reduced levels of seed germination

in the absence of previous stratification and hypersensitivity of seed germination to ABA (318), resembling phenotypes of *gpa1* mutants (311). GCR1, GPA1 and PRN1 were shown to act together in defining ABA and BL-induced transcription of *Lhcb* even under very low light conditions (317). PRN1 thus appears to be one component to integrate light-stimuli with G-protein signaling.

G-protein signaling has long been discussed as a fast acting phytochrome signaling pathway within the cytoplasm. Initial evidences arose from the observation of Ca^{2+}-dependent R induced swelling of etiolated wheat mesophyll protoplasts. This reaction could be artificially induced by addition of GTPγS in darkness or after FR illumination, but was inhibited after addition of GDPβS (319). R enhancement and FR inhibition of GTP binding to proteins contained within a crude extract of *Avena* seedlings further supported the idea of an involvement of G-proteins in phytochrome action (320). Expression of *CAB:GUS* and *CHS:GUS* fusion constructs in the holophytochrome-free *aurea* background were shown to be inducible by oat phyA, GTPγS, cGMP and Ca^{2+} or activated calmodulin (91, 92). Under the same conditions also anthocyanin synthesis and chloroplast development could be induced. Shortly thereafter, transcriptional activation of *rbcS* and *chs* was reported to be mediated by Ca^{2+}- and cGMP-pathways by targeting of Box II and Unit I *cis*-elements by direct application of phyA, GTPγS and Ca^{2+} (321).

In silico analysis of the *Physcomitrella* genome confirmed homologous proteins for all key components of the G-protein signaling machinery. Homologs of GCR1 were identified by BLAST search (predicted protein, XP_001765654.1 and XP_001784721.1) and both GPA1 (PpGPA1, XP_001772174.1) and AGB1 (Pp.GPB1, XP_001753169.1 and Pp.GPB2, XP_001757493.1) homologs have been annotated within the *Physcomitrella* protein database. The γ-subunit of the putative *Physcomitrella* G-protein, however, appears to have only a weak homology with either AGG1 or AGG2; only AGG2 gave a score with reasonable homology within *Physcomitrella* (predicted protein, XP_001756327.1). Thus, a functional heterotrimeric G-protein complex is likely to exist in *Physcomitrella* and might be connected with pirin action as described in *Arabidopsis*.

Pp.Pirin interacted with full-length phy4 in the Pfr state and R/FR-reversibly. Interestingly, Pp.Pirin was the only protein identified which also bound the N-terminal partial of phy4 (see fig. 30) pointing to the binding site being located within the photosensory module. Notably this interaction was light independent, but appeared to be rather dependent on the formation of holo-phy4_N, since apo-PHY4_N did not show interaction under the same selection conditions. Constitutive binding was observed for apo-PHY4_C (see fig. 31). The specific binding to holo-phy4_N may give a hint on structural implications underlying phytochrome-pirin interaction, as chromophore assembly apparently induces structural / conformational changes, even in the Pr form, which are required for Pp.Pirin binding. Pfr state-dependent interaction required the full-length holo-phytochrome suggesting a role for the C-terminal module for light-dependent interaction. Presumably, the Pp.Pirin binding site within the photosensory domain is accessible in the full-length phytochrome dimer only upon Pfr formation, whereas it maybe generally accessible in the case of an (un-)dimerised N-terminal module. This hypothesis could be proved by fusion of the N-terminal module with a dimerizing C-terminal tag, such as GUS. Assuming the hypothesis being correct, such fusion

constructs should exhibit Pfr state-dependent interaction as well. In case other functions of the C-terminal module are involved in Pfr specific binding (e.g. kinase-activity), Pfr state-dependent interaction would not be expected for the artificial phytochrome dimer construct.
Fluorescent fusions of Pp.Pirin appeared to be nuclear localised independent of light, which could be due to its small molecular weight below the exclusion size of passive nuclear diffusion. Despite this localisation pattern, sYFP interaction occurred strictly within the cytoplasm under both D and R conditions (see fig. 34); a strong hint to an interaction with cytoplasmic phytochrome.
Inferring from the *Arabidopsis* data described and the apparently conserved G-protein signaling machinery in *Physcomitrella*, Pp.Pirin could be a candidate to connect phytochrome-perceived light signals with G-protein signaling events. As many directional phytochrome responses require preceding changes in intracellular Ca^{2+} concentrations, with or without participation of calmodulin, G-proteins could serve as one possible phytochrome downstream signaling pathway. As G-protein signaling generally requires plasma membrane bound receptors, phytochrome interaction with PRN could connect cytoplasmic phytochrome and plasma membrane associated α-subunits of the heterotrimeric G-protein. Plasma membrane localisation would not necessarily be required for this type of G-protein signaling cascade of phytochrome, yet phytochrome-PRN interaction would not exclude the possibility of membrane-bound phytochrome serving as the initial receptor.

5.4. Phytochrome - Phototropin Interaction

5.4.1. Intracellular localisation of *Physcomitrella* phototropins

Localisation of *Arabidopsis* phototropins has been investigated in great detail and both phot1 and phot2 were described as being plasma membrane associated (100, 101, 217). However, both phot1 and phot2 detach from the plasma membrane upon B detection. phot1 was shown to organise into punctuate spots within the membrane after B irradiation, finally loosening from the plasma membrane and being internalised into the cytoplasm (100, 102). Likewise, B induces translocation of phot2 from the plasma membrane into punctuate structures within the cytoplasm corresponding to Golgi-apparatus localisation (101). Interestingly, R irradiation prior to B perception was shown to inhibit this internalisation process of phot1; phyA was identified as the responsible photoreceptor (103). It could be shown that intermolecular autophosphorylation of phot1 precedes the internalisation process which is mediated by a clathrin dependent endocytotic pathway additionally involving microtubule action (322, 323). Although a similar clathrin dependence was shown for internalisation of phot2 in the same studies, no kinase activity is needed for phot2 association with the Golgi-apparatus; the kinase domain is nevertheless required (101). Although the concrete physiological function of phototropin internalisation is not yet known, it might be part of the phototropin signaling cascade or a desensitising / adaptation reaction. However the mechanism by which phototropins associate with the plasma membrane remains unknown. As phototropins do not seem to possess any transmembrane domain or isoprenylation motif, it might be that this association is mediated by a phototropin-interacting anchoring protein.

Regardless of detailed physiological analyses of *Physcomitrella* phototropin knockout mutants (8), nothing was known about moss phototropin localisation prior to this study. N-terminal CFP-fusions to each of the four phototropins localised to the cell periphery (see fig. 40). Comparison with the localisation patterns of both PIP2a:GFP (180) and a membrane specific dye (see fig. 39) implied plasma membrane association for all of them. In contrast to higher plants, however the localisation pattern did not change under either R or B. No internalisation reaction was observed for any of the phototropins investigated, suggesting the observed plasma membrane association was independent of light (see suppl. figs. 17 and 18). Although N-terminal fusion of CFP to phototropin did not affect plasma membrane association, it might have an influence on B dependent cytoplasmic internalisation and/or signal transduction. Localisation and complementation of phototropin mutants in higher plants were conducted with C-terminal fusion proteins (100, 101). Detailed phenotypic complementation assays using N-terminal phototropin fusions in mosses have not been reported do date.

As expression of N-terminal fluorescent fusions of *Physcomitrella* phototropins in the heterologous system of higher plant cells using onion epidermis cells similarly yielded plasma membrane association of the photoreceptors (see fig. 43) it is likely that the mechanism of plasma membrane association of higher plants phototropins is able to also function in the attachment of lower plants phototropins. Consequently it would be interesting to know whether phot1 or phot2 localises to the plasma membrane in lower plant cells as well.

Arabidopsis phototropins, like phytochromes, are functional dimers (213) and intermolecular phosphorylation of phot1 is fundamental to its cytoplasmic localisation. To investigate *Physcomitrella* phototropin dimerisation, sYFP complementation assays were carried out. All four phototropins examined showed homodimerisation at the plasma membrane independent of light conditions (see fig. 41). Homodimerisation does therefore not interfere with membrane attachment and *Physcomitrella* phototropins likely act as functional dimers. Possible heterodimerisation between the phototropins has not been addressed yet.

5.4.2. Physical interaction of phy4 with *Physcomitrella* phototropins

Indeed, all four *Physcomitrella* phototropins showed direct interaction with full-length PHY4 in an Y2H assay (see fig. 35). Further analysis on PBC-complemented selection medium revealed Pfr state-dependency of this interaction, comparable to the phyA - FHY1 interaction (see fig. 35). Although phy4-photA1 initially showed no obvious R dependency, quantitative measurements of the interaction strength under pulsed light conditions revealed strong enhancement of the phy4-photA1 interaction following R irradiation, even exceeding interaction strength of phyA-FHY1 measured under the same conditions (see figs. 35 and 36). Notably B irradiation did not enhance interaction. Moreover, phytochrome specificity was proven by FR reversibility of R-enhanced interaction for all of the phototropins tested (see fig. 36). Interestingly, apo-PHY4 is able to interact independently of light with photA1, photA2 and photB1. Binding to photB2 was not detected under such conditions (see fig. 35); however, phy4-photB2 interaction was by far the weakest interaction observed, even with supplemented chromophore in R. This might be due to structural changes in the overall protein structure upon chromophore assembly, influencing binding sites for

interacting partners. Whatever structural changes precede chromophore attachment and Pr formation, it abolishes phot interaction in D, B and FR. In respect to interaction with phototropin, apo-PHY4 seems to resemble more the Pfr conformation in the Y2H assay.

The nature of apo-PHY4 interaction with phototropins nevertheless remains unclear at this point. In order to further investigate the impact of apo-PHY4 and its similarity to Pfr conformation, it might be interesting to investigate holo-phytochrome mutants like *hy1* or *aurea* in regard to R modulation of B induced directional responses. Assuming apo-PHY to be structurally similar to Phy-Pfr, an enhancement of B induced phototropism of hypocotyls would be present even in the absence of a previous R stimulus. One can speculate on the underlying mechanism based on apo-PHY-phot interaction: phot1 is B dependently internalised, which is discussed to act as a desensitizing mechanism (100, 322). R treatments prior to B irradiation delay this plasma membrane dissociation in a phyA-dependent manner (103). Binding of apo-phyA to phot1 might be able to likewise retard phot1 internalisation, possibly by prohibiting phot1 autophosphorylation, and thus lead to an enhancement of B phototropism.

Y2H spot assays employing N- and C-terminal partials of PHY4 and full length phototropins did not result in binding to either apo- or holo-phy4_N, while constitutive binding to apo-PHY4_C was observed. This points to an interaction interface located within the C-terminal module of PHY4. Notably, interaction of phytochrome with any of the phototropins investigated was generally abolished using C-terminally tagged phy4-baits, also hinting to the necessity for C-terminal accessibility for phy-phot interaction. Weak interaction was only detected for photA1 with the apo-PHY4_C:BD bait construct, probably deriving from the very strong nature of phy4-phot1 interaction. As interaction with the C-terminus loses light and conformation dependency, this again might reflect structural changes of the Pfr conformation which are transduced to the C-terminal part. Alternatively, conformation dependency might be introduced by a signaling event, rapidly following Pfr formation, such as phosphorylation.

Directional responses of lower plants are mainly phytochrome mediated, in strong contrast to higher plants, where phototropins initiate B dependent directional responses (324). However, many of the directional responses in lower plants are not strictly R dependent but may also be induced by phototropins in B, like chloroplast photorelocation (8). R and B perception and signaling thus seem to be tightly connected with each other in lower plants and the former were even proposed to feed in a common signaling pathway (175). This becomes even more evident in the convergent evolution of the photoreceptor chimera neochrome in both algae and ferns (12). Based on genome sequence, *Physcomitrella* and higher plants do not contain a similar genetic fusion of phytochrome and phototropin. A physical interaction of phytochrome with phototropin though would allow plasma membrane association of both photoreceptors in *Physcomitrella*.

After observation of physical interaction of full length phy4 with *Physcomitrella* phototropins in yeast systems, *in vivo* interaction was investigated using sYFP-complementation assays in *Physcomitrella* protonemata cells. Exclusively N-terminal fusions were used within the sYFP-assays due to the experiences in the Y2H assays. Emitted YFP-signals further confirmed *in vivo* interaction of phy4 with all of the four

phototropins. Moreover plasma membrane association of the interacting complex was revealed (see fig. 42). Both the plasma membrane association of CFP:phot fusions (see fig. 40) and the exclusive cytoplasmic localisation of GFP:phy4 fusions (see fig. 9) are reflected in this observation. The capability of phytochrome to interact with phototropin appears to be dependent upon either a structural feature and / or a signaling mechanism involving the C-terminus of phytochrome. Although partial nuclear accumulation of phy4 was observed with C-terminal FP-fusions, phy4 largely remained cytosolic under any light conditions investigated. These observations clearly hint on a phytochrome pool with dual functions. A proportion of phytochrome appears to fulfil gene regulatory function in the nucleus even in lower plants, as discussed by the identification of key regulators in *Physcomitrella* connected with photomorphogenic responses in higher plants (174). However, another proportion of phytochrome seems to be retained within the cytoplasm and to regulate directional responses to both R and B in direct interaction with phototropins. Notably, this applies to the observations made for the R modulation of B directional responses in higher plants, too.

Whether or not phy4 is the only phytochrome interacting with phototropins A1-B2 remains an open question at this point. Although phy4 is predominantly responsible for directional light sensing in *Physcomitrella*, the remaining phytochromes might share overlapping functions and act probably redundantly under high light conditions. phy2 was described as the phytochrome predominantly inducing chloroplast photomovements (172) and phylogenetic analysis grouped *PHY2* and *PHY4* within the same clade (9); both genes probably resulting from an ancient gene duplication event (9, 126). Thus it is likely that at least phy2 might also interact with phototropins.

5.4.3. Functional relevance of the phy4-phot signaling complex in directional light sensing

To investigate the physiological relevance of the direct phy-phot interaction at the plasma membrane, phototropin knockout mutants of *Physcomitrella* were analysed regarding R directional responses. Triple mutants of *photA2photB1photB2* and double mutants of *photA2photB1* were strongly impaired in responses to either unidirectional or polarised R; the phenotype of *photB1photB2* was still significant but considerably weaker (see figs. 45 and 46). This might reflect the low interaction strength of phy4-photB2. In Y2H assays, phy4-photB2 did interact significantly less than photA2 and photB1 (see figs. 35 and 36). Interestingly, the phenotypes of phototropin mutants were generally stronger than the phenotype of *phy4* single knockouts. Thus loss of plasma membrane association seems to have a more severe impact on directional light sensing as loss of only phy4; again, partial redundancy of the remaining phytochromes may account for the comparably weak phenotype. As phy2 was shown to be predominantly responsible for chloroplast avoidance movements in R, phy2 might be a good candidate to partially compensate loss of phy4 (172). Irradiation of the phytochrome and phototropin mutant lines with unidirectional B however did not induce phototropism (see fig. 47). Thus phototropins are apparently involved in phototropic responses but cannot induce phototropic responses on their own.

Interaction of both photoreceptors at the plasma membrane is of particular interest, as it might explain the long existing paradox of how a soluble photoreceptor induces directional responses and simultaneously offers an explanation about the B involvement in such responses. Upon unidirectional irradiation of a cell, soluble phytochrome molecules are eventually converted into Pfr and establish a gradient with molecules closer to the illumination side, thus converting earlier. Pfr-phytochrome subsequently binds phototropin molecules, hence establishing a locally fixed Pfr gradient at the plasma membrane. Following rapid establishment of the Pfr gradient, downstream signaling events could occur as previously described, i.e. formation of a local Ca^{2+} gradient, actin cytoskeleton reorganisation and actin-mediated vesicle trafficking, finally leading to a phototropic bending and re-orientation of tip-cell growth.
Polarotropism would also be understandable through this mechanism. Plasma membrane association of phytochrome by direct interaction with phototropin would yield anisotropy, allowing the long proposed flip-flop dichroism to occur (148, 325, 326). A parallel orientation of the dipole moments of phytochrome's attached chromophore thus would explain responses to vectorial light information. Overall adjustment of bending and growth according to the vectorial information is likely to involve similar downstream signaling events as described for phototropic responses. As small amounts of photA1 and photA2 appear to be bound to phytochrome in dark conditions as well (see fig. 36) a small amount of phytochrome may be constitutively associated with phototropins at the plasma membrane, a situation which matches exactly the proposed properties of phytochrome necessary to induce directional responses. Chloroplast photorelocation has been investigated in both *phy4* and *phot* knockout lines. Chloroplast repositioning under R_{pol} conditions was only weakly affected by loss of *phy4* (9), while avoidance and accumulation responses under both R and B conditions were severely affected in *phot*-knockout mutants (8). This resembles the phenotypes of *phy4* and triple and double *phot* knockouts observed for R phototropism and polarotropism in the study presented here. Repositioning of chloroplasts not only involves rearrangements of the F-actin cytoskeleton and the formation of and interaction with a cp-actin meshwork around the chloroplasts, but also reorganisation between the actin-filaments and the plasma membrane, which is mediated by CHUP1 (164). As chloroplast relocation in mosses is inducible by both R and B, again phy-phot interaction would make a sound foundation for both directional light sensing and downstream signaling for actin-rearrangement.
Spore germination and protoplast regeneration are inducible by both R and B (124, 130, 131). Although evidence emerges that nuclear phytochromes are needed for induction of spore germination in lower plants (173, 230), both responses inherit directional character. The initial polarisation of the round cell is a strictly directional light response, likely to be explained by a local Pfr gradient formed upon unidirectional or vectorial R stimulus as explained before.

5.4.4. G-protein signaling of plasma membrane associated phytochrome

Cytoplasmic phytochrome signaling mediated by G-proteins has been long discussed. Although there have been clear connections to Ca^{2+} / calmodulin and G-protein signaling (87), the role of phytochrome as a plasma membrane coupled receptor

inducing G-protein signaling remained elusive. However, plasma membrane association of phytochrome by direct interaction with phototropin might open a new view on this shut down phytochrome signaling route.
The intriguing connection of R and B signaling events is reflected within rapid downstream signaling employing Ca^{2+}, which is also implied in directional responses mediated by phototropins (327). This work also provides new insights into how phytochrome could be connected to G-protein signaling by interaction with newly identified proteins, as both EF1α and PRN1 participate in G_{α}-function and are candidates to connect phytochrome with G-protein binding and interaction.
Usually, cAMP or phosphatidylinositol phosphate (IP) serve as second messengers in transmitting signals from activated G-proteins. The photosensory module of cyanobacterial and probably all phytochromes is a tandem GAF-protein and shares structural similarities with adenylate cyclases (44), responsible for cyclisation of ATP. cAMP indeed plays a role in phytochrome signaling in certain cyanobacteria (328) and macroalgae (329). However, its general involvement in plant signaling events has been controversially discussed ((330) retracted) and a role in phytochrome signaling could not be unequivocally shown (91, 331). On the other hand, IPs are known as second messengers in several cellular responses, like vesicle trafficking and modulation of the actin cytoskeleton (332). Kinases involved in the formation of active inositol-1,4,5-triphosphate (IP_3) are conserved in both *Arabidopsis* and *Physcomitrella* (333, 334). Especially IP_3 and diacylglycerol (DAG) are implied in Ca^{2+} and phytochrome signaling, as IP_3 was able to substitute for R in protoplast swelling (85). In *Physcomitrella*, knockout of Pp.PIPK1 resulted in severe impairment of tip growth as displayed by defects in caulonemata development and rhizoid growth (335).
A long sought connection to G-protein signaling may now be reconsidered, as a phototropin bound phytochrome might indeed function as a plasma membrane coupled receptor in a broader sense and G-proteins might be partially involved in the phytochrome induced Ca^{2+} signaling cascade.

5.4.5. Phytochrome - Phototropin Interaction in *Arabidopsis*

As the multicellular tissue of higher plants scatters, vectorial responses might be obscured in higher plants. Nevertheless, a similar phytochrome arrangement might exist. sYFP-based analysis using N-terminal fusions to both phyA and phot1 could detect interaction between both photoreceptors in onion epidermis cells; the signal is plasma membrane localised, as previously observed for *Physcomitrella* phy-phot interaction (see fig. 51). However, this putatively direct interaction could not be confirmed in an Y2H assay, suggesting an indirect interaction requiring at least one further bridging partner which is not available within the yeast system, but is present in the heterologous system of onion epidermis cells. As homodimerisation and the associated light-dependent localisation of both phyA and phot1 were observed in onion cells (see figs. 48 and 50), functionality of N-terminal sYFP-fusions can be assumed. Although indirect interaction has not specifically been shown with the sYFP method, they might still be detectable, as the method is proximity based and requires protein distances shorter than 100 Å (210). Candidates to enable a phyA-phot1 complex formation are possibly involved in directional sensing. PKS1 would qualify as a suitable bridging partner, as it directly interacts with both, phyA and

phot1 and is required for B induced phototropism of hypocotyls (336) and root phototropism (110, 337). As the putative bridging partner is a novelty of higher plant phy-phot interaction and is not a prerequisite in mosses it might not be conserved among the two organisms. Members of the PKS family could not be identified based on sequence similarity searches in the moss genome and are also absent from other lower plants (214). Another possible candidate is NPH3, which has a strong phototropism phenotype and was suggested to be involved in scaffolding (338).

Thus phytochromes appear to have additional modes of function apart from their described role in gene regulation. Via light-dependent translocation into the nucleus they are capable of interacting with transcription factors, coupling light and transcriptional control of gene expression. Both inducing and repressing actions of phytochromes are described in gene regulation, all of which lead to an adjustment of the developmental program from germination to photomorphogenesis, flower induction and circadian clock entrainment (75). Additionally phytochromes have cytoplasmic function which is connected to B sensing and signaling by phototropins. Directional light signaling in higher plants is B induced and, as phot knockout lines show, solely dependent on plasma membrane associated phototropins (324). Nevertheless, R modulates B induced responses via phytochromes. For example, B induced phototropism of etiolated hypocotyls is enhanced by previous R irradiation mediated by phyA (107, 215) and chloroplast relocation responses occur in both R and B, mediated by phyB, phot1 and phot2 (112). Likewise root phototropism is inducible by both R and B (108, 109, 216), although the quality of responses differ in dependence of the light stimulus applied: B induces negative root phototropism, R induces positive root phototropism. These phenomena are consistent with the emerging role of cytoplasmic phytochrome function in higher plants (71, 80, 81) and the findings presented here show that part of the cytoplasmic phytochrome pool is membrane associated via phototropin either by direct or by indirect interaction. A proportion of the remaining cytoplasmic phytochrome pool appears to be involved in translational regulation of light-dependent genes (81). Whether or not those diverse functions of phytochrome are all initiated by one primary action mechanism can only be speculated. As phosphorylation of phyA is not only necessary for FHY1-mediated transport (232) but also for interaction with proteins involved in the modulation and induction of directional responses such as PKS1 (58), it might also play a role in the regulation of phot1 internalisation and B induced phototropism (322). As phosphorylation also regulates the activity of EF1α (280, 281) and PRL1 (261), which were identified as putative interacting partners of phy4, higher and lower plant's primary phytochrome action mechanism might be conserved.

6. Summary

The work presented focussed on the elucidation of cytoplasmic phytochrome function. *Physcomitrella patens*, a lower plant model system, offered exquisite experimental conditions to access investigation on the cytoplasmic signaling system underlying directional light sensing: a sequenced genome, excellent accessibility of molecular genetics, cellular and microscopic applications and developmental and physiological analysis.

Studies using fluorescent fusions proofed phy4 localisation to be sensitive to tag-positioning in *Physcomitrella*, with predominant cytoplasmic localisation and the ability to enter the nucleus in a light-independent manner. Further localisation studies on higher plant phytochromes phyA and phyB in *Physcomitrella* and phy4 expression in higher plant cells revealed the existence of a phytochrome nuclear transport machinery in *Physcomitrella*. As both phyA and phy4 nuclear translocation was affected by tag-positioning this transport mechanism appeared to share features with the fhy1/fhl-transport mechanism acquired by angiosperms and may be considered a common ancestor of phytochrome nuclear translocation. *In silico* analysis of the *Physcomitrella* genome pointed on a gene probably involved in this mechanism with considerable homology to the C-terminus of FHY1.

The assembly of holo-phy4 on PCB-complemented medium resulted in a functional, i.e. R/FR-reversible phytochrome in yeast cells. Positioning of the BD-tag did not impair phytochrome function but affected binding of putative interactors. Using holo-BD:phy4 four putative cytoplasmic interaction partners could be identified from a cDNA library, 2 of which exhibited state-dependent interaction and R/FR-reversibility in Y2H. *In silico* analysis characterised those putative interactors as (i) a transmembrane protein with ATP / GTP binding function (PLP), (ii) a WD40-domain protein (PRL), (iii) a protein involved in actin filaments binding and cytoskeleton assembly (EF1α) and (iv) an interactor of the heterotrimeric G-protein's alpha subunit (Pirin). Further analysis by sYFP confirmed *in vivo* interaction of all putative interactors with phy4 within the cytoplasm. Possible functions in phy4 cytoplasmic signaling, however, can only be deduced from *in silico* analysis and will need further elucidation on the physiological level by analysis of knockdown or knockout mutants.

The notion of exclusively cytoplasmic GFP:phy4 and the establishment of functional holo-BD:phy4 in yeast encouraged the investigation of the tight connection between R and B in directional light sensing observed in both *Physcomitrella* and *Arabidopsis* by assuming a physical interaction between phytochrome and phototropin. Using Y2H assays a direct interaction of N-terminally tagged phy4 with any of the four described *Physcomitrella* phototropins was demonstrated, while the reciprocal C-terminal BD-fusion clearly inhibited direct binding of phy4 to phototropin. phy4-phot interaction was additionally shown to be strengthened in a R dependent manner and was further consolidated to by phytochrome-specific in terms of R/FR-reversibility. sYFP methods moreover proofed i*n vivo* interaction and simultaneously revealed plasma membrane association of the phy-phot complex in accordance with phototropin localisation previously shown by fluorescent-fusions. The loss of directional R responses in *phot* knockout mutants finally confirmed physiological necessity of phy4-phot interaction at the plasma membrane. These results supported the hypothesis of phy4's plasma membrane fixation with the help of phototropins, thereby not only fulfilling the requirements of the Jaffe/Etzold/Haupt hypothesis but also explaining the intrinsic tight connection between

R and B signaling in directional light sensing of lower plants. The physical interaction of the two photoreceptors is also reflected by the occurrence of neochrome, a phytochrome - phototropin-chimera, twice in evolution.
Since a connection of R and B in directional responses has been reported for higher plants too, consequently a phyA-phot1 interaction was hypothesised. Y2H analysis in the beginning turned out with no direct phyA - phot1 interaction. Astonishingly, an *in vivo* interaction could still be demonstrated using sYFP methods. In accordance with the notion of the establishment of a more elaborate phytochrome system, especially in regard of phyA, an angiosperm-specific light-labile phytochrome, an indirect, more complex interaction between phyA and phot1 involving other proteins has to be assumed for higher plants. A possible candidate to mediate this complex formation is PKS1. Taken the results of this work together, phytochromes appear to fulfil different functions: (i) as integrators of light in regulation of gene expression by interaction with transcription factors within the nucleus, (ii) as sensors and mediators of directional responses connected to phototropins and thereby associated with the plasma membrane and a yet uncharacterised cytoplasmic signaling cascade and (iii) as regulators of genproduct abundance by tranlationally control as recently reported.

7. Zusammenfassung

Die vorgelegte Arbeit befasste sich mit Untersuchungen zur cytoplasmatischen Phytochrom Funktion. *Physcomitrella patens*, ein Modelorganismus niederer Pflanzen, bietet ausgezeichnete Experimentalbedingungen um ein der direktionalen Lichtwahrnehmung unterliegenden cytoplasmatisches Signaltransduktionssystem zu untersuchen: ein sequenziertes Genom, exzellente Zugänglichkeit sowohl molekular-genetischer als auch zellulärer und mikroskopischer Methoden wie auch entwicklungsbiologischer und physiologischer Analyse.

Untersuchungen mit Fluoreszenz markierten Fusionsproteinen zeigten, dass die Lokalisation von phy4 in *Physcomitrella* sensibel gegenüber der Positionierung des Fluorophors ist, sich jedoch weitestgehend als cytoplasmatisch erwies, mit der Möglichkeit zur nuklearen Translokation; allerdings in einem Licht-unabhängigen Modus. Weitere Lokalisationsstudien der Phytochrome phyA und phyB in *Physcomitrella* sowie die Expression von phy4 in höheren Pflanzenzellen offenbarten die Existenz eines nuklearen Phytochrom Transport Mechanismus in *Physcomitrella.* Da der Kerntransport sowohl von phyA als auch von phy4 durch die Positionierung des Fluorophors betroffen war, scheint der vorliegende Transportmechanismus Eigenschaften des fhy1/fhl-Systems der Angiospermen zu teilen und kann daher möglicherweise als gemeinsamer Vorläufer verstanden werden. *In silico* Analysen des *Physcomitrella* Genoms identifizierten ein Genprodukt mit großer Homologie zum C-Terminus von FHY1. Hieraus könnte sich eine Rolle innerhalb des nuklearen Transportmechanismus in *Physcomitrella* ableiten lassen.

Die Assemblierung von Holo-phy4 auf PCB-komplettiertem Medium führte zur Bildung eines funktionellen, R/FR-revertierbaren Phytochroms in Hefezellen. Die Position der Bindedomäne beeinflusste die Phytochromfunktion dabei nicht, jedoch wurde die Bindung putativer Interaktoren beeinträchtigt. Mit Holo-phy4 konnten 4 putativ cytoplasmatische Interaktionsproteine aus einer *cDNA-library* identifiziert werden; zwei dieser Proteine zeigten R-spezifische Interaktion mit phy4 und R/FR-Revertierbarkeit im Y2H-System. *In silico* Analysen charakterisierten diese Interaktoren als (i) ein Transmembran-Protein mit ATP / GTP bindender Funktion (PLP), (ii) ein WD40-Domänen Protein (PRL), (iii) ein Protein, das an Aktinbindung und Assemblierung des Cytoskeletts beteiligt ist (EF1α) und (iv) als einen Interaktor der Alpha-Untereinheit des heterotrimeren G-Proteins (Pirin). Weitere Untersuchungen mit der sYFP-Methode bestätigten die *in vivo* Interaktion aller putativer Interaktoren mit phy4 im Cytoplasma. Mögliche Funktionen innerhalb der cytoplasmatischen phy4-Signaltransduktion jedoch können nur aus den *in silico* Daten abgeleitet werden und bedürfen weiterer physiologischer Untersuchungen von *knockdown*- bzw. *knockout*-Mutanten.

Die Feststellung von ausschließlich cytoplasmatisch lokalisiertem GFP:phy4 und des funktionellen holo-BD:phy4's in Hefe ermunterten zu weiteren Untersuchung der engen Verbindung zwischen R und B-Licht innerhalb der direktionalen Lichtwahrnehmung in *Physcomitrella.* Hier wurde eine physische Interaktion zwischen Phytochrom und Phototropin vermutet. Y2H-Experimente zeigten eine direkte Interaktion von N-terminal fusioniertem phy4 mit jedem der vier untersuchten Phototropine, während die reziproke C-terminale Fusion diese Interaktion verhinderte. Die phy4-phot Bindung konnte weiterhin als R-Licht abhängig und R/FR-revertierbar, und damit als Phytochrom spezifisch, dargestellt werden. sYFP-Experimente konnten weiterhin eine *in vivo* Interaktion nachweisen und offenbarten eine Assoziation des phy-phot-Komplexes an der Plasmamembran im Einklang mit der zuvor bestätigten Plasmamembran-Lokalisation

der *Physcomitrella* Phototropine. Der Verlust direktionaler R-Licht Antworten in *phot*-Mutanten bestätigte zuletzt auch die physiologische Notwendigkeit des phy-phot-Komplexes an der Plasmamembran. Diese Ergebnisse bestätigen die Plasmamembran-Fixierung von Phytochrom bei der Detektion direktionaler Lichtstimuli und erfüllen damit nicht nur die Vorraussetzungen der Jaffe/Etzold/Haupt-Hypothese sondern erklären gleichzeitig auch die enge Verknüpfung von R und B-Licht bei der Auslösung direktionaler Antworten in niederen Pflanzen. Die physikalische Interaktion der beiden Photorezeptoren ist außerdem reflektiert durch das zweimalige, unabhängige Auftreten von Neochrom, einer genetischen Phytochrom-Phototropin-Chimäre. Da auch für höhere Pflanzen eine R/B-Licht-Verknüpfung direktionaler Antworten besteht, wurde eine Interaktion von phyA mit phot1 vermutet. Y2H-Experimente zeigten jedoch eindeutig, dass keine direkte phyA-phot1 Interaktion vorliegt. Erstaunlicherweise konnte jedoch mit Hilfe des sYFP-Systems *in vivo* eine Interaktion an der Plasmamembran nachgewiesen werden. Im Einklang mit dem Auftreten eines komplexeren Phytochrom Systems in höheren Pflanzen, insbesondere mit dem Angiospermen-spezifischen, lichtlabilen phyA, wird nun eine indirekte Interaktion von phyA mit phot1 in höheren Pflanzen angenommen, sehr wahrscheinlich unter der Beteiligung weiterer Proteine. PKS1 könnte einen Kandidaten zur Vermittlung einer solchen Interaktion darstellen.

Abschließend ist festzustellen, dass Phytochrome mehrere verschiedene Funktionsmodi besitzen: Zum einen als Integratoren von Licht innerhalb der Regulation von Genexpression durch Interaktion mit Transkriptionsfaktoren innerhalb des Zellkerns, außerdem als Sensoren und Vermittler direktionaler Antworten in Verbindung mit Phototropinen an der Plasmamembran und einem, bisher unbekannten, cytoplasmatischen Signaltransduktionssystem und zuletzt in der Regulation von lichtinduzierten Genprodukten auf Ebene der tranlationalen Kontrolle, wie jüngst veröffentlich.

8. References

1. **Smith H** (2000) Phytochromes and light signal perception by plants--an emerging synthesis. *Nature* 407:585-591.
2. **Franklin KA**, Quail PH (2010) Phytochrome functions in Arabidopsis development. *J. Exp. Bot.* 61:11-24.
3. **Rizzini L**, Favory JJ, Cloix C, Faggionato D, O'Hara A, Kaiserli E, Baumeister R, Schafer E, Nagy F, Jenkins GI *et al.* (2011) Perception of UV-B by the Arabidopsis UVR8 protein. *Science* 332:103-106.
4. **Briggs WR**, Huala E (1999) Blue-light photoreceptors in higher plants. *Annu. Rev. Cell Dev. Biol.* 15:33-62:33-62.
5. **Ahmad M** (1999) Seeing the world in red and blue: insight into plant vision and photoreceptors. *Curr. Opin. Plant Biol.* 2:230-235.
6. **Somers DE**, Schultz TF, Milnamow M, Kay SA (2000) ZEITLUPE Encodes a Novel Clock-Associated PAS Protein from Arabidopsis. *Cell* 101:319-329.
7. **Wolf L**, Rizzini L, Stracke R, Ulm R, Rensing SA (2010) The molecular and physiological responses of Physcomitrella patens to ultraviolet-B radiation. *Plant Physiol* 153:1123-1134.
8. **Kasahara M**, Kagawa T, Sato Y, Kiyosue T, Wada M (2004) Phototropins mediate blue and red light-induced chloroplast movements in *Physcomitrella patens*. *Plant Physiol* 135:1388-1397.
9. **Mittmann F**, Brücker G, Zeidler M, Repp A, Abts T, Hartmann E, Hughes J (2004) Targeted knockout in *Physcomitrella* reveals direct actions of phytochrome in the cytoplasm. *Proc. Natl. Acad. Sci. U. S. A* 101:13939-13944.
10. **Imaizumi T**, Kiyosue T, Kanegae T, Wada M (1999) Cloning of the cDNA encoding the blue-light photoreceptor cryptochrome from the moss *Physcomitrella patens* (Accession No. AB027528). *Plant Physiol.* 120:1205.
11. **Briggs WR**, Olney MA (2001) Photoreceptors in plant photomorphogenesis to date. Five phytochromes, two cryptochromes, one phototropin, and one superchrome. *Plant Physiol* 125:85-88.
12. **Suetsugu N**, Mittmann F, Wagner G, Hughes J, Wada M (2005) A chimeric photoreceptor gene, NEOCHROME, has arisen twice during plant evolution. *Proc Natl Acad Sci U S A* 102:13705-13709.
13. **Nozue K**, Kanegae T, Imaizumi T, Fukuda S, Okamoto H, Yeh KC, Lagarias JC, Wada M (1998) A phytochrome from the fern *Adiantum* with features of the putative photoreceptor NPH1. *Proc. Natl. Acad. Sci. U. S. A* 95:15826-15830.
14. **Sharrock R** (2008) The phytochrome red/far-red photoreceptor superfamily. *Genome Biology* 9:230.
15. **Vierstra R**, Quail PH (1982) Native phytochrome: inhibition of proteolysis yields a homogeneous monomer of 124 kilodaltons from *Avena*. *Proc. Natl. Acad. Sci. USA* 79:5272-5276.
16. **Furuya, M**. & Song, P. S. (1994) in *Photomorphogenesis in Plants*, eds. Kendrick, R. E. & Kronenberg, G. H. M. (Kluwer, Dortrecht), pp. 105-140.
17. **Lagarias JC**, Rapoport H (1980) Chromopeptides from phytochrome. The structure and linkage of the Pr form of the phytochrome chromophore. *J. Am. Chem. Soc* 102:4821-4828.
18. **Rüdiger W**, Brandlmeier T, Blos I, Goassauer A, Weller JP (1980) Isolation of the phytochrome chromophore. The cleavage reaction with hydrogen bromide. *Z. Naturforsch.* 35c:763-769.
19. **Elich TD**, McDonagh AF, Palma LA, Lagarias JC (1989) Phytochrome chromophore biosynthesis. Treatment of tetrapyrrole- deficient *Avena* explants with natural and non-natural bilatrienes leads to formation of spectrally active holoproteins. *J. Biol. Chem.* 264:183-189.
20. **Lamparter T**, Esteban B, Hughes J (2001) Phytochrome Cph1 from the cyanobacterium Synechocystis PCC6803. Purification, assembly, and quaternary structure. *Eur. J. Biochem.* 268:4720-4730.
21. **Lagarias JC**, Lagarias DM (1989) Self-assembly of synthetic phytochrome holoprotein *in vitro*. *Proc. Natl. Acad. Sci. USA* 86:5778-5780.
22. **Borthwick HA**, Hendricks SB, Parker MW, Toole EH, Toole VK (1952) A Reversible Photoreaction Controlling Seed Germination. *Proc. Natl. Acad. Sci. U. S. A* 38:662-666.
23. **Kneip C**, Hildebrandt P, Schlamann W, Braslavsky SE, Mark F, Schaffner K (1999) Protonation state and structural changes of the tetrapyrrole chromophore during the Pr --> Pfr phototransformation of phytochrome: a resonance Raman spectroscopic study. *Biochemistry* 38:15185-15192.
24. **Rüdiger W**, Thümmler F, Cmiel E, Schneider S (1983) Chromophore structure of the physiologically active form Pfr of phytochrome. *Proc. Natl. Acad. Sci. U. S. A* 80:6244-6248.
25. **Eilfeld P**, Rüdiger W (1985) Absoprtion spectra of phytochrome intermediates. *Z. Naturforsch.* 40c:109-114.

26. **Hsiao AI**, Vidaver WILL (1984) Effects of Temperature and Various Red or Far-red Irradiations on Phytochrome- and Gibberellin A3-mediated Germination Control in Partially Hydrated Lettuce Seeds. *J. Exp. Bot.* 35:1771-1781.
27. **Litts JC**, Kelly JM, Lagarias JC (1983) Structure-function studies on phytochrome. Preliminary characterization of highly purified phytochrome from Avena sativa enriched in the 124-kilodalton species. *J Biol. Chem.* 258:11025-11031.
28. **Flint LH**, McAlister ED (1937) Wavelengths of radiation in the visible spectrum promoting the germination of light-sensitive lettuce seed. *Smiths. Misc. Coll.* 96:1-8.
29. **Chen M**, Chory J (2011) Phytochrome signaling mechanisms and the control of plant development. *Trends in Cell Biology* 21:664-671.
30. **Somers DE**, Devlin PF, Kay SA (1998) Phytochromes and cryptochromes in the entrainment of the Arabidopsis circadian clock. *Science* 282:1488-1490.
31. **Millar AJ** (2004) Input signals to the plant circadian clock. *J. Exp. Bot.* 55:277-283.
32. **Searle I**, Coupland G (2004) Induction of flowering by seasonal changes in photoperiod. *EMBO J.* 23:1217-1222.
33. **Smith H**, Whitelam GC (1997) The shade avoidance syndrome: multiple responses mediated by multiple phytochromes. *Plant Cell and Environment* 20:840-844.
34. **Franklin KA** (2008) Shade avoidance. *New Phytol.* 179:930-944.
35. **Sharrock RA**, Clack T (2002) Patterns of expression and normalized levels of the five Arabidopsis phytochromes. *Plant Physiol* 130:442-456.
36. **Furuya M** (1989) Molecular properties and biogenesis of phytochrome I and II. *Adv. Biophys.* 25:133-167.
37. **Deng XW**, Caspar T, Quail PH (1991) cop1: a regulatory locus involved in light-controlled development and gene expression in Arabidopsis. *Genes Dev.* 5:1172-1182.
38. **Seo HS**, Watanabe E, Tokutomi S, Nagatani A, Chua NH (2004) Photoreceptor ubiquitination by COP1 E3 ligase desensitizes phytochrome A signaling. *Genes Dev.* 18:617-622.
39. **Saijo, Y**., Zhu, D., Li, J., Rubio, V., Zhou, Z., Shen, Y., Hoecker, U., Wang, H., & Deng, X. W. (2008) pp. 607-613.
40. **Shinomura** T, Nagatani A, Hanzawa H, Kubota M, Watanabe M, Furuya M (1996) Action spectra for phytochrome A- and B-specific photoinduction of seed germination in Arabidopsis thaliana. *Proc. Natl. Acad. Sci. U. S. A.* 93:8129-8133.
41. **Montgomery BL**, Lagarias JC (2002) Phytochrome ancestry: sensors of bilins and light. *Trends Plant Sci.* 7:357-366.
42. **Rockwell NC**, Su YS, Lagarias JC (2006) Phytochrome structure and signaling mechanisms. *Annu. Rev. Plant Biol.* 57:837-858.
43. **Rockwell NC**, Lagarias JC (2006) The structure of phytochrome: a picture is worth a thousand spectra. *Plant Cell* 18:4-14.
44. **Essen L-O**, Mailliet J, Hughes J (2008) The structure of a complete phytochrome sensory module in the Pr ground state. *Proc. Natl. Acad. Sci. U. S. A* 105:14709-14714.
45. **Beavo JA**, Brunton LL (2002) Cyclic nucleotide research - still expanding after half a century. *Nat Rev Mol Cell Biol* 3:710-718.
46. **Wagner JR**, Brunzelle JS, Forest KT, Vierstra RD (2005) A light-sensing knot revealed by the structure of the chromophore-binding domain of phytochrome. *Nature* 438:325-331.
47. **Yang X**, Kuk J, Moffat K (2008) Crystal structure of Pseudomonas aeruginosa bacteriophytochrome: photoconversion and signal transduction. *Proc. Natl. Acad. Sci. U. S. A* 105:14715-14720.
48. **Kikis EA**, Oka Y, Hudson ME, Nagatani A, Quail PH (2009) Residues clustered in the light-sensing knot of phytochrome B are necessary for conformer-specific binding to signaling partner PIF3. *PLoS. Genet.* 5:e1000352.
49. **Oka Y**, Matsushita T, Mochizuki N, Quail PH, Nagatani A (2008) Mutant screen distinguishes between residues necessary for light-signal perception and signal transfer by phytochrome B. *PLoS Genet* 4:e1000158.
50. **Nordmeier**, W, Johnen, P, & Hiltbrunner, A (2011). Residues in the light-sensing knot of phytochrome A are important for nuclear transport and downstream signaling. (Poster presentation, *Botanikertagung* Berlin 2011).
51. **Schneider-Poetsch HA** (1992) Signal transduction by phytochrome: phytochromes have a module related to the transmitter modules of bacterial sensor proteins. *Photochem. Photobiol.* 56:839-846.

52. **Quail PH**, Boylan MT, Parks BM, Short TW, Xu Y, Wagner D (1995) Phytochromes: photosensory perception and signal transduction. *Science* 268:675-680.
53. **Vreede J**, van der Horst MA, Hellingwerf KJ, Crielaard W, van Aalten DM (2003) PAS domains. Common structure and common flexibility. *J. Biol. Chem.* 278:18434-18439.
54. **Lindebro MC**, Poellinger L, Whitelaw ML (1995) Protein-protein interaction via PAS domains: role of the PAS domain in positive and negative regulation of the bHLH/PAS dioxin receptor-Arnt transcription factor complex. *EMBO J.* 14:3528-3539.
55. **Yeh KC**, Wu SH, Murphy JT, Lagarias JC (1997) A cyanobacterial phytochrome two-component light sensory system. *Science* 277:1505-1508.
56. **Yeh KC**, Lagarias JC (1998) Eukaryotic phytochromes: light-regulated serine/threonine protein kinases with histidine kinase ancestry. *Proc. Natl. Acad. Sci. U. S. A* 95:13976-13981.
57. **Kim JI**, Park JE, Zarate X, Song PS (2005) Phytochrome phosphorylation in plant light signaling. *Photochem. Photobiol. Sci.* 4 (9):681-687.
58. **Fankhauser C**, Yeh KC, Lagarias JC, Zhang H, Elich TD, Chory J (1999) PKS1, a substrate phosphorylated by phytochrome that modulates light signaling in Arabidopsis. *Science* 284:1539-1541.
59. **Al Sady B**, Ni W, Kircher S, Schafer E, Quail PH (2006) Photoactivated Phytochrome Induces Rapid PIF3 Phosphorylation Prior to Proteasome-Mediated Degradation. *Mol. Cell* 23:439-446.
60. **Ahmad M**, Jarillo JA, Smirnova O, Cashmore AR (1998) The CRY1 blue light photoreceptor of Arabidopsis interacts with phytochrome A in vitro. *Mol. Cell* 1:939-948.
61. **Colon-Carmona** A, Chen DL, Yeh KC, Abel S (2000) Aux/IAA proteins are phosphorylated by phytochrome in vitro. *Plant Physiol* 124:1728-1738.
62. **Matsushita T**, Mochizuki N, Nagatani A (2003) Dimers of the N-terminal domain of phytochrome B are functional in the nucleus. *Nature* 424:571-574.
63. **Coleman RA**, Pratt LH (1974) Electron microscopic localization of phytochrome in plants using an indirect antibody-labeling method. *J. Histochem. Cytochem.* 22:1039-1047.
64. **Pratt LH**, Coleman RA (1971) Immunocytochemical Localization of Phytochrome. *Proceedings of the National Academy of Sciences* 68:2431-2435.
65. **Sakamoto K**, Nagatani A (1996) Nuclear localization activity of phytochrome B. *Plant J.* 10:859-868.
66. **Kircher S**, Kozma-Bognar L, Kim L, Adam E, Harter K, Schäfer E, Nagy F (1999) Light quality-dependent nuclear import of the plant photoreceptors phytochrome A and B. *Plant Cell* 11:1445-1456.
67. **Hisada A**, Hanzawa H, Weller JL, Nagatani A, Reid JB, Furuya M (2000) Light-induced nuclear translocation of endogenous pea phytochrome A visualized by immunocytochemical procedures. *Plant Cell* 12:1063-1078.
68. **Kim L**, Kircher S, Toth R, Adam E, Schäfer E, Nagy F (2000) Light-induced nuclear import of phytochrome-A:GFP fusion proteins is differentially regulated in transgenic tobacco and Arabidopsis. *Plant J.* 22:125-133.
69. **Hiltbrunner A**, Viczian A, Bury E, Tscheuschler A, Kircher S, Toth R, Honsberger A, Nagy F, Fankhauser C, Schäfer E (2005) Nuclear accumulation of the phytochrome A photoreceptor requires FHY1. *Curr. Biol.* 15:2125-2130.
70. **Hiltbrunner A**, Tscheuschler A, Viczian A, Kunkel T, Kircher S, Schäfer E (2006) FHY1 and FHL act together to mediate nuclear accumulation of the phytochrome A photoreceptor. *Plant Cell Physiol*.
71. **Rösler J**, Klein I, Zeidler M (2007) Arabidopsis fhl/fhy1 double mutant reveals a distinct cytoplasmic action of phytochrome A. *Proc Natl Acad Sci U S A* 104:10737-10742.
72. **Gil P**, Kircher S, Adam E, Bury E, Kozma-Bognar L, Schäfer E, Nagy F (2000) Photocontrol of subcellular partitioning of phytochrome-B:GFP fusion protein in tobacco seedlings. *Plant J* 22:135-145.
73. **Kircher S**, Gil P, Kozma-Bognar L, Fejes E, Speth V, Husselstein-Muller T, Bauer D, Adam E, Schäfer E, Nagy F (2002) Nucleocytoplasmic partitioning of the plant photoreceptors phytochrome A, B, C, D, and E is regulated differentially by light and exhibits a diurnal rhythm. *Plant Cell* 14:1541-1555.
74. **Chen M**, Tao Y, Lim J, Shaw A, Chory J (2005) Regulation of phytochrome B nuclear localization through light-dependent unmasking of nuclear-localization signals. *Curr. Biol* 15:637-642.
75. **Quail PH** (2010) Phytochromes. *Curr. Biol.* 20:R504-R507.
76. **Monte E**, Tepperman JM, Al Sady B, Kaczorowski KA, Alonso JM, Ecker JR, Li X, Zhang Y, Quail PH (2004) The phytochrome-interacting transcription factor, PIF3, acts early, selectively, and positively in light-induced chloroplast development. *Proc. Natl. Acad. Sci. U. S. A* 101:16091-16098.
77. **Tepperman JM**, Zhu T, Chang HS, Wang X, Quail PH (2001) Multiple transcription-factor genes are early targets of phytochrome A signaling. *Proc. Natl. Acad. Sci. USA* 98:9437-9442.

78. **Tepperman JM**, Hwang YS, Quail PH (2006) phyA dominates in transduction of red-light signals to rapidly responding genes at the initiation of Arabidopsis seedling de-etiolation. *Plant J* 48:728-742.
79. **Ma L**, Li J, Qu L, Hager J, Chen Z, Zhao H, Deng XW (2001) Light control of Arabidopsis development entails coordinated regulation of genome expression and cellular pathways. *Plant Cell* 13:2589-2607.
80. **Rösler J**, Jaedicke K, Zeidler M (2010) Cytoplasmic phytochrome action. *Plant Cell Physiol* 51:1248-1254.
81. **Paik I**, Yang S, Choi G (2012) Phytochrome regulates translation of mRNA in the cytosol. *PNAS* 109:1335-1340.
82. **Barnes SA**, Nishizawa NK, Quaggio RB, Whitelam GC, Chua N-H (1996) Far-red light blocks greening of Arabidopsis seedlings via a phytochrome A-mediated change in plastid development. *Plant Cell* 8:601-615.
83. **Roux SJ** (1983) A possible role for Ca2+ in mediating phytochrome responses. *Symp. Soc. Exp. Biol.* 36:561-80:561-580.
84. **Tretyn A** (1999) Calcium-dependent signal transduction pathways in plants-- phytochrome mechanism of action as an example. *Pol. J. Pharmacol.* 51:145-151.
85. **Shacklock PS**, Read ND, Trewavas AJ (1992) Cytosolic free calcium mediates red light-induced photomorphogenesis. *Nature* 358:753-755.
86. **Millar AJ**, McGrath RB, Chua N-H (1994) Phytochrome phototransduction pathways. *Ann. Rev. Genet.* 28:325-349.
87. **Tretyn A**, Kendrick RE, Wagner G (1991) The role(s) of calcium ions in phytochrome action. *Photochem. Photobiol.* 54:1135-1155.
88. **Blakeley SD**, Thomas B, Hall JL, Vince-Prue D (1983) Regulation of swelling of etiolated-wheat-leaf protoplasts by phytochrome and gibberellic acid. *Planta* 158:416-421.
89. **Parks BM**, Jones AM, Adamse P, Koornneef M, Kendrick RE, Quail PH (1987) The *aurea* mutant of tomato is deficient in spectrophotometrically and immunochemically detectable phytochrome. *Plant Mol. Biol.* 9:97-107.
90. **Sharrock RA**, Parks BM, Koornneef M, Quail PH (1988) Molecular analysis of the phytochrome deficiency in an *aurea* mutant of tomato. *Mol. Gen. Genet.* 213:9-14.
91. **Neuhaus G**, Bowler C, Kern R, Chua N-H (1993) Calcium/calmodulin-dependent and -independent phytochrome signal transduction pathways. *Cell* 73:937-952.
92. **Bowler C**, Neuhaus G, Yamagata H, Chua N-H (1994) Cyclic GMP and calcium mediate phytochrome phototransduction. *Cell* 77:73-81.
93. **Okamoto H**, Matsui M, Deng XW (2001) Overexpression of the heterotrimeric G-protein alpha-subunit enhances phytochrome-mediated inhibition of hypocotyl elongation in Arabidopsis. *Plant Cell* 13:1639-1652.
94. **Wei Q**, Zhou W, Hu G, Wei J, Yang H, Huang J (2008) Heterotrimeric G-protein is involved in phytochrome A-mediated cell death of Arabidopsis hypocotyls. *Cell Res* 18:949-960.
95. **Botto JF**, Ibarra S, Jones AM (2009) The Heterotrimeric G-protein Complex Modulates Light Sensitivity in Arabidopsis thaliana Seed Germination. *Photochem. Photobiol.* 85:949-954.
96. **Jones AM**, Ecker JR, Chen JG (2003) A reevaluation of the role of the heterotrimeric G protein in coupling light responses in Arabidopsis. *Plant Physiol* 131:1623-1627.
97. **Guo H**, Duong H, Ma N, Lin C (1999) The Arabidopsis blue light receptor cryptochrome 2 is a nuclear protein regulated by a blue light-dependent post-transcriptional mechanism. *The Plant Journal* 19:279-287.
98. **Kleiner O**, Kircher S, Harter K, Batschauer A (1999) Nuclear localization of the Arabidopsis blue light receptor cryptochrome 2. *The Plant Journal* 19:289-296.
99. **Yang, H**. Q., Wu, Y. J., Tang, R. H., Liu, D., Liu, Y., & Cashmore, A. R. (2000) The C termini of Arabidopsis cryptochromes mediates a constitutive light response. *Cell* 103:815-827.
100. **Sakamoto K**, Briggs WR (2002) Cellular and subcellular localization of phototropin 1. *Plant Cell* 14:1723-1735.
101. **Kong SG**, Suzuki T, Tamura K, Mochizuki N, Hara-Nishimura I, Nagatani A (2006) Blue light-induced association of phototropin 2 with the Golgi apparatus. *Plant J.* 45:994-1005.
102. **Wan YL**, Eisinger W, Ehrhardt D, Kubitscheck U, Baluska F, Briggs W (2008) The subcellular localization and blue-light-induced movement of phototropin 1-GFP in etiolated seedlings of *Arabidopsis thaliana*. *Mol. Plant* 1:103-117.
103. **Han IS**, Tseng TS, Eisinger W, Briggs WR (2008) Phytochrome A regulates the intracellular distribution of phototropin 1-green fluorescent protein in *Arabidopsis thaliana*. *Plant Cell* 20:2835-2847.

104. **Christie JM**, Reymond P, Powell GK, Bernasconi P, Raibekas AA, Liscum E, Briggs WR (1998) Arabidopsis NPH1: a flavoprotein with the properties of a photoreceptor for phototropism. *Science* 282:1698-1701.
105. **Liscum E**, Briggs WR (1995) Mutations in the NPH1 locus of *Arabidopsis* disrupt the perception of phototropic stimuli. *Plant Cell* 7:473-485.
106. **Sakai T**, Kagawa T, Kasahara M, Swartz TE, Christie JM, Briggs WR, Wada M, Okada K (2001) Arabidopsis nph1 and npl1: blue light receptors that mediate both phototropism and chloroplast relocation. *Proc. Natl. Acad. Sci. USA* 98:6969-6974.
107. **Stowe-Evans EL**, Luesse DR, Liscum E (2001) The enhancement of phototropin-induced phototropic curvature in *Arabidopsis* occurs via a photoreversible phytochrome A-dependent modulation of auxin responsiveness. *Plant Physiol.* 126:826-834.
108. **Kiss JZ**, Mullen JL, Correll MJ, Hangarter RP (2003) Phytochromes A and B mediate red-light-induced positive phototropism in roots. *Plant Physiol.* 131:1411.
109. **Ruppel NJ**, Hangarter RP, Kiss JZ (2001) Red-light-induced positive phototropism in Arabidopsis roots. *Planta* 212:424-430.
110. **Molas ML**, Kiss JZ (2008) PKS1 plays a role in red-light-based positive phototropism in roots. *Plant, Cell & Environment* 31:842-849.
111. **DeBlasio SL**, Mullen JL, Luesse DR, Hangarter RP (2003) Phytochrome Modulation of Blue Light-Induced Chloroplast Movements in Arabidopsis. *Plant Physiol.* 133:1471-1479.
112. **Luesse DR**, DeBlasio SL, Hangarter RP (2010) Integration of phot1, phot2, and PhyB signalling in light-induced chloroplast movements. *J. Exp. Bot.* 61:4387-4397.
113. **Theißen G**, Münster T, Henschel K (2001) Why don't mosses flower? *New Phytol.* 150:1-8.
114. **Quatrano RS**, McDaniel SF, Khandelwal A, Perroud PF, Cove DJ (2007) Physcomitrella patens: mosses enter the genomic age. *Current Opinion in Plant Biology* 10:182-189.
115. **Cove D**, Bezanilla M, Harries P, Quatrano R (2006) Mosses as model systems for the study of metabolism and development. *Annu. Rev. Plant Biol.* 57:497-520.
116. **Cove D** (2005) The moss Physcomitrella patens. *Annu. Rev. Genet.* 39:339-358.
117. **Schaefer DG**, Zrÿd J-P, Knight CD, Cove DJ (1991) Stable transformation of the moss *Physcomitrella patens*. *Mol. Gen. Genet.* 226:418-424.
118. **Schaefer DG**, Zrÿd J-P (1997) Efficient gene targeting in the moss *Physcomitrella patens*. *Plant J.* 11:1195-1206.
119. **Grimsley NH**, Ashton NW, Cove DJ (1977) The production of somatic hybrids by protoplast fusion in the moss *Physcomitrella patens*. *Mol. Gen. Genet.* 154:97-100.
120. **Cove DJ**, Quatrano RS, Hartmann E (1996) The alignment of the axis of asymmetry in regenerating protoplasts of the moss *Ceratodon purpureus* is determined independently of axis polarity. *Development* 122:371-379.
121. **Cove DJ** (2000) The generation and modification of cell polarity. *J. Exp. Bot.* 51:831-838.
122. **Jenkins GI**, Cove DJ (1983a) Light requirements for regeneration of protoplasts of the moss Physcomitrella patens. *Planta* 157:39-45.
123. **Jenkins GI**, Cove DJ (1983b) Phototropism and polarotropism of primary chloronemata of the moss Physcomitrella patens: responses of mutant strains. *Planta* 159:432-438.
124. **Jenkins GI**, Cove DJ (1983c) Phototropism and polarotropism of primary chloronemata of the moss Physcomitrella patens: responses of the wild-type. *Planta* 158:357-364.
125. **Rensing SA**, Lang D, Zimmer AD, Terry A, Salamov A, Shapiro H, Nishiyama T, Perroud PF, Lindquist EA, Kamisugi Y *et al.* (2008) The *Physcomitrella* genome reveals evolutionary insights into the conquest of land by plants. *Science* 319:64-69.
126. **Rensing SA**, Ick J, Fawcett JA, Lang D, Zimmer A, Van de PY, Reski R (2007) An ancient genome duplication contributed to the abundance of metabolic genes in the moss Physcomitrella patens. *BMC. Evol. Biol.* 7:130.
127. **Burgess J**, Linstead PJ (1981) Studies on the Growth and Development of Protoplasts of the Moss, *Physcomitrella patens*, and its Control by light. *Planta* 331-338.
128. **Hartmann E**, Klingenberg B, Bauer L (1983) Phytochrome-mediated phototropism in protonemata of *Ceratodon purpureus*. *Photochem. Photobiol.* 38:599-603.
129. **Bauer L**, Mohr H (1959) Der Nachweis des reversiblen Hellrot-Dunkelrot Reaktionssystems bei Laubmoosen. *Planta* 54:68-73.
130. **Schild, A**. (1981) Untersuchungen zur Sporenkeimung und Protonemaentwicklung be idem Laubmoos *Physcomitrella patens*. (PhD thesis, University of Mainz).

131. **Cove D**, Schild A, Ashton NW, Hartmann E (1978) Genetic and physiological studies of the effect of light on the development of the moss, *Physcomitrella patens*. *Photochem. Photobiol.* 27:249-254.
132. **Valanne N** (1966) The germination of moss spores and their control by light. *Annals Botanici Fennici* 3:1-40.
133. **Nebel BJ** (1969) Responses of moss protonemata to red and far-red polarized light: evidence for disc-shaped phytochrome photoreceptors. *Planta* 87:170-179.
134. **Esch H**, Hartmann E, Cove D, Wada M, Lamparter T (1999) Phytochrome-controlled phototropism of protonemata of the moss *Ceratodon purpureus*: physiology of the wild type and class 2 ptr-mutants. *Planta* 209:290-298.
135. **Lamparter T**, Hughes J, Hartmann E (1998) Blue light- and genetically-reversed gravitropic response in protonemata of the moss *Ceratodon purpureus*. *Planta* 206:95-102.
136. **Lamparter T**, Esch H, Cove D, Hughes J, Hartmann E (1996) Aphototropic mutants of the moss *Ceratodon purpureus* with spectrally normal and with spectrally dysfunctional phytochrome. *Pl. Cell &. Environ.* 19:560-568.
137. **Kagawa T**, Sakai T, Suetsugu N, Oikawa K, Ishiguro S, Kato T, Tabata S, Okada K, Wada M (2001) Arabidopsis NPL1: a phototropin homolog controlling the chloroplast high-light avoidance response. *Science* 291:2138-2141.
138. **Kadota A**, Sato Y, Wada M (2000) Intracellular chloroplast photorelocation in the moss *Physcomitrella patens* is mediated by phytochrome as well as by a blue-light receptor. *Planta* 210:932-937.
139. **Cove DJ**, Ashton NW (1988) Growth regulation and development in *Physcomitrella patens*: an insight into growth regulation and development in bryophytes. *Botanical Journal of the Linnean Society* 98:247-254.
140. **Kagawa T**, Lamparter T, Hartmann E, Wada M (1997) Phytochrome-mediated branch formation in protonemata of the moss *Ceratodon purpureus*. *Journal of Plant Research* 110:363-370.
141. **Imaizumi T**, Kadota A, Hasebe M, Wada M (2002) Cryptochrome light signals control development to suppress auxin sensitivity in the moss Physcomitrella patens. *Plant Cell* 14:373-386.
142. **Uenaka H**, Wada M, Kadota A (2005) Four distinct photoreceptors contribute to light-induced side branch formation in the moss *Physcomitrella patens*. *Planta* 222:623-631.
143. **Uenaka H**, Kadota A (2008) Phototropin-Dependent Weak and Strong Light Responses in the Determination of Branch Position in the Moss Physcomitrella patens. *Plant Cell Physiol.* 49:1907-1910.
144. **Racusen R**, Satter RL (1975) Rhythmic and phytochrome-regulated changes in transmembrane potential in samanea pulvini. *Nature* 255:408-410.
145. **Tanada T** (1968) A rapid photoreversible response of barley root tips in the presence of 3-indoleacetic acid. *Proc. Natl. Acad. Sci. U. S. A* 59:376-380.
146. **Takagi S**, Kong SG, Mineyuki Y, Furuya M (2003) Regulation of actin-dependent cytoplasmic motility by type II phytochrome occurs within seconds in *Vallisneria gigantea* epidermal cells. *Plant Cell* 15:331-345.
147. **Kraml, M**. (1994) in *Photomorphogenesis in plants*, eds. Kendrick, R. E. & Kronenberg, G. H. M. (Kluwer, Dortrecht), pp. 417-446.
148. **Sundqvist C**, Björn LO (1983) Light-induced linear dichroism in photoreversibly phytochrome sensor pigements - II. Chromophore rotation in immobilized phytochrome. *Photochem Photobiol* 37:69-75.
149. **Kraml M**, Enders M, Bürkel N (1984) Kinetics of the dichroic reorientation of phytochrome during photoconversion in Mougeotia. *Planta* 161:216-222.
150. **Kadota A**, Wada M, Furuya M (1982) Phytochrome-mediated phototropism and different dichroic orientation of P_r and P_{fr} in protonemata of the fern *Adiantum capillus-veneris* . *Photochem. Photobiol.* 35:533-536.
151. **Haupt W** (1970) Über den Dichroismus von Phytochrom-660 und Phytochrom-730 bei *Mougeotia*. *Z. Pflanzenphysiol.* 62:287-298.
152. **Haupt W** (1960) Die Chloroplastendrehung bei Mougeotia. II: Die Induktion der Schwachlichtbewegung durch linear polarisiertes Licht. *Planta* 55:465-479.
153. **Etzold H (**1965) Der Polarotropismus und Phototropismus der Chloronemen von *Dryopteris filix-mas* (L.) Schott. *Planta* 64:254-280.
154. **Herrmann H**, Kraml M (1997) Time-dependent formation of Pfr-mediated signals for the interaction with blue light in Mesotaenium chloroplast orientation. *Journal of Photochemistry and Photobiology B: Biology* 37:60-65.

155. **Böse G**, Schwille P, Lamparter T (2004) The mobility of phytochrome within protonemal tip cells of the moss *Ceratodon purpureus*, monitored by fluorescence correlation spectroscopy. *Biophys. J* 87:2013-2021.
156. **Nagatani A**, Jenkins GI, Furuya M (1988) Non-specific association of phytochrome to nuclei during isolation from dark-grown pea. *Plant Cell Physiol* 29:1141-1145.
157. **Kidd DG**, Lagarias JC (1990) Phytochrome from the green alga Mesotaenium caldariorum. Purification and preliminary characterization. *J. Biol. Chem.* 12:7029-7035.
158. **Quail PH** (1991) Phytochrome: a light-activated molecular switch that regulates plant gene expression. *Annu. Rev. Genet.* 25:389-409.
159. **Meske V**, Hartmann E (1995) Reorganisation of microfilaments in protonemal tip cells of the moss *Ceratodon purpureus* during the phototropic response. *Protoplasma* 188:59-69.
160. **Meske V**, Rupert V, Hartmann E (1996) Structural basis for the red light induced repolarisation of tip growth in caulonemal cells of *Ceratodon purpureus*. *Protoplasma* 192:189-198.
161. **Perroud PF**, Quatrano R (2006) The role of ARPC4 in tip growth and alignment of the polar axis in filaments of *Physcomitrella patens*. *Cell Motility and the Cytoskeleton*162-171.
162. **Yamashita H**, Sato Y, Kanegae T, Kagawa T, Wada M, Kadota A (2011) Chloroplast actin filaments organize meshwork on the photorelocated chloroplasts in the moss Physcomitrella patens. *Planta* 233:357-368.
163. **Oikawa K**, Kasahara M, Kiyosue T, Kagawa T, Suetsugu N, Takahashi F, Kanegae T, Niwa Y, Kadota A, Wada M (2003) CHLOROPLAST UNUSUAL POSITIONING1 Is Essential for Proper Chloroplast Positioning. *The Plant Cell Online* 15:2805-2815.
164. **Oikawa K**, Yamasato A, Kong SG, Kasahara M, Nakai M, Takahashi F, Ogura Y, Kagawa T, Wada M (2008) Chloroplast Outer Envelope Protein CHUP1 Is Essential for Chloroplast Anchorage to the Plasma Membrane and Chloroplast Movement. *Plant Physiol.* 148:829-842.
165. **Ichikawa S**, Yamada N, Suetsugu N, Wada M, Kadota A (2011) Red Light, Phot1 and JAC1 Modulate Phot2-Dependent Reorganization of Chloroplast Actin Filaments and Chloroplast Avoidance Movement. *Plant Cell Physiol.* 52:1422-1432.
166. **Yamada N**, Suetsugu N, Wada M, Kadota A (2011) Phototropin-dependent biased relocalization of cp-actin filaments can be induced even when chloroplast movement is inhibited. *Plant Signal. Behav.* 6:1651-1653.
167. **Lau OS**, Deng XW (2010) Plant hormone signaling lightens up: integrators of light and hormones. *Current Opinion in Plant Biology* 13:571-577.
168. **Saijo Y**, Sullivan JA, Wang H, Yang J, Shen Y, Rubio V, Ma L, Hoecker U, Deng XW (2003) The COP1-SPA1 interaction defines a critical step in phytochrome A-mediated regulation of HY5 activity. *Genes Dev.* 17:2642-2647.
169. **Laubinger S**, Fittinghoff K, Hoecker U (2004) The SPA Quartet: A Family of WD-Repeat Proteins with a Central Role in Suppression of Photomorphogenesis in Arabidopsis. *Plant Cell* 9:2293-2306.
170. **Osterlund MT**, Hardtke CS, Wei N, Deng XW (2000) Targeted destabilization of HY5 during light-regulated development of Arabidopsis. *Nature* 405:462-466.
171. **Lee J**, He K, Stolc V, Lee H, Figueroa P, Gao Y, Tongprasit W, Zhao H, Lee I, Deng XW (2007) Analysis of Transcription Factor HY5 Genomic Binding Sites Revealed Its Hierarchical Role in Light Regulation of Development. *The Plant Cell Online* 19:731-749.
172. **Uenaka H**, Kadota A (2007) Functional analyses of the *Physcomitrella patens* phytochromes in regulating chloroplast avoidance movement. *The Plant Journal*.
173. **Tsuboi H**, Nakamura S, Sch+ñfer E, Wada M (2012) Red Light-Induced Phytochrome Relocation into the Nucleus in Adiantum capillus-veneris. *Molecular Plant*.
174. **Yamawaki S**, Yamashino T, NAKANISHI H, Mizuno T (2011) Functional Characterization of HY5 Homolog Genes Involved in Early Light-Signaling in Physcomitrella patens. *Bioscience, Biotechnology, and Biochemistry* 75:1533-1539.
175. **Suetsugu N**, Wada M (2007) Phytochrome-dependent Photomovement Responses Mediated by Phototropin Family Proteins in Cryptogam Plants. *Photochem. Photobiol.* 83:87-93.
176. **Ashton NW**, Cove DJ (1977) The isolation and preliminary characterisation of auxotrophic and analogue resistant mutants of the moss *Physcomitrella patens*. *Mol. Gen. Genet.* 154:87-95.
177. **Rösler, J**. (2010) Charakterisierung und Identifizierung von Komponenten und Ereignissen der frühen Phytochrom A Signaltransduktion in *Arabidopsis thaliana.* (PhD thesis, Justus Liebig Universität, Giessen).

178. **Karimi M**, Inzé D, Depicker A (2002) GATEWAY (TM) vectors for *Agrobacterium*-mediated plant transformation. *Trends in Plant Science* 7:193-195.
179. **Citovsky V**, Lee LY, Vyas S, Glick E, Chen MH, Vainstein A, Gafni Y, Gelvin SB, Tzfira T (2006) Subcellular localization of interacting proteins by bimolecular fluorescence complementation *in planta*. *J. Mol. Biol.* 362:1120-1131.
180. **Nelson BK**, Cai X, Nebenfühhr A (2007) A multicolored set of in vivo organelle markers for co-localization studies in Arabidopsis and other plants. *The Plant Journal* 51:1126-1136.
181. **Kost B**, Spielhöfer P, Chua N-H (1998) A GFP-mouse talin fusion protein labels plant actin filaments in vivo and visualizes the actin cytoskeleton in growing pollen tubes. *The Plant Journal* 16:393-401.
182. **Gasch, P**. (2010). Untersuchungen zur Signaltransduktion von Phytochrom A in Arabidopsis thaliana. (Master thesis, Justus Liebig Universität, Giessen).
183. **Zeidler M**, Bolle C, Chua NH (2001) The phytochrome A specific signaling component PAT3 is a positive regulator of Arabidopsis photomorphogenesis. *Plant Cell Physiol* 42:1193-1200.
184. **Sambrook, J**. & Russell, D. W. (2001) *Molecular Cloning. A Laboratory Manual. 3rd edition* (Cold Spring Harbor Laboratory Press.
185. **Hanahan, D**. (1985) in *DNA cloning a practical approach*, ed. Glover, D. M. (IRL Press, Oxford), pp. 109-135.
186. **Jaedicke K**, Rösler J, Gans T, Hughes J (2011) *Bellis perennis*: a useful tool for protein localization studies. *Planta* 234:759-768.
187. **Vain P**, Keen NT, Murillo J, Rathus C, Nemes C, Finer JJ (1993) Development of the Particle Inflow Gun. *Plant Cell Tissue and. Organ. Culture* 33:237-246.
188. **Drummond, A**, Asthon, B, Buxton, S, Cheung, M, Cooper, A, Duran, C, Field, M, Heled, J, Kearse, M, Markowitz, S *et al.* (2011). Geneious v 5.4. (http://www.geneious.com/).
189. **Jordan ET**, Cherry JR, Walker JM, Vierstra RD (1996) The amino-terminus of phytochrome A contains two distinct functional domains. *Plant J.* 9:243-257.
190. **Cherry JR**, Hondred D, Walker JM, Vierstra RD (1992) Phytochrome requires the 6-kDa N-terminal domain for full biological activity. *Proc. Natl. Acad. Sci. U. S. A.* 89:5039-5043.
191. **Yang X**, Stojkovic EA, Kuk J, Moffat K (2007) Crystal structure of the chromophore binding domain of an unusual bacteriophytochrome, RpBphP3, reveals residues that modulate photoconversion. *Proc Natl Acad Sci U S A* 104:12571-12576.
192. **Howard EA**, Zupan JR, Citovsky V, Zambryski PC (1992) The VirD2 protein of A. tumefaciens contains a C-terminal bipartite nuclear localization signal: Implications for nuclear uptake of DNA in plant cells. *Cell* 68:109-118.
193. **Haseloff J**, Siemering KR, Prasher DC, Hodge S (1997) Removal of a cryptic intron and subcellular localization of green fluorescent protein are required to mark transgenic *Arabidopsis* plants brightly. *Proc. Natl. Acad. Sci. U. S. A* 94:2122-2127.
194. **Hill C**, Gartner W, Towner P, Braslavsky SE, Schaffner K (1994) Expression of phytochrome apoprotein from Avena sativa in Escherichia coli and formation of photoactive chromoproteins by assembly with phycocyanobilin. *Eur. J. Biochem.* 223:69-77.
195. **Ni M**, Tepperman JM, Quail PH (1998) PIF3, a phytochrome-interacting factor necessary for normal photoinduced signal transduction, is a novel basic helix-loop-helix protein. *Cell* 95:657-667.
196. **Choi G**, Yi H, Lee J, Kwon YK, Soh MS, Shin B, Luka Z, Hahn TR, Song PS (1999) Phytochrome signalling is mediated through nucleoside diphosphate kinase 2. *Nature* 401:610-613.
197. **Bölter B**, Sharma R, Soll J (2007) Localisation of Arabidopsis NDPK2--revisited. *Planta* 226:1059-1065.
198. **Marchler-Bauer A**, Lu S, Anderson JB, Chitsaz F, Derbyshire MK, Weese-Scott C, Fong JH, Geer LY, Geer RC, Gonzales NR *et al.* (2011) CDD: a Conserved Domain Database for the functional annotation of proteins. *Nucleic Acids Res.* 39:D225-D229.
199. **Ramakrishnan C**, Dani VS, Ramasarma T (2002) A conformational analysis of Walker motif A [GXXXXGKT (S)] in nucleotide-binding and other proteins. *Protein Eng.* 15:783-798.
200. **Saraste M**, Sibbald PR, Wittinghofer A (1990) The P-loop--a common motif in ATP- and GTP-binding proteins. *Trends Biochem. Sci.* 15:430-434.
201. **Walker JE**, Saraste M, Runswick MJ, Gay NJ (1982) Distantly related sequences in the alpha- and beta-subunits of ATP synthase, myosin, kinases and other ATP-requiring enzymes and a common nucleotide binding fold. *EMBO J.* 1:945-951.
202. **Klein M**, Papenbrock J (2004) The multi-protein family of Arabidopsis sulphotransferases and their relatives in other plant species. *J. Exp. Bot.* 55:1809-1820.

203. **Sprague ER**, Redd MJ, Johnson AD, Wolberger C (2000) Structure of the C-terminal domain of Tup1, a corepressor of transcription in yeast. *EMBO J* 19:3016-3027.
204. **Smith TF**, Gaitatzes C, Saxena K, Neer EJ (1999) The WD repeat: a common architecture for diverse functions. *Trends Biochem. Sci.* 24:181-185.
205. **Li D**, Roberts R (2001) Human Genome and Diseases:-WD-repeat proteins: structure characteristics, biological function, and their involvement in human diseases. *Cellular and Molecular Life Sciences* 58:2085-2097.
206. **Axelos M**, Bardet C, Liboz T, Le Van TA, Curie C, Lescure B (1989) The gene family encoding the Arabidopsis thaliana translation elongation factor EF-1 alpha: molecular cloning, characterization and expression. *Mol Gen. Genet.* 219:106-112.
207. **Ransom-Hodgkins W** (2009) The application of expression analysis in elucidating the eukaryotic elongation factor one alpha gene family in Arabidopsis thaliana. *Molecular Genetics and Genomics* 281:391-405.
208. **Zeidler M**, Lamparter T, Hughes J, Hartmann E, Remberg A, Braslavsky S, Schaffner K, Gärtner W (1998) Recombinant phytochrome of the moss *Ceratodon purpureus*: heterologous expression and kinetic analysis of Pr-->Pfr conversion. *Photochem. Photobiol.* 68:857-863.
209. **Strauss HM**, Schmieder P, Hughes J (2005) Light-dependent dimerisation in the N-terminal sensory module of cyanobacterial phytochrome 1. *FEBS Lett.* 18:3970-3974.
210. **Kerppola TK** (2008) Bimolecular fluorescence complementation (BiFC) analysis as a probe of protein interactions in living cells. *Annu. Rev Biophys.* 37:465-487.
211. **Jarillo JA**, Gabrys H, Capel J, Alonso JM, Ecker JR, Cashmore AR (2001) Phototropin-related NPL1 controls chloroplast relocation induced by blue light. *Nature* 410:952-954.
212. **Kagawa T** (2003) The phototropin family as photoreceptors for blue light-induced chloroplast relocation. *J. Plant Res.* 116:77-82.
213. **Salomon M**, Lempert U, Rüdiger W (2004) Dimerization of the plant photoreceptor phototropin is probably mediated by the LOV1 domain. *FEBS Lett.* 572:8-10.
214. **Banks JA**, Nishiyama T, Hasebe M, Bowman JL, Gribskov M, dePamphilis C (2011) The *Selaginella* genome identifies genetic changes associated with the evolution of vascular plants. *Science* 332:960-963.
215. **Parks BM**, Quail PH, Hangarter RP (1996) Phytochrome A regulates red-light induction of phototropic enhancement in Arabidopsis. *Plant Physiol* 110:155-162.
216. **Kiss JZ**, Ruppel NJ, Hangarter RP (2001) Phototropism in Arabidopsis roots is mediated by two sensory systems. *Adv. Space Res* 27:877-885.
217. **Knieb E**, Salomon M, Rüdiger W (2004) Tissue-specific and subcellular localization of phototropin determined by immuno-blotting. *Planta* 218:843-851.
218. **Harries PA**, Pan A, Quatrano RS (2005) Actin-related protein2/3 complex component ARPC1 is required for proper cell morphogenesis and polarized cell growth in *Physcomitrella patens*. *Plant Cell* 17:2327-2339.
219. **Schaefer DG** (2002) A new moss genetics: targeted mutagenesis in *Physcomitrella patens*. *Annu. Rev. Plant. Biol* 53:477-501.
220. **Castillon A**, Shen H, Huq E (2007) Phytochrome Interacting Factors: central players in phytochrome-mediated light signaling networks. *Trends Plant Sci* 12:514-521.
221. **Van Buskirk EK**, Decker PV, Chen M (2012) Photobodies in light signaling. *Plant Physiol* 158:52-60.
222. **Wang ZY**, Kenigsbuch D, Sun L, Harel E, Ong MS, Tobin EM (1997) A Myb-related transcription factor is involved in the phytochrome regulation of an Arabidopsis Lhcb gene. *Plant Cell* 9:491-507.
223. **Martinez-Garcia JF**, Huq E, Quail PH (2000) Direct targeting of light signals to a promoter element-bound transcription factor. *Science* 288:859-863.
224. **Shimizu M**, Ichikawa K, Aoki S (2004) Photoperiod-regulated expression of the PpCOL1 gene encoding a homolog of CO/COL proteins in the moss Physcomitrella patens. *Biochem. Biophys. Res. Commun.* 324:1296-1301.
225. **Okada R**, Satbhai SB, Aoki S (2009) Photoperiod-dependent regulation of cell growth by PpCCA1a and PpCCA1b genes encoding single-myb clock proteins in the moss Physcomitrella patens. *Genes Genet. Syst.* 84:379-384.
226. **Okada R**, Kondo S, Satbhai SB, Yamaguchi N, Tsukuda M, Aoki S (2009) Functional characterization of CCA1/LHY homolog genes, PpCCA1a and PpCCA1b, in the moss Physcomitrella patens. *Plant J.* 60:551-563.

227. **Satbhai SB**, Yamashino T, Mizuno T, AOKI S (2011) Heterologous Expression and Functional Characterization of a Physcomitrella Pseudo Response Regulator Homolog, PpPRR2, in Arabidopsis. *Biosci. , Biotechnol. , Biochem.* 75:786-789.
228. **Ichikawa K**, Sugita M, Imaizumi T, Wada M, Aoki S (2004) Differential expression on a daily basis of plastid sigma factor genes from the moss Physcomitrella patens. Regulatory interactions among PpSig5, the circadian clock, and blue light signaling mediated by cryptochromes. *Plant Physiol* 136:4285-4298.
229. **Sathbhai SB**, Yamashino T, Okada R, Nomoto Y, Mizuno T, Tezuka Y, Itoh T, Tomita M, Otsuki S, AOKI S (2011) Pseudo-Response Regulator (PRR) Homologues of the Moss Physcomitrella patens: Insights into the Evolution of the PRR Family in Land Plants. *DNA Research* 18:39-52.
230. **Possart, A**, Rensing, S., & Hiltbrunner, A. (2011). A novel view on cryptogam light signalling: Rapid nuclear accumulation of phytochromes and FR-induced responses in Physcomitrella patens. (Poster presentation, *Botanikertagung* Berlin 2011).
231. **Sokolova V**, Bindics J, Kircher S, Adam E, Schafer E, Nagy F, Viczian A (2012) Missense mutation in the amino terminus of phytochrome A disrupts the nuclear import of the photoreceptor. *Plant Physiol* 158:107-118.
232. **Genoud T**, Schweizer F, Tscheuschler A, Debrieux D, Casal JJ, Schafer E, Hiltbrunner A, Fankhauser C (2008) FHY1 mediates nuclear import of the light-activated phytochrome A photoreceptor. *PLoS. Genet.* 4:e1000143.
233. **Putterill J**, Robson F, Lee K, Simon R, Coupland G (1995) The CONSTANS gene of Arabidopsis promotes flowering and encodes a protein showing similarities to zinc finger transcription factors. *Cell* 80:847-857.
234. **Kim DH**, Yamaguchi S, Lim S, Oh E, Park J, Hanada A, Kamiya Y, Choi G (2008) SOMNUS, a CCCH-type zinc finger protein in Arabidopsis, negatively regulates light-dependent seed germination downstream of PIL5. *Plant Cell* 20:1260-1277.
235. **Park J**, Lee N, Kim W, Lim S, Choi G (2011) ABI3 and PIL5 collaboratively activate the expression of SOMNUS by directly binding to its promoter in imbibed Arabidopsis seeds. *Plant Cell* 23:1404-1415.
236. **Kang X**, Zhou Y, Sun X, Ni M (2007) HYPERSENSITIVE TO RED AND BLUE 1 and its C-terminal regulatory function control FLOWERING LOCUS T expression. *Plant J* 52:937-948.
237. **Kang X**, Chong J, Ni M (2005) HYPERSENSITIVE TO RED AND BLUE 1, a ZZ-type zinc finger protein, regulates phytochrome B-mediated red and cryptochrome-mediated blue light responses. *Plant Cell* 17:822-835.
238. **Chen M**, Ni M (2006) RED AND FAR-RED INSENSITIVE 2, a RING-domain zinc finger protein, mediates phytochrome-controlled seedling deetiolation responses. *Plant Physiol* 140:457-465.
239. **Schwechheimer C**, Deng XW (2000) The COP/DET/FUS proteins-regulators of eukaryotic growth and development. *Semin. Cell Dev. Biol.* 11:495-503.
240. **Deng XW**, Matsui M, Wei N, Wagner D, Chu AM, Feldmann KA, Quail PH (1992) COP1, an Arabidopsis regulatory gene, encodes a protein with both a zinc-binding motif and a G beta homologous domain. *Cell* 71:791-801.
241. **Oyama T**, Shimura Y, Okada K (1997) The Arabidopsis HY5 gene encodes a bZIP protein that regulates stimulus-induced development of root and hypocotyl. *Genes Dev.* 11:2983-2995.
242. **Chattopadhyay S**, Ang LH, Puente P, Deng XW, Wei N (1998) Arabidopsis bZIP protein HY5 directly interacts with light- responsive promoters in mediating light control of gene expression. *Plant Cell* 10:673-684.
243. **Jang IC**, Henriques R, Seo HS, Nagatani A, Chua NH (2010) Arabidopsis PHYTOCHROME INTERACTING FACTOR Proteins Promote Phytochrome B Polyubiquitination by COP1 E3 Ligase in the Nucleus. *The Plant Cell Online* 22:2370-2383.
244. **Osterlund MT**, Deng XW (1998) Multiple photoreceptors mediate the light-induced reduction of GUS-COP1 from Arabidopsis hypocotyl nuclei. *Plant J.* 16:201-208.
245. **Klein M**, Reichelt M, Gershenzon J, Papenbrock J (2006) The three desulfoglucosinolate sulfotransferase proteins in Arabidopsis have different substrate specificities and are differentially expressed. *FEBS Journal* 273:122-136.
246. **Rouleau Ml**, Marsolais Fdr, Richard M, Nicolle L, Voigt B, Adam G, Varin L (1999) Inactivation of Brassinosteroid Biological Activity by a Salicylate-inducible Steroid Sulfotransferase from Brassica napus. *J. Biol. Chem.* 274:20925-20930.

247. **Marsolais Fdr**, Boyd J, Paredes Y, Schinas AM, Garcia M, Elzein S, Varin L (2007) Molecular and biochemical characterization of two brassinosteroid sulfotransferases from Arabidopsis, AtST4a (At2g14920) and AtST1 (At2g03760). *Planta* 225:1233-1244.
248. **Gidda SK**, Miersch O, Levitin A, Schmidt J, Wasternack C, Varin L (2003) Biochemical and Molecular Characterization of a Hydroxyjasmonate Sulfotransferase from Arabidopsis thaliana. *J. Biol. Chem.* 278:17895-17900.
249. **Komori R**, Amano Y, Ogawa-Ohnishi M, Matsubayashi Y (2009) Identification of tyrosylprotein sulfotransferase in Arabidopsis. *Proceedings of the National Academy of Sciences* 106:15067-15072.
250. **Zhou W**, Wei L, Xu J, Zhai Q, Jiang H, Chen R, Chen Q, Sun J, Chu J, Zhu L *et al.* (2010) Arabidopsis Tyrosylprotein Sulfotransferase Acts in the Auxin/PLETHORA Pathway in Regulating Postembryonic Maintenance of the Root Stem Cell Niche. *The Plant Cell Online* 22:3692-3709.
251. **Matsuzaki Y**, Ogawa-Ohnishi M, Mori A, Matsubayashi Y (2010) Secreted Peptide Signals Required for Maintenance of Root Stem Cell Niche in Arabidopsis. *Science* 329:1065-1067.
252. **Doyle JJ**, Luckow MA (2003) The Rest of the Iceberg. Legume Diversity and Evolution in a Phylogenetic Context. *Plant Physiol.* 131:900-910.
253. **Suzuki A**, Suriyagoda L, Shigeyama T, Tominaga A, Sasaki M, Hiratsuka Y, Yoshinaga A, Arima S, Agarie S, Sakai T *et al.* (2011) Lotus japonicus nodulation is photomorphogenetically controlled by sensing the red/far red (R/FR) ratio through jasmonic acid (JA) signaling. *Proceedings of the National Academy of Sciences* 108:16837-16842.
254. **Zhai Q**, Li CB, Zheng W, Wu X, Zhao J, Zhou G, Jiang H, Sun J, Lou Y, Li C (2007) Phytochrome Chromophore Deficiency Leads to Overproduction of Jasmonic Acid and Elevated Expression of Jasmonate-Responsive Genes in Arabidopsis. *Plant Cell Physiol.* 48:1061-1071.
255. **Gangappa SN**, Prasad VBR, Chattopadhyay S (2010) Functional Interconnection of MYC2 and SPA1 in the Photomorphogenic Seedling Development of Arabidopsis. *Plant Physiol.* 154:1210-1219.
256. **Cartieaux F**, Thibaud MC, Zimmerli L, Lessard P, Sarrobert C, David P, Gerbaud A, Robaglia C, Somerville S, Nussaume L (2003) Transcriptome analysis of Arabidopsis colonized by a plant-growth promoting rhizobacterium reveals a general effect on disease resistance. *The Plant Journal* 36:177-188.
257. **Stumpe M**, Gobel C, Faltin B, Beike AK, Hause B, Himmelsbach K, Bode J, Kramell R, Wasternack C, Frank W *et al.* (2010) The moss Physcomitrella patens contains cyclopentenones but no jasmonates: mutations in allene oxide cyclase lead to reduced fertility and altered sporophyte morphology. *New Phytol.* 188:740-749.
258. **Morikawa T**, Saga H, Hashizume H, Ohta D (2009) CYP710A genes encoding sterol C22-desaturase in Physcomitrella patens as molecular evidence for the evolutionary conservation of a sterol biosynthetic pathway in plants. *Planta* 229:1311-1322.
259. **Koncz C**, Nemeth K, Redei GP, Schell J (1992) T-DNA insertional mutagenesis in Arabidopsis. *Plant Mol Biol* 20:963-976.
260. **Xia G**, Ramachandran S, Hong Y, Chan YS, Simanis V, Chua NH (1996) Identification of plant cytoskeletal, cell cycle-related and polarity-related proteins using Schizosaccharomyces pombe. *The Plant Journal* 10:761-769.
261. **Nemeth K**, Salchert K, Putnoky P, Bhalerao R, Koncz-Kalman Z, Stankovic-Stangeland B, Bako L, Mathur J, Okresz L, Stabel S *et al.* (1998) Pleiotropic control of glucose and hormone responses by PRL1, a nuclear WD protein, in Arabidopsis. *Genes Dev.* 12:3059-3073.
262. **Coello P**, Hirano E, Hey SJ, Muttucumaru N, Martinez-Barajas E, Parry MAJ, Halford NG (2012) Evidence that abscisic acid promotes degradation of SNF1-related protein kinase (SnRK) 1 in wheat and activation of a putative calcium-dependent SnRK2. *J. Exp. Bot.* 63:913-924.
263. **Halford NG**, Hey SJ (2009) Snf1-related protein kinases (SnRKs) act within an intricate network that links metabolic and stress signalling in plants. *Biochem. J* 419:247-259.
264. **Bhalerao RP**, Salchert K, Bakó L, Okrész L, Szabados L, Muranaka T, Machida Y, Schell J, Koncz C (1999) Regulatory interaction of PRL1 WD protein with Arabidopsis SNF1-like protein kinases. *Proceedings of the National Academy of Sciences* 96:5322-5327.
265. **Halford NG**, Grahame Hardie D (1998) SNF1-related protein kinases: global regulators of carbon metabolism in plants? *Plant Mol. Biol.* 37:735-748.
266. **Thelander M**, Olsson T, Ronne H (2004) Snf1-related protein kinase 1 is needed for growth in a normal day-night light cycle. *EMBO J* 23:1900-1910.
267. **Decker EL**, Frank W, Sarnighausen E, Reski R (2006) Moss systems biology en route: phytohormones in Physcomitrella development. *Plant Biol. (Stuttg)* 8:397-405.

268. **von Schwartzenberg K** (2006) Moss Biology and Phytohormones - Cytokinins in Physcomitrella. *Plant biol (Stuttg)* 8:382,388.
269. **Thelander M**, Olsson T, Ronne H (2005) Effect of the energy supply on filamentous growth and development in Physcomitrella patens. *J Exp. Bot.* 56:653-662.
270. **Olsson T**, Thelander M, Ronne H (2003) A Novel Type of Chloroplast Stromal Hexokinase Is the Major Glucose-phosphorylating Enzyme in the Moss Physcomitrella patens. *J. Biol. Chem.* 278:44439-44447.
271. **Moore B**, Zhou L, Rolland F, Hall Q, Cheng WH, Liu YX, Hwang I, Jones T, Sheen J (2003) Role of the Arabidopsis glucose sensor HXK1 in nutrient, light, and hormonal signaling. *Science* 300:332-336.
272. **Thelander M**, Nilsson A, Olsson T, Johansson M, Girod PA, Schaefer DG, Zryd JP, Ronne H (2007) The moss genes PpSKI1 and PpSKI2 encode nuclear SnRK1 interacting proteins with homologues in vascular plants. *Plant Mol Biol* 64:559-573.
273. **Farras R**, Ferrando A, Jasik J, Kleinow T, Okresz L, Tiburcio A, Salchert K, del Pozo C, Schell J, Koncz C (2001) SKP1-SnRK protein kinase interactions mediate proteasomal binding of a plant SCF ubiquitin ligase. *EMBO J* 20:2742-2756.
274. **Andersen GR**, Nissen P, Nyborg J (2003) Elongation factors in protein biosynthesis. *Trends Biochem. Sci.* 28:434-441.
275. **Demma M**, Warren V, Hock R, Dharmawardhane S, Condeelis J (1990) Isolation of an abundant 50,000-dalton actin filament bundling protein from Dictyostelium amoebae. *J. Biol. Chem.* 265:2286-2291.
276. **Dharmawardhane S**, Demma M, Yang F, Condeelis J (1991) Compartmentalization and actin binding properties of ABP-50: The elongation factor-1 alpha of Dictyostelium. *Cell Motil. Cytoskeleton* 20:279-288.
277. **Kaur KJ**, Ruben L (1994) Protein translation elongation factor-1 alpha from Trypanosoma brucei binds calmodulin. *J. Biol. Chem.* 269:23045-23050.
278. **Gonen H**, Smith CE, Siegel NR, Kahana C, Merrick WC, Chakraburtty K, Schwartz AL, Ciechanover A (1994) Protein synthesis elongation factor EF-1 alpha is essential for ubiquitin-dependent degradation of certain N alpha-acetylated proteins and may be substituted for by the bacterial elongation factor EF-Tu. *Proceedings of the National Academy of Sciences* 91:7648-7652.
279. **Yang W**, Burkhart W, Cavallius J, Merrick WC, Boss WF (1993) Purification and characterization of a phosphatidylinositol 4-kinase activator in carrot cells. *J. Biol. Chem.* 268:392-398.
280. **Izawa T**, Fukata Y, Kimura T, Iwamatsu A, Dohi K, Kaibuchi K (2000) Elongation Factor-1+¦ Is a Novel Substrate of Rho-Associated Kinase. *Biochem. Biophys. Res. Commun.* 278:72-78.
281. **Yang W**, Boss WF (1994) Regulation of phosphatidylinositol 4-kinase by the protein activator PIK-A49. Activation requires phosphorylation of PIK-A49. *J. Biol. Chem.* 269:3852-3857.
282. **Menand BT**, Calder G, Dolan L (2007) Both chloronemal and caulonemal cells expand by tip growth in the moss Physcomitrella patens. *J. Exp. Bot.* 58:1843-1849.
283. **Eklund DM**, Svensson EM, Kost B (2010) Physcomitrella patens: a model to investigate the role of RAC/ROP GTPase signalling in tip growth. *J. Exp. Bot.* 61:1917-1937.
284. **Gu Y**, Vernoud V, Fu Y, Yang Z (2003) ROP GTPase regulation of pollen tube growth through the dynamics of tip-localized F-actin. *J. Exp. Bot.* 54:93-101.
285. **Gu Y**, Fu Y, Dowd P, Li S, Vernoud V, Gilroy S, Yang Z (2005) A Rho family GTPase controls actin dynamics and tip growth via two counteracting downstream pathways in pollen tubes. *The Journal of Cell Biology* 169:127-138.
286. **De Simone S**, Oka Y, Inoue Y (2000) Effect of Light on Root Hair Formation in *Arabidopsis thaliana* Phytochrome-Deficient Mutants. *Journal of Plant Research* 113:63-69.
287. **Shin DH**, Cho MH, Kim TL, Yoo J, Kim JI, Han YJ, Song PS, Jeon JS, Bhoo SH, Hahn TR (2010) A Small GTPase Activator Protein Interacts with Cytoplasmic Phytochromes in Regulating Root Development. *J. Biol. Chem.* 285:32151-32159.
288. **Perroud PF**, Quatrano RS (2008) BRICK1 Is Required for Apical Cell Growth in Filaments of the Moss Physcomitrella patens but Not for Gametophore Morphology. *The Plant Cell Online* 20:411-422.
289. **Szymanski DB** (2005) Breaking the WAVE complex: the point of Arabidopsis trichomes. *Curr. Opin. Plant Biol* 8:103-112.
290. **Li S**, Blanchoin L, Yang Z, Lord EM (2003) The Putative Arabidopsis Arp2/3 Complex Controls Leaf Cell Morphogenesis. *Plant Physiol.* 132:2034-2044.
291. **Mathur J** (2005) The ARP2/3 complex: giving plant cells a leading edge. *BioEssays* 27:377-387.

292. **Van Gestel**, Slegers H, von Witsch M, Samaj J, Baluska F, Verbelen JP (2003) Immunological evidence for the presence of plant homologues of the actin- related protein Arp3 in tobacco and maize: subcellular localization to actin-enriched pit fields and emerging root hairs. *Protoplasma* 222:45-52.
293. **Hable WE**, Kropf DL (2005) The Arp2/3 complex nucleates actin arrays during zygote polarity establishment and growth. *Cell Motil. Cytoskeleton* 61:9-20.
294. **Augustine RC**, Vidali L, Kleinman KP, Bezanilla M (2008) Actin depolymerizing factor is essential for viability in plants, and its phosphoregulation is important for tip growth. *The Plant Journal* 54:863-875.
295. **Augustine RC**, Pattavina KA, Tützel E, Vidali L, Bezanilla M (2011) Actin Interacting Protein1 and Actin Depolymerizing Factor Drive Rapid Actin Dynamics in Physcomitrella patens. *The Plant Cell Online* 23:3696-3710.
296. **Henty JL**, Bledsoe SW, Khurana P, Meagher RB, Day B, Blanchoin L, Staiger CJ (2011) Arabidopsis Actin Depolymerizing Factor4 Modulates the Stochastic Dynamic Behavior of Actin Filaments in the Cortical Array of Epidermal Cells. *The Plant Cell Online* 23:3711-3726.
297. **Hartmann E**, Weber M (1988) Storage of the phytochrome-mediated phototropic stimulus of moss protonematal cells. *Planta* 175:39-49.
298. **Picton JM**, Steer MW (1983) Evidence for the role of Ca^{2+}-ions in tip extension in pollen tubes. *Protoplasma* 115:11-17.
299. **Schnepf E** (1986) Cellular polarity. *Ann. Rev. Plant Physiol.* 37:23-47.
300. Hartmann, E. (1984) Influence of light on phototropic bending of moss protonemata of *Ceratodon purpureus. Brid. J Hattori Bot Lab.* 55:87-98.
301. **Takác**, Pechan T, Richter H, Müller J, Eck C, Böhm N, Obert B, Ren H, Niehaus K, Samaj J (2010) Proteomics on Brefeldin A-Treated Arabidopsis Roots Reveals Profilin 2 as a New Protein Involved in the Cross-Talk between Vesicular Trafficking and the Actin Cytoskeleton. *J. Proteome Res.* 10:488-501.
302. **Vidali L**, Augustine RC, Kleinman KP, Bezanilla M (2007) Profilin Is Essential for Tip Growth in the Moss Physcomitrella patens. *Plant Cell*.
303. **Schmidt von Braun S**, Schleiff E (2008) The chloroplast outer membrane protein CHUP1 interacts with actin and profilin. *Planta* 227:1151-1159.
304. **Sato Y**, Wada M, Kadota A (2001) Choice of tracks, microtubules and/or actin filaments for chloroplast photo-movement is differentially controlled by phytochrome and a blue light receptor. *J Cell Sci* 114:269-279.
305. **Kandasamy MK**, Meagher RB (1999) Actin-organelle interaction: Association with chloroplast in Arabidopsis leaf mesophyll cells. *Cell Motil. Cytoskeleton* 44:110-118.
306. **Kadota A**, Yamada N, Suetsugu N, Hirose M, Saito C, Shoda K, Ichikawa S, Kagawa T, Nakano A, Wada M (2009) Short actin-based mechanism for light-directed chloroplast movement in Arabidopsis. *Proceedings of the National Academy of Sciences* 106:13106-13111.
307. **Suetsugu N**, Yamada N, Kagawa T, Yonekura H, Uyeda TQP, Kadota A, Wada M (2010) Two kinesin-like proteins mediate actin-based chloroplast movement in Arabidopsis thaliana. *Proceedings of the National Academy of Sciences* 107:8860-8865.
308. **Finka A**, Schaefer DG, Saidi Y, Goloubinoff Pierre, Zryd JP (2007) *In vivo* localisation of F Actin structures during the development of the moss *Physcomitrella patens*. *New Phytol.*
309. **Ma H**, Yanofsky MF, Meyerowitz EM (1990) Molecular cloning and characterization of GPA1, a G protein alpha subunit gene from Arabidopsis thaliana. *Proceedings of the National Academy of Sciences* 87:3821-3825.
310. **Ullah H**, Chen JG, Young JC, Im KH, Sussman MR, Jones AM (2001) Modulation of cell proliferation by heterotrimeric G protein in Arabidopsis. *Science* 292:2066-2069.
311. **Ullah H**, Chen JG, Wang S, Jones AM (2002) Role of a heterotrimeric G protein in regulation of Arabidopsis seed germination. *Plant Physiol* 129:897-907.
312. **Plakidou-Dymock, S**, Dymock, D, & Hooley, R (1998) A higher plant seven-transmembrane receptor that influences sensitivity to cytokinins. *Curr Biol.* 8(6):315-324.
313. **Josefsson LG**, Rask L (1997) Cloning of a Putative G-Protein-Coupled Receptor from Arabidopsis thaliana. *Eur. J. Biochem.* 249:415-420.
314. **Pandey S**, Assmann SM (2004) The Arabidopsis Putative G Protein-ûCoupled Receptor GCR1 Interacts with the G Protein α-Subunit GPA1 and Regulates Abscisic Acid Signaling. *The Plant Cell Online* 16:1616-1632.
315. **Pandey S**, Chen JG, Jones AM, Assmann SM (2006) G-Protein Complex Mutants Are Hypersensitive to Abscisic Acid Regulation of Germination and Postgermination Development. *Plant Physiol.* 141:243-256.

316. **Chen JG**, Pandey S, Huang J, Alonso JM, Ecker JR, Assmann SM, Jones AM (2004) GCR1 Can Act Independently of Heterotrimeric G-Protein in Response to Brassinosteroids and Gibberellins in Arabidopsis Seed Germination. *Plant Physiol.* 135:907-915.
317. **Warpeha KM**, Upadhyay S, Yeh J, Adamiak J, Hawkins SI, Lapik YR, Anderson MB, Kaufman LS (2007) The GCR1, GPA1, PRN1, NF-Y Signal Chain Mediates Both Blue Light and Abscisic Acid Responses in Arabidopsis. *Plant Physiol.* 143:1590-1600.
318. **Lapik YR**, Kaufman LS (2003) The Arabidopsis cupin domain protein AtPirin1 interacts with the G protein alpha-subunit GPA1 and regulates seed germination and early seedling development. *Plant Cell* 15:1578-1590.
319. **Bossen ME**, Kendrick RE, Vredenberg WJ (1990) The involvement of a G-protein in phytochrome-regulated Ca+ dependent swelling of etiolated wheat protoplasts. *Physiol. Plant.* 80:55-62.
320. **Romero LC**, Sommer D, Gotor C, Song PS (1991) G-proteins in etiolated Avena seedlings. Possible phytochrome regulation. *FEBS Lett.* 282:341-346.
321. **Wu Y**, Hiratsuka K, Neuhaus G, Chua N-H (1996) Calcium and cGMP target distinct phytochrome-responsive elements [published erratum appears in Plant J 1997 Apr;11(4):905]. *Plant J.* 10:1149-1154.
322. **Kaiserli E**, Sullivan S, Jones MA, Feeney KA, Christie JM (2009) Domain Swapping to Assess the Mechanistic Basis of Arabidopsis Phototropin 1 Receptor Kinase Activation and Endocytosis by Blue Light. *The Plant Cell Online* 21:3226-3244.
323. **Sullivan S**, Thomson CE, Kaiserli E, Christie JM (2009) Interaction specificity of Arabidopsis 14-3-3 proteins with phototropin receptor kinases. *FEBS Lett.* 583:2187-2193.
324. **Lin C** (2002) Blue light receptors and signal transduction. *Plant Cell* 14 Suppl:S207-S225.
325. **Tokutomi S**, Sugimoto T, Mimuro M (1992) A model for the molecular structure and orientation of the chromophore in a dimeric phytochrome molecule. *Photochem Photobiol* 56:545-552.
326. **Ekelund NGA**, Sundqvist C, Quail PH, Vierstra RD (1985) Chromophore rotation in 124-kdalton *Avena* phytochrome as measured by light-induced changes in linear dichroism. *Photochem Photobiol* 41:221-223.
327. **Harada A**, Shimazaki Ki (2007) Phototropins and Blue Light-dependent Calcium Signaling in Higher Plants. *Photochem. Photobiol.* 83:102-111.
328. **Ohmori M**, Terauchi K, Okamoto S, Watanabe M (2002) Regulation of cAMP-mediated Photosignaling by a Phytochrome in the Cyanobacterium Anabaena cylindrica. *Photochem. Photobiol.* 75:675-679.
329. **Gordillo FJ**, Segovia M, Lopez-Figueroa F (2004) Cyclic AMP levels in several macroalgae and their relation to light quantity and quality. *J Plant Physiol* 161:211-217.
330. **Ichikawa T**, Suzuki Y, Czaja I, Schommer C, LeBnick A, Schell J, Walden R (1997) Identification and role of adenylyl cyclase in auxin signalling in higher plants. *Nature* 390:698-701.
331. **Volotovski ID** (1998) Ca^{2+} and intracellular signalling in plant cells: a role in phytochrome transduction. *Membr. Cell Biol.* 12:721-742.
332. **Heck JN**, Mellman DL, Ling K, Sun Y, Wagoner MP, Schill NJ, Anderson RA (2007) A conspicuous connection: structure defines function for the phosphatidylinositol-phosphate kinase family. *Crit Rev Biochem. Mol Biol* 42:15-39.
333. **Mueller-Roeber B**, Pical C (2002) Inositol Phospholipid Metabolism in Arabidopsis. Characterized and Putative Isoforms of Inositol Phospholipid Kinase and Phosphoinositide-Specific Phospholipase C. *Plant Physiol.* 130:22-46.
334. **Saavedra L**, Balbi V, Dove SK, Hiwatashi Y, Mikami K, Sommarin M (2009) Characterization of Phosphatidylinositol Phosphate Kinases from the Moss Physcomitrella patens: PpPIPK1 and PpPIPK2. *Plant Cell Physiol.* 50:595-609.
335. **Saavedra L**, Balbi V, Lerche J, Mikami K, Heilmann I, Sommarin M (2011) PIPKs are essential for rhizoid elongation and caulonemal cell development in the moss Physcomitrella patens. *The Plant Journal* 67:635-647.
336. **Lariguet P**, Schepens I, Hodgson D, Pedmale UV, Trevisan M, Kami C, de Carbonnel M, Alonso JM, Ecker JR, Liscum E *et al.* (2006) PHYTOCHROME KINASE SUBSTRATE 1 is a phototropin 1 binding protein required for phototropism. *Proc. Natl. Acad. Sci. U. S. A* 103:10134-10139.
337. **Boccalandro HE**, De Simone SN, Bergmann-Honsberger A, Schepens I, Fankhauser C, Casal JJ (2008) PHYTOCHROME KINASE SUBSTRATE1 regulates root phototropism and gravitropism. *Plant Physiol* 146:108-115.
338. **Motchoulski A**, Liscum E (1999) Arabidopsis NPH3: A NPH1 photoreceptor-interacting protein essential for phototropism. *Science* 286:961-964.

9. List of figures

10. List of tables

11. Abbreviations

aa	Amino acids
ABA	Abscisic acid
AD	Gal4 DNA activation domain
ADE2	Phosphoribosylaminoimidazole carboxylase
Amp	Ampicillin
3-AT	3-Amino-1,2,4-triazole (suppressor of the HIS3-gene product imidazoleglycerol-phosphate dehydratase)
B	Blue Light (450 nm)
BD	Gal4 DNA binding domain
BF	Bight field (filter cube)
BiFC	Bimolecular fluorescence complementation
BLAST	Basic Local Alignment Tool
bp	Base pairs
BP	Band pass (filter cube)
BR	Brassinosteroid
BSA	Bovine serum albumin
BV	Biliverdin
ca	*circa*
CaMV	Cauliflower mosaic virus
CDPK	Ca-dependent protein kinase
CDS	Coding sequence
CFP	Cyan fluorescent protein
cfu	Colony forming units
cGMP	cyclic guanosine monophosphate
CRY	Cryptochrome
D	Dark
d	Day
DAG	Diacylglycerol
DDO	Double dropout medium (-Trp/-Leu)
DIC	Differential interference contrast (filter cube)
DNA	Deoxyribonucleic acid
EDTA	Ethylenediaminetetraacetic acid
EF1α	*Elongation factor 1 α*
e.g.	*exempli gratia*
etc.	*et cetera*
E-Vector	Electric vector of light
fhl	FHY1-*like* mutant
fhy1	Far-red elongated hypocotyl mutant
fig.	Figure
FL	Full length
FMN	Flavin mononucleotide
FP	Fluorescence protein
FR	Far-red light (730 nm)
f/w	forward (primer)
g	Gravity (gravitational acceleration)
g	gram
GA	Gibberellic acid (phytohormone)
GAF	cGMP-specific phosphodiesterase from vertebrates / cyanobacterial adenylate cyclase / transcription factor Fhl-A domain

GFP	Green fluorescent protein
GW	GATEWAY technology (Invitrogen)
h	Hours
HA	Hemagglutinin epitope
HIR	High irradiance response
HKRD	Histidine kinase related domain
HRM	High range marker
Hyg	Hygromycin
IAA	Isoamyl alcohol
i.e.	*id est*
IP3	Inositol-3-phosphate
JA	Jasmonic acid (phytohormone)
Kan	Kanamycin
kD	Kilo Dalton
λ	Wavelength
λ_{max}	Wavelength of maximal absorbance
LB	Lysogeny broth medium
LD	Long day (16 h W / 8 h D)
LFR	Low fluence response
mCherry	Derivative of a red fluorescent protein. Used here referring to the VirD2:NLS:mCherry construct
MEL1	α-Galactosidase
µg	Microgram
mg	Milligram
min	Minutes
NES	Nuclear export signal
NLS	Nuclear import signal
OD	Optical density
o.n.	Over night
ORF	Open Reading Frame
PAS	Period clock/ ARNT/ single-minded domain
PCB	Phycocyanobilin
PCR	Polymerase chain reaction
PEG	Polyethylene glycol
Pfr	Phytochrome in its far-red light absorbing state
PHY	Phytochrome specific domain
phy4	*Physcomitrella patens* holophytochrome 4
phyA	*Arabidopsis thaliana* holophytochrome A
phyB	*Arabidopsis thaliana* holophytochrome B
PIG	Particle inflow gun
PLP	Phosphate-loop containing protein (p-loop is also known as *walker motif*)
Pp	*Physcomitrella patens*
Pr	Phytochrome in its red light absorbing state
PRL1	Pleiotropic Regulator 1
PSM	Prestained marker
P_{tot}	Total amount of phytochrome per cell
PΦB	Phytochromobilin
QDO	Quadruple dropout Medium (-Trp/-Leu/-His/-Ade)
R	Red light (660 nm)
R_{pol}	Polarised red light (660 nm)
RT	Room temperature (21 °C)
r/v	reverse (primer)

S	Selection medium
SAP	Sequestered areas of phytochrome
SD	Short day (8 h W / 16 h D)
SDS	Sodium Dodecyl Sulfate
Ser/Thr	Serine/Threonine
STE	Salt TE buffer
sYFP	Split YFP (bimolecular fluorescence complementation system)
T_{an}	Annealing temperature
TB	Terrific broth medium
TBE	Tris Borat EDTA buffer
TDO	Triple dropout medium (-Trp/-Leu/-His)
TE	Tris EDTA buffer
TRIS	Tris(hydroxymethyl)-aminomethane
UTR	Untranslated region
VLFR	Very low fluence response
Vol	Volume
v/v	Volume per volume
W	White light
W_{pol}	Polarised white light
WT	Wild type (if not stated otherwise, *Physcomitrella patens* wild type selected by David Cove in Gransden, Huntingdonshire, Cambridge, UK, was used)
w/	With
w/o	Without
w/v	Weight per volume
XαGal	5-Bromo-4-chloro-3-indoxyl-α-D-galactopyranoside
Y2H	Yeast two hybrid system
Y3H	Yeast three hybrid system
YFP	Yellow fluorescent protein

12. Appendix

12.1. *In silico* analysis of *PHY4* sequences

12.1.1. *PHY4* cDNAs

```
Pp.PHY4(2004)       ATGTCGACCACCAAGTTGGCATACTCGTCAGGGAGTTCTGTGAAGTCGAAGCATAGTGTA 60
Pp.PHY4(2007)       ATGTCGACCACCAAGTTGGCATACTCGTCAGGGAGTTCTGTGAAGTCGAAGCATAGTGTA 60

Pp.PHY4(2004)       CGGGTTGCGCAAACTACAGCAGATGCCAAGCTGCAGGCAGTGTATGAAGAATCCGGAGAT 120
Pp.PHY4(2007)       CGGGTTGCGCAAACTACAGCAGATGCCAAGCTGCAGGCAGTGTATGAAGAATCCGGAGAT 120

Pp.PHY4(2004)       TCGGGAGACTCATTTGATTATTCCAAATCAGTTCATGCGTCCAAATCCACTGGCGAGAAT 180
Pp.PHY4(2007)       TCGGGAGACTCATTTGATTATTCCAAATCAGTTCATGCGTCCAAATCCACTGGCGAGAAT 180

Pp.PHY4(2004)       GTCCCTGCCCTAGCAGTCACCGCGTACCTTCAGCGCATGCAAAGAGGGGGTTTGGTGCAG 240
Pp.PHY4(2007)       GTCCCTGCCCTAGCAGTCACCGCGTACCTTCAGCGCATGCAAAGAGGGGGTTTGGTGCAG 240

Pp.PHY4(2004)       ACATTCGGGTGTATGCTATGTGTGGACGAGAGTAGTTTTAGGGTTATTGCTTACAGCGAG 300
Pp.PHY4(2007)       ACATTCGGGTGTATGCTATGTGTGGACGAGAGTAGTTTTAGGGTTATTGCTTACAGCGAG 300

Pp.PHY4(2004)       AATGCGCCAGAGATGCTTGACCTGATGCCACAAGCGGTGCCCAGTGTGGGTCAGCAGGAA 360
Pp.PHY4(2007)       AATGCGCCAGAGATGCTTGACCTGATGCCACAAGCGGTGCCCAGTGTGGGTCAGCAGGAA 360

Pp.PHY4(2004)       GTTCTGGGCATTGGAACCGATGCAAGAACTTTGTTCACCCCTTCCAGTGCGGCCGCCCTG 420
Pp.PHY4(2007)       GTTCTGGGCATTGGAACCGATGCAAGAACTTTGTTCACCCCTTCCAGTGCGGCCGCCCTG 420

Pp.PHY4(2004)       GAGAAATGTGCCGGAGCGGTGGATGTGACCATGCTGAACCCTATCTCAGTGCACTGTCGA 480
Pp.PHY4(2007)       GAGAAATGTGCCGGAGCGGTGGATGTGACCATGCTGAACCCTATCTCAGTGCACTGTCGA 480

Pp.PHY4(2004)       AGCTCGGGGAAGCCGTTCTATGCGATTCTGCACCGTATTGACGTAGGACTGGTAATTGAT 540
Pp.PHY4(2007)       AGCTCGGGGAAGCCGTTCTATGCGATTCTGCACCGTATTGACGTAGGACTGGTAATTGAT 540

Pp.PHY4(2004)       TTTGAACCAGTGCGCCCGAATGATGCCGTTGTGTCCTCCGCAGGGGCTTTGCAGTCGCAT 600
Pp.PHY4(2007)       TTTGAACCAGTGCGCCCGAATGATGCCGTTGTGTCCTCCGCAGGGGCTTTGCAGTCGCAT 600

Pp.PHY4(2004)       AAGTTGGCTGCAAAAGCGATATCTCGGCTGCAGGCACTTCCTGGCGGAGACATTGGCCTC 660
Pp.PHY4(2007)       AAGTTGGCTGCAAAAGCGATATCTCGGCTGCAGGCACTTCCTGGCGGAGACATTGGCCTC 660

Pp.PHY4(2004)       CTTTGTGATACAGTTGTAGAAGAGGTACGCCAGCTTTCCGGTTACGATCGTGTCATGGCA 720
Pp.PHY4(2007)       CTTTGTGATACAGTTGTAGAAGAGGTACGCCAGCTTTCCGGTTACGATCGTGTCATGGCA 720

Pp.PHY4(2004)       TACAAATTCCACGAAGACGAACATGGTGAGGTCTTGGCGGAGATTCGAAGATCAGATTTA 780
Pp.PHY4(2007)       TACAAATTCCACGAAGACGAACATGGTGAGGTCTTGGCGGAGATTCGAAGATCAGATTTA 780

Pp.PHY4(2004)       GAACCTTACTTAGGTCTACATTACCCAGCAACAGATATCCCACAGGCGTCAAGATTCCTG 840
Pp.PHY4(2007)       GAACCTTACTTAGGTCTACATTACCCAGCAACAGATATCCCACAGGCGTCAAGATTCCTG 840

Pp.PHY4(2004)       TTTATGAAGAACAGGGTGCGAATGATAGGTGATTGCTATGCTCCTCCTGTTAAAGTGGTT 900
Pp.PHY4(2007)       TTTATGAAGAACAGGGTGCGAATGATAGGTGATTGCTATGCTCCTCCTGTTAAAGTGGTT 900

Pp.PHY4(2004)       CAGGACAAGGATTTGAGGCAGCCTATTAGTCTGGCCGGGTCTACTTTACGGGCCCCTCAT 960
Pp.PHY4(2007)       CAGGACAAGGATTTGAGGCAGCCTATTAGTCTGGCCGGGTCTACTTTACGGGCCCCTCAT 960

Pp.PHY4(2004)       GGCTGCCATGCGCAATACATGGGCAACATGAACTCCATCGCTTCGTTGGTGATGGCAGTT 1020
Pp.PHY4(2007)       GGCTGCCATGCGCAATACATGGGCAACATGAACTCCATCGCTTCGTTGGTGATGGCAGTT 1020

Pp.PHY4(2004)       ATCGTGAATGATCCGGATGAGGATCCTAATTCACGTGGGGGCCAGCAGAGAGGGCGCAAG 1080
Pp.PHY4(2007)       ATCGTGAATGATCCGGATGAGGATCCTAATTCACGTGGGGGCCAGCAGAGAGGGCGCAAG 1080

Pp.PHY4(2004)       CTCTGGGGATTGGTGGTTTGTCACCACACGTCTCCGAGGACCGTCTCCTTTCCTTTGAGA 1140
Pp.PHY4(2007)       CTCTGGGGATTGGTGGTTTGTCACCACACGTCTCCGAGGACCGTCTCCTTTCCTTTGAGA 1140

Pp.PHY4(2004)       TCGGCCTGTGAGTTCCTGATGCTGGTGTTCGGTCTGCAGCTGAACATGGAAGTTGAACTT 1200
Pp.PHY4(2007)       TCGGCCTGTGAGTTCCTGATGCAGGTGTTCGGTCTGCAGCTGAACATGGAAGTTGAACTT 1200

Pp.PHY4(2004)       GCAGCTCAGCTAAGAGAAAAACATATTTTGAGAACACAAACCCTTCTCTGTGACATGTTA 1260
Pp.PHY4(2007)       GCAGCTCAGCTAAGAGAAAAACATATTTTGAGAACACAAACCCTTCTCTGTGACATGTTA 1260

Pp.PHY4(2004)       TTGCGGGATGCACCCATCGGAATTGTTTCTCAGTCACCCAATATCATGGACTTGGTTAAA 1320
Pp.PHY4(2007)       TTGCGGGATGCACCCATCGGAATTGTTTCTCAGTCACCCAATATCATGGACTTGGTTAAA 1320

Pp.PHY4(2004)       TGCGACGGTGCAGCACTTTACTATGGGAAAAGGTTTTGGCTTTTGGGAATCACACCTAAC 1380
Pp.PHY4(2007)       TGCGACGGTGCAGCACTTTACTATGGGAAAAGGTTTTGGCTTTTGGGAATCACACCTAAC 1380
```

```
Pp.PHY4(2004)    GAGGTCCAGATTAAGGAAATCGCGGACTGGTTCCTAGAACATCATCAAGATTCGACCGGT 1440
Pp.PHY4(2007)    GAGGTCCAGATTAAGGAAATCGCGGACTGGCTCCTAGAACATCATCAAGATTCGACCGGT 1440

Pp.PHY4(2004)    TTGAGTACAGACAGCCTGGCCGATGCTGGTTACCCTGGCGCAGCGCAACTTGGTGATGCT 1500
Pp.PHY4(2007)    TTGAGTACAGACAGCCTGGCCGATGCTGGTTACCCTGGCGCAGCGCAACTTGGTGATGCT 1500

Pp.PHY4(2004)    GTGTGTGGAATGGCTGCGGCAAAGATCACTCCAAGGGACTTTCTTTTCTGGTTCAGGTCA 1560
Pp.PHY4(2007)    GTGTGTGGAATGGCTGCGGCAAAGATCACTCCAAGGGACTTTCTTTTCTGGTTCAGGTCA 1560

Pp.PHY4(2004)    CACACCGCCAAGGAGATTAAGTGGGGTGGTGCCAAGCACGATCCTGATGAAAAGGATGAT 1620
Pp.PHY4(2007)    CACACCGCCAAGGAGATTAAGTGGGGTGGTGCCAAGCACGATCCTGATGAAAAGGATGAT 1620

Pp.PHY4(2004)    GGGAGGAAAATGCATCCCCGCTCCTCGTTCAAGGCCTTTCTAGAAGTTGTGAAGAGAAGA 1680
Pp.PHY4(2007)    GGGAGGAAAATGCATCCCCGCTCCTCGTTCAAGGCCTTTCTAGAAGTTGTGAAGAGAAGA 1680

Pp.PHY4(2004)    AGTTTGCCATGGGAGGACATAGAAATGGACGCAATTCATTCTCTTCAACTCATTTCGAGA 1740
Pp.PHY4(2007)    AGTTTGCCATGGGAGGACATAGAAATGGACGCAATTCATTCTCTTCAACTCATTTTGAGA 1740

Pp.PHY4(2004)    GGTTCATTCCAGGATATAGACGACAGTGATACCAAAACTATGATACACGCCCGACTCAAC 1800
Pp.PHY4(2007)    GGTTCATTCCAGGATATAGACGACAGTGATACCAAAACTATGATACACGCCCGACTCAAC 1800

Pp.PHY4(2004)    GACTTAAAGCTCCAGGGCATGGATGAACTCAGTACAGTTGCTAATGAAATGGTTAGATTG 1860
Pp.PHY4(2007)    GACTTAAAGCTCCAGGGCATGGATGAACTCAGTACAGTTGCTAATGAAATGGTTAGATTG 1860

Pp.PHY4(2004)    ATAGAGACAGCGACTGCACCAATTCTCGCTGTCGATTCGAGTGGATTCATCAATGGTTGG 1920
Pp.PHY4(2007)    ATAGAGACAGCGACTGCACCAATTCTCGCTGTCGATTCGAGTGGATTCATCAATGGTTGG 1920

Pp.PHY4(2004)    AATGCCAAAGTAGCTGAACTGACTGGACTTCCAGTTGGAGAAGCCATGGGTCGGTCGCTG 1980
Pp.PHY4(2007)    AATGCCAAAGTAGCTGAACTGACTGGACTTCCAGTTGGAGAAGCCATGGGTCGGTCGCTG 1980

Pp.PHY4(2004)    GTTAAAGATTTAATTTTAGAGGAATCAATTGATGTTGTTCAGCGACTTCTCTACCTTGCA 2040
Pp.PHY4(2007)    GTTAAAGATTTAATTTTAGAGGAATCAATTGATGTTGTTCAGCGACTTCTCTACCTTGCA 2040

Pp.PHY4(2004)    TTACAAGGTGAAGAAGAACAAAATATTGAGATTCAGTTGAAGACCTTTGGGCCACAAAAA 2100
Pp.PHY4(2007)    TTACAAGGTGAAGAAGAACAAAATATTGAGATTCAGTTGAAGACCTTTGGGCCACAAAAA 2100

Pp.PHY4(2004)    GAGAAGGGCGCAGTGATTTTGATAGTGAATGCGTGCTCCAGCAGGGATGTACAAGACAAT 2160
Pp.PHY4(2007)    GAGAAGGGCGCAGTGATTTTGATAGTGAATGCGTGCTCCAGCAGGGATGTACAAGACAAT 2160

Pp.PHY4(2004)    GTCGTTGGAGTTTGTTTTGTGGGGCAAGATGTGACAGGTCAAAAACAAGTTTTGGATAAA 2220
Pp.PHY4(2007)    GTCGTTGGAGTTTGTTTTGTGGGGCAAGATGTGACAGGTCAAAAACAAGTTTTGGATAAA 2220

Pp.PHY4(2004)    TTTACTCGGATACAAGGCGACTACAAAGCAATAGTTCAGAACCCAAACCCTTTGATTCCT 2280
Pp.PHY4(2007)    TTTACTCGGATACAAGGCGACTACAAAGCAATAGTTCAGAACCCAAACCCTTTGATTCCT 2280

Pp.PHY4(2004)    CCTATATTTGGCACTGATGAATATGGATATTGCTCTGAGTGGAATCCTTCAATGGAGAAG 2340
Pp.PHY4(2007)    CCTATATTTGGCACTGATGAATATGGATATTGCTCTGAGTGGAATCCTTCAATGGAGAAG 2340

Pp.PHY4(2004)    CTGACTGGATGGAAGAGAGAAGAGGTGCTTGGGAAACTGCTAGTGGGTGAAATTTTTGGA 2400
Pp.PHY4(2007)    CTGACTGGATGGAAGAGAGAAGAGGTGCTTGGGAAACTGCTAGTGGGTGAAATTTTTGGA 2400

Pp.PHY4(2004)    ATGCAACTTATGTGTTGCCGACTGAAAGGTCAAGATGCAATGACGAAATTTATGATTGCA 2460
Pp.PHY4(2007)    ATGCAACTTATGTGTTGCCGACTGAAAGGTCAAGATGCAATGACGAAATTTATGATTGCA 2460

Pp.PHY4(2004)    TTAAATAGTGCAATGGATGGTCAAGATACAGATCGGTTTCCCTTTTCCTTCTTTGATCGA 2520
Pp.PHY4(2007)    TTAAATAGTGCAATGGATGGTCAAGATACAGATCGGTTTCCCTTTTCCTTCTTTGATCGA 2520

Pp.PHY4(2004)    CAAGGGAAATACGTAGATGCCCTACTCACAGTCAATAAAAGAACGGATGCAGAGGGAAGC 2580
Pp.PHY4(2007)    CAAGGGAAATACGTAGATGCCCTACTCACAGTCAATAAAAGAACGGATGCAGAGGGAAGC 2580

Pp.PHY4(2004)    ATCACTGGCGTATTCTGCTTTTTGCACACAACCAGTGTGGAATTATTGCAAGCATTGACT 2640
Pp.PHY4(2007)    ATCACTGGCGTATTCTGCTTTTTGCACACAACCAGTGTGGAATTATTGCAAGCATTGACT 2640

Pp.PHY4(2004)    GTCCAACGTGCGACGGAGAAAGTAGCCTTCGCAAAACTCAAGGAGTTGGCTTACATTCGA 2700
Pp.PHY4(2007)    GTCCAACGTGCGACGGAGAAAGTAGCCTTCGCAAAACTCAAGGAGTTGGCTTACATTCGA 2700

Pp.PHY4(2004)    CAGGAGATCAAGAATCCTTTGTATGGGATTATGTTTACACGTAATTTAATGGAAGATACG 2760
Pp.PHY4(2007)    CAGGAGATCAAGAATCCTTTGTATGGGATTATGTTTACACGTAATTTAATGGAAGATACG 2760
```

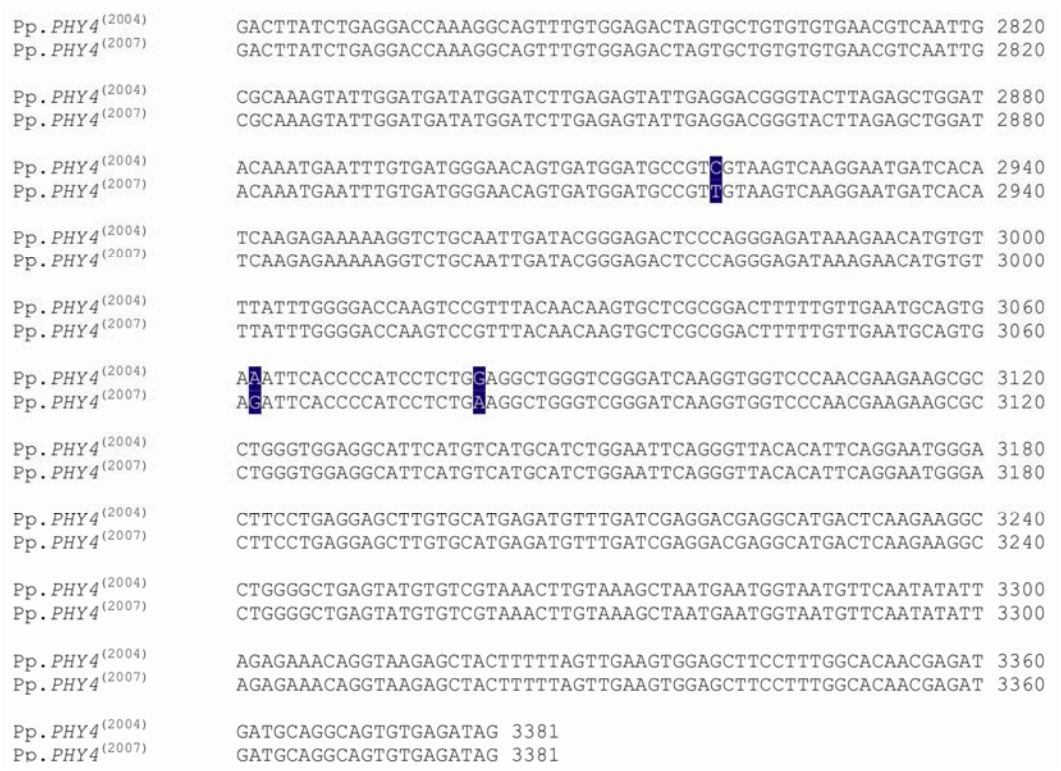

Suppl. Fig. 1 Alignment of *PHY4* cDNAs cloned by Mittmann *et al.* (2004) and after genome sequencing (2007). CLUSTALW2-alignment. Point mutations are marked in purple.

12.1.2. Alignment of phytochrome sequences from higher and lower plants

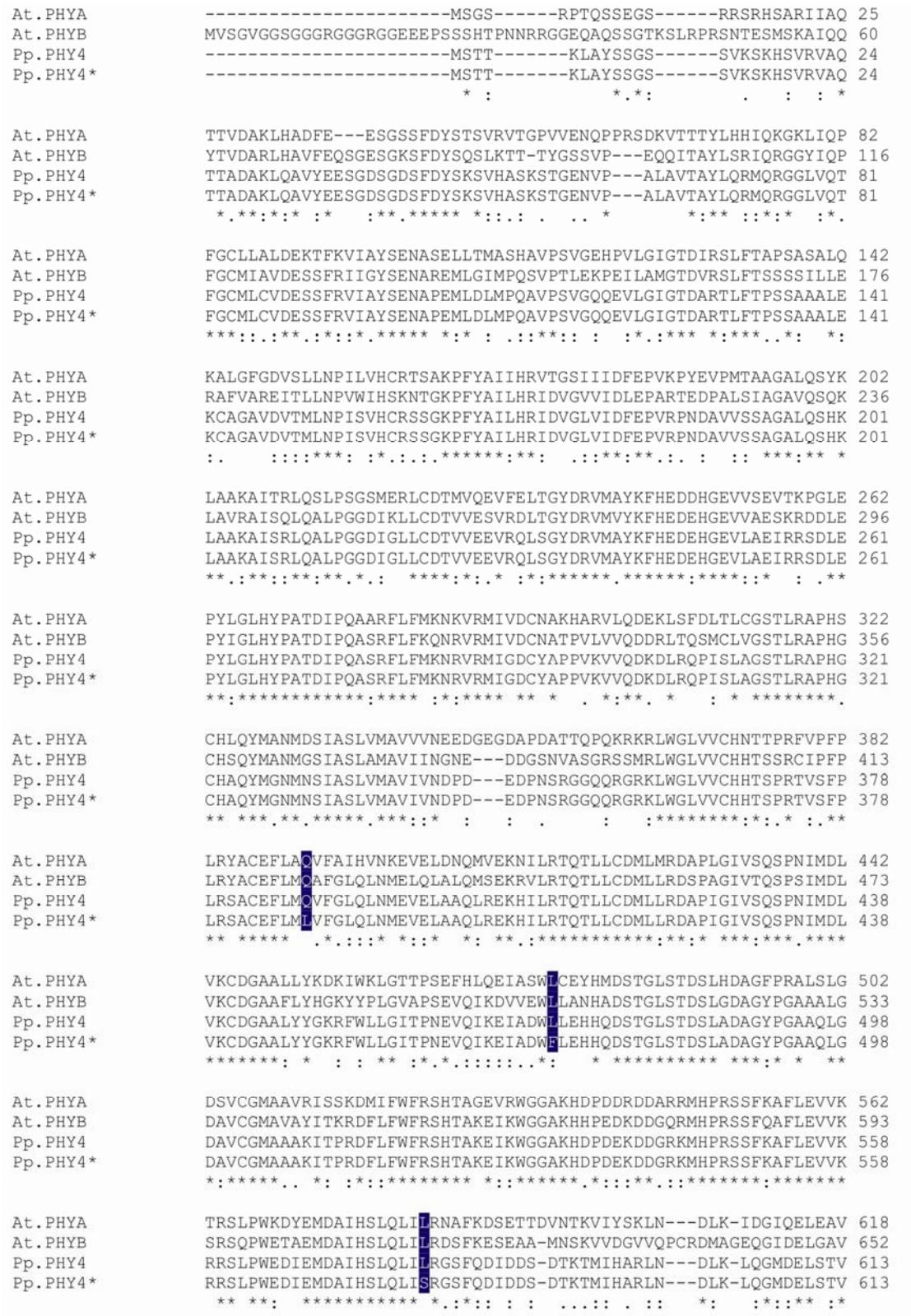

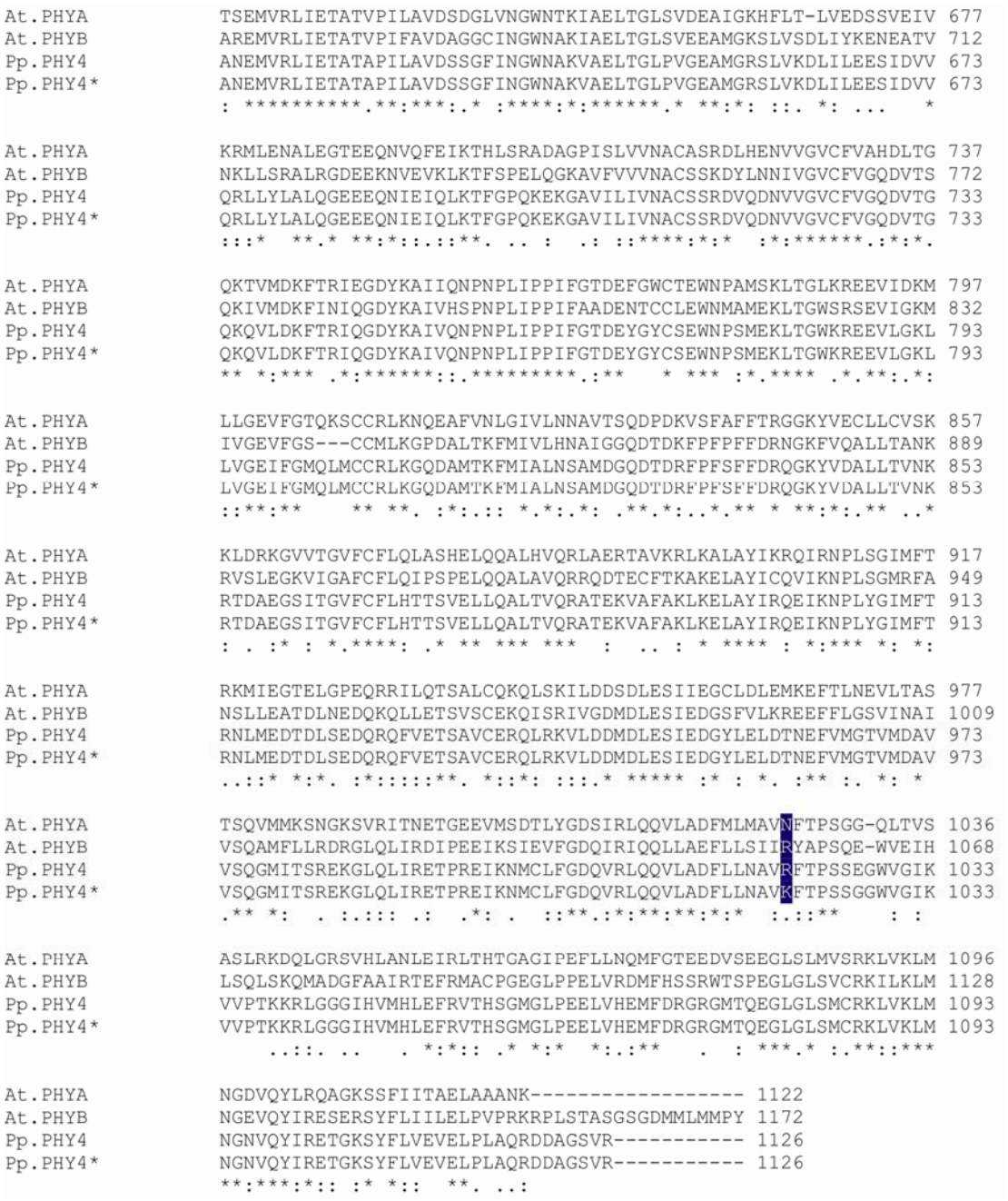

Suppl. Fig. 2 Alignment of *Arabidopsis* PHYA and PHYB with *Physcomitrella* PHY4 and PHY4^{2004} protein sequences. CLUSTALW2-alignment. PHY4^{2004} is designated Pp.PHY4*. Point mutations in conserved residues are marked in purple.

12.2. Y2H

12.2.1. Establishment of internal system controls

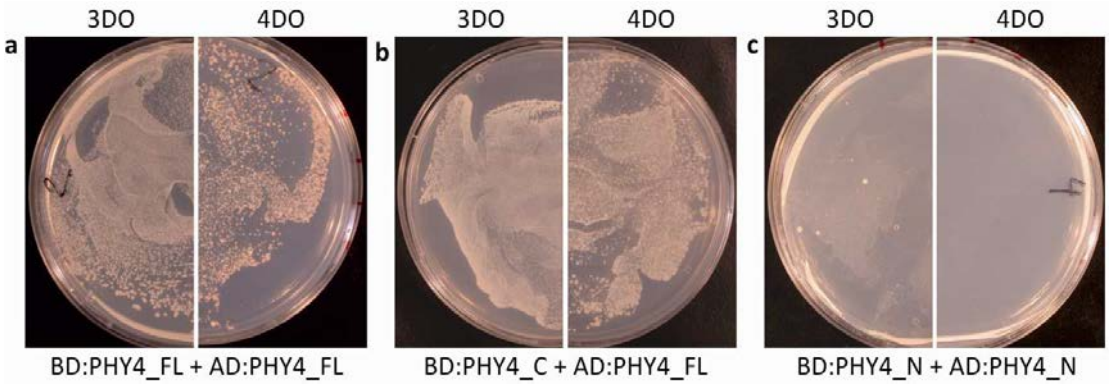

Suppl. Fig. 3 Dimerisation of BD:PHY4 and AD:PHY4 fusions in yeast strain AH109. Quantitative approach, nutritional selection as indicated (3DO: -Trp/-Leu/-His, 4DO: -Trp/-Leu/-His/-Ade).

12.3. *In silico* analysis of putative PHY4 interactors identified by Y2H screening

12.3.1. #16.1, p-loop containing nucleoside triphophaste hydrolase (PLP)

Suppl. Table 1 Homologs of Pp.PLP used for alignment and phylogenetic analysis (in light yellow).

Accession no	Description	Organism
NP_190631	nodulation-related protein [Arabidopsis thaliana]	Arabidopsis thaliana
NP_179175	nodulation protein-like protein [Arabidopsis thaliana]	Arabidopsis thaliana
NP_195168	P-loop containing nucleoside triphosphate hydrolase family protein-like protein	Arabidopsis thaliana
BAJ96976	predicted protein [Hordeum vulgare subsp. vulgare]	Hordeum vulgare
EEE59097	hypothetical protein OsJ_10950 [Oryza sativa Japonica Group]	Oryza sativa
NP_001050289	Os03g0394900 [Oryza sativa Japonica Group]	Oryza sativa
EAY76082	hypothetical protein OsI_04009 [Oryza sativa Indica Group]	Oryza sativa
EAZ13778	hypothetical protein OsJ_03703 [Oryza sativa Japonica Group]	Oryza sativa
NP_001173434	Os03g0363950 [Oryza sativa Japonica Group]	Oryza sativa
ABF96111	nodulation protein, putative, expressed [Oryza sativa Japonica Group]	Oryza sativa
NP_001060447	Os07g0644200 [Oryza sativa Japonica Group]	Oryza sativa
AAP04177	unknown protein [Oryza sativa Japonica Group]	Oryza sativa
XP_001781728	predicted protein [Physcomitrella patens subsp. patens]	Physcomitrella patens
XP_001762870	predicted protein [Physcomitrella patens subsp. patens]	Physcomitrella patens
XP_002510263	conserved hypothetical protein [Ricinus communis]	Ricinus communis
XP_002525546	conserved hypothetical protein [Ricinus communis]	Ricinus communis
XP_002518797	conserved hypothetical protein [Ricinus communis]	Ricinus communis
XP_002981588	hypothetical protein SELMODRAFT_114849 [Selaginella moellendorffii]	Selaginella moellendorffii
XP_002963204	hypothetical protein SELMODRAFT_80417 [Selaginella moellendorffii]	Selaginella moellendorffii
XP_002445915	hypothetical protein SORBIDRAFT_07g027970 [Sorghum bicolor]	Sorghum bicolor
XP_002461118	hypothetical protein SORBIDRAFT_02g041100 [Sorghum bicolor]	Sorghum bicolor
XP_002465172	hypothetical protein SORBIDRAFT_01g033350 [Sorghum bicolor]	Sorghum bicolor
XP_002281772	PREDICTED: hypothetical protein [Vitis vinifera]	Vitis vinifera
XP_002284367	PREDICTED: hypothetical protein [Vitis vinifera]	Vitis vinifera
CAN66236	hypothetical protein VITISV_022815 [Vitis vinifera]	Vitis vinifera
XP_002285039	PREDICTED: hypothetical protein [Vitis vinifera]	Vitis vinifera
CAN68800	hypothetical protein VITISV_008807 [Vitis vinifera]	Vitis vinifera
XP_002265782	PREDICTED: hypothetical protein [Vitis vinifera]	Vitis vinifera
ACF85229	unknown [Zea mays]	Zea mays
NP_001144194	uncharacterized protein LOC100277054 [Zea mays]	Zea mays
NP_001131369	hypothetical protein LOC100192694 [Zea mays]	Zea mays
ACN25401	unknown [Zea mays]	Zea mays
ACF82278	unknown [Zea mays]	Zea mays
NP_001142398	hypothetical protein LOC100274572 [Zea mays]	Zea mays
NP_001145331	uncharacterized protein LOC100278656 [Zea mays]	Zea mays
NP_001167842	uncharacterized protein LOC100381543 [Zea mays]	Zea mays
NP_001142620	uncharacterized protein LOC100274889 [Zea mays]	Zea mays

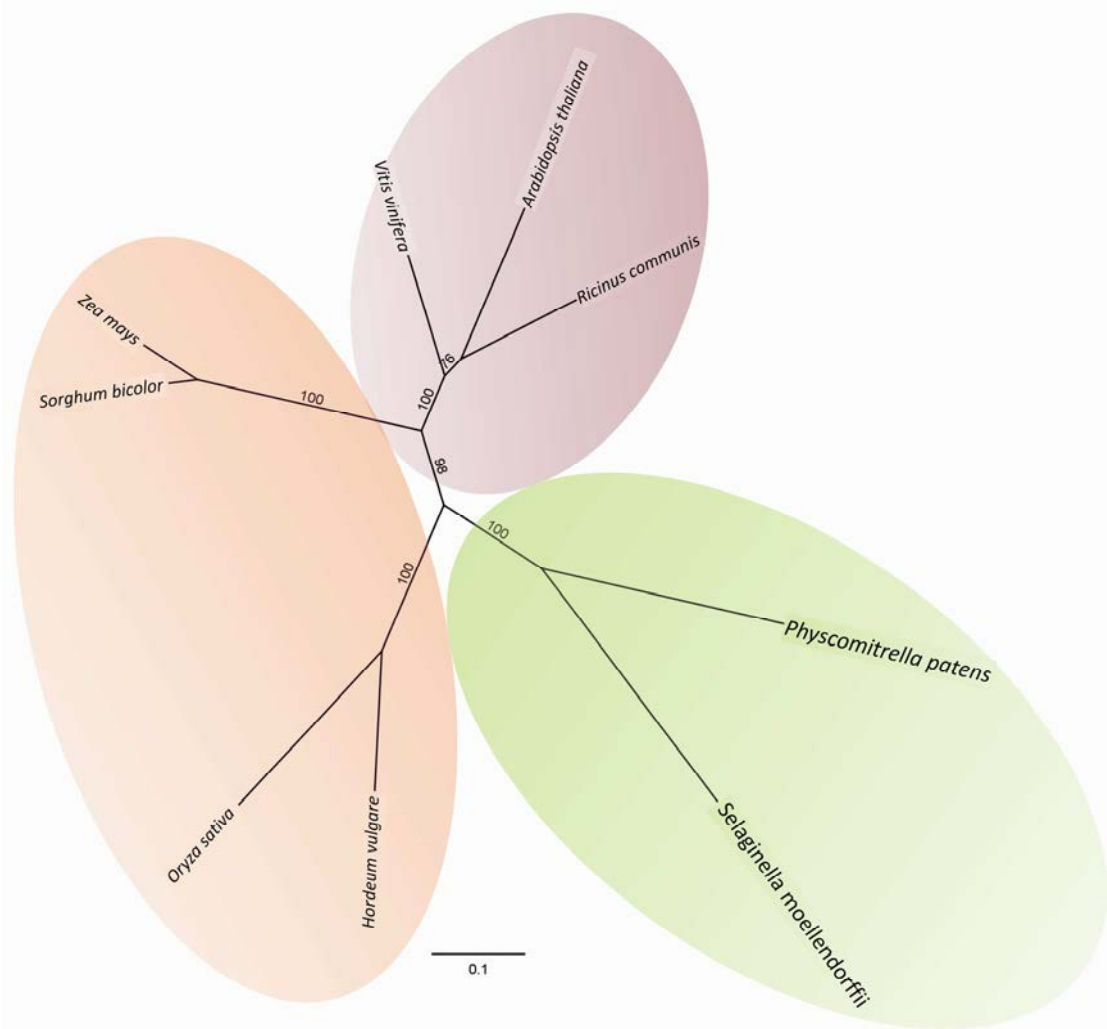

Suppl. Fig. 4: Phylogenetic tree of PLP homologs in different plant species.
PLP homologs are conserved throughout the plant kingdom, from lower plants (in light green) to higher plants (monocots in light red, dicots in purple). Homologs were identified by protein BLAST. Distances and groupings were determined by Jukes-Cantor and Neighbour-Joining method and correspond to 500 replications. Bootstrap values are given at the branches. Scale bar represents protein distance as substitutions per site. Accession numbers together with a table of further information are given in the appendix.

12.3.2. #33.7, pleiotropic regulator locus (PRL)

Suppl. Table 2 Homologs of Pp.PRL used for alignment and phylogenetic analysis (in light yellow).

Accession no	Description	Organism
NP_193325	protein pleiotropic regulatory locus 1 [Arabidopsis thaliana]	Arabidopsis thaliana PRL1
NP_566557	protein pleiotropic regulator PRL2 [Arabidopsis thaliana]	Arabidopsis thaliana PRL2
XP_001698474	predicted protein, partial [Chlamydomonas reinhardtii]	Chlamydomonas reinhardtii
NP_001050058	Os03g0339100 [Oryza sativa Japonica Group]	Oryza sativa
XP_001784373	predicted protein [Physcomitrella patens subsp. patens]	Physcomitrella patens
ABK22482	unknown [Picea sitchensis]	Picea sitchensis
XP_002315516	predicted protein [Populus trichocarpa]	Populus trichocarpa
XP_002516938	PP1/PP2A phosphatases pleiotropic regulator PRL1, putative [Ricinus communis]	Ricinus communis
XP_002981714	hypothetical protein SELMODRAFT_115108, partial [Selaginella moellendorffii]	Selaginella moellendorffii
XP_002262991	PREDICTED: hypothetical protein [Vitis vinifera]	Vitis vinifera
NP_001149303	LOC100282926 [Zea mays]	Zea mays

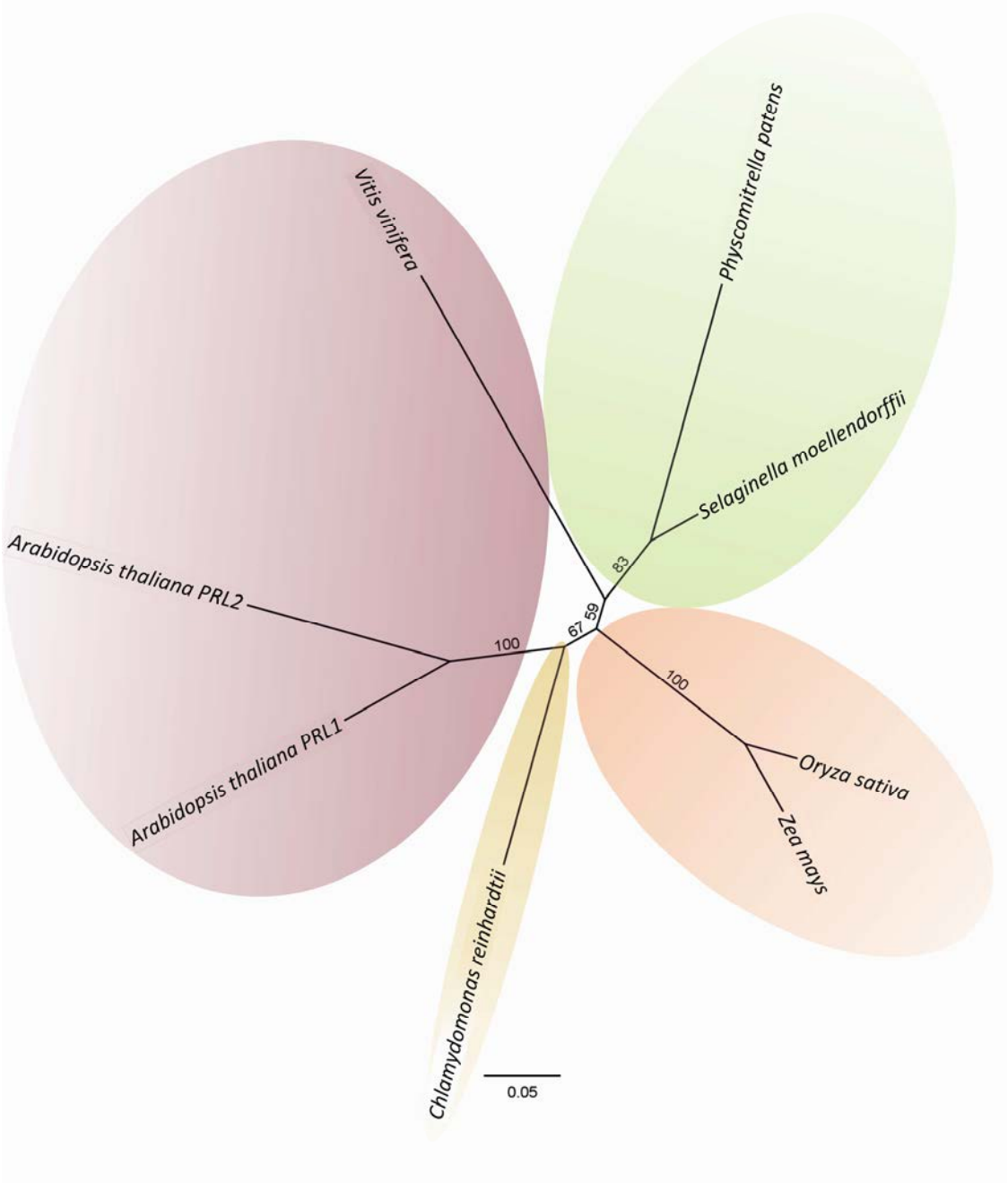

Suppl. Fig. 5: Phylogenetic tree of PRL1 homologs in different plant species.
PRL1 homologs are conserved throughout the plant kingdom, from algae (brown) to lower (in light green) and higher plants (monocots in light red, dicots in purple). Homologs were identified by protein BLAST. Distances and groupings were determined by Jukes-Cantor and Neighbour-Joining method and correspond to 500 replications. Bootstrap values are given at the branches. Scale bar represents protein distance as substitutions per site. Accession numbers together with a table of further information are given in the appendix.

12.3.3. #54.1, elongation factor 1 α (EF1α)

Suppl. Table 3 Homologs of Pp.EF1α used for alignment and phylogenetic analysis (in light yellow).

Accesssion no	Description	Organism
NP_200847	Elongation factor 1-alpha [Arabidopsis thaliana]	Arabidopsis thaliana
NP_563800	Elongation factor 1-alpha [Arabidopsis thaliana]	Arabidopsis thaliana
NP_563799	Elongation factor 1-alpha [Arabidopsis thaliana]	Arabidopsis thaliana
NP_563801	Elongation factor 1-alpha [Arabidopsis thaliana]	Arabidopsis thaliana
ACS68200	elongation factor 1 alpha [Brassica napus]	Brassica napus
ACS68201	elongation factor 1 alpha [Brassica napus]	Brassica napus
XP_001696568	eukaryotic translation elongation factor 1 alpha 1 [Chlamydomonas reinhardtii]	Chlamydomonas reinhardtii
XP_001702347	eukaryotic translation elongation factor 1 alpha 2 [Chlamydomonas reinhardtii]	Chlamydomonas reinhardtii
ACI42861	elongation factor-1A [Glycine max]	Glycine max
EF1A_SOYBN	RecName: Full=Elongation factor 1-alpha; Short=EF-1-alpha	Glycine max
EF1A2_HORVU	RecName: Full=Elongation factor 1-alpha; Short=EF-1-alpha	Hordeum vulgare
EF1A1_HORVU	RecName: Full=Elongation factor 1-alpha; Short=EF-1-alpha	Hordeum vulgare
BAA09709	elongation factor-1 alpha [Nicotiana tabacum]	Nicotiana tabacum
BAA23658	EF-1 alpha [Oryza sativa]	Oryza sativa
NP_001049145	Os03g0177400 [Oryza sativa Japonica Group]	Oryza sativa
XP_001753059	predicted protein [Physcomitrella patens subsp. patens]	Physcomitrella patens
XP_001753181	predicted protein [Physcomitrella patens subsp. patens]	Physcomitrella patens
XP_001753167	predicted protein [Physcomitrella patens subsp. patens]	Physcomitrella patens
XP_001766482	predicted protein [Physcomitrella patens subsp. patens]	Physcomitrella patens
XP_001763194	predicted protein [Physcomitrella patens subsp. patens]	Physcomitrella patens
XP_001763201	predicted protein [Physcomitrella patens subsp. patens]	Physcomitrella patens
ABK25072	unknown [Picea sitchensis]	Picea sitchensis
ABK24265	unknown [Picea sitchensis]	Picea sitchensis
ACN41180	unknown [Picea sitchensis]	Picea sitchensis
ABK24843	unknown [Picea sitchensis]	Picea sitchensis
ACN40740	unknown [Picea sitchensis]	Picea sitchensis
ACN40081	unknown [Picea sitchensis]	Picea sitchensis
XP_002518073	elongation factor 1-alpha, putative [Ricinus communis]	Ricinus communis
XP_002528028	elongation factor 1-alpha, putative [Ricinus communis]	Ricinus communis
XP_002968419	hypothetical protein SELMODRAFT_270693 [Selaginella moellendorffii]	Selaginella moellendorffii
XP_002970583	hypothetical protein SELMODRAFT_171512 [Selaginella moellendorffii]	Selaginella moellendorffii
XP_002968422	hypothetical protein SELMODRAFT_169717 [Selaginella moellendorffii]	Selaginella moellendorffii
XP_002970579	hypothetical protein SELMODRAFT_270852 [Selaginella moellendorffii]	Selaginella moellendorffii
XP_002460859	hypothetical protein SORBIDRAFT_02g036420 [Sorghum bicolor]	Sorghum bicolor
XP_002277159	PREDICTED: hypothetical protein [Vitis vinifera]	Vitis vinifera
XP_002284964	PREDICTED: hypothetical protein [Vitis vinifera]	Vitis vinifera
XP_002279598	PREDICTED: hypothetical protein [Vitis vinifera]	Vitis vinifera
ACG25290	elongation factor 1-alpha [Zea mays]	Zea mays
NP_001104939	elongation factor alpha6 [Zea mays]	Zea mays
NP_001105587	elongation factor 1-alpha [Zea mays]	Zea mays
NP_001105935	elongation factor alpha8 [Zea mays]	Zea mays
NP_001105933	elongation factor alpha2 [Zea mays]	Zea mays
NP_001105617	elongation factor alpha3 [Zea mays]	Zea mays
NP_001105565	elongation factor alpha5 [Zea mays]	Zea mays
NP_001105934	elongation factor alpha7 [Zea mays]	Zea mays
NP_001104938	elongation factor 1 alpha [Zea mays]	Zea mays
NP_001152668	LOC100286309 [Zea mays]	Zea mays

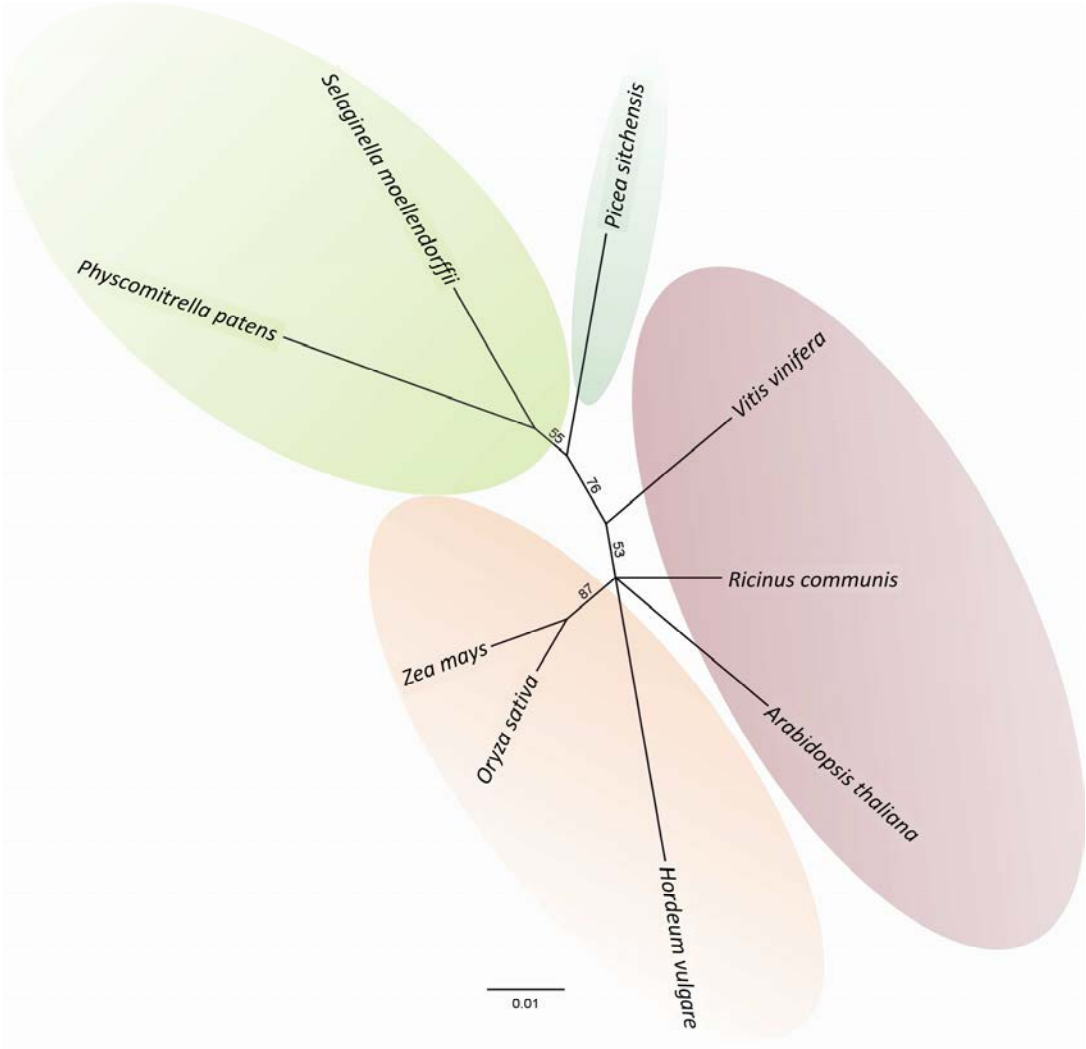

Suppl. Fig. 6 Consensus tree of EF1α homologs in different plant species.
EF1α homologs are conserved from archae to eukaryotes and are thus also found throughout the plant kingdom, from lower plants (in light green) to higher plants (gymnosperms in light blue, monocots in light red, dicots in purple). Homologs were identified by protein BLAST. Distances and groupings were determined by Jukes-Cantor and Neighbour-Joining method and correspond to 500 replications. Bootstrap values are given at the branches. Scale bar represents protein distance as substitutions per site. Accession numbers together with a table of further information are given in the appendix.

12.3.4. #61.4, Pirin-like protein (Pirin)

Suppl. Table 4 Homologs of Pp.Pirin used for alignment and phylogenetic analysis (in light yellow).

Accession no	Description	Organism
NP_191485	putative pirin [Arabidopsis thaliana]	Arabidopsis thaliana
NP_191481	pirin [Arabidopsis thaliana]	Arabidopsis thaliana
NP_850385	pirin-like protein [Arabidopsis thaliana]	Arabidopsis thaliana
XP_001695785	hypothetical protein CHLREDRAFT_149072 [Chlamydomonas reinhardtii]	Chlamydomonas reinhardtii
ACU20099	unknown [Glycine max]	Glycine max
ACU23860	unknown [Glycine max]	Glycine max
BAK02287	predicted protein [Hordeum vulgare subsp. vulgare]	Hordeum vulgare
BAJ91650	predicted protein [Hordeum vulgare subsp. vulgare]	Hordeum vulgare
NP_001061644	Os08g0364900 [Oryza sativa Japonica Group]	Oryza sativa
NP_001051876	Os03g0845000 [Oryza sativa Japonica Group]	Oryza sativa
XP_001766405	predicted protein [Physcomitrella patens subsp. patens]	Physcomitrella patens
ABK27098	unknown [Picea sitchensis]	Picea sitchensis
XP_002529028	pirin, putative [Ricinus communis]	Ricinus communis
XP_002527385	pirin, putative [Ricinus communis]	Ricinus communis
XP_002987558	hypothetical protein SELMODRAFT_446995 [Selaginella moellendorffii]	Selaginella moellendorffii
XP_002992823	hypothetical protein SELMODRAFT_430965 [Selaginella moellendorffii]	Selaginella moellendorffii
XP_002460441	hypothetical protein SORBIDRAFT_02g028180 [Sorghum bicolor]	Sorghum bicolor
XP_002445387	hypothetical protein SORBIDRAFT_07g015030 [Sorghum bicolor]	Sorghum bicolor
XP_002275409	PREDICTED: hypothetical protein [Vitis vinifera]	Vitis vinifera
XP_002268298	PREDICTED: hypothetical protein [Vitis vinifera]	Vitis vinifera !
NP_001150652	pirin-like protein [Zea mays]	Zea mays
NP_001131711	hypothetical protein LOC100193073 [Zea mays]	Zea mays
NP_001131808	hypothetical protein LOC100193181 [Zea mays]	Zea mays
NP_001137098	hypothetical protein LOC100217274 [Zea mays]	Zea mays

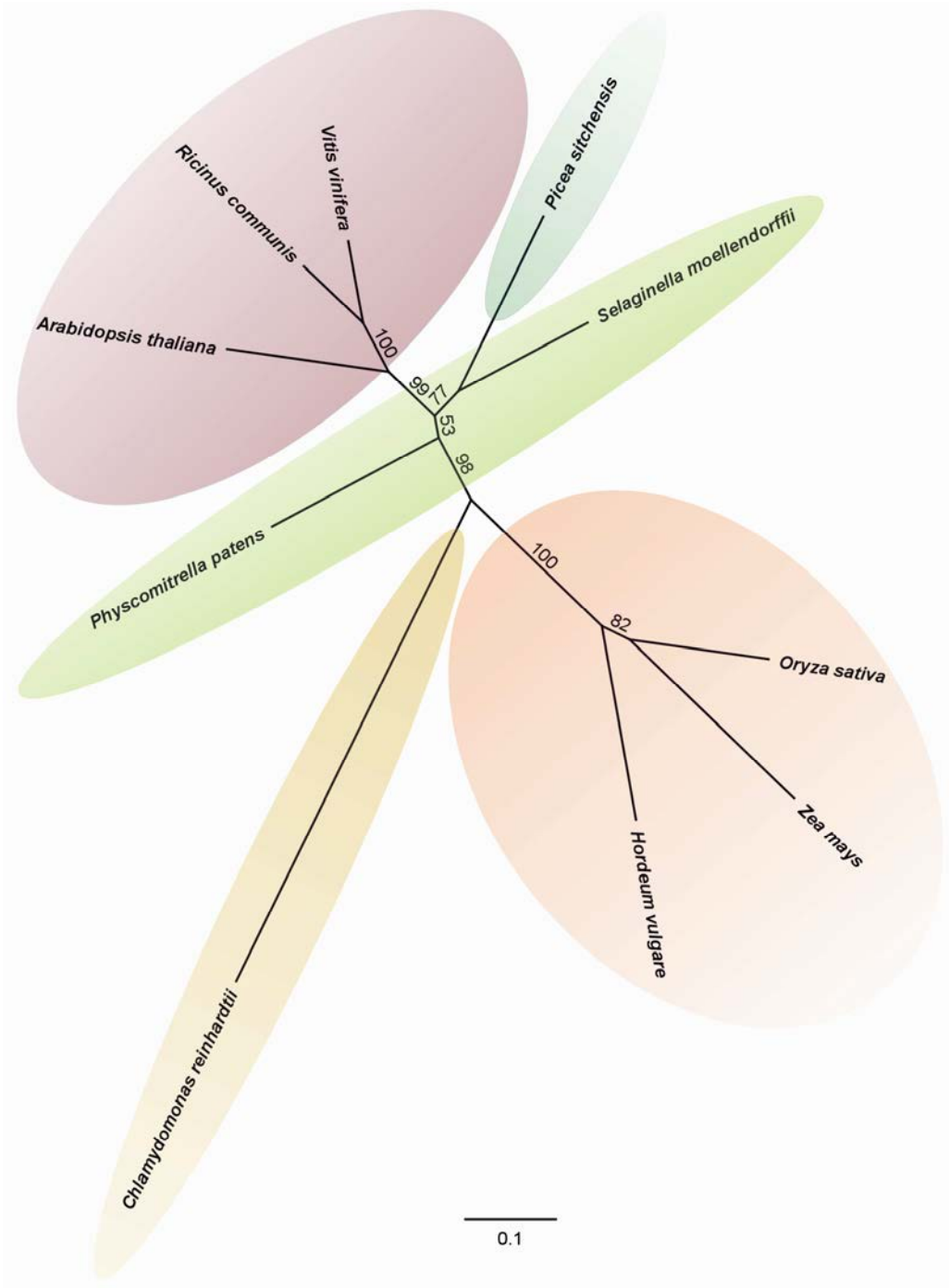

Suppl. Fig. 7 Consensus tree of pirin (-like) homologs in different plant species.
Pirin (-like) homologs are conserved throughout the plant kingdom, from lower plants (in light green) to higher plants (gymnosperms in light blue, monocots in light red, dicots in purple). Homologs were identified by protein BLAST. Distances and groupings were determined by Jukes-Cantor and Neighbour-Joining method and correspond to 500 replications. Bootstrap values are given at the branches. Scale bar represents protein distance as substitutions per site. Accession numbers together with a table of further information are given in the appendix.

12.4. Light dependent interaction of phy4:BD with putative interactors in yeast

12.4.1. Quantitative growth assay on PCB-complemented medium: full-length phy4:BD

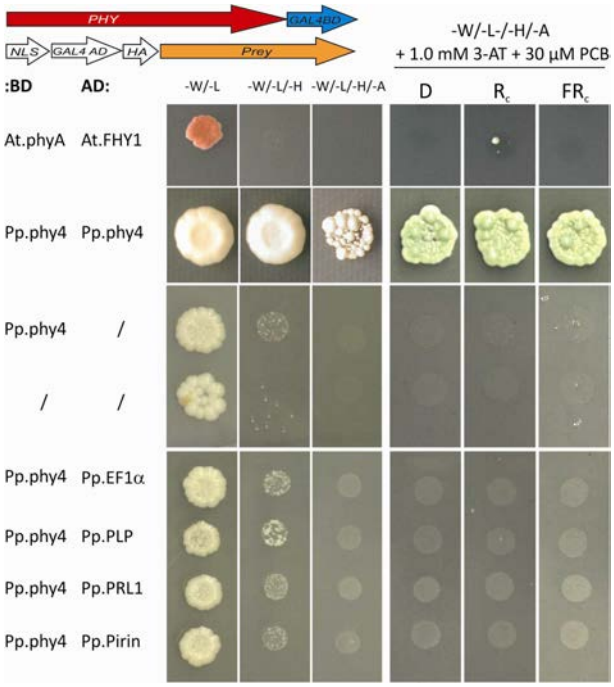

Suppl. Fig. 8 Analysis of light dependent phy4:BD interaction with putative interacting proteins. No interaction with the given putative interacting proteins was observed.

12.4.2. Quantitative growth assay on PCB-complemented medium: phy4_N:BD

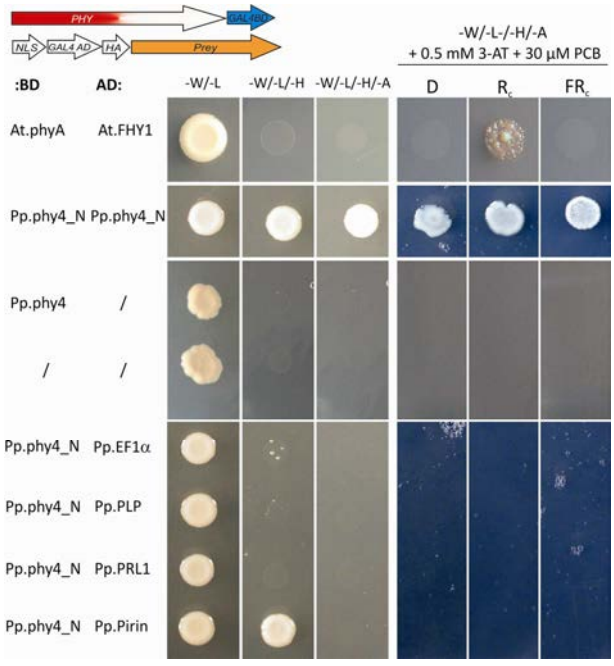

Suppl. Fig. 9 Analysis of light dependent phy4_N:BD interaction with putative interacting proteins. No interaction with the given putative interacting proteins was observed.

12.4.3. Quantitative growth assay on PCB-complemented medium: PHY4_C:BD

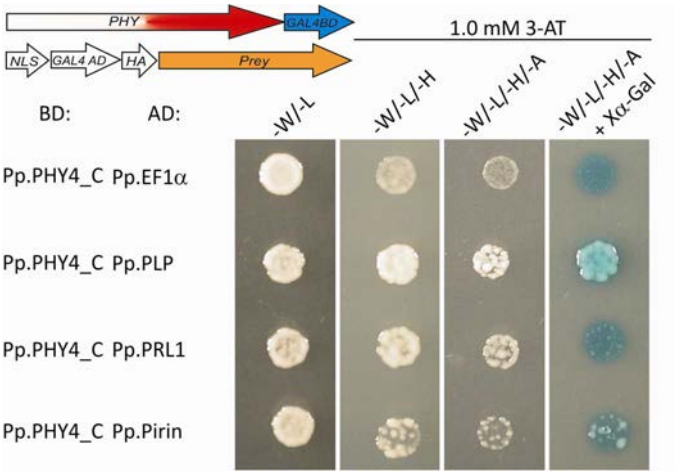

Suppl. Fig. 10 Analysis of light dependent interaction of PHY4_C:BD with putative interactors. Apo-PHY4_C interacted only weakly with PLP and Pirin prey-proteins under most stringent selection conditions. No interaction was seen for EF1α and PRL1.

12.5. sYFP-based i*n vivo* interaction studies of phy4 with its putative interactors

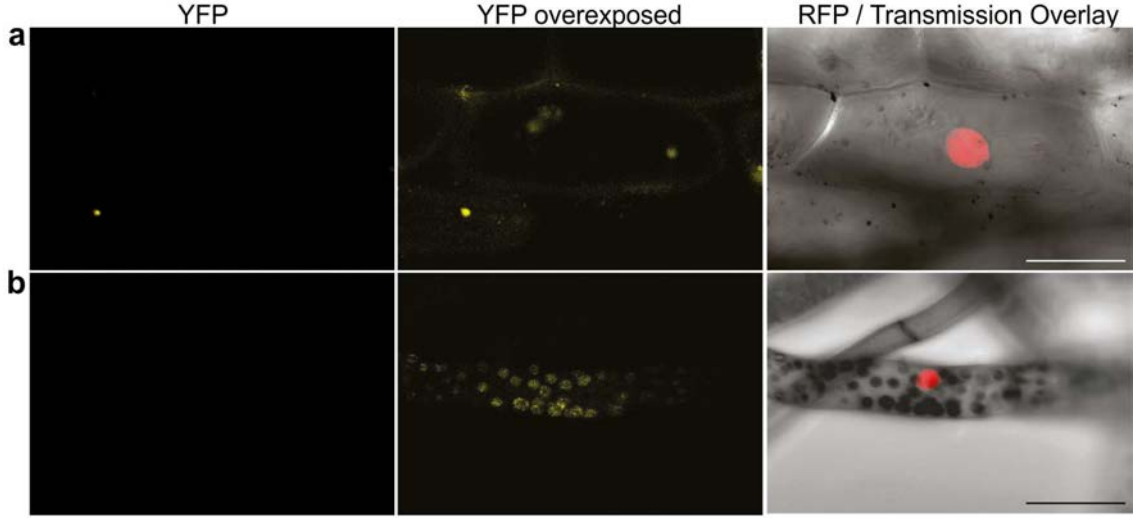

Suppl. Fig. 11 Expression of YFP_N:[empty] and YFP_C:[empty] did not lead to emission of sYFP fluorescence signals. Scale bars 50 µm.

12.6. Light dependent localisation studies of putative phy4 interactors in *Physcomitrella*

These localisation studies were carried out by Rabea Krikor in course of her master thesis project under my supervision.

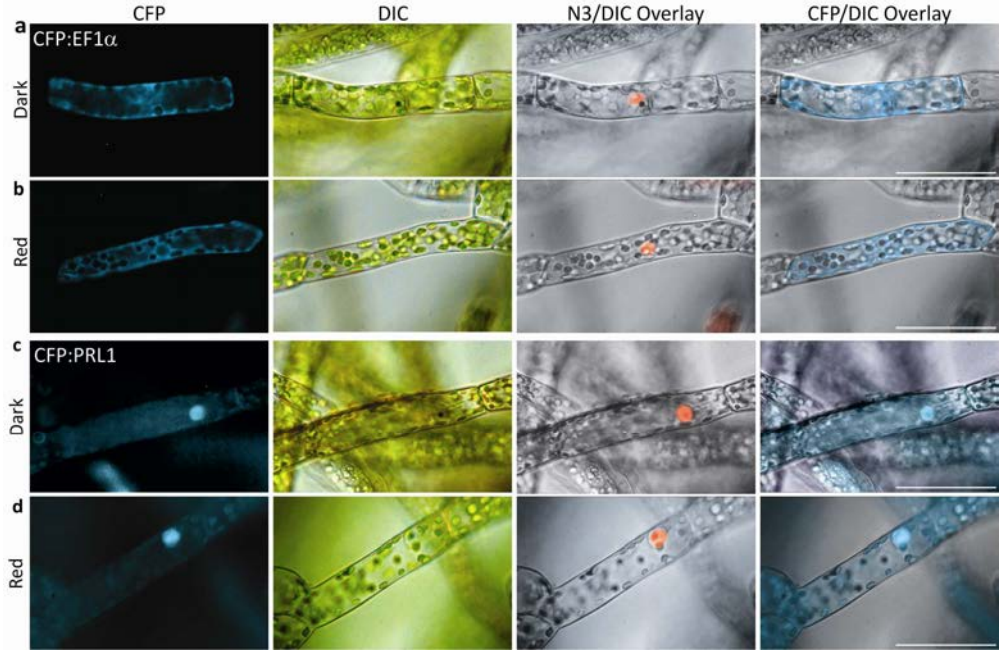

Suppl. Fig. 12 Localisation of N-terminally tagged CFP-fusions of EF1α and PRL1 in darkness and after red light incubation. EF1α was strictly localised to the cytoplasm, as seen from the clear exclusion of the signal from the nucleus (b). PRL1 was clearly located to the nucleus in both darkness and after red light treatment. Scale bars 50 µm.

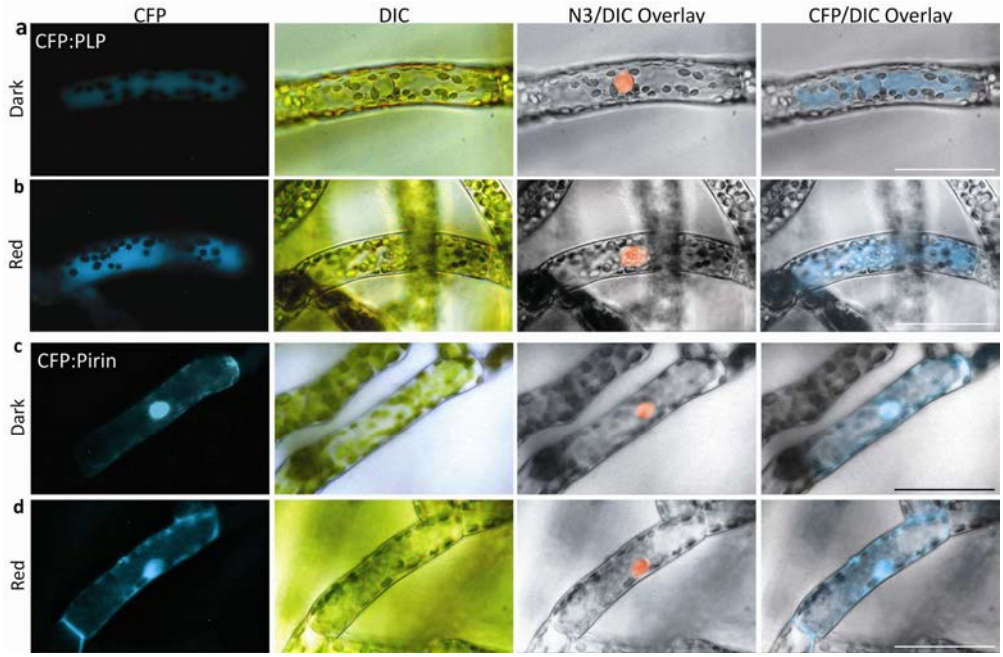

Suppl. Fig. 13 Localisation of N-terminally tagged CFP-fusions of PLP and Pirin in darkness and after red light incubation. PLP showed homogenous fluorescence in both darkness and after red illumination, whereas Pirin exhibited clear accumulation within the nucleus under both light conditions. A considerable cytoplasmic signal remained, however. Scale bars 50 µm.

12.7. Studies on *Physcomitrella* phytochrome 4-phototropin interaction

12.7.1. Quantitative growth assay on PCB-complemented medium: full-length phy4:BD

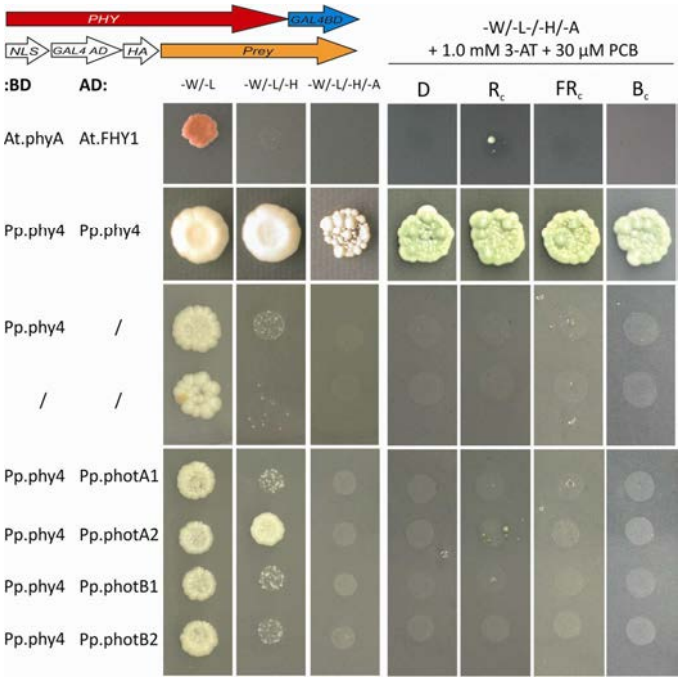

Suppl. Fig. 14 Analysis of light dependent interaction of C-terminally fused phy4 with any of the four phototropins by Y2H. No interaction was observed.

12.7.2. Quantitative growth assay on PCB-complemented medium: phy4_N:BD

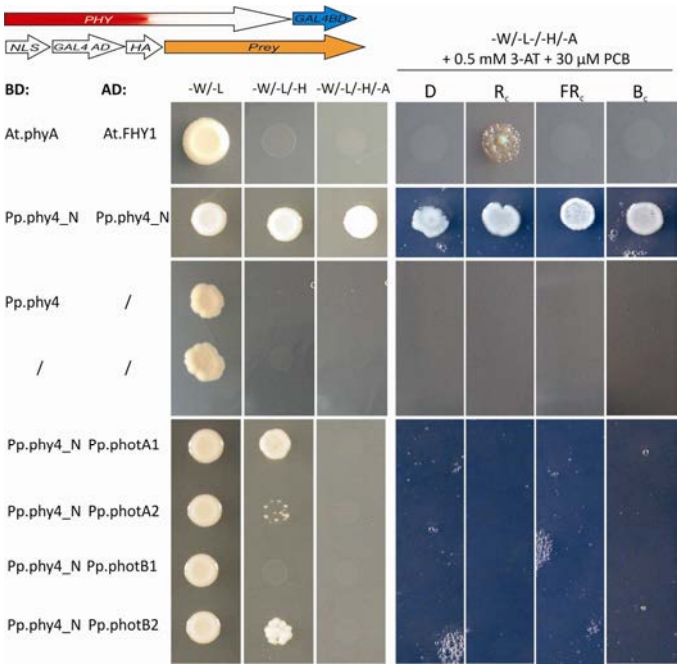

Suppl. Fig. 15 Analysis of light dependent interaction of C-terminally fused phy4_N with any of the four phototropins by Y2H. No interaction was observed.

12.7.3. Quantitative growth assay on PCB-complemented medium: PHY4_C:BD

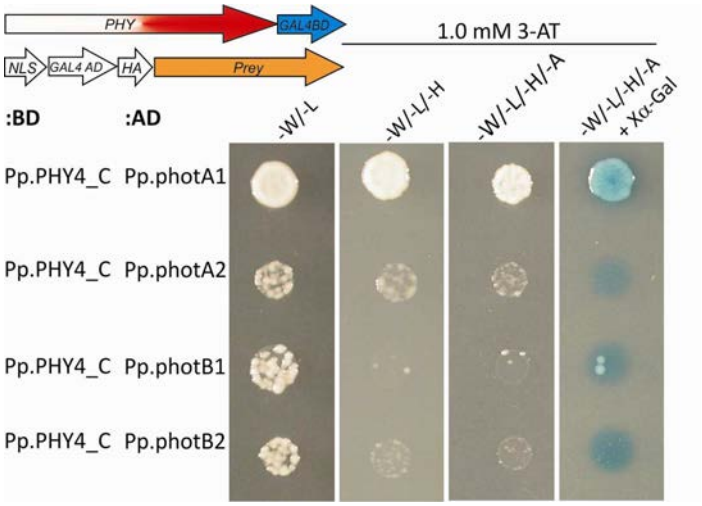

Suppl. Fig. 16 Analysis of light dependent interaction of C-terminally fused PHY4_C with any of the four phototropins by Y2H. Interaction only with photA1 was observed, whereas no other phototropin was bound by PHY4_C.

12.7.4. sYFP-based analysis of phototropin homodimerisation

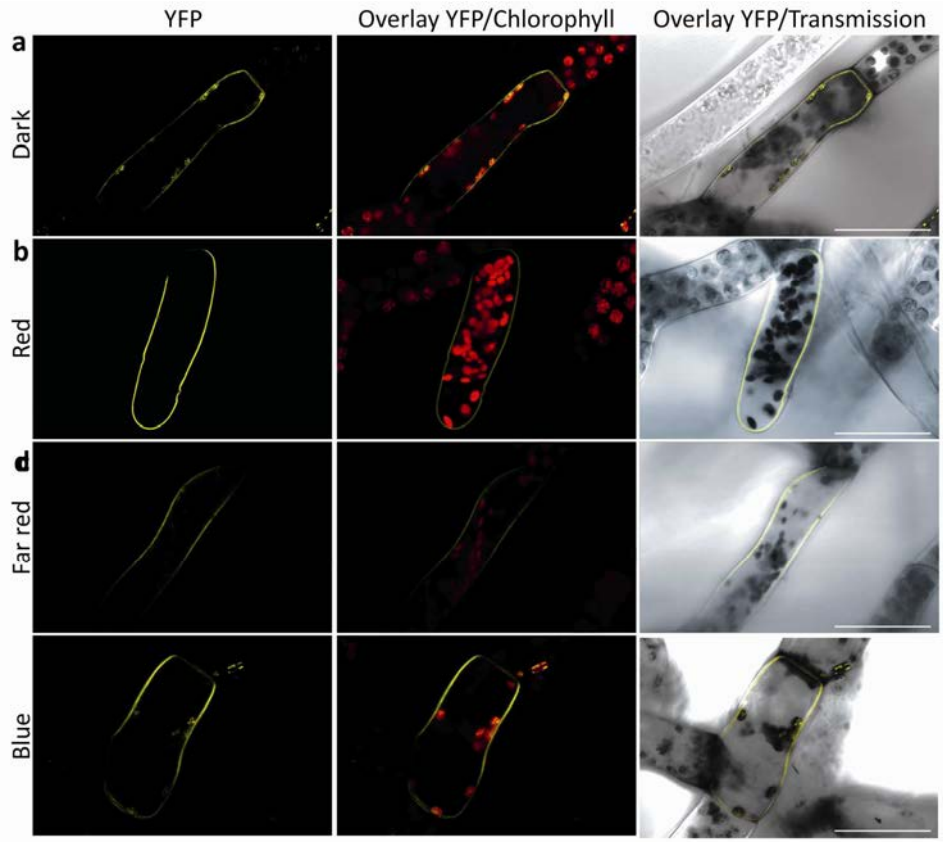

Suppl. Fig. 17 N-terminal fusions of $YFP_{N/C}$ to photA2 form homodimers independent from light. Scale bars 50 µm.

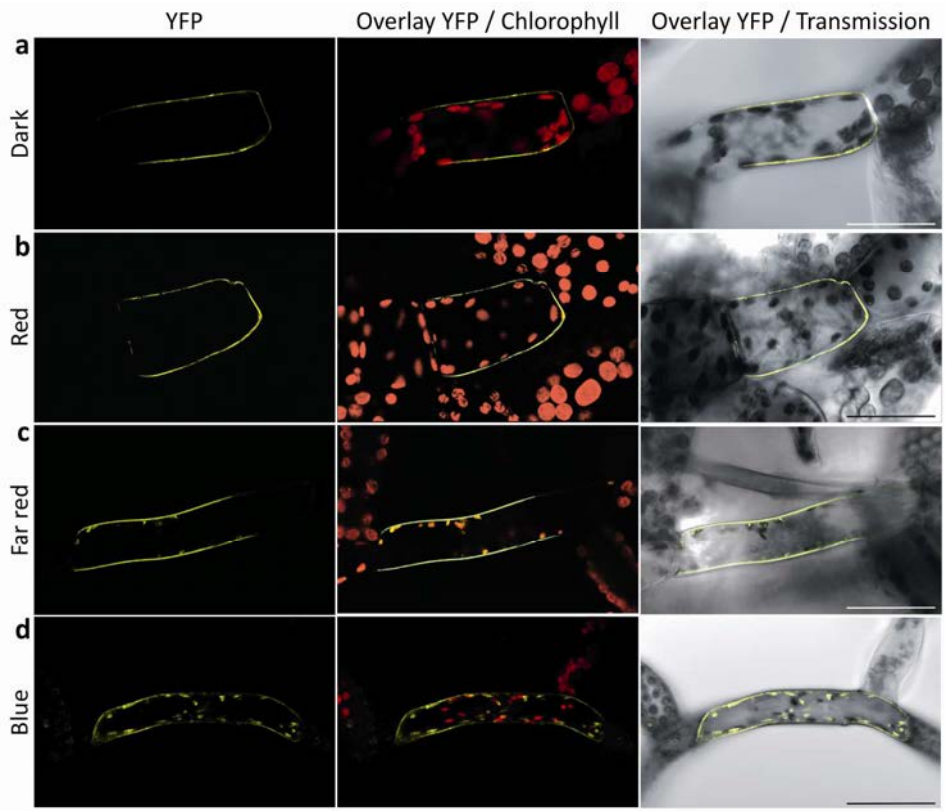

Suppl. Fig. 18 N-terminal fusions of $YFP_{N/C}$ to photB2 form homodimers independent from light. Scale bars 50 µm.

12.8. Y2H-based studies on phyA-phototropin interaction

12.8.1. Quantitative Y2H growth assay on PCB-complemented medium

To test for direct phyA-phot1/2 interaction N-terminal BD/AD:fusions of phyA (BD:phyA) and phot1/2 (AD:phot1/2) were cloned, following the example of Y2H experiments carried out with *Physcomitrella* phy4 and phototropin fusions. phyA_pGBKT7 was cloned by Anna Lena Lichtenthäler, phot1_pGADT and phot2_pGADT7 were cloned by Melanie Bingel.

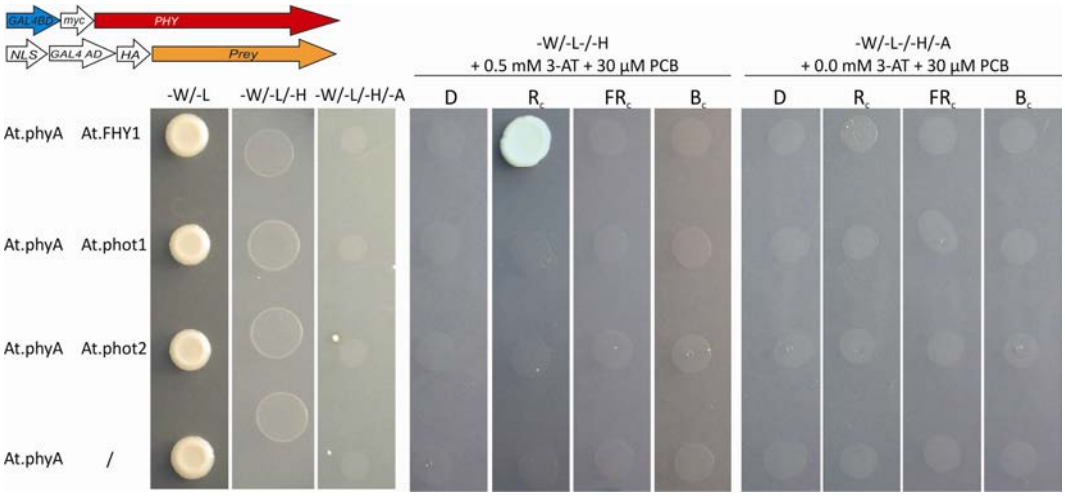

Suppl. Fig. 19 Analysis of light dependent phyA - phototropin interaction by conventional Y2H approach. Scheme in the upper left corner indicates bait and prey molecules used. N-terminal fused BD:phyA fusion proteins exhibited red light dependent growth only upon interaction with FHY1 under medium (middle panel). No interaction was observed for phyA with phot1 or phot2.

Danksagung

Jon Hughes möchte ich von Herzen danken für ein offenes Gespräch zur Weihnachtszeit 2006, das eine Kehrtwende meiner Pläne bedeutete und mich in ein brandneues und unwahrscheinlich faszinierendes *Physcomitrella* Projekt brachte. Ich bin dankbar für alle Unterstützung und das Vertrauen, das mir die Gelegenheit gab, zu lernen, dass man meist doch immer noch einen Schritt weiter gehen kann. Und noch einen. Und noch einen… Komm nach Jülich!
Ich bin dankbar und froh Mathias Zeidler als Moos-Veteranen begleitend an meiner Seite gewusst zu haben. Seine bewundernswerte Eigenschaft Motivation eimerweise über mich zu schütten hat mehr als einmal meine frühzeitige Kapitulation abgewendet und dazu geführt, dass mein Ehrgeiz wieder entfacht wurde. Er war Netz und doppelter Boden - ohne ihn hätte es Knochenbrüche gegeben.

Sehr dankbar bin ich TanJA! Gans und Andrea Weisert - unser gemeinsamer Weg begann schon früher als diese Arbeit und hat nun zu diesem kleinen Meilenstein geführt. Nicht nur die exzellente technische Assistenz, sondern auch Unterstützung, Motivation und Hilfestellungen im Großen wie im Kleinen hat dazu geführt, dass ich diese Arbeit zu einem Ende bringen konnte. Von ganzem Herzen Danke auch an Melanie Bingel, die unzählige DNA-Präparationen für mich übernommen habt. Tina Lang und *Spirulina* danke ich für PCB-Präparationen im mg-Bereich – ohne Euch wäre es bloß grau in grau! Für alle pflegerische Unterstützung danke ich Roland Kürschner bei der Versorgung mehrerer Generationen von Gänseblümchen und Zwiebeln. Es tut mir im Nachhinein Leid um die vielen schönen Blumen, die unter mir so schwer zu leiden hatten. Anette Münndelein danke ich für all die Herzlichkeit, die staunenden Augen und den frischen Wind.

Anna Lena Lichtenthäler und Rabea Krikor möchte ich von Herzen danken für einige experimentelle Unterstützung während der letzten Züge meiner Arbeit und der aufregenden Zeit des „großen Manuskript“ Schreibens.
Adriaan Dorresteijn und Anne Holz danke ich für hilfsbereite Unterstützung und Einführung in die hohe Kunst der konfokalen *Laser Scanning Microscopy.*

Jutta Rösler bin ich für so viele verschiedene Dinge dankbar, dass ich sie hier unmöglich aufzählen kann. Es gibt kaum einen Menschen, der mich und meine Arbeit schon seit dem allerersten Moment derart beeinflusst hat, von dem ich soviel Unterstützung bekommen habe und der mich, bis zuletzt!, gleichzeitig so häufig in den Wahnsinn getrieben hat.

Einen großen Anteil am Gelingen meiner Doktorarbeit haben meine Freunde, allen voran Ilse Klein, Silke Krüger, Marika Midon und Ines Winkler – einfach dafür, dass sie mit Phytochrom nichts (mehr) am Hut haben.
Ich bin froh, von meiner Familie soviel Kraft und Verständnis bekommen zu haben, jedes Mal wenn ich nicht vom Phytochrom los kam. Jo danke ich für das gemeinsame Forschen, Diskutieren, Leben, Arbeiten, Schimpfen, Herzrasen, Kochen, Doktorarbeit schreiben, Köpfe schütteln und Lachen, Lachen, Lachen!

(In Ge-)danke(n) an Gottfried Wagner, der sicher seine große Freude mit dieser Arbeit gehäbt hätte.

Selbständigkeitsversicherung

Ich erkläre hiermit, dass ich die vorliegende Arbeit ohne unzulässige Hilfe Dritter und ohne Benutzung anderer als der angegebenen Hilfsmittel angefertigt habe. Aus fremden Quellen direkt oder indirekt übernommene Gedanken sind als solche kenntlich gemacht.

Gießen, den 28.02.2012